

Rational Drug Design  
and Synthesis of  
Selective FKBP51 Ligands

Xixi Feng

2015

Dissertation zur Erlangung des Doktorgrades  
der Fakultät für Chemie und Pharmazie  
der Ludwig-Maximilians-Universität München

Dissertation zur Erlangung des Doktorgrades  
der Fakultät für Chemie und Pharmazie  
der Ludwig-Maximilians-Universität München

**Rational Drug Design and Synthesis  
of Selective FKBP51 Ligands**

Xixi Feng

aus

Tangshan, Hebei, VR China

2015



## **Erklärung**

Diese Dissertation wurde im Sinne von § 7 der Promotionsordnung vom 28. November 2011 von Herrn PD Dr. Felix Hausch betreut.

## **Eidesstattliche Versicherung**

Diese Dissertation wurde eigenständig und ohne unerlaubte Hilfe erarbeitet.

München, den 05. November 2015

.....Xixi Feng.....

(Unterschrift der Autorin)

**Dissertation eingereicht am 05. November 2015**

1. Gutachter: PD Dr. Felix Hausch

2. Gutachter: Prof. Christoph Turck

**Mündliche Prüfung am 17. Dezember 2015**



# Abstract

## Abstract

The FK506-binding protein 51 (FKBP51) has an important role in several diseases and pathologic states like stress-related depressive disorder, obesity and cancer. Gaali et al. just recently developed the first series of selective FKBP51 inhibitors. All ligands known before bind to FKBP51 and the structurally very similar, but functionally opposing, FKBP52 with the same binding affinity. With the most advanced ligands SAFit1 and SAFit2 the first studies to assess the effects of pharmacological FKBP51 inhibition were finally realizable. In these studies FKBP51 was validated as a promising drug target and FKBP51 inhibition as possible treatment option.



**Scheme 1:** Central coupling step of the FKBP ligand series.

Nevertheless, both SAFit compounds are rather research tools than real drug candidates, since they don't exhibit optimal drug-like parameters. The aim of this thesis is therefore to find more appropriate lead structures for further drug optimization studies, explore the FKBP51 binding pocket by structure-affinity-relationship (SAR) analysis and to further assess the role of FKBP51 as a drug target. With this aim three structurally novel ligand series, classified on their chemical synthesis (Scheme 1), were developed and synthesized. The novel ligands were derived from the SAFit compounds, whereby either the "Bottom Group" (BG) or the "Top Group" (TG) was replaced by new moieties.

Inspired by FK506 and previous FKBP ligands we assessed the role of a hydroxyl group in the binding pocket in the first BG series, whereby the building blocks were derived from a stereo-selective Aldol reaction. At the same time we developed a series of ligands to analyze the structural requirements for selective binding. In the second BG series a rigidification strategy was used and a series of bicyclic scaffolds were designed and synthesized via an asymmetric Diels Alder cyclization. In both series we were able to reproduce the selective binding mechanism. In the last series a SAR on various different amino acids as TG was performed that all contained the highly selective SAFit-derived BG. For this project an

## Abstract

efficient solid phase-based synthesis was developed and conducted in collaborative work. All three ligand series gave new insight into the FKBP51 binding pocket and valuable information for further drug research. Additionally, they represent the first systematic analysis on FKBP51 selective ligands after the discovery of the SAFit compounds.

In order to further validate FKBP51 as a drug target in different indications an upscaling of the SAFit synthesis was performed. In several *in vitro* and *in vivo* studies it was possible to reproduce FKBP51 knock out results with pharmacological inhibition by SAFit1 or SAFit2. In these studies FKBP51 inhibition was either confirmed or even newly discovered as possible treatment, encouraging our attempts to further optimize FKBP51 selective ligands.

# Contents

## CONTENTS

### A - INTRODUCTION

<b>1. FKBP51 as a promising drug target</b>	1
1.1. The role of FKBP51 in diseases	1
1.2. Druggability of FKBP51	2
<b>2. The biology of FKBP51</b>	3
2.1. Structure and function	3
2.2. The important role of FKBP51 in HPA axis regulation	5
<b>3. Development of FKBP51-selective ligands</b>	6
3.1. The necessity of FKBP51 selectivity	6
3.2. Flipping Phenylalanine – the key to selectivity	7
3.3. Open issues	8
<b>4. Aim of this work</b>	9

### B – RESEARCH ARTICLES

<b>5. Publication I: “Recent Progress in FKBP ligand development”</b>	11
• Summary	11
• Original Publication	12
<b>6. Publication/Manuscript II-V: Pharmacological effects of SAFit1 and SAFit2</b>	30
6.1. <b>II: “FKBP51 employs both scaffold and isomerase functions to promote NFκB activation in melanoma”</b>	30
• Summary	30
• Original Publication	31
6.2. <b>III: “The stress regulator FKBP51 drives chronic pain by modulating spinal glucocorticoid signaling” (submitted manuscript)</b>	42
• Summary	42
6.3. <b>IV: “Loss or inhibition of FKBP51 protects against diet-induced metabolic disorders by shaping insulin signaling” (manuscript in preparation)</b>	43
• Summary	43
• Original Manuscript	44
6.4. <b>V: “The FKBP51 antagonist SAFit2 decreases basal ultradian corticosterone secretion in the rat” (manuscript in preparation)</b>	56
• Summary	56

# Contents

<b>7. Publication/Manuscript VI-VIII: Own publication</b>	<b>57</b>
<b>VI: “Structure–Affinity Relationship Analysis of Selective FKBP51 Ligands”</b>	<b>57</b>
• Summary	57
• An asymmetric aldol reaction as key synthesis step	58
• Original Publication	61
• Supporting Information	72
<b>7.2. VII: “A novel decalin-based bicyclic scaffold for FKBP51-selective ligands”</b> (manuscript in preparation)	<b>92</b>
• Summary	92
• Prescreening of bicyclic aromating scaffolds	93
• An asymmetric intramolecular Diels-Alder (IMDA) reaction as key synthesis step	93
• Original Manuscript	97
• Supporting Information	107
<b>7.3. VIII: “Rapid, structure-based exploration of pipercolic acid amides as novel</b> selective antagonists of the FK506-binding protein 51” (submitted manuscript)	<b>140</b>
• Summary	140
• Original Manuscript	141
• Supporting Information	173
<b>C – SUMMARY AND OUTLOOK</b>	<b>179</b>
<b>D – REFERENCES</b>	<b>182</b>
<b>E – CURRICULUM VITAE</b>	<b>189</b>

# A. Introduction

## A. INTRODUCTION

### 1. FKBP51 as a promising drug target

#### 1.1. The role of FKBP51 in diseases

The immunophilin FK506-binding protein 51 (FKBP), among other FKBP, is best known for its immunosuppressant-enabling properties due to its role as the binding target of the immunosuppressant FK506 (Tacrolimus) and also rapamycin (Sirolimus) (Fig. 1). Even the name of this protein family is derived from this function. But beside this role, FKBP, are also enrolled in numerous other intracellular pathways and are therefore involved in different diseases.

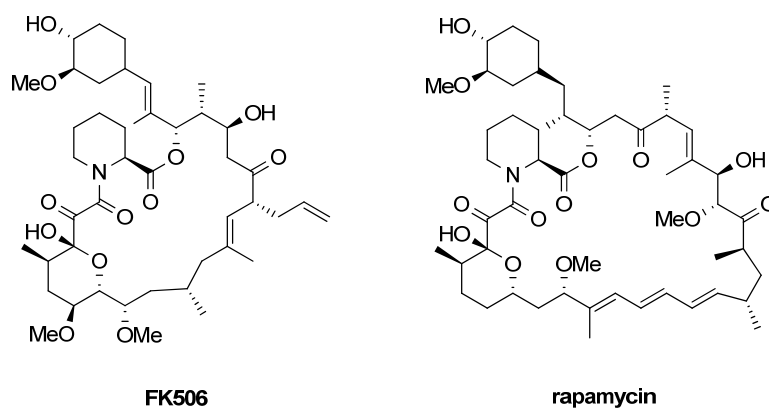


**Fig. 1:** Chemical structure of FK506 (Tacrolimus) and rapamycin (Sirolimus).

In genetic studies single nucleotide polymorphisms in FKBP5, the gene encoding FKBP51, have repeatedly been associated with stress-related disorders. An upregulation of FKBP51, caused by genetic variations of FKBP5, were linked to numerous stress-related endophenotypes and affective disorders like depression or post-traumatic stress disorder.<sup>1, 2</sup> Studies in FKBP51 knockout mice showed enhanced active stress-coping behavior after stress. Also on the endocrine level the animals were protected from hyperactive stress responses, likely due to an improved feedback regulation of the hypothalamus-pituitary-adrenal (HPA) axis. In behavioral studies FKBP51 deficiency led to enhanced recovery after stress exposure and actually an antidepressive-like effect, confirming the influence of FKBP51 on HPA axis regulation.<sup>3-6</sup> FKBP51 is therefore an established risk factor for stress-related disorders.

Beside this a strong expression of FKBP51 was also observed in adipocytes during differentiation. It might therefore influence mitotic cell growth.<sup>7</sup> Additionally, reduction of

## A. Introduction

the protein by knockout protected mice from weight gain after a high fat diet. In selected organs and pathways a loss of functional FKBP51 is supposed to create a hyperactivated glucocorticoid receptor that in the end induces fatty acid catabolism and better expenditure of energy.<sup>8</sup> Generally, mice with reduced FKBP51 exhibited a slightly reduced weight.<sup>4</sup> In this context an inhibition of FKBP51 is supposed to have positive effects on obese conditions. It has also been shown that a reduction of FKBP51 leads to chemoresistance in malignant melanoma by influencing NF- $\kappa$ B activation.<sup>9-11</sup> However, also in several other cancers a strong expression of FKBP51 was found. An inhibition of the protein by rapamycin showed positive effects in, for example, glioma and in childhood acute lymphoblastic leukemia.<sup>9, 10</sup> Another auspicious indication for FKBP51 inhibition is the treatment of musculoskeletal pain after trauma, like motor vehicle collision or sexual assault to improve recovery. Also here, it has been shown in genetic studies that single nucleotide polymorphisms in FKBP5 cause increased FKBP5 mRNA levels that are associated with increased pain development.<sup>14</sup>

For all these diseases FKBP51 is a promising drug target and pharmacological inhibition could therefore be a possible treatment.<sup>15-17</sup>

### 1.2. Druggability of FKBP51

Since FK506 and rapamycin were known inhibitors of FKBP51, a principle druggability of FKBP51 was acknowledged. But to further go on with FKBP51-directed drug discovery for the treatment of FKBP1-related diseases two major hurdles had to be taken. The first one was to develop non-immunosuppressant inhibitors. The second obstacle was to selectively target FKBP51 without affecting other FKBP5s, especially its closest homolog FKBP52, to avoid undesired side-effects.

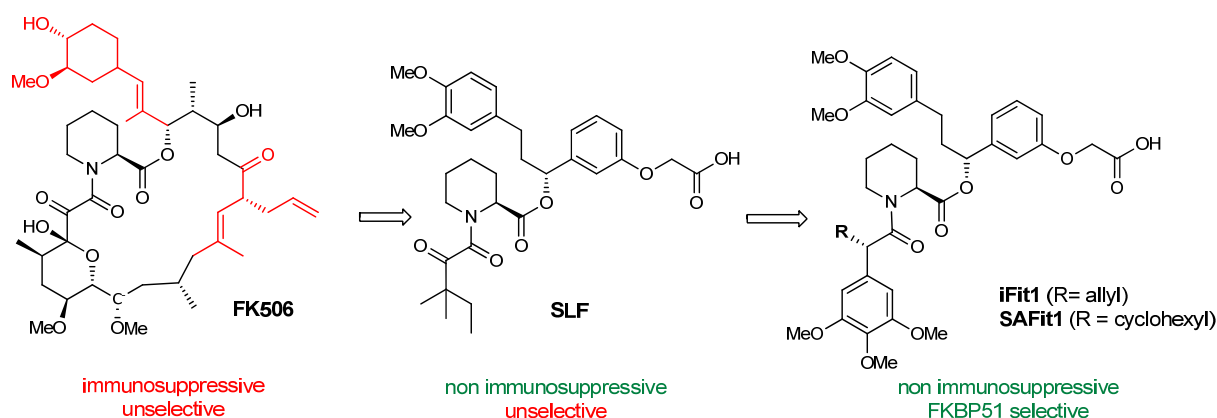


**Fig. 2:** Evolution of FKBP ligands and their characteristics. The calcineurin binding domain of FK506 is shown in green.

## A. Introduction

By removing and changing the immunosuppressive effector domain (calcineurin binding domain) a series of non-immunosuppressive FKBP ligands were developed. The development of FK1706, for example, was based on the chemical structure of FK506.<sup>18</sup> Like several other non-immunosuppressive FKBP ligands, it was shown that FK1706 exhibits neurotrophic activity. This class of non-immunosuppressive FKBP ligands was therefore supposed to be promising for the treatment for neurodegenerative diseases upon binding to FKBP12. To find more binders for FKBP51 a high throughput screening of more than 380,000 compounds and chemical scaffold was conducted. Unfortunately, no promising hit was found after the screening.<sup>19</sup> A more successful strategy was the use of structure-based rational design, whereby a crystal structure of FKBP51 and the non-immunosuppressive ligand SLF was used as starting point.<sup>20</sup> With this method a series of novel non-immunosuppressive FKBP inhibitors were developed by Gopalakrishnan et al.<sup>20, 21</sup>, Wang et al.<sup>22</sup> and Pomplun et al.<sup>23</sup>. Although novel scaffolds and highly efficient synthetic strategies were developed to obtain a variety of chemically different and highly affine ligands, all compounds bound to FKBP12, 51 and 52 with almost the same binding affinity. No significant FKBP51 selectivity could be achieved.

A milestone in FKBP51 drug development was reached when Gaali et al.<sup>24</sup> discovered a first series of ligands that exhibited high binding affinities for FKBP51, but no binding towards FKBP52. The compounds SAFit1 and SAFit2 from this series are the best published FKBP51 selective ligands so far. SAFit2, due to its more lipophilic structure and therefore better blood-brain-barrier permeability, allowed the first *in vivo* pharmacological studies for FKBP51 in mice. In several animal models SAFit2 showed clear antidepressant-like and anxiolytic effects.<sup>24, 25</sup> Additionally, a plausible mechanistic explanation of the selective binding mode was provided that, together with the first pharmacological data, represent a great progress in FKBP51-directed drug development.

### **2. The biology of FKBP51**

#### *2.1. Structure and function*

FKBP51 as well as the other members of the FKBP family exhibit rotamase activity. The proteins are peptidyl-prolyl isomerases (Fig. 3) and catalyze cis-trans conversion around peptidyl-prolyl bonds of proteins. Therefore it is assumed that they play an important role in

## A. Introduction

protein folding and intracellular trafficking. The enzyme activity can be inhibited by both FK506 and rapamycin.<sup>7</sup>

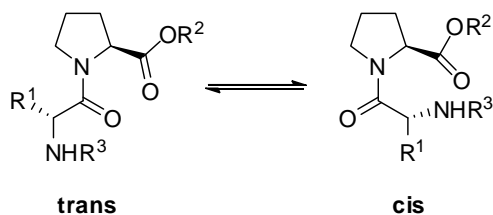


**Fig. 3:** Proline cis/trans isomerization

FKBP51 (as well as FKBP52) belongs to the large FKBP homologs and are named after their size (in kD). As most FKBP s they are located in cytosolic cell compartments.<sup>26</sup> The protein consists of three domains (Fig. 4): two consecutive structurally similar FKBP domains (FK1, FK2) and at the C-terminus a three-unit repeat of the TPR (tetratricopeptide repeat) domain. As typical FKBP domains the FK1 and FK2 domains of FKBP51 are composed of an  $\alpha$ -helix enclosed by five  $\beta$ -sheets. In contrast, the TPR domain is all-helical.<sup>27</sup>

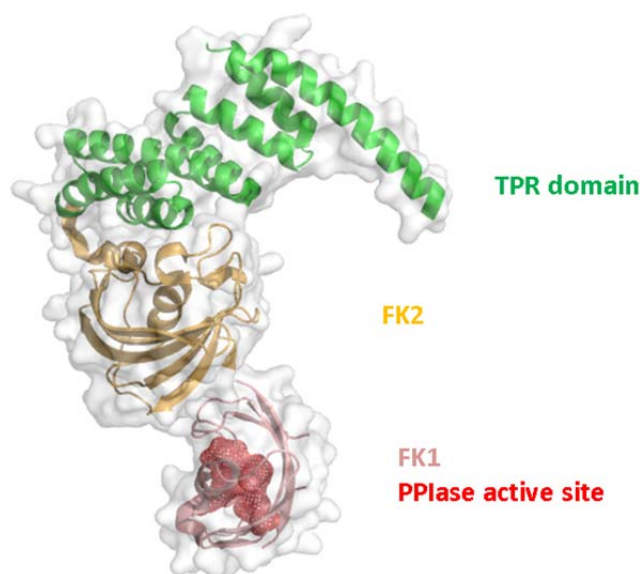


**Fig. 4:** Crystal structure of human FKBP51 (pdb: 1KT0). TPR domain is shown in green; FK2 domain is shown in yellow; FK1 domain is shown in salmon; PPIase active site is shown in red.

Although both FK domains are structurally similar, the FK2 domain has no PPIase activity. Double point mutations in FK1 almost abolished the enzyme activity in human FKBP51<sup>27</sup>, making this part of the protein the main target and focus in FKBP51-directed drug development.

# A. Introduction

## 2.2. The important role of FKBP51 in HPA axis regulation

Although FK506 and rapamycin also show high binding affinity towards the large FKBP51 (51 and 52) the immunosuppressive effect is mainly mediated by FKBP12 and only partly by FKBP51, whereby the effect is independent from PPIase inhibition.<sup>26</sup> The immunosuppressive effect is enabled by ternary complexes that are formed by FKBP51-FK506-calcineurin and FKBP51-rapamycin-mTOR, whereby a specific part of the ligands is responsible for binding the effector proteins. In the end both complexes, by different pathways, lead to an absence of important key regulators for T-cell activation, a major component of the human immune system.<sup>28</sup>

Although this is the most prominent role of FKBP51, FKBP51 itself is mainly considered in context with stress-related diseases due to its important role in the stress regulating system, which is the hypothalamus-pituitary-adrenal (HPA) axis (Fig. 5). Stress is a trigger for the hypothalamus to produce CRH (corticotropin releasing hormone), which activates the pituitary gland to secrete ACTH (adrenocorticotrophic hormone). This stimulates the production of cortisol in the adrenal glands.<sup>29</sup>

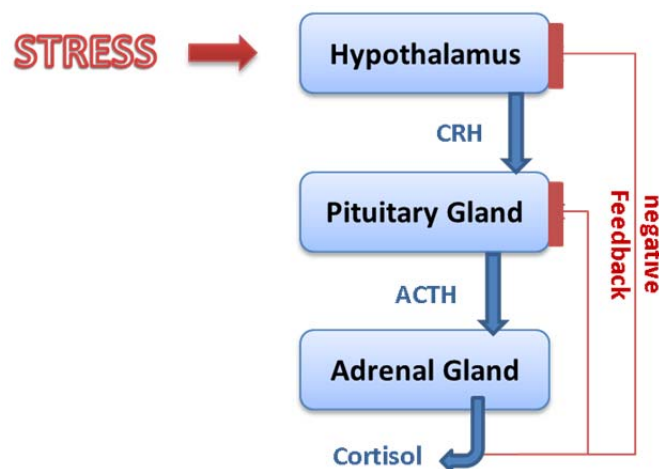


**Fig. 5:** The hypothalamus-pituitary-adrenal axis regulation cascade.

Upon binding to the glucocorticoid receptor (GR), cortisol activates energy metabolism in different tissues. At the same time it inhibits exaggerated CRH and ACTH release in the respective tissues to maintain a homeostasis of the HPA axis. FKBP51 is a negative modulator of GR activity by decreasing the affinity of GR for cortisol. Simultaneously, GR activation increases FKBP51 expression. Changes in these feedback loops can lead to an inappropriate reaction of the HPA axis to stress. Overactive FKBP51 leads to decreased GR sensitivity. In depressive patients this is a typical functional phenotype.<sup>29</sup> Reduced GR

## A. Introduction

sensitivity is also associated with the evolvement of posttraumatic pain states.<sup>14</sup> Enhancement of GR sensitivity to restore a balanced feedback mechanism by pharmacological inhibition of FKBP51 has already shown successful results in first *in vivo* studies in mice.<sup>24</sup>

### 3. Development of FKBP51-selective ligands

#### 3.1. The necessity of FKBP51 selectivity

A key issue in the drug discovery process is the development of preferably selective compounds to avoid undesired side-effects by interacting with different target proteins.<sup>30</sup> In the field of FKBP51 research, achieving selectivity, especially over FKBP52, was a big hurdle. In a cellular model of neuronal differentiation in N2a cells it has been shown that FKBP52 has exactly the opposite effect of FKBP51. While FKBP52 exhibited a neuritotropic effect by stimulating neurite outgrowth, FKBP51 showed an inhibitory effect (Fig. 6).<sup>24</sup> Also on a physiological level opposing effects of FKBP51 and 52 have been reported. Both proteins affect the binding affinity of steroids on their respective steroid hormone receptors, for example the androgen receptor, progesterone receptor and the glucocorticoid receptor. In the presence of FKBP51 the binding affinity of the hormones, e.g. cortisol, are decreased. In contrast, FKBP52 enhances the binding affinity of the respective hormones.<sup>31-35</sup> Therefore it is supposed that that a pharmacological regulation of both proteins at the same time would have no effect at all since it would cancel each other out.

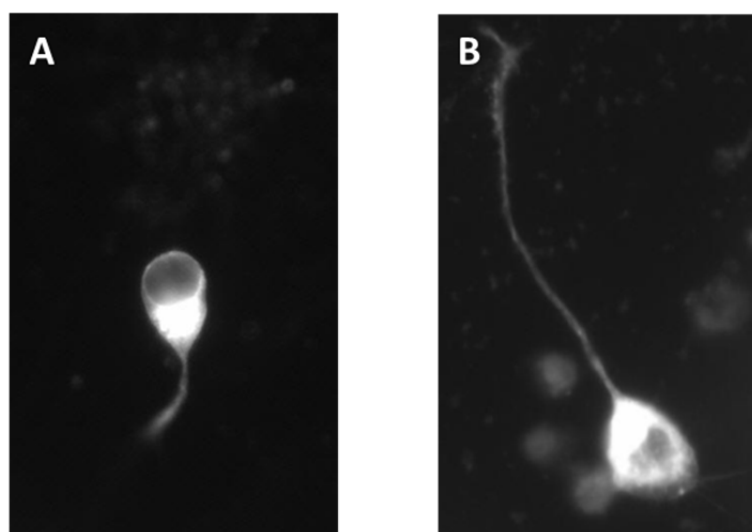


**Fig. 6:** Effect of FKBP51 (A) and FKBP52 (B) on neurite outgrowth of N2a cells.<sup>38</sup>

## A. Introduction

In addition to that, reduction of endogen FKBP52 in knockout mice had severe effects on the reproductive system. Female mice were complete sterile and male mice showed significant undesirable phenotypic changes in the secondary sex organs. Functional FKBP52 is essential for the formation of fully functional reproductive organs.<sup>32, 36, 37</sup> A pharmacological inhibition of this protein should therefore be clearly avoided.

In contrast, no severe phenotypic but even positive changes in the stress-regulating system were observed in FKBP51 knockout mice as described in the previous chapter, suggesting that inhibition of FKBP51 is probably well tolerated

Although these issues have been known for a while, FKBP51 drug discovery was hindered since it was not possible to pharmacologically differentiate between these proteins. Before 2014 all known ligands showed virtually the same binding affinity on both proteins, like FK506 and rapamycin.

### 3.2. Flipping Phenylalanine – the key to selectivity

The discovery of the first FKBP51 selective ligands was a serendipitous incident. iFit1, a ligand that was developed to only bind to mutated FKBP51, surprisingly showed weak binding to wildtype FKBP51. But, paradoxically, at the same time no binding towards FKBP52 was observed.<sup>24</sup>

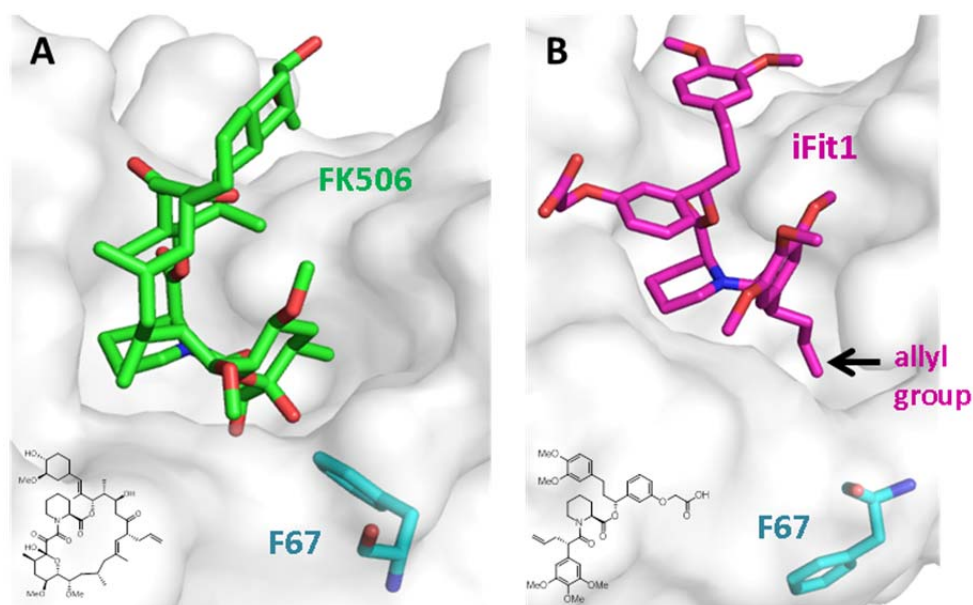


**Fig. 7:** X-ray structure of FK506 (A, green, pdb: 3O5R) and iFit1 (B, magenta, pdb: 4TW6) in the FK506 binding domain of FKBP51. Phenylalanine 67 is shown in blue.

## A. Introduction

The cocrystal structure of FKBP51-iFit1 showed a significantly enlarged binding pocket compared to earlier published structures of FKBP51-ligand complexes (Fig. 7), like FK506, although the rest of the ligand adopts virtually the same binding conformation. The allyl substituent points into this enlarged cavity, which is in the apo-form of the protein occupied by Phe67. A comparison of this crystal structure with a FK506-FKBP51 crystal structure confirmed that Phe67 is flipped into a new position. It is hypothesized that this conformational change is energetically less favored in FKBP52 due to the sterically more hindered amino acids Thr58, Trp60, Val129 in the Phe67 surrounding. In FKBP51 Phe67 is in close proximity to Lys58 and Lys60 that are stabilized by Phe129.<sup>24</sup>

Due to its orientation the allyl substituent seemed to be very important for this kind of binding mode. A structure affinity relationship analysis of this particular substituent was therefore performed by Gaali et al to explore the enlarged binding pocket. They could show a positive correlation between the size of the substituent and the binding affinity. Also the right stereochemistry was shown to be essential for binding. In this series the cyclohexyl-substituted ligands SAFit1 and SAFit2 (Fig. 8) showed the highest binding affinities towards FKBP51 and at the same time > 10,000 fold selectivity over FKBP52. With these ligands it was, for the very first time, possible to assess the pharmacological effect of selective FKBP51 inhibition (see 1.1.), representing a turning point in FKBP51 research.<sup>24</sup>

### *3.3. Open issues*

SAFit2, due to its more lipophilic structure and therefore better blood-brain-barrier permeability, has already shown promising pharmacological effects in animal studies. Although these effects are very intriguing and encouraging, both (SAFit1 & SAFit2) compounds should be rather considered as tool compounds for research than seen as drug-like inhibitors. Their physicochemical properties (Tab.1) are clearly outside the range of typical CNS-directed drugs (90 % of CNS drugs) and have clearly to be optimized.<sup>39</sup> It was shown by Leeson et. al.<sup>40</sup> that compounds, which match with the suggested drug-like parameters, have higher chances to pass the clinical trials and reach the market.

## A. Introduction

	SAFit1	SAFit2	typ. CNS drug
<b>molecular weight (g/mol)</b>	743	803	< 426
<b>lipophilicity (clogD)</b>	3.5	7.1	< 3.8
<b>polar surface area (Å<sup>2</sup>)</b>	139	114	< 86
<b>hydrogen bond acceptors</b>	14	12	< 7

**Tab. 1:** Overview of the physicochemical parameters of SAFit1, SAFit2 and typical CNS drugs.

Due to their high molecular weights, SAFit1 and SAFit2 are also not useful chemical starting points for further drug development. Towards this end, more suitable molecular entities have to be found that optimally further retain the just recently discovered selective binding characteristics.

### 4. Aim of this work

Derived from the open issues in current FKBP51 drug research the aim of this study was to identify molecular entities that can serve as starting points for improving drug-likeness of FKBP51 ligands. Using rational drug design methods novel ligands should be developed based on the knowledge about previous developed ligand series and on the information about the protein obtained from the respective crystal structures. To perform a structure-based approach, using SAFit1 and SAFit2 as starting points, we divided the compounds into three parts based on the chemical synthesis of the compounds. Hereby the (*S*)-pipercolic acid represents the “core group”, which we decided to keep constant in all compounds since a preliminary chemical exploration of this moiety has already been performed by Gaali.<sup>41</sup>

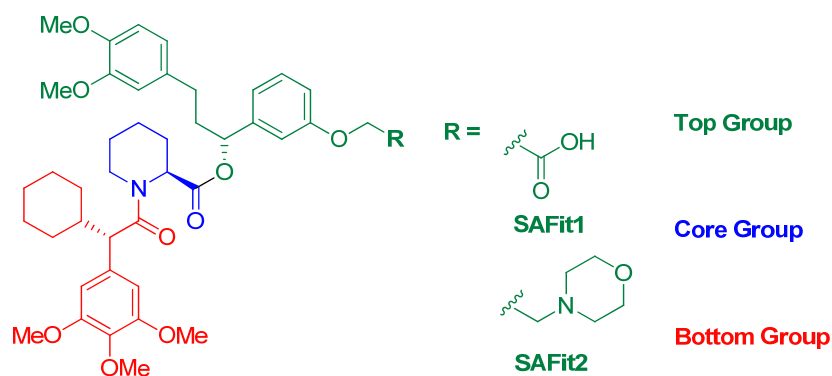


**Fig. 8:** Chemical structure of SAFit1 and SAFit2. The chemical building blocks are shown in different colors (Top Group in green, Core Group in blue, Bottom Group in red).

## A. Introduction

First of all, the trimethoxyphenylring of the bottom group should be systematically replaced to analyze the structural requirements for the selective binding mechanism. Since we expect a significant loss of binding affinity during this step, potential methods to again increase the affinity will be tested. This includes incorporating a hydroxyl group in the bottom group that has proven to be important for previous developed ligands. Additionally, a scaffold should be designed that rigidifies the flexible cyclohexylring to decrease entropy loss during binding. Furthermore, we set out to find biologically more stable and smaller residues to replace the labile ester “Top Group”.

A scale-up of the SAFit1&2 syntheses should be developed and conducted to provide sufficient of these compounds for further animal studies. The promising effects of pharmacological FKBP51 inhibition should be confirmed by more experiments to justify our drug optimization ambitions.

## B. Research Articles – Publication I

### B. RESEARCH ARTICLES

#### 5. Publication I

##### Recent Progress in FKBP ligand development

(Xixi Feng, Sebastian Pomplun, Felix Hausch, *Current Molecular Pharmacology* 2015)

##### Summary

The review article “Recent Progress in FKBP ligand development” gives an overview of the latest achievements in FKBP ligand research. It provides information about the relevance of FKBP5s, especially FKBP51, as potential drug targets and the structural and chemical development of different series of FKBP ligands.

Within this article I contributed to the section “Development of the first FKBP51-selective ligands”, where the serendipitous discovery of the first FKBP51-ligand is described, and the section “Induced Fit-The Key to FKBP51 Selectivity”. In this part a detailed explanation of the selectivity mechanism is given and the development of the currently most advanced ligands SAFit1 and SAFit2 is explained.

## B. Research Articles – Publication I

### ORIGINAL PUBLICATION

#### Recent progress in FKBP ligand development

Xixi Feng, Sebastian Pomplun, Felix Hausch

Max Planck Institute of Psychiatry, Kraepelinstr. 2, 80804 Munich, Germany

#### Abstract

FK506-binding proteins have been implicated in numerous human diseases suggesting novel therapeutic opportunities. In particular, the large FKBP51 has emerged as an important regulator of the stress-coping system and as an established risk factor for stress-related disorders. The principal druggability of FKBP51 is evidenced by the prototypical high affinity ligands FK506 and rapamycin but the development of more refined and selective chemical probes for FKBP51 has been challenging. In this review we summarize recent advances in the development of FKBP51 ligands, which culminated in the first highly selective ligands for FKBP51. The best ligand SAFit2 allowed the proof-of-concept in mice for FKBP51 inhibitors as potentially novel antidepressants. Finally, we discuss pending issues that need to be addressed for the further development of FKBP51-directed drugs.

#### Introduction

FK506-binding proteins (FKBPs) comprise a family of 16 proteins in humans that share sequence homology to the prototypic FKBP12, the first discovered and best characterized FKBP. Many members of the FKBP family possess a peptidyl-prolyl-isomerase activity and to bind to the natural products FK506 or rapamycin.[1,2]

FKBPs are best known for their ability to enable the immunosuppressive effect of FK506 and rapamycin (Fig. 1).[3,4] Remarkably, this is a gain-of-function mechanism that is biochemically achieved by forming an FK506-induced ternary complex with the phosphatase calcineurin or a rapamycin-induced ternary complexes with the kinase mTOR. As a result the activity of calcineurin or mTOR is inhibited, leading to a blockade of pathways that are essential for allograft rejection after transplantation. While this immunosuppressant-enabling property was historically assigned to the prototypic FKBP12, it has recently become clear that other cytosolic FKBPs like FKBP12.6 and FKBP51 can also exert this effect, especially in the case of rapamycin, where direct contacts between FKBPs and mTOR are minimal within the

## B. Research Articles – Publication I

ternary complex.[5] Since the mTOR pathway is also critical for cell growth, rapamycin and its analogs are also clinically used to treat several types of cancer.

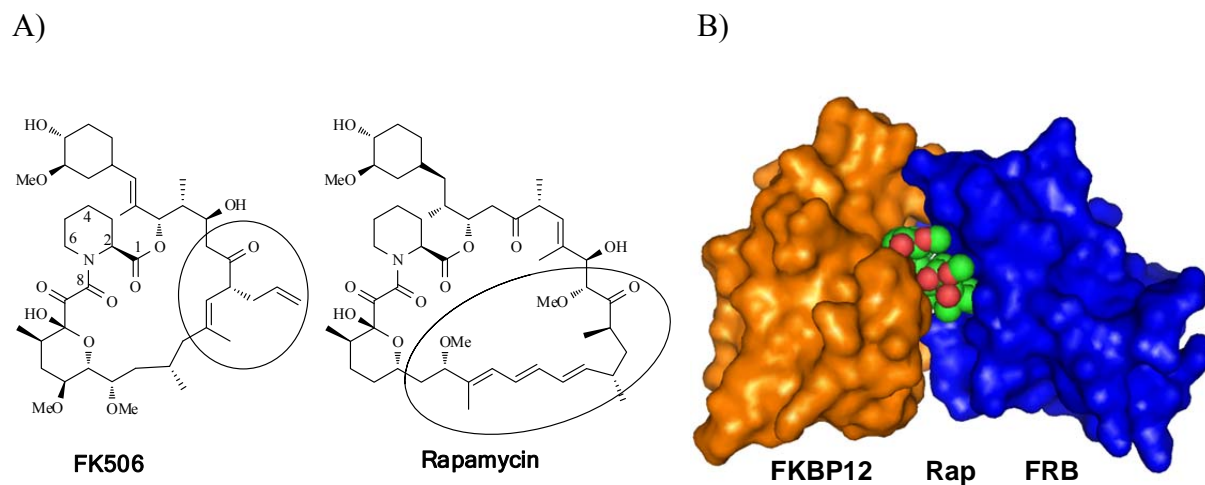


**Fig. 1:** A) Chemical structures of the prototypic immunosuppressive FKBP ligands FK506 and rapamycin. The conserved FKBP-binding part of the molecules is shadowed in gray. The effector part of the molecules that induces the inhibitory ternary complexes with calcineurin or with mTOR is circled. B) Crystal structure of the ternary complex of FKBP12-Rapamycin-FRB (FKBP/Rapamycin binding domain of mTOR; pdb code: 1FAP)

### FKBPs in disease

In addition to their immunosuppressant-enabling properties, FKBP on their own have been implicated in numerous intracellular signaling pathways. Early work focused on the role of FKBP12 in neurological disorders since FKBP12 were found to be highly expressed in the central nervous system and FKBP ligands showed neuroprotective and neuroregenerative properties. However, the relevant target of the in-vivo effects of those FK506-derived ligands could never be elucidated and it remained unclear if FKBP were involved at all.[6] In consequence, drug discovery for FKBP within the pharmaceutical industry largely stopped. Very recently, the development of more specific tools allowed to unambiguously show that inhibition of the large FKBP51 accounts, at least in part, for the neuritotropic effect of FKBP ligands *in vitro*.

Transgenic studies in mice have provided more direct evidence for the role of individual FKBP in mammalian physiology. It is clear that FKBP12 and FKBP12.6 are important in the development of skeletal and heart muscle.[7] FKBP12 knockout mice display severe developmental heart defects that seem to be mediated at least in part by a stabilization of Notch1.[8] FKBP36 deficiency results in male infertility but FKBP36<sup>-/-</sup>-mice are otherwise healthy.[9] Knockout of FKBP38 leads to lethal neurodevelopmental defects.[10] Several

## B. Research Articles – Publication I

studies have shown that deletion of FKBP51 protects mice from the negative consequences of stress exposure. FKBP52<sup>-/-</sup>-mice display defects in male sexual development and female infertility, confirming the essential role of FKBP52 in sex hormone signaling.[11]

More recently, genetic studies in humans have indicated a contribution of several FKBP5s to human diseases. Germ-line mutations in the gene encoding FKBP37 (also known as AIP, XAP2 or ARA9) are a major cause for the development of pituitary adenomas.[12] The gene encoding FKBP36 is part of a large genomic deletion that causes sporadic Williams syndrome.[13] Single nucleotide polymorphisms in FKBP5, the gene encoding FKBP51, have repeatedly been associated with numerous stress-related endophenotypes and affective disorders.[14] Recently, mutations in the ER-localized FKBP22 and FKBP65 have been associated with matrix disorders.[15,16]

FKBP5s are also present in many human pathogens, where they have been proposed to play an important role in the infection process.[17] The macrophage infectivity potentiator belongs to the FKBP family and has been pursued as an anti-infective target.[18] Inhibitors of FKBP35 from plasmodium species have been suggested as anti-malaria agents.[19] Finally, the translocation of clostridial toxins seem to require co-chaperone assistance from immunophilin proteins (Cyp18 and FKBP51), which may therefore be useful for detoxification of these pathogens.[20]

### **FKBP51 as drug target**

The data gathered for FKBP51 over the last decade have converged to a compelling case suggesting FKBP51 inhibition as a novel drug target.[21] Single nucleotide polymorphisms in the FKBP5 gene have been shown to enhance the induction of FKBP51 expression by glucocorticoid stress hormones through transcriptional and epigenetic mechanisms.[22] The same single nucleotide polymorphisms have repeatedly been associated in humans with stress-coping, fear perception, cognition, aggression and emotionality. The genetic FKBP5 variations have also been associated with the susceptibility for stress-related disorders like post-traumatic stress disorder, especially in combination with early life trauma.[14] Collectively, these results firmly established FKBP51 as risk factor for stress-related disorders.

The spatial and temporal expression pattern of FKBP51 in the brain is consistent with its role as a regulator of stress-related behavior. Notably, the expression of FKBP51 is robustly

## B. Research Articles – Publication I

induced by glucocorticoids and by various forms of stress in several regions of the brain that are important for stress-coping behaviours.[23]

Several studies have shown that FKBP51-knockout mice are protected from exaggerated stress responses. They display lower levels of the stress hormone corticosterone during the peak of the circadian glucocorticoid rhythm, reduced corticosterone secretion after acute or chronic stress, enhanced feedback regulation of the hypothalamus-pituitary-adrenal axis, enhanced cognitive flexibility and more active stress-coping behavior after stress.[24-29] Importantly, only very mild phenotypic alterations were observed in FKBP51-deficient mice beyond stress biology. In an analysis of peripheral processes controlled by the glucocorticoid receptor, blood and immune markers, glucose metabolism, and life span were found to be only marginally affected by FKBP51 deletion, suggesting that pharmacological inhibition of FKBP51 might be tolerated and devoid of target-based adverse side effects.[28]

One of the few minor phenotypes of FKBP51<sup>-/-</sup> mice under basal conditions was slightly reduced weight.[25] This might be important, however, since FKBP51<sup>-/-</sup> mice were described to be protected from excessive weight gain after a high-fat diet.[30] This is consistent with a pronounced expression of FKBP51 in adipocytes and in adipose tissue. FKBP51 expression in human omental adipose tissue correlated with reduced insulin responsiveness and single nucleotide polymorphism in the FKBP5 gene were associated with type 2 diabetes.[31] In the 3T3 cellular model, FKBP51 knockdown affected a variety of markers of adipogenesis.[32] *In vivo*, FKBP51 might also affect metabolism via central mechanism, since higher FKBP51 expression in the hypothalamus was associated with increased weight gain[33] and viral overexpression of FKBP51 in the hypothalamus promoted an obese phenotype after a high-fat diet.[34] It is therefore clear that FKBP51 plays an important role in metabolism. Metabolic disorders like obesity or diabetes might thus be an alternative indication for FKBP51 inhibitors.

An open question in FKBP51 drug development is the molecular mechanism by which FKBP51 exerts its physiological effects. While initially FKBP51 was largely viewed as an inhibitor of steroid hormone receptors, most importantly of the glucocorticoid receptor, it is now clear that FKBP51 has many other interaction partners. In addition to the established binding to Hsp90, FKBP51 was co-immunoprecipitated with transcription factors or coactivators like PPAR $\gamma$ ,[Steichschulte Mol Endo 2014], NF- $\kappa$ B,[35,36] p300[37] or Smad2/3,[38], kinases like IKK, Akt and SGK1,[39-41], phosphatases like PHLPP and calcineurin,[41,42] TRAF scaffolding proteins,[43] or the miRNA/siRNA effector Ago2.[44]

## B. Research Articles – Publication I

More recently, 90 putative interaction partners of FKBP51 were identified in a proteomic analysis.[45] For most of these interactions, it is unclear if FKBP51 binds to these proteins directly or indirectly via a third partner such as Hsp90. Mirroring its broad protein binding potential, FKBP51 has also been implicated in several other cellular pathways beyond steroid hormone signaling such as the Akt/mTOR pathway, the IKK/ NF- $\kappa$ B pathway, TGF/Smad pathway, or the Tau phosphorylation. An important open question is how FKBP51 affects these pathways at the biochemically level. It is noteworthy that biochemical assays that reconstitute the effect of FKBP51 on a relevant substrate protein in a defined system are lacking in most cases.

### **Medicinal Chemistry of FKBP inhibitors**

Early work on FKBP ligands focused on improving the properties of the natural products FK506 and rapamycin for their use in immunosuppression and related applications. This led to the development of the semisynthetic drugs pimecrolimus and everolimus. In addition, in the late 1990s many pharmaceutical companies pursued drug development programs for non-immunosuppressive FKBP ligands as potential neuroprotective or neuroregenerative agents.[3] These studies were mainly focused on FKBP12 ligands and resulted in the clinical candidates FK1706 and Biricodar. FK1706 was tested in a phase I clinical trial, where it was well tolerated.[46] Biricodar is a dual FKBP12/P-glycoprotein inhibitor that was tested as a chemosensitizer in several phase II clinical phases for several types of cancer.[47] Because of the lack of success of these clinical candidates and due to substantial controversies on the underlying mechanistic concept, by 2005 most FKBP drug discovery efforts were stopped. In recent years the field got some revival by the intriguing biological findings for FKBP38, FKBP52 and especially for FKBP51.

FKBP inhibition can be determined by a peptidyl-prolyl-isomerase inhibition assay.[48,49] However, as this assay demands laborious experimental conditions (short time window, anhydrous reagents) the development of a practical assay was an important step for the development of new inhibitors. The synthetic non-immunosuppressive FKBP12 inhibitor **1a** (Fig. 2), first described by Keenan et al.,[50] was shown to retain binding affinity to the larger FKBP51 and FKBP52.[2] Compound **1a** was coupled to a fluorescein derivative, affording **1b** (also called FL-SFL[51]), which allowed competitive fluorescence polarization assay for most FK506 binding-competent FKBP51s (FKBP12, 12.6, 13, 25, 51 and 52). This assay was used for a high throughput screening of more than 380,000 compounds for binders to the FK506-binding pocket of FKBP51. However, while FK506 and rapamycin were routinely identified in

## B. Research Articles – Publication I

an unbiased fashion, no other chemically tractable starting point could be identified for FKBP51. This suggests that FKBP51 might be rather difficult to target with the chemical scaffolds typically present in the contemporary screening libraries.

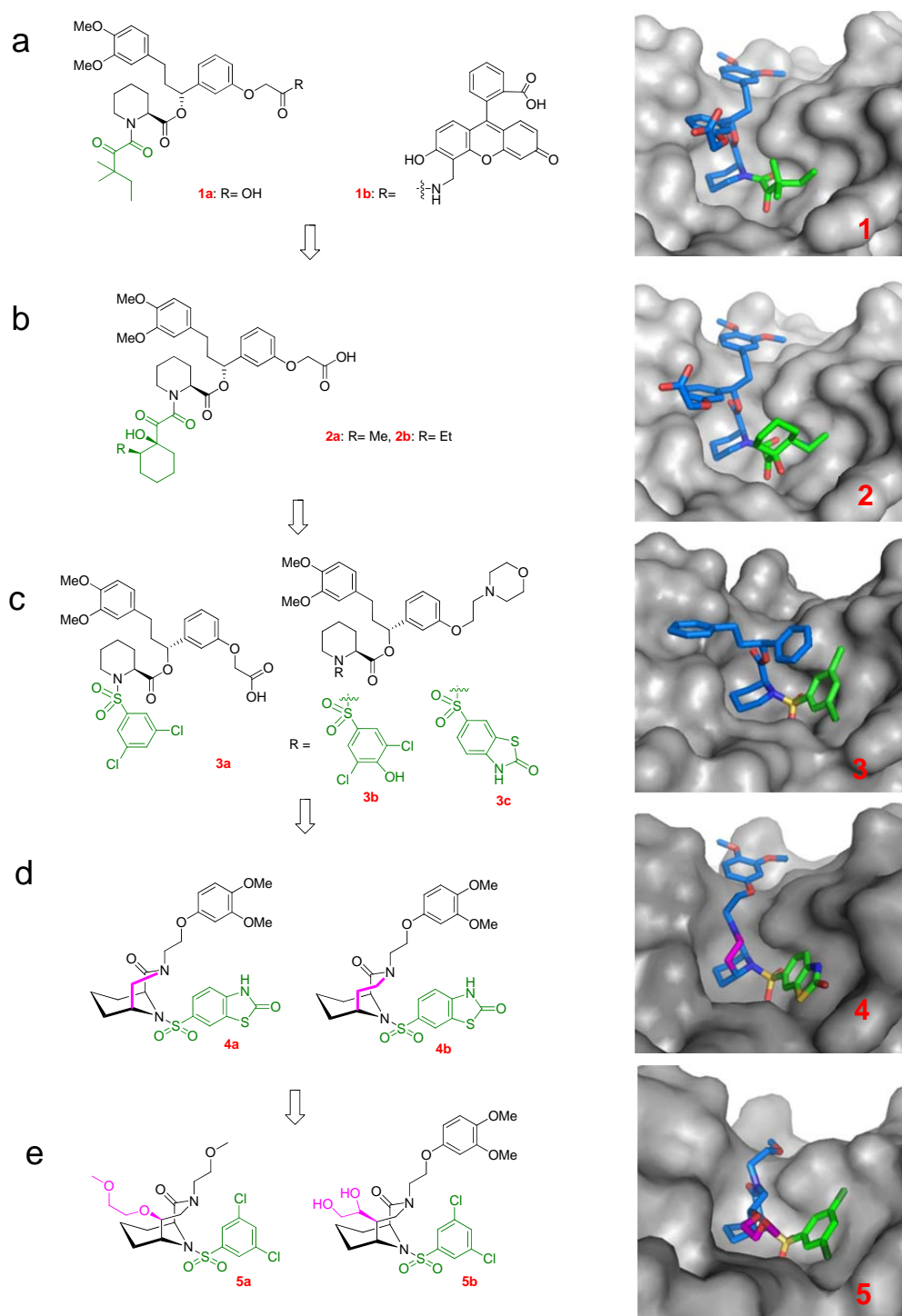


**Fig. 2:** Progressive generations of FKBP ligands developed by rational design, with chemical structures of selected examples (left side) and crystal structures of complexes with the FK506-binding domain of FKBP51.

Like for FKBP12, the most effective strategy to develop FKBP51 inhibitors turned out to be structure-based rational design. Towards this end, cocrystal structures of the FK506-binding

## B. Research Articles – Publication I

domain of FKBP51 with FK506 and **1a** were generated[52,53]. This clarified the most important protein-ligand interactions, affording a suitable starting point for a further rational ligand development. The core interactions of FK506 in the FKBP51 binding domain (Fig. 3) are conserved for **1a**: the pipercolate ring is situated over Trp90, the basement of the binding pocket. The C<sup>1</sup>-carbonyl of the pipercolate forms a hydrogen bond with Ile87 and the C<sup>8</sup>-carbonyl (for numbering of FK506 see Fig.1) of the amide forms a hydrogen bond with Tyr113. With **1a** ( $K_i^{\text{FKBP51}} = 8\mu\text{M}$ ,  $K_i^{\text{FKBP52}} = 10\mu\text{M}$ ,  $K_i^{\text{FKBP12}} = 0.17\mu\text{M}$ ) as starting point Gopalakrishnan *et al.* performed the first structure-activity-relationship analysis of small synthetic molecules for the human FKBP51 and FKBP52. This confirmed the important role of the pipercolate core of the ligands: substitution by proline or 4,5-dehydropipercolinic acid caused 4-6 fold decreased binding affinity of the ligands, while a thiomorpholine-3-carboxylic acid as core component completely abrogated the binding affinity to FKBP51 and 52. The successive attempt to substitute the  $\alpha$ -keto amide *tert*-pentyl group of **1a** with  $\alpha$ -keto amide hydroxyl-cyclohexyl moieties, which were supposed to emulate the pyranose functionality of the highly affine FK506, did not afford substantially enhanced affinities of the inhibitors (**2a**, **2b**, Fig. 2).[53]

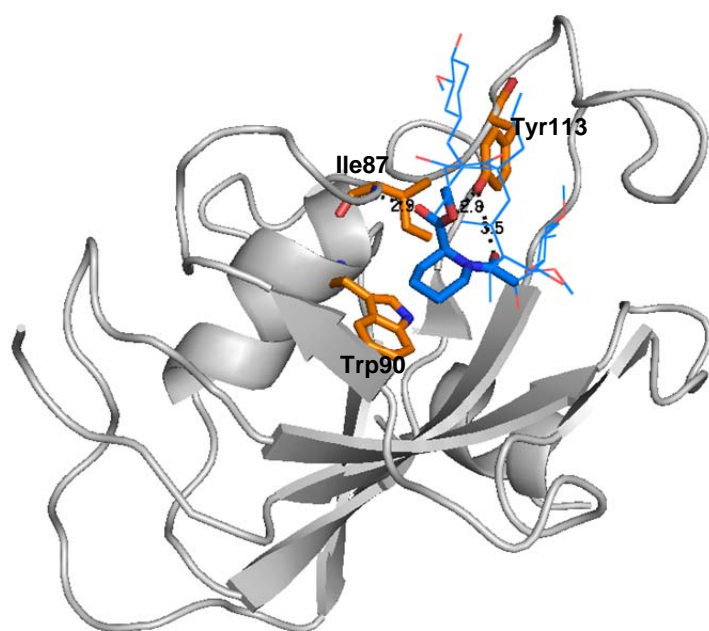


**Fig. 3** Cocrystal structure of FK506 (blue lines) in complex with the FKBP51 binding domain (grey cartoon, pdb code: 3O5R). The pipercolate core of FK506 is highlighted as blue sticks. Trp90 (orange sticks) forms the basement of the binding pocket, while Ile87 and Tyr113 (orange sticks) form hydrogen bonds with the C1- and C8-carbonyls FK506.[52]

## B. Research Articles – Publication I

In a second approach the  $\alpha$ -ketoamide-moiety was bioisosterically replaced by an aryl sulfonamide moiety. With a solid phase synthetic strategy a small focused library of > 50 ligands with the general structure 7 was prepared (Fig. 4).[54]

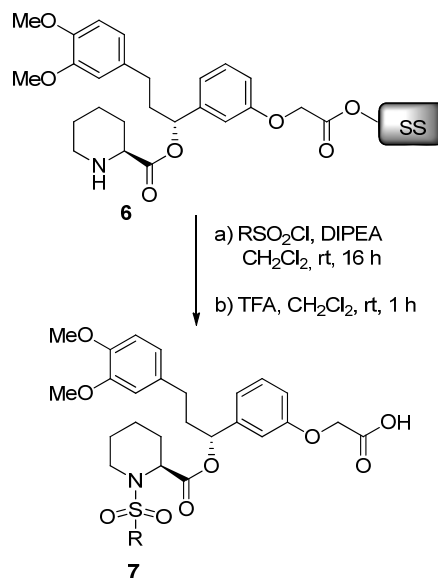


**Fig. 4:** Solid phase-assisted reaction of the immobilized building block 6 with various sulfonyl chlorides and subsequent cleavage under acidic conditions afforded a focused library of > 50 sulfonamide FKBP ligands.[54]

As revealed by the cocrystal structure of **3a**, the ortho-hydrogens of the aryl-sulfonamides engage in aromatic hydrogen bonds with Asp68 and Tyr113 of FKBP51 and therefore functionalization of the ortho position caused loss of activity in this class of compounds. The *m*-halogen substituted aromatic sulfonamides showed the most promising binding affinities to FKBP51 and FKBP52 due to the formation of a halogen bond with Ser118 (Fig. 2, 3a). When the free acid of the piperolate-ester-top group was substituted by a morpholine-containing group, the *m*-dichloro, *p*-hydroxy sulfonamide analogue (Fig. 2, 3b) showed submicromolar affinities for FKBP51, 52 and 12 (456 nM, 710 nM, 115 nM respectively).

The initial structure-activity relationship analysis showed minimal differences in affinity for FKBP51 or FKBP52, in line with the almost complete structural conservation of the active site residues between these two proteins.[52,55] There was also a general trend for higher affinities for FKBP12 (5-10 fold on average). Surprisingly, the benzothiazole-2(3H)-one sulfonamide analogue (Fig 2, 3c) showed a striking selectivity for FKBP12 over FKBP51 and FKBP52,[54] making it a useful tool compound probe to the specific role of FKBP12.[5]

It became clear that simple substitutions or modifications of piperolate-based ligands would be insufficient to provide drug-like ligands for FKBP51 or FKBP52. Due to the high

## B. Research Articles – Publication I

molecular weights ( $> 650$ ) and the moderate binding affinities the ligand efficiencies (defined as free binding energy  $\Delta G$ /Number of non-hydrogen atoms) were far away from values typically required for brain-penetrant drugs.[56] It was thus necessary to improve the core structure of the FKBP ligands. In all cocrystal structures up to that date the pipecolate core of the ligands occupied virtually superimposable positions. This suggested the idea to fix this active conformation by bridging the pipecolate scaffold from the carbonyl  $C^1$  to the  $C^6$  position either with an ethylene or with a methylene linker to form a preorganized bicyclic core scaffold (Fig. 2d, examples 4a and 4b). As predicted by modelling studies the ethylene linker afforded considerably better results, preorganizing the pipecolic core exactly in the desired active conformation (Fig. 5).[57]

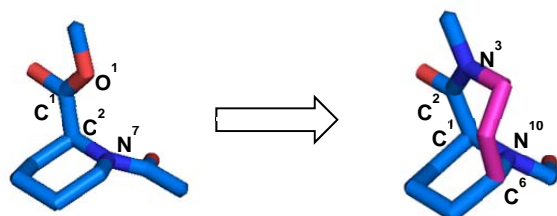


**Figure 5** The core scaffold of the monocyclic, pipecolate-based ligands (blue sticks) is converted from an ester to an amide and bridged by an ethylene linker (magenta sticks) connecting  $N^3$  and carbon  $C^6$ . The resulting aza-amido [4.3.1] bicycle rigidifies the active conformation of the pipecolate core maintaining exactly the same  $O^1-C^1-C^2-N^7 / N^3-C^2-C^1-N^{10}$  dihedral angles.

The combination of the [4.3.1]-bicycles with sulfonamide moieties afforded a robust improvement of ligand efficiency (up to  $LE = 0.29$ ). The cocrystal structures of the bicyclic sulfonamides partially explained this by revealing a very unusual hydrogen bond between the sulfonamide nitrogen ( $N^{10}$  in Fig. 5) and Tyr113. The pyramidalized geometry of this nitrogen resembles the postulated transition state of peptidyl-prolyl-peptide bond during the cis-trans isomerisation catalyzed by FKBP. The [4.3.1]-bicyclic sulfonamides may thus be very efficient FKBP ligands because they are very close transition state analogs.

The binding mode of the rigid bicyclic core scaffold suggested a further improvement of the ligands by rational design. The analysis of the cocrystal structure of bicyclic [4.3.1] aza-amide ligands with the binding domain of FKBP51 indicated that a substituent in the pro-(*S*)- $C^5$  position could fit into the binding pocket while offering the potential for further interactions with the protein (Fig. 2, 4b). For the construction of  $C^5$ -substituted bicycles with defined stereochemistry two new synthetic strategies had to be developed. In the first approach,  $C^5$ -hydroxy substituted bicycles were prepared by an intramolecular epoxide opening followed

## B. Research Articles – Publication I

by a lactamization reaction (Fig. 6a).[58] In the second approach, [4.3.1] bicycles with a C<sup>5</sup>-vinyl substituent were prepared by an intramolecular N-acyliminium cyclization (Fig. 6b).[59] Both approaches offered the possibility for further chemical variation of the new C<sup>5</sup>-functionality, furnishing ligands with binding affinities in the low nanomolar range (< 50 nM) and highly improved ligand efficiencies (up to 0.38) (Figure 2, examples 5a and 5b). Substance **5b** potently facilitated neurite outgrowth of N2a neuroblastoma cells.[59]

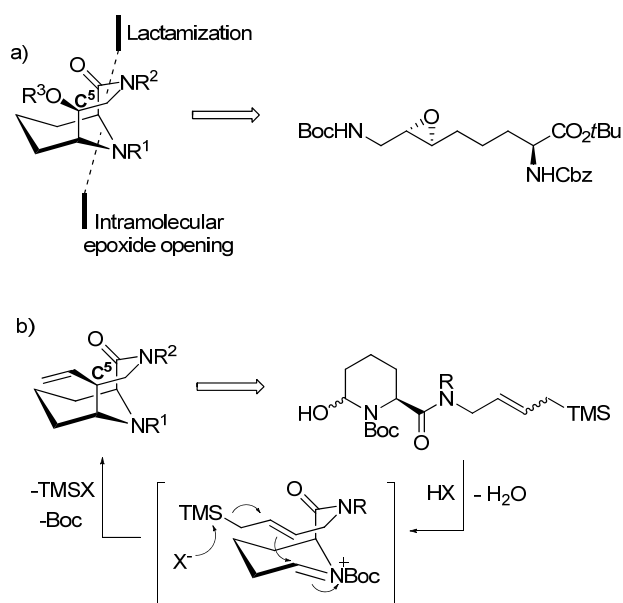


**Fig. 6** a) Retrosynthetic analysis for the synthesis of C<sup>5</sup>-hydroxy [4.3.1] bicycles: an intramolecular epoxide opening is followed by a lactamization step.[58] b) Mechanism of the intramolecular acyliminium cyclization, key step for the synthesis of C<sup>5</sup>-vinyl substituted [4.3.1] bicyclic FKBP ligands.[59]

### Development of the first FKBP51-selective ligands

Although antagonists of FKBP51 have been known for a while, selectivity within the FKBP family was regarded difficult.[60] The selectivity issue was particularly important for FKBP51 and FKBP52 since these proteins have opposite effects on glucocorticoid signaling in cells and partially also *in vivo*. However, achieving selectivity between FKBP51 and FKBP52 was also extremely challenging since their FK506-binding pockets are completely conserved. Until very recently, none of the tested FKBP ligands differentiated between FKBP51 and FKBP52.

To solve this issue in model systems, a chemical genetics approach was used by Gaali *et al.* to generate artificial selectivity.[61] The FK506-binding sites of FKBP51 and 52 were enlarged via mutation, whereby the large hydrophobic Phe<sup>67</sup> is replaced by a smaller valine, leading to a new cavity in the mutant protein. A similar method had been previously used by Clackson *et*

## B. Research Articles – Publication I

al.,[62] who introduced a F36V mutation in FKBP12 fusion proteins. The aim of such a mutation in the binding pocket is to allow designing complementary ligand that fit into the new binding pocket but clash with the wildtype protein. This way artificial selectivity for the mutant FKBP can be achieved (Fig. 7). For the FKBP51<sup>F67V</sup>/FKBP52<sup>F67V</sup> system ligand 1 was designed and synthesized, showing IC<sub>50</sub> values of 60 nM and 80 nM, respectively. The binding affinities for the wild type proteins were >30 μM. In this ligand the allyl substituent in the C<sub>α</sub>-position is responsible for the artificial selectivity towards the mutant proteins compared to the wildtype proteins.

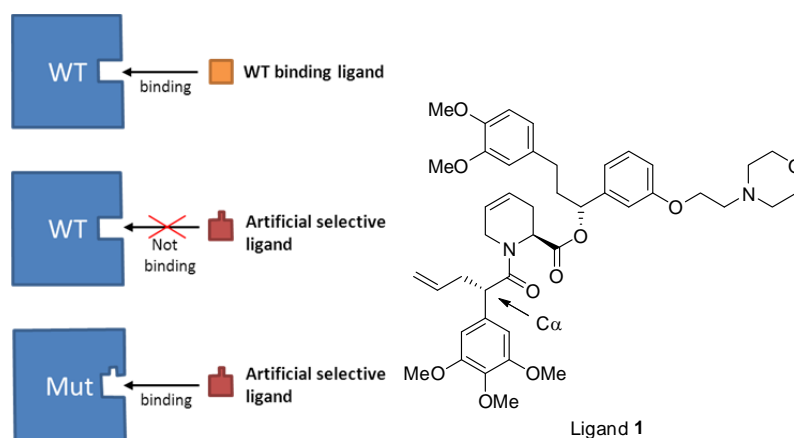


**Fig. 7:** A) Ligand mutant pair for artificial selectivity. B) The FKBP51/52<sup>F67V</sup> mutant-selective ligand 1

The FKBP51/52<sup>F67V</sup> mutant-ligand system was tested in murine N2a neuroblastoma cells, a cellular model of neuronal differentiation that is reciprocally regulated by FKBP51 and FKBP52.[63] In this system, overexpression of the point-mutated proteins recapitulated the effect of their wildtype counterparts on neurite differentiation. FKBP51<sup>WT</sup> and FKBP51<sup>F67V</sup> inhibited neurite outgrowth while FKBP52<sup>WT</sup> and FKBP52<sup>F67V</sup> enhanced it. With ligand 1 it was now possible to selectively block the effects of the mutated FKBP51 or of FKBP52, while sparing the wildtype FKBP5s. Using this system, it was possible to unambiguously show that inhibition of FKBP51 is neuritotrophic while inhibition of FKBP52 is anti-neuritotrophic.

Strikingly, inhibition of both FKBP5s at the same time showed no effect, emphasizing the necessity for selective ligands.

### Induced fit – The key to FKBP51 selectivity

The results in the N2a cell model made the need for selective FKBP51 ligands even more pressing. The turning point in the development of selective FKBP51 ligands was eventually a serendipitous discovery. During development of the artificial FKBP51/52<sup>F67V</sup> ligand series,

## B. Research Articles – Publication I

the ligand iFit1 (Fig. 8) showed weak binding affinity to FKBP51<sup>WT</sup>. This was not expected since the C<sub>α</sub> substituent was supposed to clash with the protein according to the canonical binding mode. Even more surprising was the absence of binding to FKBP52<sup>WT</sup>.

The crystal structure of the FKBP51-iFit1 complex uncovered that iFit1 induces a conformational change in the protein, whereby the C<sub>α</sub> substituent points into a newly formed cavity. In the apo-form of the protein, this cavity is occupied by the phenyl side chain of Phe67. An overlay of this crystal structure with FKBP51 co-crystal structures of unselective ligands reveals a flip of Phe67. In the new binding conformation Phe67 formed a close contact with Lys58 and Lys60 of FKBP51. Lys58 and Lys60 themselves were stabilized by Phe129. Notably, in FKBP52 these amino acids are replaced by the sterically hindered residues Thr58, Trp60, Val129, which likely make a conformational rearrangement of Phe67 energetically less favored for FKBP52. Interestingly, apart from the C<sub>α</sub> substituent the rest of iFit1 adopted a similar binding mode in the FKBP51 binding pocket as the unselective ligands described in the chapter before.

There are already many proteins known, beside FKBP51, that show ligand-induced conformational rearrangement, e.g. COX-2, the estrogen receptor or the enzyme neuraminidase. Although crystal structures of their different binding conformations exist, *a priori* theoretical predictions are difficult to make due to the highly flexible binding sites.[64] To explore the newly formed subpocket of FKBP51<sup>WT</sup> a series of ligands was synthesized that contained different substituents in the C<sub>α</sub> position, which represent the first series of FKBP51<sup>WT</sup> selective ligands (Fig. 2).

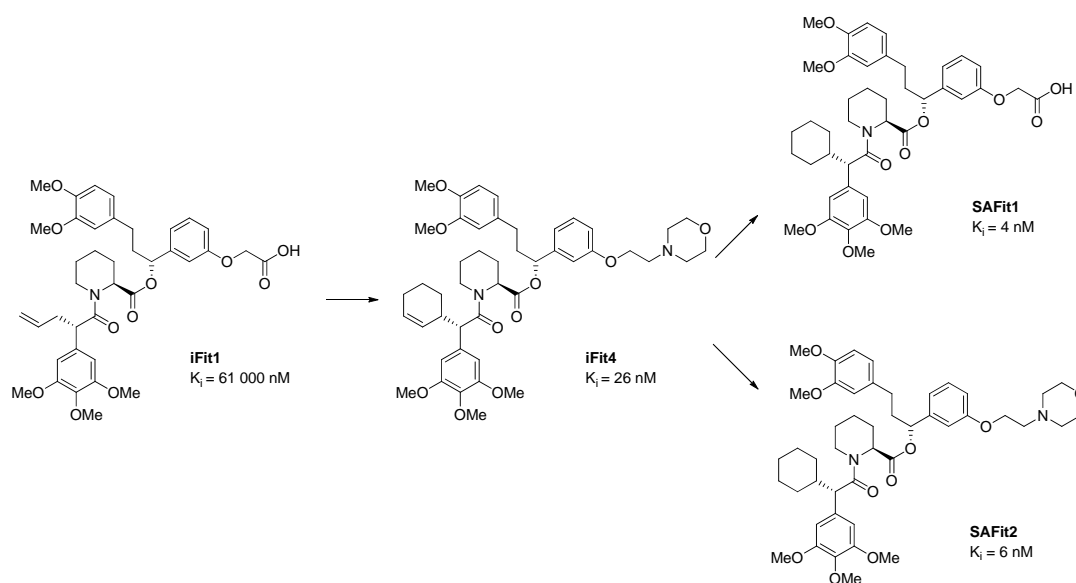


**Fig. 8:** Discovery of the iFit series of FKBP51-selective ligands and their binding affinities to FKBP51<sup>WT</sup>

## B. Research Articles – Publication I

The binding data showed that an increasing size of the C<sub>α</sub> substituent did not affect the selectivity, since still no binding to FKBP52<sup>WT</sup> could be detected. In contrast the enlarged substituents had a significant effect on the binding affinity for FKBP51. A clear correlation between size of the substituent and K<sub>i</sub> was observed, whereby increasing size of the substituent resulted in higher binding affinities. Crucial for all ligands, regarding affinity and selectivity, was the stereochemistry of the C<sub>α</sub> substituent.

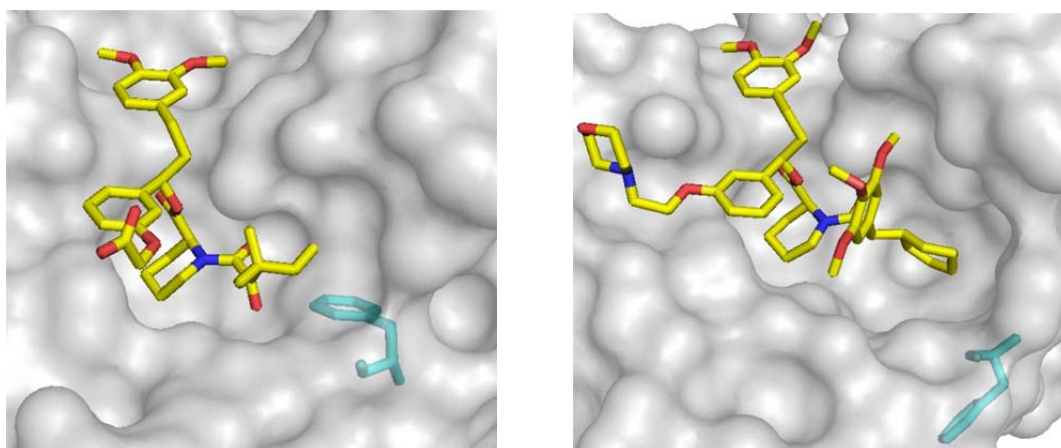


**Fig. 9:** Co-crystal structure of 1a/ FKBP51<sup>WT</sup> (left, pdb code: 4DRK) and iFit4/FKBP51<sup>WT</sup> (right, pdb code: 4TW7). The key residue F67, which is displaced by iFit ligands, is highlighted in cyan

The introduction of a six-membered ring as C<sub>α</sub> substituent led to a strong increase of binding affinity suggesting an optimal match between the substituent and the subpocket. The co-crystal structure of FKBP51-iFit4 (Fig. 9) confirmed this by revealing that the cyclohexenyl ring is sitting tightly in the new protein cavity. A reduction of the double bond of the cyclohexenyl moiety further increased the affinity for FKBP51, leading to SAFit1 and SAFit2, the best FKBP51 ligands published so far. SAFit1 and SAFit2 (selective antagonists of the FK506-binding protein 51 by induced fit) had K<sub>i</sub> values of 4 nM and 6 nM respectively. Both show > 10,000 fold selectivity over FKBP52<sup>WT</sup>. SAFit1 did not show any immunosuppressive effects, which is expected since it lacks the effector domain necessary to form ternary complexes with calcineurin or mTOR (Fig. 1). While SAFit1 was the ligand of choice for cellular assays, SAFit2 had better *in vivo* stability and improved brain permeability and was therefore chosen for animal studies. Upon sub-chronic dosing in mice, SAFit2 reduced the corticosterone levels during the peak time of the circadian rhythm of glucocorticoid secretion. A similar effect was observed in FKBP51<sup>-/-</sup> mice, supporting the idea that the effect of SAFit2 was due to FKBP51 inhibition. SAFit2 also sensitized mice to low doses of the glucocorticoid dexamethasone in a combined dexamethasone-CRF test. This test measures the suppressability of the hypothalamus-pituitary-adrenal axis, one of the major

## B. Research Articles – Publication I

endocrine stress-coping systems in mammals. Notably, a blunted regulation of the hypothalamus-pituitary-adrenal axis is a recurrent finding in subpopulation of depressive patients. Finally, SAFit2 promoted a more active stress-coping behavior in the forced swim test, the classical test to characterize clinically used antidepressants.[61]

The discovery of the iFit class of FKBP51 ligands can be considered a landmark in FKBP research. It provided extremely powerful tools to study the role FKBP51. In addition, the understanding of the underlying structural basis for selectivity offers the possible to develop more drug-like FKBP51-selective ligands by rational design. In the absence of the serendipitously discovered FKBP51-specific conformation it would have been very difficult if not impossible to achieve selectivities like the ones displayed by SAFit1 or SAFit2.

### **Open issues in FKBP51 drug development**

The *in vivo* results of SAFit2 provided the proof-of-concept that compounds directed to the FK506-binding site of FKBP51 might have beneficial therapeutic effects. However, several important questions remain to be addressed during the further development. For example, it is unknown by which molecular mechanism SAFit2-like compounds work. The binding of FKBP51 to at least some interactions partners (Akt, PHLPP or calcineurin) are not mediated by the PPIase active site and thus unaffected by FK506 analogs.[40,42] Clarifying the drug sensitivity of FKBP51-regulated signaling pathways is important to predict the efficacy profile or potential target-based side effects.

When considering depression as a potential indication, two distinguishing aspects of FKBP51, compared to other targets, are its established human genetic association and the strong mechanistic link to stress endocrinology. This offers possibilities for patient stratification. For example, patients with an early life trauma and FKBP51 high-inducing (epi)genetic variants might benefit preferentially from FKBP51 inhibitors. Likewise, patients with a hypo-sensitive feedback regulation of the hypothalamus-pituitary adrenal axis (clinically measurable by a dexamethasone suppression test) might be a preferred population for FKBP51 inhibitors. Normalization of the HPA axis regulation by FKBP51 inhibitors should be fast and this could be used as a functional biomarker.

The current FKBP51-selective ligands such as SAFit1 and SAFit2 should be regarded primarily as tool compounds for research. The molecular weight is prohibitively high and their usefulness as chemical starting points for the development of FKBP51-directed drugs remains to be seen. Like for the bicyclic pan-selective FKBP ligand series, we expect

## B. Research Articles – Publication I

innovative chemistry bolstered by structure-based rational design to be instrumental for the development of FKBP51-selective drug candidates.

### Acknowledgement:

This work was supported by the M4 Award 2011 from the Bayrisches Staatsministerium für Wirtschaft, Infrastruktur Verkehr und Technologie (to F.H.). We thank Dr. S. Gaali for support with the art work.

### References:

1. Edlich F, Weiwad M, Wildemann D, Jarczowski F, Kilka S, Moutty M-C, Jahreis G, Lucke C, Schmidt W, Striggow F, et al.: The Specific FKBP38 Inhibitor N-(N',N'-Dimethylcarboxamidomethyl)cycloheximide Has Potent Neuroprotective and Neurotrophic Properties in Brain Ischemia. *J. Biol. Chem.* 2006, 281:14961-14970.
2. Kozany C, März A, Kress C, Hausch F: Fluorescent Probes to Characterise FK506-Binding Proteins. *ChemBioChem* 2009, 10:1402-1410.
3. Gaali S, Gopalakrishnan R, Wang Y, Kozany C, Hausch F: The chemical biology of immunophilin ligands. *Curr Med Chem* 2011, 18:5355-5379.
4. Schreiber SL: Chemistry and biology of the immunophilins and their immunosuppressive ligands. *Science* 1991, 251:283-287.
5. Marz AM, Fabian A-K, Kozany C, Bracher A, Hausch F: Large FK506-Binding Proteins Shape the Pharmacology of Rapamycin. *Mol Cell Biol* 2013, 33:1357-1367.
6. Gerard M, Deleersnijder A, Demeulemeester J, Debyser Z, Baekelandt V: Unraveling the Role of Peptidyl-Prolyl Isomerases in Neurodegeneration. *Molecular Neurobiology* 2011:1-15.
7. Li BY, Chen H, Maruyama M, Zhang W, Zhang J, Pan ZW, Rubart M, Chen PS, Shou W: The role of FK506-binding proteins 12 and 12.6 in regulating cardiac function. *Pediatr Cardiol* 2012, 33:988-994.
8. Chen H, Zhang W, Sun X, Yoshimoto M, Chen Z, Zhu W, Liu J, Shen Y, Yong W, Li D, et al.: Fkbp1a controls ventricular myocardium trabeculation and compaction by regulating endocardial Notch1 activity. *Development* 2013, 140:1946-1957.
9. Crackower MA, Kolas NK, Noguchi J, Sarao R, Kikuchi K, Kaneko H, Kobayashi E, Kawai Y, Kozieradzki I, Landers R, et al.: Essential role of Fkbp6 in male fertility and homologous chromosome pairing in meiosis. *Science* 2003, 300:1291-1295.
10. Shirane M, Ogawa M, Motoyama J, Nakayama KI: Regulation of apoptosis and neurite extension by FKBP38 is required for neural tube formation in the mouse. *Genes Cells* 2008, 13:635-651.
11. Sivils JC, Storer CL, Galigniana MD, Cox MB: Regulation of steroid hormone receptor function by the 52-kDa FK506-binding protein (FKBP52). *Current Opinion in Pharmacology* 2011, 11:314-319.
12. Lloyd C, Grossman A: The AIP (aryl hydrocarbon receptor-interacting protein) gene and its relation to the pathogenesis of pituitary adenomas. *Endocrine* 2014, 46:387-396.
13. Meng X, Lu X, Morris CA, Keating MT: A novel human gene FKBP6 is deleted in Williams syndrome. *Genomics* 1998, 52:130-137.
14. Zannas AS, Binder EB: Gene–environment interactions at the FKBP5 locus: sensitive periods, mechanisms and pleiotropism. *Genes, Brain and Behavior* 2014, 13:25-37.

## B. Research Articles – Publication I

15. Baumann M, Giunta C, Krabichler B, Ruschendorf F, Zoppi N, Colombi M, Bittner RE, Quijano-Roy S, Muntoni F, Cirak S, et al.: Mutations in FKBP14 cause a variant of Ehlers-Danlos syndrome with progressive kyphoscoliosis, myopathy, and hearing loss. *Am J Hum Genet* 2012, 90:201-216.
16. Steinlein OK, Aichinger E, Trucks H, Sander T: Mutations in FKBP10 can cause a severe form of isolated Osteogenesis imperfecta. *BMC Med Genet* 2011, 12:152.
17. Unala CM, Steinert M: Microbial peptidyl-prolyl cis/trans isomerases (PPIases): virulence factors and potential alternative drug targets. *Microbiol Mol Biol Rev* 2014, 78:544-571.
18. Juli C, Sippel M, Jäger J, Thiele A, Weiwad M, Schweimer K, Roisch P, Steinert M, Sottriffer CA, Holzgrabe U: Pipecolic Acid Derivatives As Small-Molecule Inhibitors of the Legionella MIP Protein. *Journal of Medicinal Chemistry* 2011, 54:277-283.
19. Harikishore A, Niang M, Rajan S, Preiser PR, Yoon HS: Small molecule Plasmodium FKBP35 inhibitor as a potential antimalaria agent. *Sci. Rep.* 2013, 3.
20. Kaiser E, Bohm N, Ernst K, Langer S, Schwan C, Aktories K, Popoff M, Fischer G, Barth H: FK506-binding protein 51 interacts with Clostridium botulinum C2 toxin and FK506 inhibits membrane translocation of the toxin in mammalian cells. *Cell Microbiol* 2012, 14:1193-1205.
21. Schmidt MV, Paez-Pereda M, Holsboer F, Hausch F: The Prospect of FKBP51 as a Drug Target. *ChemMedChem* 2012, 7:1351-1359.
22. Klengel T, Mehta D, Anacker C, Rex-Haffner M, Pruessner JC, Pariante CM, Pace TWW, Mercer KB, Mayberg HS, Bradley B, et al.: Allele-specific FKBP5 DNA demethylation mediates gene-childhood trauma interactions. *Nat Neurosci* 2013, 16:33-41.
23. Scharf SH, Liebl C, Binder EB, Schmidt MV, Müller MB: Expression and Regulation of the FKBP5 Gene in the Adult Mouse Brain. *PLoS ONE* 2011, 6:e16883.
24. Albu S, Romanowski C, Curzi M, Jakubcakova V, Flachskamm C, Gassen N, Hartmann J, Schmidt M, Schmidt U, Rein T, et al.: Deficiency of FK506-binding protein (FKBP) 51 alters sleep architecture and recovery sleep responses to stress in mice. *J Sleep Res* 2014, 23:176-185.
25. Hartmann J, Wagner KV, Liebl C, Scharf SH, Wang X-D, Wolf M, Hausch F, Rein T, Schmidt U, Touma C, et al.: The involvement of FK506-binding protein 51 (FKBP5) in the behavioral and neuroendocrine effects of chronic social defeat stress. *Neuropharmacology* 2012, 62:332-339.
26. Hoeijmakers L, Harbich D, Schmid B, Lucassen PJ, Wagner KV, Schmidt MV, Hartmann J: Depletion of FKBP51 in female mice shapes HPA axis activity. *PLoS One* 2014, 9:e95796.
27. O'Leary JC, 3rd, Dharia S, Blair LJ, Brady S, Johnson AG, Peters M, Cheung-Flynn J, Cox MB, de Erausquin G, Weeber EJ, et al.: A new anti-depressive strategy for the elderly: ablation of FKBP5/FKBP51. *PLoS One* 2011, 6:e24840.
28. Sabbagh JJ, O'Leary JC, 3rd, Blair LJ, Klengel T, Nordhues BA, Fontaine SN, Binder EB, Dickey CA: Age-Associated Epigenetic Upregulation of the FKBP5 Gene Selectively Impairs Stress Resiliency. *PLoS One* 2014, 9:e107241.
29. Touma C, Gassen NC, Herrmann L, Cheung-Flynn J, Bull DR, Ionescu IA, Heinzmann JM, Knapman A, Siebertz A, Depping AM, et al.: FK506 binding protein 5 shapes stress responsiveness: modulation of neuroendocrine reactivity and coping behavior. *Biol Psychiatry* 2011, 70:928-936.
30. Warriar M: Role of Fkbp51 and Fkbp52 in Glucocorticoid Receptor Regulated Metabolism. *Thesis, University of Toledo* 2008.
31. Pereira MJ, Palming J, Svensson MK, Rizell M, Dalenbäck J, Hammar Mr, Fall T, Sidibeh CO, Svensson P-A, Eriksson JW: FKBP5 expression in human adipose tissue increases following dexamethasone exposure and is associated with insulin resistance. *Metabolism* 2014:DOI: 10.1016/j.metabol.2014.1005.1015.

## B. Research Articles – Publication I

32. Stechschulte LA, Hinds TD, Khuder SS, Shou W, Najjar SM, Sanchez ER: FKBP51 Controls Cellular Adipogenesis through p38 Kinase-Mediated Phosphorylation of GR $\alpha$  and PPAR $\gamma$ . *Molecular Endocrinology* 2014, 28:1265-1275.
33. Balsevich G, Uribe A, Wagner KV, Hartmann J, Santarelli S, Labermaier C, Schmidt MV: Interplay between diet-induced obesity and chronic stress in mice: potential role of FKBP51. *J Endocrinol* 2014, 222:15-26.
34. Yang L, Isoda F, Yen K, Kleopoulos SP, Janssen W, Fan X, Mastaitis J, Dunn-Meynell A, Levin B, McCrimmon R, et al.: Hypothalamic Fkbp51 is induced by fasting, and elevated hypothalamic expression promotes obese phenotypes. *Am J Physiol Endocrinol Metab* 2012, 302:E987-991.
35. Romano S, Mallardo M, Romano MF: FKBP51 and the NF- $\kappa$ B regulatory pathway in cancer. *Current Opinion in Pharmacology* 2011, In Press, Corrected Proof.
36. Erlejman AG, De Leo SA, Mazaira GI, Molinari AM, Camisay MF, Fontana V, Cox MB, Piwien-Pilipuk G, Galigniana MD: NF- $\kappa$ B Transcriptional Activity Is Modulated by FK506-binding Proteins FKBP51 and FKBP52: A ROLE FOR PEPTIDYL-PROLYL ISOMERASE ACTIVITY. *J Biol Chem* 2014, 289:26263-26276.
37. Romano S, Staibano S, Greco A, Brunetti A, Nappo G, Iardi G, Martinelli R, Sorrentino A, Di Pace A, Mascolo M, et al.: FK506 binding protein 51 positively regulates melanoma stemness and metastatic potential. *Cell Death Dis* 2013, 4:e578.
38. Romano S, D'Angelillo A, D'Arrigo P, Staibano S, Greco A, Brunetti A, Scalvenzi M, Bisogni R, Scala I, Romano MF: FKBP51 increases the tumour-promoter potential of TGF- $\beta$ . *Clin Transl Med* 2014, 3:1.
39. Bouwmeester T, Bauch A, Ruffner H, Angrand P-O, Bergamini G, Croughton K, Cruciat C, Eberhard D, Gagneur J, Ghidelli S, et al.: A physical and functional map of the human TNF- $\alpha$ /NF- $\kappa$ B signal transduction pathway. *Nat Cell Biol* 2004, 6:97 - 105.
40. Fabian A-K, März A, Neimanis S, Biondi RM, Kozany C, Hausch F: InterAKTions with FKBP51 - Mutational and Pharmacological Exploration. *PLoS ONE* 2013, 8:e57508.
41. Pei H, Li L, Fridley BL, Jenkins GD, Kalari KR, Lingle W, Petersen G, Lou Z, Wang L: FKBP51 Affects Cancer Cell Response to Chemotherapy by Negatively Regulating Akt. *Cancer Cell* 2009, 16:259-266.
42. Li TK, Baksh S, Cristillo AD, Bierer BE: Calcium- and FK506-independent interaction between the immunophilin FKBP51 and calcineurin. *J Cell Biochem* 2002, 84:460-471.
43. Akiyama T, Shiraishi T, Qin J, Konno H, Akiyama N, Shinzawa M, Miyauchi M, Takizawa N, Yanai H, Ohashi H, et al.: Mitochondria-Nucleus Shuttling FK506-Binding Protein 51 Interacts with TRAF Proteins and Facilitates the RIG-I-Like Receptor-Mediated Expression of Type I IFN. *PLoS One* 2014, 9:e95992.
44. Martinez NJ, Chang HM, Borrajo JD, Gregory RI: The co-chaperones Fkbp4/5 control Argonaute2 expression and facilitate RISC assembly. *RNA* 2013, 19.
45. Taipale M, Tucker G, Peng J, Krykbaeva I, Lin Z-Y, Larsen B, Choi H, Berger B, Gingras A-C, Lindquist S: A Quantitative Chaperone Interaction Network Reveals the Architecture of Cellular Protein Homeostasis Pathways. *Cell* 2014, 158:434-448.
46. Minematsu T, Lee J, Zha J, Moy S, Kowalski D, Hori K, Ishibashi K, Usui T, Kamimura H: Time-dependent inhibitory effects of (1R,9S,12S,13R,14S,17R,18E,21S,23S,24R,25S,27R)-1,14-dihydroxy-12-(E)-2-[(1R,3R,4R)-4-hydroxy-3-methoxycyclohexyl]-1-methylvinyl-23,25-dimethoxy-13, 19,21,27-tetramethyl-17-(2-oxopropyl)-11,28-dioxo-4-azatricyclo[2.2.3.1.0(4,9)]octacos-18-ene-2,3,10,16-tetrone (FK1706), a novel nonimmunosuppressive immunophilin ligand, on CYP3A4/5 activity in humans *in vivo* and *in vitro*. *Drug Metab Dispos* 2010, 38:249-259.
47. Dey S: Biricodar. Vertex Pharmaceuticals. *Curr Opin Investig Drugs* 2002, 3:818-823.
48. Fischer G, Bang H, Mech C: Determination of enzymatic catalysis for the cis-trans-isomerization of peptide binding in proline-containing peptides. *Biomed Biochim Acta* 1984, 43:1101-1111.

## B. Research Articles – Publication I

49. Kofron JL, Kuzmic P, Kishore V, Colon-Bonilla E, Rich DH: Determination of kinetic constants for peptidyl prolyl cis-trans isomerases by an improved spectrophotometric assay. *Biochemistry* 1991, 30:6127-6134.
50. Keenan T, Yaeger DR, Courage NL, Rollins CT, Pavone ME, Rivera VM, Yang W, Guo T, Amara JF, Clackson T, et al.: Synthesis and activity of bivalent FKBP12 ligands for the regulated dimerization of proteins. *Bioorg Med Chem* 1998, 6:1309-1335.
51. Banaszynski LA, Liu CW, Wandless TJ: Characterization of the FKBP-rapamycin-FRB ternary complex. *J Am Chem Soc* 2005, 127:4715-4721.
52. Bracher A, Kozany C, Thost AK, Hausch F: Structural characterization of the PPIase domain of FKBP51, a cochaperone of human Hsp90. *Acta Crystallogr D Biol Crystallogr* 2011, 67:549-559.
53. Gopalakrishnan R, Kozany C, Gaali S, Kress C, Hoogeland B, Bracher A, Hausch F: Evaluation of Synthetic FK506 Analogues as Ligands for the FK506-Binding Proteins 51 and 52. *J Med Chem* 2012, 55:4114-4122.
54. Gopalakrishnan R, Kozany C, Wang Y, Schneider S, Hoogeland B, Bracher A, Hausch F: Exploration of Pipecolate Sulfonamides as Binders of the FK506-Binding Proteins 51 and 52. *J Med Chem* 2012, 55:4123-4131.
55. Bracher A, Kozany C, Hähle A, Wild P, Zacharias M, Hausch F: Crystal Structures of the Free and Ligand-Bound FK1-FK2 Domain Segment of FKBP52 Reveal a Flexible Inter-Domain Hinge. *J Mol Biol* 2013, 425:4134-4144.
56. Wager TT, Chandrasekaran RY, Hou X, Troutman MD, Verhoest PR, Villalobos A, Will Y: Defining desirable central nervous system drug space through the alignment of molecular properties, *in vitro* ADME, and safety attributes. *ACS Chem Neurosci* 2010, 1:420-434.
57. Wang Y, Kirschner A, Fabian AK, Gopalakrishnan R, Kress C, Hoogeland B, Koch U, Kozany C, Bracher A, Hausch F: Increasing the Efficiency of Ligands for FK506-Binding Protein 51 by Conformational Control. *J Med Chem* 2013, 56:3922-3935.
58. Bischoff M, Sippel C, Bracher A, Hausch F: Stereoselective Construction of the 5-Hydroxy Diazabicyclo[4.3.1]decane-2-one Scaffold, a Privileged Motif for FK506-Binding Proteins. *Organic Letters* 2014, 16:5254-5257.
59. Pomplun S, Wang Y, Kirschner A, Kozany C, Bracher A, Hausch F: Rational design and asymmetric synthesis of potent and neurotrophic FKBP ligands. *Angew Chem Int Ed* 2014:DOI: 10.1002/ange.201408776R201408771.
60. Blackburn EA, Walkinshaw MD: Targeting FKBP isoforms with small-molecule ligands. *Current Opinion in Pharmacology* 2011, 11:365-371.
61. Gaali S, Kirschner A, Cuboni S, Hartmann J, Kozany C, Balsevich G, Namendorf C, Fernandez-Vizarra P, Sippel C, Zannas AS, et al.: Selective inhibitors for the psychiatric risk factor FKBP51 enabled by an induced-fit mechanism. *Nat Chem Biol* 2014:in press.
62. Clackson T, Yang W, Rozamus LW, Hatada M, Amara JF, Rollins CT, Stevenson LF, Magari SR, Wood SA, Courage NL, et al.: Redesigning an FKBP-ligand interface to generate chemical dimerizers with novel specificity. *PNAS* 1998, 95:10437-10442.
63. Quintá HR, Maschi D, Gomez-Sanchez C, Piwien-Pilipuk G, Galigniana MD: Subcellular rearrangement of hsp90-binding immunophilins accompanies neuronal differentiation and neurite outgrowth. *J Neurochem* 2010, 115:716-734.
64. Sherman W, Day T, Jacobson MP, Friesner RA, Farid R: Novel procedure for modeling ligand/receptor induced fit effects. *J Med Chem* 2006, 49:534-553.

## B. Research Articles – Publication/Manuscript II

### 6. Publication/Manuscript II-IV: Pharmacological effects of SAFit1 and SAFit2

SAFit1 and SAFit2 currently represent the most advanced selective FKBP51 ligands. With these compounds, for the first time, pharmacological selective FKBP51 inhibition is possible. In preliminary *in vitro* and *in vivo* studies both ligands have already proven their usefulness as research tools. In order to further verify FKBP51 as drug target in FKBP51-related disease and to show that pharmacological FKBP51 inhibition could be a possible treatment, an optimization and scale up of the chemical synthesis of SAFit1 and SAFit2 was conducted. Both compounds were then synthesized in gram scales and used in collaborative FKBP51 research projects, which are described in the following chapter.

#### 6.1. Publication II

##### **FKBP51 employs both scaffold and isomerase functions to promote NFκB activation in melanoma**

(Simona Romano, Yichuan Xiao, Mako Nakaya, Anna D'Angelillo, Mikyoung Chang, Jin Jin, Felix Hausch, Mariorosario Masullo, **Xixi Feng**, Maria Fiammetta Romano, Shao-Cong Sun, *Nucleic Acids Research* **2015**, Vol. 43, No. 14, 6983-6993, doi: 10.1093/nar/gkv615)

##### **Summary**

FKBP51 is linked to the severity of skin cancer due to its role in NFκB activation, which influences tumor progression, metastasis and apoptosis resistance. The presented study aimed to explain the underlying molecular mechanisms.

It was shown that FKBP51, as a scaffold, enhances IKK activity upon binding to the subunits and assisting the assembly of the kinase complex that activates NFκB. Hereby different FKBP51 domains interact with the different subunits. Both SAFit compounds, as well as FKBP51 knock out, reduced IKK activation, whereby the contact between both proteins was not abolished (indicating the importance of the PPIase activity for the effect). Additionally an interaction between FKBP51 and TRAF2 was observed which is supposed to facilitate IKK activation. Disturbing NFκB activation by FKBP51 inhibition could hence be a starting point for novel melanoma therapies.

## ORIGINAL PUBLICATION

Published online 22 June 2015

Nucleic Acids Research, 2015, Vol. 43, No. 14 6983–6993  
doi: 10.1093/nar/gkv615**FKBP51 employs both scaffold and isomerase functions to promote NF- $\kappa$ B activation in melanoma**Simona Romano<sup>1,2</sup>, Yichuan Xiao<sup>2,3</sup>, Mako Nakaya<sup>2</sup>, Anna D'Angelillo<sup>1</sup>, Mikyoung Chang<sup>2</sup>, Jin Jin<sup>2</sup>, Felix Hausch<sup>4</sup>, Mariorosario Masullo<sup>1,5</sup>, Xixi Feng<sup>4</sup>, Maria Fiammetta Romano<sup>1,\*</sup> and Shao-Cong Sun<sup>2</sup><sup>1</sup>Department of Molecular Medicine and Medical Biotechnologies, Federico II University, Naples 80131, Italy,<sup>2</sup>Department of Immunology, The University of Texas MD Anderson Cancer Center, Houston, TX 77030, USA,<sup>3</sup>Institute of Health Sciences, Shanghai Institutes for Biological Sciences, Chinese Academy of Sciences/Shanghai Jiao Tong University School of Medicine, Shanghai 200031, China, <sup>4</sup>Department Translational Research in Psychiatry, Max Planck Institute of Psychiatry, München 80804, Germany and <sup>5</sup>Department of Movement Sciences and Wellness, University of Naples 'Parthenope', Naples 80133, Italy

Received October 03, 2014; Revised May 13, 2015; Accepted June 02, 2015

**ABSTRACT**

Melanoma is the most aggressive skin cancer; its prognosis, particularly in advanced stages, is disappointing largely due to the resistance to conventional anticancer treatments and high metastatic potential. NF- $\kappa$ B constitutive activation is a major factor for the apoptosis resistance of melanoma. Several studies suggest a role for the immunophilin FKBP51 in NF- $\kappa$ B activation, but the underlying mechanism is still unknown. In the present study, we demonstrate that FKBP51 physically interacts with IKK subunits, and facilitates IKK complex assembly. FKBP51 knockdown inhibits the binding of IKK $\gamma$  to the IKK catalytic subunits, IKK $\alpha$  and  $\beta$ , and attenuates the IKK catalytic activity. Using FK506, an inhibitor of the FKBP51 isomerase activity, we found that the IKK-regulatory role of FKBP51 involves both its scaffold function and its isomerase activity. Moreover, FKBP51 also interacts with TRAF2, an upstream mediator of IKK activation. Interestingly, both FKBP51 TPR and PPIase domains are required for its interaction with TRAF2 and IKK $\gamma$ , whereas only the TPR domain is involved in interactions with IKK $\alpha$  and  $\beta$ . Collectively, these results suggest that FKBP51 promotes NF- $\kappa$ B activation by serving as an IKK scaffold as well as an isomerase. Our findings have profound implications for designing novel melanoma therapies based on modulation of FKBP51.

**INTRODUCTION**

FK506 binding proteins (FKBPs) are multifunctional proteins highly conserved across the species and abundantly expressed in the cell. FKBPs belong to the family of immunophilins, which includes also cyclophilins (Cyp) (1). The term immunophilin derives from the immunosuppressant action of the complexes formed between these proteins and the natural products cyclosporine A, FK506 and rapamycin (1). In addition to a well-established role in immunosuppression, immunophilins modulate several signal transduction pathways in the cell, due to their isomerase activity and the capability to interact with other proteins, inducing changes in conformation and function of partner proteins (2,3). Many immunophilins have a peptidyl-prolyl *cis*-*trans* isomerase activity (PPIase), which is inhibited by drug ligand binding (1). FKBP51, encoded by the *FKBP5* gene, has a C-terminal tetratricopeptide repeat (TPR) domain, known to be involved in interaction with Hsp90 as well as other proteins (4,5). This structural feature suggests that FKBP51 may share some functions with heat shock proteins (6). The N-terminal region of FKBP51 contains two FKBP-like domains (FK1 and FK2). Only the FK1 domain is capable of PPIase activity and immunosuppressant drug binding, while the FK2 domain seems to have a structural role (5,6).

FKBP51 is highly expressed in melanoma (7,8) and plays an important role in tumor progression and metastasis (9,10). Several lines of evidence support an essential role for FKBP51 in the control of NF- $\kappa$ B activation (7,8,11–14). An interaction of FKBP51 with IKK $\alpha$  was firstly identified in a study mapping the protein interaction network of the TNF $\alpha$ /NF- $\kappa$ B pathway (13). In addition, tandem affinity purification-tagged FKBP51 resulted in the identification of several other kinases, indicating that FKBP51

\*To whom correspondence should be addressed. Tel: +39 0817463125; Fax: +39 0817463205; Email: mariafiammetta.romano@unina.it

might be a prominent multifunctional kinase cofactor (15). RNA interference for FKBP51 confirmed an essential role for this immunophilin in the overall signaling process of NF- $\kappa$ B activation (13). Other studies identified FKBP51 as an essential factor for chemotherapy induced NF- $\kappa$ B activation in melanoma and leukemia (7,11). Rapamycin, indeed, counteracted NF- $\kappa$ B activation induced by doxorubicin and decreased the nuclear translocation of NF- $\kappa$ B by inhibiting the ability of IKK kinase complex to phosphorylate I $\kappa$ B. The effect of rapamycin was reproduced by FKBP51 depletion (7), while the over expression of p65/RelA counteracted the action of the macrocyclic agent (10). This immunophilin was also found essential in the activation of NF- $\kappa$ B by ionizing radiation. Irradiated FKBP51-silenced melanoma cells showed reduced clonogenic potential due to impaired capability to activate NF- $\kappa$ B. Evidence of FKBP51 involvement in radioresistance was also provided by studies with a melanoma xenograft mouse model (8). In addition to melanoma and leukemia, the relevant roles of FKBP51 in NF- $\kappa$ B activation, chemoresistance, and tumor growth have also been demonstrated in glioma (14). In ovarian cancer, FKBP51 was recently identified as critical factor of chemoresistance (16).

Despite the numerous studies in support of a role for FKBP51 in promoting NF- $\kappa$ B activation, and IKK complex function (7,8,11–14), molecular mechanisms underlying the interplay between this large immunophilin and  $\kappa$ B signal transduction proteins are still unknown. The present study supports the conclusion that, both enzymatic and scaffold functions of FKBP51, are essential for IKK complex assembly and activation. In addition, we show that FKBP51 is essential for IKK $\gamma$  recruitment to TRAF2, an adaptor protein central in the IKK kinase activation cascade, that links IKK to TAK1.

## MATERIALS AND METHODS

### Cell cultures, plasmids, antibodies and reagents

The melanoma cell lines SAN and A375 were cultured as described (8). The pcDNA expression vectors encoding hemagglutinin (HA)-tagged human IKK $\alpha$ , IKK $\beta$ , IKK $\gamma$ , TAK1 and TRAF2 have been described previously (17–20); the pCMV Myc-DDK-tagged human FKBP51-transcript variant 1 (canonical FKBP51 [Myc-Flag-FKBP51]) and FKBP51-transcript variant 4 (short FKBP51 lacking of TPR domains [Myc-Flag-FKBP51s]) were from OriGene Technologies (MD, USA); samples of plasmids encoding pRK5 Flag-tagged FKBP51 or mutants (pRK5 empty vector [EV]; pRK5 FKBP51 WT [Flag-FKBP51]; pRK5 FKBP51-TPR-mut [Flag-FKBP51-mutTPR; K352A/R356A]; pRK5 FKBP51-PPIase-mut [Flag-FKBP51-mutPPIase; FD67DV]) were kindly provided by Theo Rein (Max Planck Institute of Psychiatry, Munich, Germany) (21). Antibodies to human Bax (B-9, mouse monoclonal), anti-IKK $\gamma$  (FL419, rabbit polyclonal), anti-IKK $\alpha/\beta$  (H-470, rabbit polyclonal), anti-IKK $\beta$  (H4, mouse monoclonal), anti-I $\kappa$ B $\alpha$  (C-21, rabbit polyclonal), anti-lamin B (C-20, goat polyclonal), anti-TRAF2 (C-20, rabbit polyclonal), Hsp60 (H300, rabbit polyclonal), anti-Tak1 (M-579, rabbit polyclonal)

were from Santa Cruz Biotechnology (CA, USA). Anti-FKBP51 was from Novus biological (CO, USA). Anti- $\beta$  Actin (C-4, mouse monoclonal), anti- $\gamma$ -Tubulin (GTU-88, mouse monoclonal), horseradish peroxidase-conjugated anti-hemagglutinin (HA-7) and anti-Flag (M2) were from Sigma Aldrich (MO, USA). Fluorescence-labeled antibody reagents are described below (see 'Flow cytometry' section). Human recombinant tumor necrosis factor  $\alpha$  (TNF $\alpha$ ), doxorubicin hydrochloride, etoposide, cyclosporin A and tacrolimus (FK506) were from Sigma-Aldrich.

### Knockdown of FKBP51 in melanoma cells

For the production of lentiviral particles, the lentiviral vector pGIPZ, either empty (pGIPZ) or encoding three different FKBP51-specific short hairpin RNA (pGIPZ-shFKBP51), was transfected into human embryonic kidney (HEK293) cells (by the calcium method) along with the packaging vectors pSPAX2 and pMD2 (provided by X. Qin). Melanoma A375 and SAN cells were infected with lentivirus carrying either pGIPZ or pGIPZ-shFKBP51. After 24 h after the infection, cells were selected with 200 ng/ml puromycin (Sigma-Aldrich) and after further 48 h, cultures were enriched for infected cells by cell sorting by flow cytometry (based on GFP expression). Sequences of the three different pGIPZ-shFKBP51 are reported:

- shFKBP51.1.Mature Antisense: TTGTCTCCAATCAT CGGCC
- shFKBP51.2.Mature Antisense: TATATAAGCTCA GCATTAG
- shFKBP51.3.Mature Antisense: TTCCAATTGGAA TGTCGTG

### Coimmunoprecipitation, immunoblot, electrophoretic mobility-shift and kinase assays

Melanoma A375 and SAN cell lines were stimulated with 20 ng/ml TNF $\alpha$ . Total and subcellular extracts were prepared from the cells and subjected to coimmunoprecipitation (co-IP), immunoblot (IB) and electrophoretic mobility-shift assay (EMSA) as described (8,20). For co-IP, cell were lysed in RIPA buffer (50 mM Tris-HCl, pH7.4; 150 mM NaCl; 1% NP-40; 0.5% Na-deoxycholate; 1 mM ethylenediaminetetraacetic acid (EDTA); 1 mM phenylmethanesulfonyl fluoride (PMSF); 1 mM dithiothreitol (DTT); protease inhibitor cocktail). PMSF and protease inhibitor cocktail were not added to the wash buffer. Antibodies used for co-IP: anti-FKBP51 antibodies were from Novus Biologicals (rabbit polyclonal, NB100-68240) and from Abnova (mouse polyclonal H00002289-B01P, Taipei, Taiwan); anti-IKK $\alpha$  antibodies were from Santa Cruz (rabbit polyclonal anti-IKK $\alpha$ , H-744; rabbit polyclonal anti-IKK $\alpha/\beta$ , H-470).

For protein-phosphorylation analysis and kinase assays (KA), cells were lysed in a kinase cell lysis buffer supplemented with phosphatase inhibitors. IKK was isolated by immunoprecipitation with anti-IKK $\gamma$  (FL-419; Santa Cruz. Biotech). A moderate effect of FK506 on IKK activation was also detected in the FKBP51-knockdown cells, probably due to the incomplete depletion of FKBP51 in these

cells chnology) and subjected to KA with a glutathione S-transferase fusion protein containing the amino-terminal 54 amino acids of I $\kappa$ B $\alpha$  (GST-I $\kappa$ B $\alpha$  [1-54]) as the substrate (20).

#### qPCR

Total RNA was isolated from cells using Trizol (Invitrogen, Carlsbad, CA, USA) and 1  $\mu$ g of each RNA was used for cDNA synthesis with iScript Reverse Transcriptase (Bio-Rad, Hercules, CA, USA). Gene expression was quantified by quantitative (q) PCR using SsoAdvanced Universal qPCR Supermixe (Bio-Rad) and specific qPCR primers for the relative quantitation of the transcripts, performed using co-amplified ribosomal  $\beta$ -Actin as an internal control for normalization. Oligo sequences are reported:

- h $\beta$ -Actin-Fw: 5'-CGAGGCCAGAGCAAGAGAG-3'
- h $\beta$ -Actin-Rev: 5'-CGGTTGGCCTTAGGGTTCAG-3'
- hI $\kappa$ B $\alpha$ -Fw: 5'-CCAGGGCTATTCTCCCTACC-3'
- hI $\kappa$ B $\alpha$ -Rev: 5'-GCTCGTCCTCTGTGAATCC-3'
- hBAX-Fw: 5'-GGACGAACTGGACAGTAACATG-3'
- hBAX-Rev: 5'-GTTGTGCGCCCTTTCTACTTTGC-3'
- hTRAF2-Fw: 5'-CAGTTCGGCCTCCAGATAA-3'
- hTRAF2-Rev: 5'-TCGTGGCAGCTCTCGTATTCTT-3'
- hCCND1-Fw: 5'-ACAAACAGATCATCCGCAAACAC-3'
- hCCND1-Rev: 5'-TGTTGGGGCTCCTCAGGTTTC-3'

Validated FKBP1A qPCR primers were purchased from Qiagen (Philadelphia, PA, USA; QT00070742: Hs.FKBP1A\_1.LG QuantiTect Primer Assay).

#### Analysis of apoptosis

Apoptosis was measured using propidium iodide in double staining with annexin V-FITC (BD Biosciences, NJ, USA). Annexin-V binds to phosphatidylserine exposed on the outer leaflet of plasmamembrane of dying cells, Propidium iodide does not stain cells with intact membrane. Both early apoptosis (cell positive for annexin-V and negative for PI) and late apoptosis (cell double positive for annexin-V and PI) were measured with a flow cytometer (LSR II, BD Biosciences).

## RESULTS

#### FKBP51 improves IKK enzymatic activity

Previous studies have shown the pivotal role of FKBP51 in promoting activation of NF- $\kappa$ B in melanoma, induced by chemotherapeutics (7,11,14) or ionizing radiation (8). Since FKBP51 has been implicated as a cofactor of IKK complex (13), we examined the role of FKBP51 in maintaining IKK kinase activity by stably knocking down FKBP51 in melanoma cell lines. FKBP51 knockdown in A375 melanoma cells, using three different shRNAs, profoundly reduced the kinase activity of IKK after stimulation with TNF $\alpha$  (Figure 1a, upper). Consistent with this finding, EMSA showed a remarkable decrease of active NF- $\kappa$ B complexes (indicated by the arrow), in the nuclear extracts

of TNF $\alpha$ -stimulated FKBP51-knockdown melanoma cells (Figure 1a, lower). Moreover, the TNF $\alpha$ -induced I $\kappa$ B $\alpha$  degradation, a central step in NF- $\kappa$ B activation, was attenuated in the FKBP51-knockdown cells (Figure 1b, upper). Since the gene encoding I $\kappa$ B $\alpha$  is the first transcriptional target of activated NF- $\kappa$ B, we also examined the level of I $\kappa$ B $\alpha$  mRNA. The induction of I $\kappa$ B $\alpha$  mRNA by TNF $\alpha$  was substantially inhibited in the FKBP51-silenced A375 cells (Figure 1b, lower), thus further confirming the reduced activation of NF- $\kappa$ B in these cells. It is worth noting that, in control cells, I $\kappa$ B- $\alpha$  production, which occurs at transcriptional level, apparently is not evident at protein level. This is consistent with high melanoma content in FKBP51, supporting an increased IKK activity and consequent I $\kappa$ B- $\alpha$  degradation. FKBP51 has been shown to inhibit apoptosis in melanoma cells (10–12). In agreement with these previous reports, we found that FKBP51 knockdown promoted TNF $\alpha$ -stimulated expression of the proapoptotic factor Bax, at both protein (Figure 1c, upper) and mRNA (Figure 1c, lower) levels. Accordingly, TNF $\alpha$  induced cell death to a greater extent in the FKBP51-silenced melanoma cells, compared to non-silenced control melanoma cells (Figure 1d). The FKBP51 knockdown also sensitized A375 cells to apoptosis induction by doxorubicin and etoposide (see supplementary information, Supplementary Figure S1). The effect of FKBP51 knockdown on IKK activity was not limited to A375 cells, since similar results were obtained with another melanoma cell line, SAN (see supplementary information, Supplementary Figure S2). Similarly to A375 cells, SAN melanoma cells depleted of FKBP51 showed impaired IKK kinase activity following TNF $\alpha$  stimulation, and a reduced NF- $\kappa$ B activation, in comparison with SAN control cells (Supplementary Figure S2). Interestingly, the FKBP51 knockdown attenuated the expression of Bcl-2 and concomitantly increased the expression of p53 in TNF $\alpha$ -stimulated SAN melanoma cells (Supplementary Figure S2).

#### Both scaffold and isomerase functions of FKBP51 are essential for IKK activity

To define the mechanisms by which FKBP51 supported IKK kinase activity, we approached the study of FKBP51 interaction with IKK proteins. When expressed in HEK293T cells, FKBP51 bound to all three subunits of IKK, IKK $\alpha$ , IKK $\beta$  and IKK $\gamma$ , with the binding to IKK $\alpha$  being most prominent (Figure 2a). The previously described FKBP51 interaction, with the IKK-activating kinase TAK1 (13), appears to be less pronounced (Figure 2a). It is feasible that the FKBP51/TAK1 association is IKK-mediated. Interestingly, FKBP51 knockdown reduced the binding of IKK $\gamma$  to the catalytic IKK subunits, IKK $\alpha$  and IKK $\beta$ , under both transfection (Figure 2b) and endogenous (Figure 2c) conditions. These findings suggested a scaffolding role for FKBP51 in facilitating the assembly of IKK kinase complex. We next addressed whether the isomerase activity of FKBP51, in addition to its scaffolding function, of FKBP51 was also important for IKK regulation. For these studies, we incubated cells with FK506, a potent ligand of FKBP51 that inhibits its PPIase activity. FK506, indeed, reduced TNF $\alpha$ -stimulated IKK activity in A375 melanoma

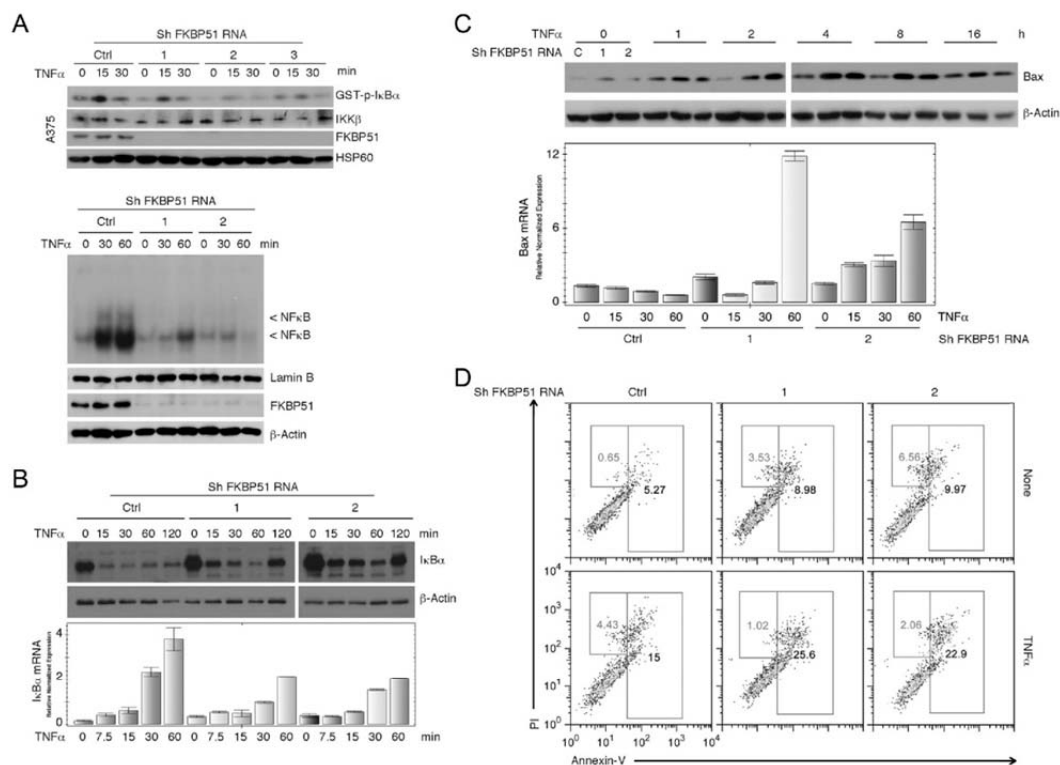


**Figure 1.** Effect of FKBP51 knockdown on NF-κB activation and apoptosis sensitivity in A375 melanoma cells. (A, upper) IB assay of IκBα phosphorylation levels in KA samples. IKK complexes were immunoprecipitated from melanoma cells stably knocked down with three different FKBP51 shRNAs (1, 2 and 3) or with a control shRNA (Ctrl) and stimulated with TNFα for 15 and 30 min. GST-IκBα served as substrate (top panel) to measure IKK activity. IB assay also monitored the IKKβ levels in immunoprecipitated-protein. Whole lysates showed the efficacy of FKBP51 knock down. HSP60 was used as a loading control. The reduced level of GST-p-IκBα in condition of FKBP51 knock down is consistent with a reduced phosphorylating capacity of immunoprecipitated IKK. (A, lower) EMSA of nuclear extracts of FKBP51-knockdown A375 cells, stimulated with TNFα for 30 and 60 min. The band was generated by NF-κB binding to a <sup>32</sup>P-radiolabeled probe. The bands indicated by the arrow are reduced in FKBP51 knock down cells. Nuclear extract was normalized using lamin B as a loading control. The expression of FKBP51 and β-actin in total lysates is also shown. (B) Assay of TNFα-induced changes in expression levels of IκBα protein (IB, upper) and mRNA (qPCR, lower). (C and D) Effect of FKBP51 knock down on TNFα-induced apoptosis. (C) Expression levels (protein and mRNA) of pro-apoptotic Bax. (D) Representative flow cytometric histograms of annex-V/PI staining. Data are representative of three independent experiments.

cells (Figure 3a). A moderate effect of FK506 on IKK activation was also detected in the FKBP51-knockdown cells, probably due to the incomplete depletion of FKBP51 in these cells or the action of other FK506-sensitive immunophilins. FK506 did not affect the physical interaction of FKBP51 with IKKα (Figure 3b), suggesting another mechanism of action. In accordance with the finding that FK506 impaired IKK function, FK506 attenuated TNFα-induced IκBα degradation (Figure 3c). A similar result was obtained with another ligand of FKBP51, rapamycin, but not with the cyclophilin A ligand cyclosporin. This result excluded a role for calcineurin phosphatase in the IKK-inhibitory action of FK506. The effect of FKBP51 inhibition on TNFα-induced IκBα degradation was confirmed using two compounds selective inhibitors of FKBP51, recently identified (22) namely SaFit1 and 2 (Figure 3d). Both

compounds inhibited expression of cyclin D1, a transcriptional target of NF-κB (Figure 3e). The expression levels of FKBP12 did not appear to be modulated in a similar fashion, which ruled out an effect of SaFits on general transcription. The observation that rapamycin is more effective than the two compounds in reducing cyclin D1 transcript levels may depend on rapamycin capacity to inhibit other FKBP51 involved in the NF-κB signaling (23). However, our result is also consistent with the notion that rapamycin has effects on Cyclin D1 expression independent of NF-κB (24).

**FKBP51 binds to TRAF2 and allows recruitment of IKK to TRAF2**

TNF receptor-associated factor 2 (TRAF2) mediates TNFα-stimulated NF-κB signaling by catalyzing K63-linked polyubiquitination, a mechanism that facilitates

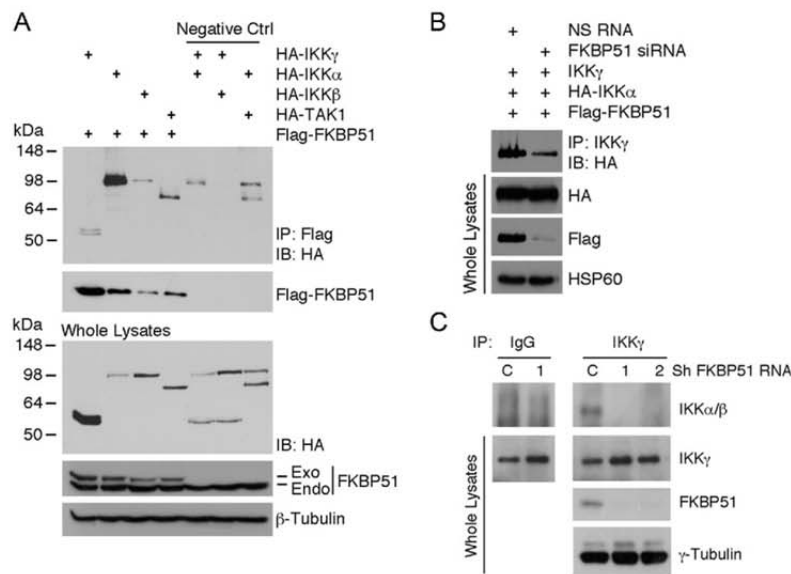


**Figure 2.** FKBP51 interacts with all IKK complex subunits and supports IKK assembly. (A) Immunoassay of HEK293 cells transfected with several combinations of expression vectors, namely HA-IKK $\gamma$ , -IKK $\alpha$ , -IKK $\beta$ , -TAK1 and Flag-FKBP51. Anti-Flag immunoprecipitated proteins were IB assayed with anti-HA and anti-Flag (upper). IB analysis of total lysates is also shown (lower). (B and C) FKBP51 knock down impairs the IKK $\gamma$ /IKK $\alpha$ /IKK $\beta$  interaction. (B) Immunoassay of HEK293 cells, silenced or not for FKBP51, and transfected with the expression vectors for IKK $\gamma$ , HA-IKK $\alpha$  and Flag-FKBP51. IKK $\gamma$  was immunoprecipitated from cell lysates; IP was analyzed by IB with anti-HA. (C) Endogenous IKK $\gamma$  was immunoprecipitated from whole lysates of stably knocked down A375 melanoma cells (1,2) and the relative negative control (C). Immunoprecipitated proteins were then assayed by IB. Data are representative of three independent experiments.

the recruitment of IKK complex to its upstream kinase TAK1 (18–19). To examine the role of FKBP51 in regulating TRAF2 function, we first analyzed the effect of FKBP51 knockdown on the expression of the TRAF2 mRNA. Interestingly, the level of TRAF2 mRNA was reduced in FKBP51 knockdown melanoma cells (Figure 4a). The reduced TRAF2 mRNA expression in the FKBP51-knockdown cells might be due to the attenuated activity of NF- $\kappa$ B or yet to be identified factors. We over expressed TRAF2 in HEK293T cells, and found that TRAF2 physically interacted with FKBP51 (Figure 4b) as well as with TAK1 and each IKK components,  $\alpha$ ,  $\beta$  and  $\gamma$  (Figure 4c). FKBP51 silencing using siRNAs did not affect the TRAF2/TAK1 interaction, but reduced the binding of TRAF2 to IKK subunits, particularly IKK $\alpha$  and IKK $\beta$  (Figure 4c). Furthermore, we performed endogenous IKK $\alpha$  and FKBP51 co-IP assays in A375 melanoma cells. A representative result of 2 independent experiments is shown in Figure 4d. These results suggest that in addition to directly modulating IKK activity, FKBP51 may also promote the recruitment of IKK to TRAF2 and, thereby, facilitates IKK activation. The role of FKBP51 as a constitutive endogenous factor of IKK complexes is supported by the observation that this immunophilin is recovered from gel filtration profiles of melanoma cell lysates associated with IKK subunits (see supplementary information, Supplementary Figure S3). HSP90 was also eluted by gel filtration (Sup-

plementary Figure S3), suggesting HSP90 can take part to FKBP51/IKK complex.

**The TPR domain of FKBP51 mediates IKK/TRAF2 interactions**

To delineate functional domains of FKBP51 involved in modulation of the IKK/TRAF2 signaling complex, we employed FKBP51 mutants harboring disrupted PPIase (FKBP51<sup>FD67DV</sup>-Flag-FKBP51-mutPPIase) or TPR (FKBP51<sup>K352A/R356A</sup>-Flag-FKBP51-mutTPR) domain. Interestingly, the TPR mutant failed to bind TRAF2, whereas the PPIase mutant retained the TRAF2-binding function (Figure 5a). Consistent with this finding, a truncated form of FKBP51 (Myc-Flag-FKBP51s), lacking the TPR tandem repeats, barely interacted with TRAF2, suggesting the involvement of the TPR domain in FKBP51/TRAF2 interaction. The mutations in the TPR domain, but not the PPIase domain, of FKBP51 also abolished its ability to promote the association between IKK $\alpha/\beta$  and IKK $\gamma$  (Figure 5b). In contrast, neither the TPR, nor the PPIase domain, was required for inducing the interaction between IKK $\gamma$  and TRAF2 (Figure 5b). On the other hand, both TPR and PPIase domains of FKBP51 were important for the IKK $\gamma$ /FKBP51 interaction, since this interaction has not been maintained by the TPR and PPIase mutants (Figure 5c). These findings also suggest that the TPR and PPIase domains of FKBP51 are not crucial for

Downloaded from <http://nar.oxfordjournals.org/> at Max Planck Inst Fur Psychiatric on September 11, 2015

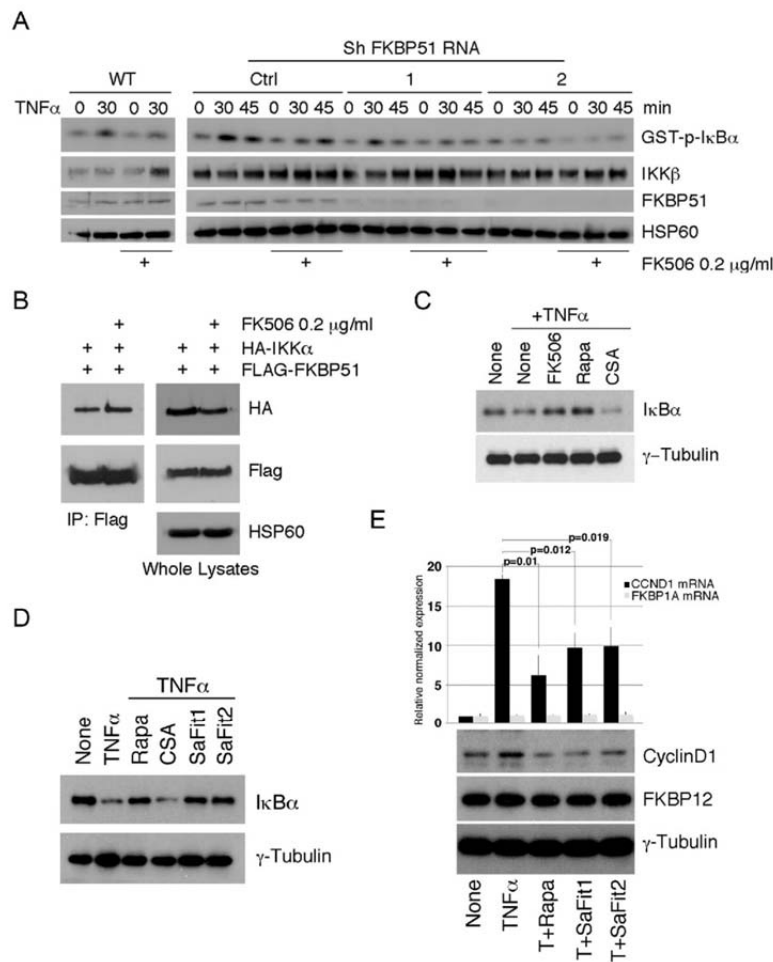


**Figure 3.** FKBP51 isomerase activity affects the enzymatic function of IKK kinase complex. (A) IB of I $\kappa$ B $\alpha$  phosphorylation levels of samples assayed in KA. IKK complexes were immunoprecipitated from WT and FKBP51-knocked down A375 cells, stimulated with TNF $\alpha$  for 30 and 45 min, in the presence or not of FK506. IKK activation was measured using GST-I $\kappa$ B $\alpha$  as substrate. IB also monitored the expression of IKK $\beta$  in immunoprecipitated protein and FKBP51 in total lysates. HSP60 served as loading control for total lysates. Data are representative of three independent experiments. (B) Immunoassay of HEK293 cells transfected with the HA-IKK $\alpha$  and Flag-FKBP51 expression vectors, in the presence or not of FK506. Data are representative of two independent experiments. (C) Study of I $\kappa$ B $\alpha$  degradation induced by TNF $\alpha$  in A375 cells pre-incubated for 1 h in the absence or the presence of FK506, rapamycin and CSA, each compound at the concentration of 0.2  $\mu$ g/ml. Data are representative of two independent experiments. (D) I $\kappa$ B $\alpha$  degradation induced by TNF- $\alpha$  in A375 cells pre-incubated for 1 h in the absence or the presence of Rapamycin, CSA and the specific FKBP51 inhibitors SaFit1 and 2, each at the concentration of 0.2  $\mu$ g/ml. Data are representative of two independent experiments. Both specific compounds inhibited TNF- $\alpha$ -induced I $\kappa$ B $\alpha$  degradation. (E) Measure by qPCR of CCND1 and FKBP1A levels showed that both SaFit1 and 2 significantly reduced TNF- $\alpha$ -induced of CCND1 levels of melanoma, in accordance with the NF- $\kappa$ B promoting ability of FKBP51. Modulation of cyclin D1 expression level was confirmed by immunoblot. Neither FKBP1A mRNA, nor FKBP12 protein, appeared to be modulated.

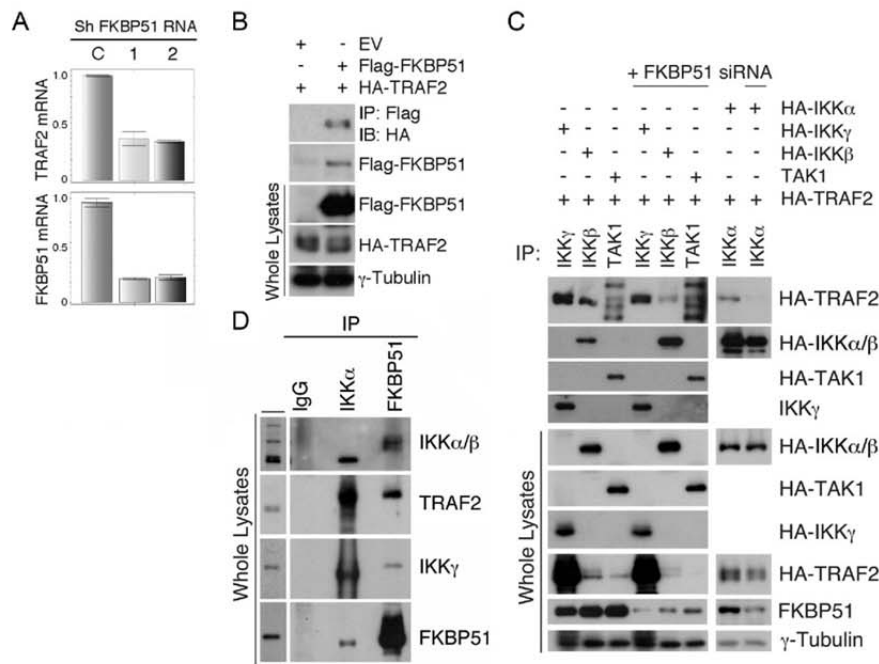


**Figure 4.** FKBP51 regulates interaction between TRAF2 and IKK. (A) Reduced TRAF2 levels in FKBP51 knocked down melanoma cells. QPCR analysis of the TRAF2 and FKBP51 mRNA levels in FKBP51-knocked down A375 cells. Data are representative of three independent experiments. (B) FKBP51 interacts with TRAF2. Immunoassay of HEK293 cells transfected with the HA-TRAF2 and Flag-FKBP51 expression vectors. Data are representative of three independent experiments. (C) FKBP51 silencing prevents TRAF2 interaction with IKK subunits. Immunoassay of whole cell extracts and immunoprecipitated proteins obtained by HEK293, silenced or not for FKBP51, and transfected with various combinations of HA-IKK $\alpha$ , -IKK $\beta$ , -IKK $\gamma$ , -TAK1, -TRAF2 and Flag-FKBP51 expression vectors. Data are representative of four independent experiments. (D) FKBP51, IKK subunits and TRAF2 interact each other. Endogenous IKK $\alpha$  and FKBP51 were immunoprecipitated from whole lysates of A375 melanoma cells. Immunoprecipitated protein was then assayed in IB. Data are representative of two independent experiments.

TRAF2/IKK $\gamma$  binding, but the TPR domain is important for facilitating the IKK complex assembly and the recruitment of IKK to TRAF2. We hypothesize that FKBP51 binding to TRAF2 (through TPR) allows recruitment of IKK $\gamma$  to TRAF2 (involving TPR and PPIase). Such TPR-mediated FKBP51 binding to TRAF2 does not appear to require HSP90 (see supplementary information, Supplementary Figure S4). It is possible that IKK $\gamma$  isomerization may virtually initiate IKK complex assembly and autophosphorylation. A proposed mechanism of interaction is depicted in Figure 6. TRAF2 interacts with the TPR domain of FKBP51, whereas IKK $\gamma$  interacts with both FK and TPR domains of FKBP51. The TPR domain promotes the assembly of IKK complex and allows IKK recruitment to TRAF2.

**DISCUSSION**

Deregulation of the NF- $\kappa$ B regulatory pathway in cancer plays a major role in mediating chemo- and radio-resistance and cancer progression. In melanoma, a relevant role for aberrant NF- $\kappa$ B activation has been assigned to FKBP51 (7,8,11). Our present work confirms previous

studies (7,8,11) showing a relevant role of FKBP51 in apoptosis resistance of melanoma and shed lights on the mechanisms by which this protein controls the cellular machinery that leads to activation of this transcription factor. Our study shows that FKBP51 interacts with all three subunits of IKK and contributes to maintaining the IKK complex formation and catalytic ability, at least in melanoma cells. The FKBP51 isomerase inhibitor FK506 did not prevent the IKK-FKBP51 interaction, but still hampered the kinase activity of IKK. In accordance with this finding, FK506 prevented TNF $\alpha$ -induced I $\kappa$ B $\alpha$  degradation. These results suggested that the PPIase activity of FKBP51 is important for supporting the enzymatic function of IKK. In further support of this hypothesis, we found that another FKBP inhibitor, rapamycin, but not the cyclophilin A inhibitor cyclosporin impaired TNF $\alpha$ -induced I $\kappa$ B $\alpha$  degradation. The fact that cyclosporin did not prevent TNF $\alpha$ -induced I $\kappa$ B $\alpha$  degradation ruled out a role for calcineurin inhibition in this effect.

By using two FKBP51 point mutants, with functionally compromised TPR or PPIase domains, and a truncated isoform lacking the TPR domain, we were able to determine the protein domains involved in interactions with IKK sub-



Proposed mechanism

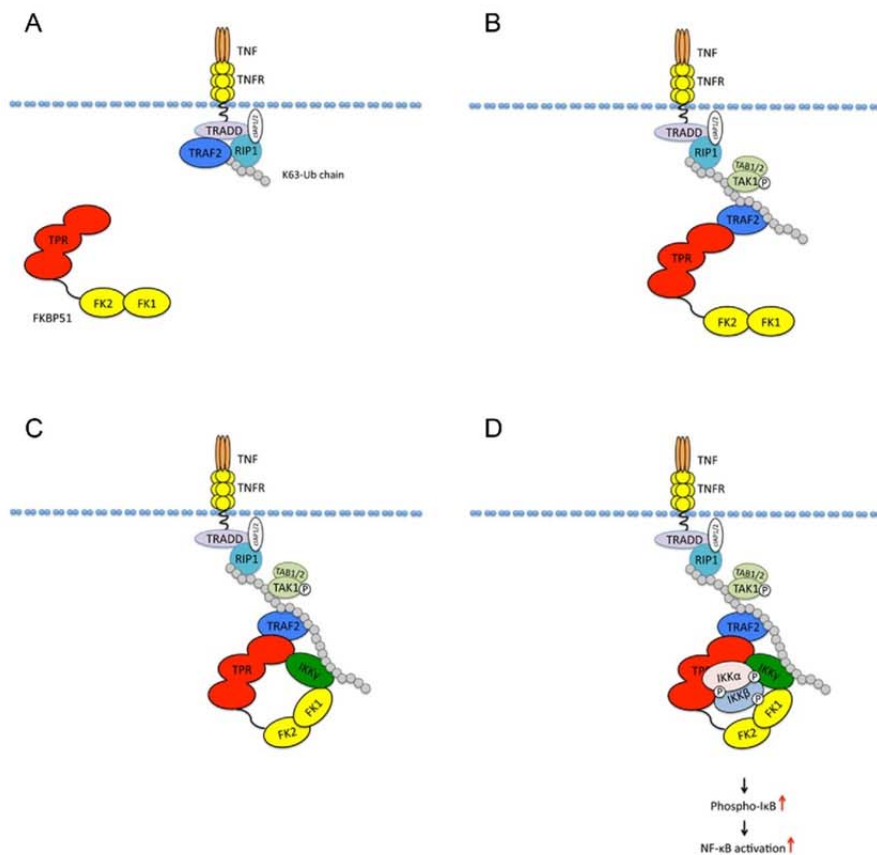


**Figure 6.** Proposed mechanism for the interaction of FKBP51 with NF- $\kappa$ B signaling proteins. (A) TNF $\alpha$ -binding to its receptor determines formation of RIP-induced K-63 ubiquitin chain. (B) TRAF2, promotes elongation of this non degradative ubiquitin chain and recruits TAK1 kinase complex. (C) TRAF2 interacts with TPR domain of FKBP51. IKK $\gamma$  interacts with both FK and TPR domains of FKBP51. IKK $\gamma$  and TRAF2 are also connected through K63 ubiquitin chain. (D) IKK $\alpha$  and  $\beta$  interact each others and with IKK $\gamma$  and TRAF2 through the TPR domain.

IKK signaling since FKBP51 was recently also identified as a TRAF3 and TRAF6 interactor (34).

Very recently, Erlejman *et al.* (23) found that another immunophilin namely FKBP52 promoted NF- $\kappa$ B activation in fibroblasts because it facilitated the nuclear translocation of the transcription factor. The authors also found that, in fibroblasts, FKBP51 counteracted the action of FKBP52 on NF- $\kappa$ B nuclear translocation. For this reason, the authors concluded that NF- $\kappa$ B activation was regulated in an antagonistic manner by the high molecular weight immunophilins FKBP51 and FKBP52, as it occurred for steroid receptor. The reduced levels of NF- $\kappa$ B complexes in nuclei of FKBP51 knockdown cells, found in EMSA, accompanied by impairment of NF- $\kappa$ B-regulated gene expression underline the strict IKK dependence on FKBP51 and the prevalence of stimulatory effect in melanoma. Thus,

even if FKBP51 regulated NF- $\kappa$ B at different levels of the activation signal, with effects that can be antagonistic, cell-context-related factors virtually affect the translocation rate of NF- $\kappa$ B heterocomplex, overcoming the suggested (23) inhibitory effects.

Taken together these results shed light on the mechanism by which FKBP51 allows NF- $\kappa$ B activation and suggest an essential role for this immunophilin in sustaining the constitutive activation of these transcriptional factors in melanoma. Finally, we show that the FKBP51 stimulating role on IKK signaling can be pharmacologically reduced, which results of this study may have an important translational implication in human therapy of this aggressive neoplasia.

## ACCESSION NUMBER

PDB ID: 4PY5.

## SUPPLEMENTARY DATA

Supplementary Data are available at NAR Online.

## ACKNOWLEDGEMENT

We thank Xuhong Cheng for the excellent technical support, Dr Annalisa Lamberti for helpful discussion.

## FUNDING

Italian Association for Cancer Research (AIRC) [10452, awarded to M.F.R.]; US National Institute of Health (NIH) [GM84459, awarded to S.C.S.]; Center for Inflammation and Cancer of MD Anderson Cancer Center; POR Progetto OCKey funded by Regione Campania. Funding for open access charge: POR Progetto OCKey funded by Regione Campania.

*Conflict of interest statement.* None declared.

## REFERENCES

- Gaali,S., Gopalakrishnan,R., Wang,Y., Kozany,C. and Hausch,F. (2011) The chemical biology of immunophilin ligands. *Curr. Med. Chem.*, **18**, 5355–5379.
- Fischer,G. and Aumüller,T. (2003) Regulation of peptide bond cis/trans isomerization by enzyme catalysis and its implication in physiological processes. *Rev. Physiol. Biochem. Pharmacol.*, **148**, 105–150.
- Hausch,F., Kozany,C., Theodoropoulou,M. and Fabian,A.K. (2013) FKBP5 and the Akt/mTOR pathway. *Cell Cycle*, **12**, 2366–2370.
- Baughman,G., Wiederrecht,G.J., Faith Campbell,N., Martin,M.M. and Bourgeois,S. (1995) FKBP51, a novel T-cell specific immunophilin capable of calcineurin inhibition. *Mol. Cell. Biol.*, **15**, 4395–4402.
- Gallo,L.I., Lagadari,M., Piwien-Pilipuk,G. and Galigniana,M.D. (2011) The 90-kDa heat-shock protein (Hsp90)-binding Immunophilin FKBP51 is a mitochondrial protein that translocates to the nucleus to protect cells against oxidative stress. *J. Biol. Chem.*, **286**, 30152–30160.
- Romano,S., Sorrentino,A., Di Pace,A.L., Nappo,G., Mercogliano,C. and Romano,M.F. (2011) The emerging role of large immunophilin FK506 binding protein 51 in cancer. *Curr. Med. Chem.*, **18**, 5424–5429.
- Romano,M.F., Avellino,R., Petrella,A., Bisogni,R., Romano,S. and Venuta,S. (2004) Rapamycin inhibits doxorubicin-induced NF-kappaB/Rel nuclear activity and enhances the apoptosis of melanoma cells. *Eur. J. Cancer*, **40**, 2829–2836.
- Romano,S., D'Angelillo,A., Pacelli,R., Staibano,S., De Luna,E., Bisogni,R., Eskelinen,E.L., Mascolo,M., Cali,G., Arra,C. et al. (2010) Role of FK 506 binding protein 51 (FKBP51) in the control of apoptosis of irradiated melanoma cells. *Cell Death Differ.*, **17**, 145–157.
- Romano,S., Staibano,S., Greco,A., Brunetti,A., Nappo,G., Ilardi,G., Martinelli,R., Sorrentino,A., Di Pace,A., Mascolo,M. et al. (2013) FK506 binding protein 51 positively regulates melanoma stemness and metastatic potential. *Cell Death Dis.*, **4**, e578.
- Romano,S., D'Angelillo,A., D'Arrigo,P., Staibano,S., Greco,A., Brunetti,A., Scalvenzi,M., Bisogni,R., Scala,I. and Romano,M.F. (2014) FKBP51 increases the tumour-promoter potential of TGF-beta. *Clin. Transl. Med.*, **3**, 1.
- Avellino,R., Romano,S., Parasole,R., Bisogni,R., Lamberti,A., Poggi,V., Venuta,S. and Romano,M.F. (2005) Rapamycin stimulates apoptosis of childhood acute lymphoblastic leukemia cells. *Blood*, **106**, 1400–1406.
- Giraudier,S., Chagraoui,H., Komura,E., Barnache,S., Blanchet,B., LeCouedic,J.P., Smith,D.F., Larbret,F., Taksin,A.L., Moreau-Gachelin,F. et al. (2002) Overexpression of FKBP51 in idiopathic myelofibrosis regulates the growth factor independence of megakaryocyte progenitors. *Blood*, **100**, 2932–2940.
- Bouwmeester,T., Bauch,A., Ruffner,H., Angrand,P.O., Bergamini,G., Croughton,K., Cruciat,C., Eberhard,D., Gagneur,J., Ghidelli,S. et al. (2004) A physical and functional map of the human TNF- $\alpha$ /NF- $\kappa$ B signal transduction pathway. *Nat. Cell Biol.*, **6**, 97–105.
- Jiang,W., Cazacu,S., Xiang,C., Zenklusen,J.C., Fine,H.A., Berens,M., Armstrong,B., Brodie,C. and Mikkelsen,T. (2008) FK506 binding protein mediates glioma cell growth and sensitivity to rapamycin treatment by regulating NF-kappaB signaling pathway. *Neoplasia*, **10**, 235–243.
- Taipale,M., Tucker,G., Peng,J., Krykbaeva,I., Lin,Z.Y., Larsen,B., Choi,H., Berger,B., Gingras,A.C. and Lindquist,S. (2014) A quantitative chaperone interaction network reveals the architecture of cellular protein homeostasis pathways. *Cell*, **158**, 434–448.
- Sun,N.K., Huang,S.L., Chang,P.Y., Lu,H.P. and Chao,C.C.K. (2014) Transcriptomic profiling of taxol-resistant ovarian cancer cells identifies FKBP5 and the androgen receptor as critical markers of chemotherapeutic response. *Oncotarget*, **5**, 11939–11956.
- Harhaj,E.W. and Sun,S.C. (1999) IKKgamma serves as a docking subunit of the IkkappaB kinase (IKK) and mediates interaction of IKK with the human T-cell leukemia virus Tax protein. *J. Biol. Chem.*, **274**, 22911–22914.
- Liao,G., Zhang,M., Harhaj,E.W. and Sun,S.C. (2004) Regulation of the NF-kappaB-inducing kinase by tumor necrosis factor receptor-associated factor 3-induced degradation. *J. Biol. Chem.*, **279**, 26243–26250.
- Wu,X. and Sun,S.C. (2007) Retroviral oncoprotein Tax deregulates NF-kappaB by activating Tak1 and mediating the physical association of Tak1-IKK. *EMBO Rep.*, **8**, 510–515.
- Uhlik,M., Good,L., Xiao,G., Harhaj,E.W., Zandi,E., Karin,M. and Sun,S.C. (1998) NF-kB-inducing kinase and I $\kappa$ B kinase participate in human T-cell leukemia virus I Tax-mediated NF-kB activation. *J. Biol. Chem.*, **273**, 21132–21136.
- Wochnik,G.M., Rüegg,J., Abel,G.A., Schmidt,U., Holsboer,F. and Rein,T. (2005) FK506-binding proteins 51 and 52 differentially regulate dynein interaction and nuclear translocation of the glucocorticoid receptor in mammalian cells. *J. Biol. Chem.*, **280**, 4609–4616.
- Gaali,S., Kirschner,A., Cuboni,S., Hartmann,J., Kozany,C., Balsevich,G., Namendorf,C., Fernandez-Vizarra,P., Sippel,C., Zannas,A.S. et al. (2015) Selective inhibitors of the FK506-binding protein 51 by induced fit-mechanism. *Nat. Chem. Biol.*, **11**, 33–37.
- Erlejan,A.G., De Leo,S.A., Mazaira,G.L., Molinari,A.M., Camisay,M.F., Fontana,V., Cox,M.B., Piwien-Pilipuk,G. and Galigniana,M.D. (2014) NF-kB transcriptional activity is modulated by FK506-binding proteins FKBP51 and FKBP52: a role for peptidyl-prolyl isomerase activity. *J. Biol. Chem.*, **289**, 26263–26276.
- Hashemolhosseini,S., Nagamine,Y., Morley,S.J., Desrivieres,S., Mercep,L. and Ferrari,S. (1998) Rapamycin inhibition of the G1 to S transition is mediated by effects on cyclin D1 mRNA and protein stability. *J. Biol. Chem.*, **273**, 14424–14429.
- Hinz,M., Broemer,M., Arslan,S.C., Otto,A., Mueller,E.C., Dettmer,R. and Scheidereit,C.J. (2007) Signal responsiveness of IkkappaB kinases is determined by Cdc37-assisted transient interaction with Hsp90. *Biol. Chem.*, **282**, 32311–32319.
- Yang,J. and Richmond,A. (2001) Constitutive IkkappaB kinase activity correlates with nuclear factor-kappaB activation in human melanoma cells. *Cancer Res.*, **61**, 4901–4909.
- Chen,Z.J. (2005) Ubiquitin signalling in the NF-kappaB pathway. *Nat. Cell Biol.*, **7**, 758–765.
- Ea,C.K., Deng,L., Xia,Z.P., Pineda,G. and Chen,Z.J. (2006) Activation of IKK by TNFalpha requires site-specific ubiquitination of RIP1 and polyubiquitin binding by NEMO. *Mol. Cell*, **22**, 245–257.
- Wu,C.J., Conze,D.B., Li,T., Srinivasula,S.M. and Ashwell,J.D. (2006) Sensing of Lys 63-linked polyubiquitination by NEMO is a key event in NF-kappaB activation. *Nat. Cell Biol.*, **8**, 398–406.
- Bertrand,M.J., Milutinovic,S., Dickson,K.M., Ho,W.C., Boudreault,A., Durkin,J., Gillard,J.W., Jaquith,J.B., Morris,S.J. and Barker,P.A. (2008) cIAP1 and cIAP2 facilitate cancer cell survival by

## B. Research Articles – Publication/Manuscript II

*Nucleic Acids Research*, 2015, Vol. 43, No. 14 6993

- functioning as E3 ligases that promote RIP1 ubiquitination. *Mol. Cell*, **30**, 689–700.
31. Shih,V.F., Tsui,R., Caldwell,A. and Hoffmann,A. (2011) A single NF $\kappa$ B system for both canonical and non-canonical signaling. *Cell Res.*, **21**, 86–102.
32. Vince,J.E., Pantaki,D., Feltham,R., Mace,P.D., Cordier,S.M., Schmukle,A.C., Davidson,A.J., Callus,B.A., Wong,W.W., Gentle,I.E. *et al.* (2009) TRAF2 must bind to cellular inhibitors of apoptosis for tumor necrosis factor (tnf) to efficiently activate nf-kappab and to prevent tnf-induced apoptosis. *J. Biol. Chem.*, **284**, 35906–35915.
33. Zarnegar,B.J., Wang,Y., Mahoney,D.J., Dempsey,P.W., Cheung,H.H., He,J., Shiba,T., Yang,X., Yeh,W.C., Mak,T.W. *et al.* (2008) Noncanonical NF-kappaB activation requires coordinated assembly of a regulatory complex of the adaptors cIAP1, cIAP2, TRAF2 and TRAF3 and the kinase NIK. *Nat. Immunol.*, **9**, 1371–1378.
34. Akiyama,T., Shiraishi,T., Qin,J., Konno,H., Akiyama,N., Shinzawa,M., Miyachi,M., Takizawa,N., Yanai,H., Ohashi,H. *et al.* (2014) Mitochondria-nucleus shuttling FK506-binding protein 51 interacts with TRAF proteins and facilitates the RIG-I-like receptor-mediated expression of type I IFN. *PLoS One*, **9**, e95992.

Downloaded from <http://nar.oxfordjournals.org/> at Max Planck Inst Fur Psychiatric on September 11, 2015

## B. Research Articles – Publication/Manuscript III

### 6.2. *Manuscript III*

**The stress regulator FKBP51 drives chronic pain by modulating spinal glucocorticoid signaling** – submitted manuscript

(Maria Maiarù, Keri Tochiki, Marc B. Cox, Leonette V. Annan, Christopher G. Bell, **Xixi Feng**, Felix Hausch, Sandrine M. Géranton)

#### **Summary**

Several studies indicated that FKBP51, as a negative regulator of the glucocorticoid receptor (GR), is involved in the severity of musculoskeletal pain after traumata. The role and direct contribution of the protein was assessed in the presented study.

An upregulation of FKBP51 as well as decreased methylation of the FKBP51 promoter sequence was observed after CFA injection. Supporting the assumption that the protein is important for long term pain states, it was shown that mice, exhibiting limited FKBP51 function by knock out, antisense silencing on spinal level or pharmacological inhibition by SAFit2 (intrathecal administration), showed reduced hypersensitivity in several persistent pain models. KO mice also showed lower levels of the pro-inflammatory cytokine IL6. Since it is known that IL6 transcription is regulated by GR, this finding supports that changes in GR activity are involved in the maintenance of chronic pain. Therefore, FKBP51 is suggested as a promising new target and pharmacological FKBP51 inhibition as possible treatment of long term pain states.

## B. Research Articles – Publication/Manuscript IV

### 6.3. *Manuscript IV*

#### **Loss or inhibition of FKBP51 protects against diet-induced metabolic disorders by shaping insulin signaling** – manuscript in preparation

(Georgia Balsevich, Nils C Gassen, Alexander Häusl, **Xixi Feng**, Carola W Meyer, Stoyo Karamihalev, Carine Dournes, Andres Uribe, Sara Santarelli, Kathrin Hafner, Marily Theodoropoulou, Christian Namendorf, Manfred Uhr, Marcelo Paez-Pereda, Felix Hausch, Alon Chen, Matthias H Tschöp, Theo Rein, Mathias V Schmidt)

#### **Summary**

Genetic variants in FKBP5, the gene encoding FKBP51, have been recently associated with type 2 diabetes and markers of insulin resistance. Also a deregulation of the enzyme AKT, which is regulated by FKBP51, was linked to diabetes and glucose metabolism. The aim of the study was therefore to assess the role of FKBP51 in energy and glucose homeostasis.

The study showed that FKBP51KO, as well as pharmacological inhibition of FKBP51 with SAFit2, protected mice from high-fat diet-induced weight gain. Also with normal chow a reduced body weight was observed. The phenotypic change is hereby caused by an increased resting metabolic rate and no decreased calorie intake was observed. A loss or inhibition of FKBP51 also resulted in improved glucose tolerance, especially in skeletal muscle by enhancing insulin signaling. Within the insulin signaling pathway it could be shown that, beside AKT and downstream effector protein, also upstream signaling is affected is influenced by FKBP51 in tissue-specific manner. These data confirm FKBP51 inhibition as a promising drug target for the treatment of obesity as well as type 2 diabetes and suggest FKBP51 inhibition as a possible pharmacological intervention.

## ORIGINAL MANUSCRIPT

**ABSTRACT**

A genome-wide association study recently demonstrated that genetic variants within the gene encoding FKBP51, *FKBP5*, associate with traits related to type 2 diabetes (T2D). Furthermore, FKBP51 is known to suppress AKT activity, a central node within the insulin signaling pathway. Based on these findings, we addressed whether FKBP51 plays a role in energy and glucose homeostasis. We found that FKBP51 knockout (51KO) mice were protected from high fat diet-induced weight gain. In addition, 51KO mice showed improved glucose tolerance and a prolonged response to insulin. This phenotype correlated with heightened insulin signaling specifically within skeletal muscle of 51KO mice. In line with this, glucose uptake was increased by FKBP5 knockout in myotubes. Importantly, pharmacological inhibition of FKBP51 recapitulated the phenotype observed in 51KO mice and likewise increased glucose uptake in myotubes. Collectively, these data implicate FKBP51 in metabolic regulation and provide physiological and mechanistic evidence for the therapeutic potential of FKBP51 in the treatment of T2D.

**INTRODUCTION**

There is an unmet need for therapeutic strategies targeting both obesity and T2D. Identification of novel multifunctional molecules, which regulate multiple key metabolic pathways, offers promise to overcome the current limitations in conventional therapeutic strategies. FKBP51 is an immunophilin protein best known as a regulator of the glucocorticoid receptor and consequently the physiological stress response (Ratajczak et al., 2015). A genome wide association study demonstrated that polymorphisms within the FK506 binding protein 51 (FKBP51) gene (*FKBP5*) loci are associated with type 2 diabetes (T2D) and markers of insulin resistance (Pereira et al., 2014). Additionally, FKBP51 is a negative regulator of the serine/threonine protein kinase, AKT and subsequently the response to chemotherapy (Pei et al., 2009). AKT is furthermore a central node within the insulin signaling pathway, and deregulation of AKT activation has been linked to the pathogenesis of diabetes and obesity (Taniguchi et al., 2006). In this context, FKBP51 may be an important regulator of insulin signaling and consequently energy and glucose homeostasis. Nevertheless, whether FKBP51 plays a critical role in whole body energy and glucose metabolism remains to be elucidated. For this purpose, we aimed to characterize the role of FKBP51 in energy and glucose homeostasis using a combination of FKBP51 knockout (51KO) mice, pharmacological manipulations, and mechanistic studies.

**Full Title** Loss or inhibition of FKBP51 protects against diet-induced metabolic disorders by shaping insulin signaling

Authors

Georgia Balsevich<sup>1, #</sup>, Nils C Gassen<sup>2</sup>, Alexander Häußl<sup>1</sup>, Xixi Feng<sup>2</sup>, Carola W Meyer<sup>3</sup>, Stoyo Karamihalev<sup>1</sup>, Carine Dourmes<sup>1</sup>, Andres Uribe<sup>1</sup>, Sara Santarelli<sup>1</sup>, Kathrin Hafner, Manily Theodoropoulou<sup>2</sup>, Christian Namendorf<sup>2</sup>, Manfred Uhr<sup>2</sup>, Marcelo Paez-Pereda<sup>2</sup>, Felix Hausch<sup>2</sup>, Alon Chen<sup>1</sup>, Matthias H Tschöp<sup>3</sup>, Theo Rein<sup>2</sup>, Mathias V Schmidt<sup>1</sup>

Affiliations

<sup>1</sup> Department of Stress Neurobiology and Neurogenetics, Max Planck Institute of Psychiatry, Munich, Germany

<sup>2</sup> Department of Translational Research in Psychiatry, Max Planck Institute of Psychiatry, Munich, Germany

<sup>3</sup> Institute of Diabetes and Obesity, Helmholtz Center, Munich, Germany

# Corresponding author:

Georgia Balsevich

Max Planck Institute of Psychiatry

Department of Stress Neurobiology and Neurogenetics

Kraepelinstr. 2-10

80804 Munich Germany

Tel: +49-89-30622-342

Fax: +49-89-30622-610

**DISCLOSURE STATEMENT:** The authors declare no conflict of interest.

## METHODS

### Animals & Animal Housing

The FKBP51 knockout (51KO) mouse line, used in experiments 1, 2, and 3, had been previously generated (Tranguch et al., 2005). C57BL/6 mice were used in experiment 4 for the pharmacological blockade of FKBP51 (Charles River Laboratories, Maastricht, The Netherlands). For all experiments, male mice between 3-4 months old were used. During each experiment, mice were singly-housed. Mice were maintained on a 12:12hr light/dark cycle, with controlled temperature (22 +/- 2°C) and humidity (55+/- 5%) conditions. Mice received ad libitum access to water and standard lab chow, unless otherwise specified. The experiments were carried out in accordance with the European Communities' Council Directive 2010/63/EU. The protocols were approved by the committee for the Care and Use of Laboratory animals of the Government of Upper Bavaria, Germany.

### Experimental Design

#### Experiment 1

Cohort 1: In the first experiment, the direct effects of FKBP51 deficiency on metabolic parameters were investigated in 51KO (n = 16) and WT (n = 18) mice. Body composition (fat and lean mass) was assessed using whole body magnetic resonance imaging (Echo-MRI, Houston, TX). Thereafter, mice were surgically implanted with a telemetric transponder (E-mitter, Mini-mitter Inc., Bend, OR). Mice were allowed to recover for approximately 2 weeks before any metabolic recordings were performed. Indirect calorimetry and telemetry were performed on mice initially under chow conditions for the assessment of energy intake, energy expenditure, body temperature, and home-cage activity (TSE PhenoMaster, TSE Systems, Bad Homburg, Germany). Each genotype groups was subsequently divided into a chow diet and high fat diet (HFD) (58% kcal from fat, D12331, Research Diets, New Brunswick, NJ, USA) group, counterbalanced for body weight in order to assess the response to HFD exposure. Body weight was measured throughout the experiment. After 8 weeks on the respective diets, 51KO and WT mice were sacrificed. Epididymal (e), inguinal (i), and perirenal (p) white adipose tissue (WAT) was harvested and weighed; brown adipose tissue (BAT) was harvested and weighed.

Cohort 2: In a second cohort of 51KO and WT mice (n = 8 per genotype), body weight and body composition were examined under HF diet conditions at 30°C to minimize the effects of thermal stress.

Cohort 3: A third cohort of 51KO and WT mice were exposed to 6 h of cold exposure (4°C) to assess cold-induced thermoregulation under both control and HF diet conditions. Briefly, 51KO and WT males were divided into a control diet (10.5%kcal fromfat.D12329, ResearchDiets, Inc., New Brunswick, NJ, USA) and HFD (D12331) group (n = 11/group). After 5 weeks on their respective diets, cold-induced thermoregulation was monitored. Initially rectal body temperature was measured for 4 days prior to the cold exposure paradigm to habituate mice to the rectal thermocouple probe. On the 5<sup>th</sup> day, rectal temperatures were monitored at 0, 2, 4, and 6 h following exposure to 4°C using an Oakton Acorn Temp JKT Thermocouple Thermometer (Oakton Instruments, IL, USA).

#### Experiment 2

To assess the contribution of food intake on body weight regulation in 51KO and WT mice, a pair-feeding experiment was performed. Mice were initially singly-housed one week prior to the experimental onset. On day one of the pair-feeding paradigm, 51KO mice (n = 9, 51KO) and WT mice (n = 11, WT) received ad libitum access to HFD (D12331, Research Diets, New Brunswick, NJ, USA). A second group of WT mice (WT-PF) were pair-fed to the 51KO mice. Each day for 6 weeks, mice in the WT-PF group received restricted access to the HFD, defined as the amount consumed by the 51KO mice 2 days earlier. Food was weighed and replaced daily at 08:00. If residual food remained in the cages of WT-PF mice, it was weighed and removed prior to the delivery of the daily food portion.

#### Experiment 3

In experiment 3, glucose tolerance and insulin tolerance were investigated in 51KO (n = 25) and WT mice (n = 18). Briefly, 51KO and WT mice were initially divided into a control diet group and a HF diet group counterbalanced for body weight. After 8 weeks on the dietary treatment, mice were subjected to a glucose tolerance test (GTT). Additionally, blood was collected to assess fasting insulin and glucose-stimulated insulin levels. Mice were allowed to recover for one week before being subjected to an insulin tolerance test (ITT). Body weight and food intake were measured regularly throughout the experiment. After 9.5 weeks on the respective diets, mice were sacrificed and tissues were collected and stored at -80°C until needed.

#### Experiment 4

To determine whether inhibition of FKBP51 may be an effective anti-obesity and/or diabetic therapeutic strategy, we treated mice for with a highly selective antagonist of FKBP51, known as SAFit2 (Gaalii et al., 2015). Briefly, SAFit2 (20 mg/kg body weight) or vehicle were administered

by intraperitoneal injections twice daily. SAFit2 was solubilized in vehicle containing 4% ethanol, 5% Tween80, 5% PEG400 in 0.9 % saline. Body weight and food intake were measured daily throughout the treatment periods.

**Cohort 1, sub-chronic administration:** Male C57BL/6 mice were singly-housed for 2 weeks prior to the treatment onset. One day before the treatment period, mice were divided into a vehicle-treated group and a SAFit2-treated group counterbalanced for body weight ( $n = 8/\text{group}$ ). On treatment day 7 locomotor activity was assessed in the open field. On treatment day 8 a GTT was performed. SAFit2 levels were assessed in plasma from blood taken from at the time of sacrifice. Animals were sacrificed on day 10 following treatment onset. Body weight and food intake were measured regularly throughout the 10-day treatment schedule.

**Cohort 2, chronic administration:** Four weeks before treatment onset, male C57BL/6 mice were divided into a control diet group ( $n = 25$ ) and a HF diet group ( $n = 25$ ) counterbalanced for body weight. One day before the treatment period, mice of each dietary group were further subdivided into a vehicle-treated group and a SAFit2-treated group counterbalanced for body weight. SAFit2 (20 mg/kg body weight) or vehicle were administered by intraperitoneal injections twice daily for 30 days. On treatment day 10 and again at the end of the treatment period (day 30), SAFit2 levels were assessed in plasma from blood taken from tail cut and decapitation, respectively (see below). The open field, dark-light transition, and elevated plus maze behavioral tests were performed on treatment days 15, 16, and 17, respectively. The GTT was performed on treatment day 25 and the ITT on treatment day 29. Animals were sacrificed on day 31 following treatment onset; tissues were harvested and stored at  $-80^{\circ}\text{C}$  for further analyses.

## Indirect Calorimetry

Energy expenditure was assessed using indirect calorimetry (TSE PhenoMaster, TSE Systems, Bad Homburg, Germany). Briefly, animals were allowed to habituate to the indirect calorimetry cages for 48h before data were collected. Following 48 h of acclimatization, O<sub>2</sub> consumption and CO<sub>2</sub> production were measured every 5 min for a total of 68.5 h. Indirect calorimetry was performed at room temperature (experiment 1, cohort 1) and at  $30^{\circ}\text{C}$  (experiment 1, cohort 2). O<sub>2</sub> consumption (VO<sub>2</sub>, [ml/h]), CO<sub>2</sub> production (VCO<sub>2</sub>, [ml/h]), and heat production (referred to as total energy expenditure (TEE), [kcal/24h]) were calculated based on the Weir equations (Weir, 1949). The respiratory exchange ratio (RER) was calculated as the ratio of CO<sub>2</sub> produced to O<sub>2</sub>

consumed (CO<sub>2</sub>/O<sub>2</sub>). Home-cage locomotor activity was assessed by beam breaks using an ActiMot infrared light beam system within the calorimetry system.

## Assessment of Energy Expenditure Components

The delay in acquisition between indirect calorimetry measurements and instantaneous locomotor activity measurements was corrected using the deconvolution procedure (Speakman, 2013) and was performed using a two-compartment gas diffusion model (Van Klinken et al., 2012), which takes into account chamber washout characteristics. Following deconvolution, total energy expenditure (TEE, kcal/24) was decomposed into its activity-related energy expenditure (AEE) and resting metabolic rate (RMR). RMR was modelled in a time-dependent manner using a method based on penalized spline regression, allowing for the detection of up to four RMR frequency components per 24h (8 knots/24h) (Van Klinken et al., 2012). Cases were excluded if the correlation between the convoluted activity and TEE did not reach an arbitrary cutoff of  $r \geq 0.7$ . Model fit was assessed by visual inspection of the component analysis residuals.

## Intraperitoneal Glucose Tolerance Test (GTT)

An intraperitoneal injection of D-glucose (2 g/kg body weight) was delivered to fasted mice (14 h fast). Blood glucose levels were measured on blood collected by tail cut at 0, 30, 60, and 120 min intervals following the glucose load. Glucose levels were measured using a handheld Contour XT glucometer (Bayer Health Care, Basel, Switzerland). Plasma was also collected from blood at 0 and 30 min to assess fasting insulin and glucose-stimulated insulin levels, respectively.

## Intraperitoneal Insulin Tolerance Test (ITT)

Mice were fasted for 14 h and subsequently received intraperitoneal injections of 0.5 IU/kg body weight of D-glucose. Blood glucose levels were assessed from tail cuts at 0, 30, 60, and 120 min following the insulin load. Glucose levels were measured using a handheld Contour XT glucometer (Bayer Health Care, Basel, Switzerland).

## Behavioral Analyses

All behavioral tests were performed during 08:00 and 12:00 (Experiment 4). General locomotor activity was examined in an empty open field arena over 15 min under 15 lux illumination. Anxiety-related behaviors were assessed using the elevated plus maze and dark-light transition

tests as previously described (Schmidt et al., 2009). Each test was videotaped by an overhead camera and analyzed using the automated video-tracking software ANYmaze4.9 (Stoelting, Wood Dale, IL, USA).

#### Tissue Collection

Mice were anesthetized with isoflurane and immediately sacrificed by decapitation. Basal trunk blood was collected and subsequently processed (plasma was collected and stored at -20°C). Skeletal muscle (extensor digitorum longus (EDL) and soleus), WAT (inguinal (i), epididymal (e), and perirenal (p)), liver, and hypothalamus were collected and stored at -80°C until used.

#### Hormone Quantification

Plasma insulin levels were determined using a mouse metabolic magnetic bead panel (Millipore Corp. Billerica, Massachusetts; sensitivity: insulin 14pg/ml). For the assessment of fasting insulin levels, blood was collected 14 h following an overnight fast by tail cut. Similarly, glucose-stimulated insulin levels were measured from plasma taken from blood collected 30 min following glucose load during the glucose tolerance test.

#### SAFit2 Quantification

The concentration of the FKBP51 antagonist SAFit2 on day 10 and 30 of treatment was quantified from plasma by LCMS/MS. Briefly, plasma was analyzed using the combined high-performance liquid chromatography/mass spectrometry (HPLC/MS-MS) technique. Analysis was performed using an Agilent 1100 Series (Agilent, Waldbronn, Germany) liquid chromatograph which was interfaced to the ESI source of an Applied Biosystems API 4000 (ABSciex, Darmstadt, Germany) triple quadrupole mass spectrometer. All samples were added to Ostro protein precipitation and phospholipid removal plates (Waters, Eschborn, Germany). Deuterated clomipramine (Clomi-D3) was used as internal standard. Chromatography was performed using a gradient elution in an Accucore RP-MS 2,6µm column (2.1 x 50 mm, Thermo Scientific, Dreieich, Germany) at a flow rate of 0.3ml/min and 30 °C.

#### Cell Lines

C2C12 myoblasts were maintained in Dulbecco's modified Eagle's medium (DMEM) supplemented with 10% fetal bovine serum and 1x penicillin streptomycin antibiotics at 37 °C in

6

a humidified atmosphere with 5% CO<sub>2</sub>. Once the cells reached ~90% confluency, C2C12 myoblasts were infected with adeno-associated viral (AAV) vectors expressing either GFP control or shRNA against FKBP51. A multiplicity of infection (MOIs) of 5 x 10<sup>4</sup> was used. Cells were induced to differentiate 8 h after infection for 3 days before the examination of glucose uptake. Differentiation was induced by switching the growth medium to DMEM containing 2% horse serum for 3 days.

#### Glucose Uptake

Basal and insulin-stimulated glucose uptake in differentiated C2C12 myotubes was examined. Briefly, C2C12 myotubes were serum-starved in low glucose (1000 mg/L) DMEM for 4h, and then incubated in Krebs-Ringer-HEPES (KRH) buffer (136 mM NaCl, 4.7 mM KCl, 10 mM sodium phosphate buffer, 1 mM MgSO<sub>4</sub>, 1 mM CaCl<sub>2</sub>, 10 mM HEPES, pH 7.4, 0.2% BSA) for 10 min. Cells were stimulated with insulin (100 nM) or left unstimulated for 1h. Glucose uptake was induced by the addition of KRH buffer containing 100 µM 2-deoxy-D-[1,2-<sup>3</sup>H]glucose, 2 µCi/ml (Perkin Elmer) to each well. 4 minutes thereafter, the reactions were terminated by washing the cells with ice-cold PSB containing 10µM cytochalasin B (inhibitor of membrane transporter-dependent glucose transport), and then 2 additional washes with ice-cold 1x PBS. Cells were lysed with 0.1 M NaOH for 30 min, and the incorporated radioactivity was determined by liquid scintillation counting. 2-deoxy-D-[1,2-<sup>3</sup>H]glucose uptake was furthermore normalized to total protein content assessed by the BCA assay (BCA Protein Assay Kit, Life Technologies, Darmstadt, Germany).

#### Western Blot Analysis

Tissues were homogenized in lysis buffer containing 62.5 mM Tris-HCl, 2% SDS, and 10% sucrose supplemented with protease (Sigma, P2714) and phosphatase (Roche, 04906837001) inhibitor cocktails, and subsequently centrifuged at 12,00 x g to remove cell debris. Lysates were sonicated three times, and protein concentrations were measured using the BCA assay (BCA Protein Assay Kit, Life Technologies, Darmstadt, Germany). After dilution, protein samples (40 µg) were heated for 5 min at 95°C in loading buffer. Equal amounts of proteins were separated by SDS-PAGE and electro-transferred onto nitrocellulose membranes. Non-specific binding was blocked in Tris-buffered saline, supplemented with 0.05% Tween (Sigma, P2287) and 5% non-fat milk for 1 h at room temperature and subsequently blots were incubated with primary antibody

7

(diluted in TBS/0.05% Tween) overnight at 4 °C. For a list of primary antibodies used, please refer to **Supplementary Table 1**. The following day, blots were washed and probed with the respective horseradish peroxidase secondary antibody for 1 h at room temperature. Immunoreactive bands were visualized either using ECL detection reagent (Millipore, Billerica, MA, USA, WBK10500). Band intensities were evaluated with the ChemiDoc Imaging System (Bio-Rad).

### Quantification of Protein Data

The level of each phosphorylated protein was normalized to its respective non-phosphorylated protein. For total protein content, actin was used as an internal control.

### Statistical Analysis

Data were analyzed by Student's t-tests or ANOVA, where appropriate, using IBM SPSS Statistics 18 software (IBM SPSS Statistics, IBM, Chicago, IL, USA). Data were transformed for ANOVA to meet the assumption of homogeneity of variance when required (See **Supplementary Table 2**). Repeated measures ANOVA was used for all body weight progression, GTT, and ITT data, in which the degrees of freedom were corrected for deviance from sphericity (Greenhouse–Geisser) for within-subjects comparisons. A Bonferroni post hoc test was used for ANOVA tests to determine statistical significance between individual groups. The decomposition of TEE into AEE and RMR was performed in MATLAB (The MathWorks, Natick, MA, USA) using a custom-designed toolbox graciously provided by JB van Klinken (Bioinformatics Center of Expertise, Leiden University Medical Center, Leiden, The Netherlands). Body weight was included as a covariate in the analyses of energy expenditure (Arch et al., 2006). Statistical analyses for all energy expenditure outcome variables, RER, home-cage activity, food intake, water intake, and body temperature were performed on either 24-hour averages. Statistical significance was set at  $p < 0.05$ ; a statistical tendency was set at  $p < 0.1$ . For interactions at  $p < 0.1$ , we also examined lower order main effects. Data are presented as the mean  $\pm$  S.E.M.

### RESULTS

#### Genetic ablation of FKBP51 prevents HF diet-induced weight gain

In order to examine the role of FKBP51 in energy and glucose homeostasis we initially characterized the metabolic outcomes arising in FKBP51 knockout (51KO) mice. We found that 51KO mice fed a chow diet showed a modest body weight phenotype, and furthermore presented reduced adiposity and increased lean mass compared to wild-type (WT) littermates (Figure 1a). Strikingly, when challenged with HF diet exposure for 8 weeks, 51KO mice were protected from both HF diet-induced weight gain and increased adiposity (Figure 1b & c). Loss of FKBP51 likewise counteracted diet-induced obesity under thermoneutral conditions (30°C), arguing against a thermoregulatory basis of the phenotype (Supplementary Figure S1). Indirect calorimetry revealed that the HF diet resistant phenotype observed in 51KO mice was accompanied by a modest increase in total energy expenditure, as a result of an increased resting metabolic rate (RMR) (Figure S2). In addition, 51KO mice presented a modest decrease in their RER and an increase in their home-cage activity. By contrast, food intake was not affected by total loss of FKBP51. To confirm a lack of FKBP51 effect on feeding behavior, a separate pair-feeding experiment was performed, in which a cohort of WT mice was pair-fed to 51KO mice. This experiment again revealed no genotype effect on energy intake (Supplementary Figure S2). No additional outcomes of FKBP51 on energy homeostasis were identified using the comprehensive lab animal monitoring system (Supplementary Figure S2).

phenotype. During an insulin tolerance test, 51KO mice presented a prolonged response to insulin under control and HF dietary conditions, despite the fact that both 51KO and WT mice remained vulnerable to HF diet-induced insulin intolerance (Figure 2f – g).

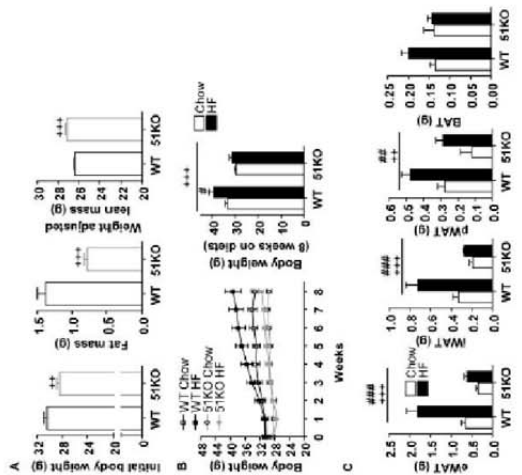
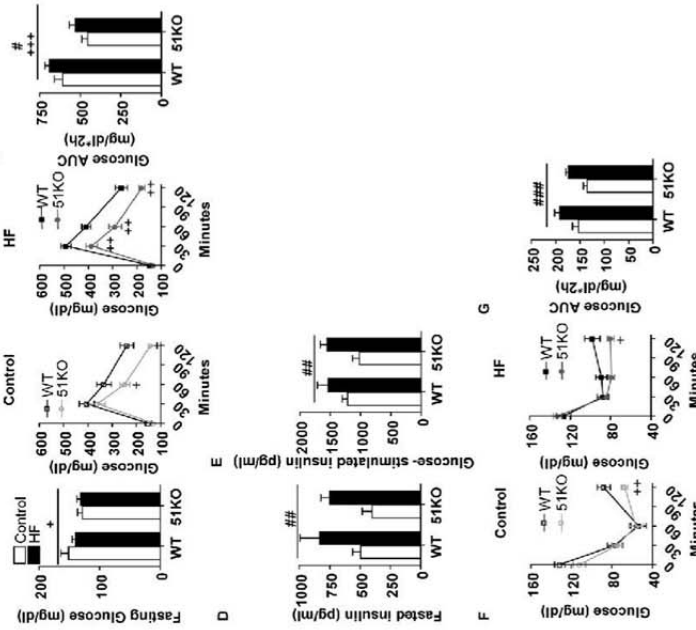


**Figure 1**

**Genetic ablation of FKBP51 improves glucose tolerance**

To determine the effects of FKBP51 on glucose metabolism and insulin sensitivity, we performed glucose tolerance and insulin tolerance tests in a separate cohort of 51KO and WT mice. Body weight data were consistent with our previous experiments (Supplementary Figure S3). FKBP51 deletion lowered fasting glucose (Figure 2a) and remarkably improved glucose tolerance under control and HF dietary conditions (Figure 2b – c). Interestingly, the levels of fasted insulin and glucose-stimulated insulin were not different between 51KO and WT mice (Figure 2d – e), indicating that differences in insulin secretion do not contribute to the improved glucose tolerance



**Genetic ablation of FKBP51 improves glucose tolerance.** (a) Blood glucose following a 14 h fast was significantly lower in 51KO mice compared to WT mice (b) In the GTT, a HF diet impaired glucose tolerance in WT mice but not in 51KO mice (c) The area under the glucose curve illustrates the effect of genotype and diet on glucose tolerance. (d, e) Fasted insulin and glucose-stimulated insulin were significantly elevated from HF diet exposure independent of genotype. (f) In HF diet-fed mice, loss of FKBP51 significantly reduced insulin tolerance. Importantly blood glucose remained significantly lower 120 min following insulin administration on account of FKBP51 deletion under both chow conditions and HF diet conditions. (g) The Area under the glucose curve for ITT demonstrates the strong diet effect and a trend for genotype. \*P < 0.05, \*\*P < 0.01, \*\*\*P < 0.001; #P < 0.05, ##P < 0.01, ###P < 0.001; + significant genotype effect; # significant diet effect; T significant trend for genotype.

**Pharmacological inhibition of FKBP51 parallels the metabolic effects resulting from genetic ablation of FKBP51**

Due to the improved metabolic phenotype of 51KO mice, we subsequently assessed the therapeutic efficacy of pharmacological blockade of FKBP51. Importantly, a highly selective antagonist for FKBP51, known as SAFit2, has recently been developed (Gaal et al., 2015; Hartmann et al., 2015). The authors described improved neurite outgrowth in neuronal cultures and improved stress coping behavior in mice from SAFit2 treatment, with possible therapeutic potential in the treatment of stress-related psychiatric disorders. In the current study, we determined the therapeutic efficacy of FKBP51 antagonism in mice on metabolic parameters. At first, SAFit2 (20mg/kg) was administered twice daily for 10 days to adult C57BL/6 mice by intraperitoneal injections under chow-fed conditions. Although 10 days of FKBP51 antagonism yielded no body weight phenotype, there was a marked lowering of glucose tolerance assessed on treatment day 8 (Figure 3a – b). To determine whether a longer treatment period was required to achieve a body weight phenotype, a second cohort of C57BL/6 mice were treated with SAFit2, this time for 30 days under both control and HF diet conditions. This injection schedule resulted in high SAFit2 plasma levels and minimal inter-animal variability (Supplementary Figure S4). At the onset of treatment, following 4 weeks of dietary exposure, there was no difference in body weight between treatment groups (Supplementary Figure S4). However, we found that 30 days of SAFit2 administration led to a reduction in body weight under both control and HF diet conditions (Figure 3c). Furthermore FKBP51 antagonism protected against HF diet-mediated glucose intolerance (Figure 3d). There was however no effect of SAFit2 on insulin tolerance or on locomotor activity tested in the open field (Supplementary Figure S4). Importantly, there were no unwanted side-effects of FKBP51 antagonism on behavioural readouts tested in the elevated plus maze and dark-light transition tests (Supplementary Figure S4). Taken together, these results clearly demonstrate that pharmacological blockade of FKBP51 phenocopies the effects of FKBP51 genetic ablation and furthermore demonstrate the therapeutic potential of SAFit2 in the treatment of obesity and T2D.

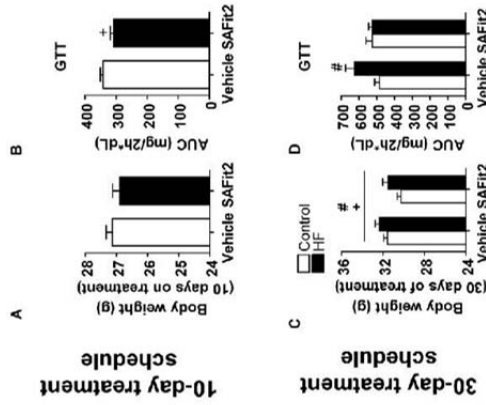


**Figure 3** Pharmacological inhibition of FKBP51 parallels the metabolic effects resulting from genetic ablation of FKBP51 (a) 10-day SAFit2 treatment had no significant effect on body weight. (b) Despite no effect on body weight, SAFit2 treatment significantly lowered glucose tolerance as reflected in the glucose AUC for the GTT measured on treatment day 8. (c) At the experimental end point (following 30 days of treatment), mice treated with SAFit2 weighed significantly less than their diet counterparts. Nevertheless mice fed the HF diet remained significantly heavier independent of treatment. (d) The extended SAFit2 treatment schedule furthermore protected against HF diet-induced impaired glucose tolerance as reflected in the glucose AUC measured on day 25. \*P < 0.05; + significant treatment effect; # significant diet effect.

**Loss of FKBP51 sensitizes insulin signaling and enhances glucose uptake**

To determine the mechanism by which FKBP51 may regulate glucose homeostasis and consequently glucose tolerance, we initially examined the phosphorylation status of critical nodes along the insulin signaling cascade as a marker of insulin signaling activation. As we found a strong effect of FKBP51 loss on glucose tolerance without any alterations of circulating insulin levels, we hypothesized that intracellular insulin signaling is enhanced following total loss of FKBP51. We found that insulin sensitivity (as reflected through the phosphorylation status of p70S6K, IRS-1, and AKT) was markedly increased in skeletal muscle of 51KO mice, whereas insulin activation in adipose tissue remained unchanged (Figure 4a – b). Indeed, skeletal muscle accounts for an estimated 80% of postprandial glucose disposal and is regarded as a principal site

modest body weight phenotype and a strong effect on glucose tolerance as early as 8 days following treatment onset. From these data, we conclude that FKBP51 is an integral component of energy and glucose homeostatic regulation, particularly in response to nutritional changes. The improved metabolic outcomes following systemic administration of a selective antagonist of FKBP51, SAFi2, offers new opportunities for drug development.

The effects of FKBP51 on body weight are likely driven by increases in RMR without compensatory increases in energy intake. Nevertheless, the present study does not allow one to identify the mechanism underlying the increased RMR. Rather the focus of the current study was to characterize the striking association in humans between single nucleotide polymorphisms with the *FKBP5* gene loci and traits related to T2D (Pereira et al., 2014). Our data highlight a fundamental role for FKBP51 in the regulation of glucose homeostasis. Glucose tolerance in 51KO is improved even in the absence of a strong body weight phenotype, under control diet settings. This suggests that the FKBP51-dependent improvement of glucose homeostasis is not secondary to body weight. In line with these findings, we found improved glucose tolerance from 10-day SAFi2 treatment, which was independent of changes in body weight. Furthermore, we found that loss of FKBP51 sensitizes the insulin signaling pathway. Interestingly, FKBP51-dependent effects on insulin signaling was highly tissue-specific, in which FKBP51-dependent increases in insulin signaling was limited to skeletal muscle. In this context, we also found that glucose uptake in mouse myotubes is enhanced on account of either FKBP51 knockdown or FKBP51 pharmacological blockade.

It has been previously shown that FKBP51 binds to AKT, a serine-threonine kinase within the insulin signaling cascade, to ultimately favour AKT inactivation (Pereira et al., 2014). Through this interaction, FKBP51 was associated with tumor growth and chemotherapy responsiveness. We have extended such previous findings by demonstrating that not only are AKT and downstream targets of AKT regulated in an FKBP51-dependent manner (reflected by the phosphorylation states of AKT and downstream effector proteins), but we have also demonstrated that FKBP51 exerts an effect on upstream signaling, whereby 51KO mice displayed enhanced activation of the insulin receptor substrate 1 (IRS-1). Within the insulin signaling pathway, the IRS-1 represents a critical node for the regulation of insulin sensitivity, and dysregulation at IRS-1 is often featured in T2D (Taniguchi et al., 2006). Tissue responsiveness to insulin in fact requires IRS-1 and IRS-2, which function to couple insulin receptor activation to the recruitment and activation of downstream signaling molecules including AKT (Copps and White, 2012). IRS-

15

responsible for the maintenance of glucose homeostasis (DeFronzo et al., 1985; Zierath and Wallberg-Henriksson, 2002). Therefore, as a natural next step we examined glucose uptake in differentiated C2C12 myotubes. Knockdown of FKBP51 in differentiated skeletal myotubes enhanced glucose uptake (Figure 4c). Importantly, inhibition of FKBP51 using SAFi2 similarly increased glucose uptake in C2C12 cells (Figure 4d). Finally, we ectopically overexpressed AKT2 within C2C12 cells, to observe (the expected) enhanced glucose uptake. When we simultaneously overexpressed both AKT2 and FKBP51, the enhanced glucose uptake arising from overexpressing AKT2 was reversed. Thus the beneficial effects of FKBP51 inhibition on glucose homeostasis require the insulin signaling pathway.

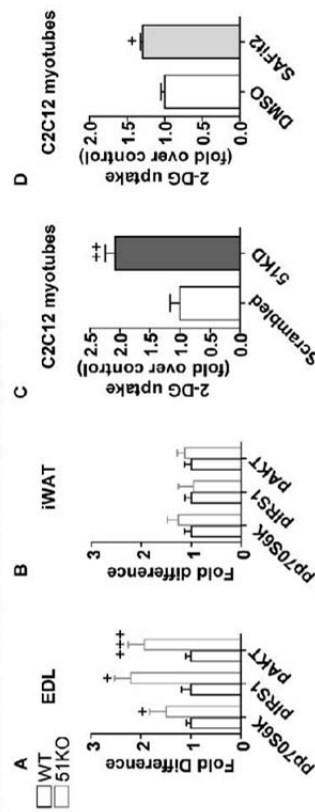


**Figure 4** Loss of FKBP51 sensitizes insulin signaling and enhances glucose uptake. (a) In EDL skeletal muscle of 51KO mice, insulin signaling was enhanced compared to WT mice as assessed by pAKT, pIRS1, and pp70S670 protein expression. (b) This outcome was specific for skeletal muscle, as protein expression was not changed in white adipose tissue (WAT) depots on account of genotype. (c) 2-deoxyglucose uptake is significantly enhanced in C2C12 myotubes in which FKBP51 has been knocked down. (d) Similarly, FKBP51 blockade with SAFi2 significantly enhanced 2-deoxyglucose uptake in C2C12 myotubes. Data are expressed as relative fold change compared to wild-type condition. \*P < 0.05, \*\*P < 0.01, \*\*\*P < 0.001; + significant genotype/treatment effect.

## DISCUSSION

Here we describe for the first time that loss of FKBP51 in mice protects against diet-induced obesity and markedly lowers glucose tolerance under both control and HF diet conditions. The effects of FKBP51 on glucose homeostasis are driven by enhanced insulin signaling within skeletal muscle and consequently heightened glucose disposal. Moreover, administration of a recently developed selective antagonist of FKBP51, SAFi2 (Gao et al., 2014), mimicked the metabolic phenotype arising from total genetic loss of FKBP51. FKBP51 blockade produced a

14

I contains over 50 possible serine-phosphorylation sites, whose phosphorylation status governs IRS-1 signaling. We specifically examined phosphorylation of serine-307 (S307), which has been shown to promote insulin sensitivity in mice (Coppes et al., 2010). Our data support this notion such that 51KO mice present increased S307 IRS-1 phosphorylation in skeletal muscle which is accompanied by enhanced downstream insulin signaling and improved glucose tolerance. An important question raised by this study is how exactly FKBP51 acts within distinct cellular/tissue environments to affect whole body energy and glucose homeostasis. Previous studies have already alluded to the importance of tissue-specific actions of FKBP51 (Toneatto et al., 2013; Hartmann et al., 2015). Here we extend our current understanding of the tissue-specific actions of FKBP51 to include FKBP51-dependent regulation of the insulin signaling exclusively within skeletal muscle. Despite microarray-based data demonstrating that skeletal muscle shows the second strongest expression profile of FKBP51 across all tissues examined (Su et al., 2004), to our knowledge, the current study is the first to define a skeletal muscle-specific role of FKBP51. These data, along with our FKBP51-dependent glucose uptake findings in cultured myotubes, suggest the possibility that targeted disruption of FKBP51 specifically within skeletal muscle may be sufficient to improve glucose homeostasis. Together, these findings define a novel role of FKBP51-dependent regulation of glucose uptake and whole body glucose homeostasis. In addition, the positive effects of FKBP51 pharmacological blockade on both body weight and glucose tolerance suggests a potential opportunity to employ FKBP51 antagonists for the treatment of obesity and T2D.

## References

- Arch.J.R., Hislop,D., Wang,S.J., and Speakman,J.R. (2006). Some mathematical and technical issues in the measurement and interpretation of open-circuit indirect calorimetry in small animals. *Int. J. Obes. (Lond)* *30*, 1322-1331.
- Coppes,K.D., Hanczer,N.J., Opare-Ado,L., Qiu,W., Walsh,C., and White,M.F. (2010). Irs1 serine 307 promotes insulin sensitivity in mice. *Cell Metab* *11*, 84-92.
- Coppes,K.D. and White,M.F. (2012). Regulation of insulin sensitivity by serine/threonine phosphorylation of insulin receptor substrate proteins IRS1 and IRS2. *Diabetologia* *55*, 2565-2582.
- DeFronzo,R.A., Gummarsson,R., Bjorkman,O., Olsson,M., and Wahren,J. (1985). Effects of insulin on peripheral and splanchnic glucose metabolism in noninsulin-dependent (type II) diabetes mellitus. *J. Clin. Invest* *76*, 149-155.
- Gaali,S., Kirschner,A., Cuboni,S., Hartmann,J., Kozany,C., Balsevich,G., Namendorf,C., Fernandez-Vizarra,P., Sippel,C., Zannas,A.S., Draenert,R., Binder,E.B., Almeida,O.F., Ruhter,G., Uhr,M., Schmidt,M.V., Touma,C., Bracher,A., and Hausch,F. (2014). Selective inhibitors of the FK506-binding protein 51 by induced fit. *Nat. Chem. Biol.*
- Gaali,S., Kirschner,A., Cuboni,S., Hartmann,J., Kozany,C., Balsevich,G., Namendorf,C., Fernandez-Vizarra,P., Sippel,C., Zannas,A.S., Draenert,R., Binder,E.B., Almeida,O.F., Ruhter,G., Uhr,M., Schmidt,M.V., Touma,C., Bracher,A., and Hausch,F. (2015). Selective inhibitors of the FK506-binding protein 51 by induced fit. *Nat. Chem. Biol.* *11*, 33-37.
- Hartmann,J., Wagner,K.V., Gaali,S., Kirschner,A., Kozany,C., Ruhter,G., Dedic,N., Hausl,A.S., Hoejmakers,L., Westerholz,S., Namendorf,C., Gerlach,T., Uhr,M., Chen,A., Deussing,J.M., Holsboer,F., Hausch,F., and Schmidt,M.V. (2015). Pharmacological Inhibition of the Psychiatric Risk Factor FKBP51 Has Anxiolytic Properties. *J. Neurosci.* *35*, 9007-9016.
- Pei,H., Li,L., Fridley,B.L., Jenkins,G.D., Kalari,K.R., Lingle,W., Petersen,G., Lou,Z., and Wang,L. (2009). FKBP51 affects cancer cell response to chemotherapy by negatively regulating Akt. *Cancer Cell* *16*, 259-266.
- Pereira,M.J., Palming,J., Svensson,M.K., Rizell,M., Dalenback,J., Hammar,M., Fall,T., Sidibeh,C.O., Svensson,P.A., and Eriksson,J.W. (2014). FKBP5 expression in human adipose tissue increases following dexamethasone exposure and is associated with insulin resistance. *Metabolism* *63*, 1198-1208.
- Ratajczak,T., Cluning,C., and Ward,B.K. (2015). Steroid Receptor-Associated Immunophilins: A Gateway to Steroid Signaling. *Clin. Biochem. Rev.* *36*, 31-52.

SUPPLEMENTARY DATA

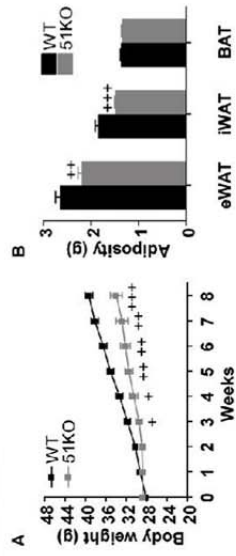


**Figure S1 Genetic ablation of FKBP51 protects against diet-induced obesity under thermoneutral conditions**  
 (a) Over 8 weeks of HF diet exposure at 30°C, 51KO mice are still resistant to HF diet-induced weight gain and (b) adiposity. Data are expressed as means ± s.e.m. \*P < 0.05, \*\*P < 0.01, \*\*\*P < 0.001; + significant genotype effect.

Schmidt, M.V., Sterlemann, V., Wagner, K., Niederleitner, B., Ganea, K., Liebl, C., Deussing, J.M., Berger, S., Schutz, G., Holsboer, F., and Müller, M.B. (2009). Postnatal glucocorticoid excess due to pituitary glucocorticoid receptor deficiency: differential short- and long-term consequences. *Endocrinology* 150, 2709-2716.

Speakman, J.R. (2013). Measuring energy metabolism in the mouse - theoretical, practical, and analytical considerations. *Front Physiol* 4, 34.

Su, A.I., Wiltshire, T., Batalov, S., Lapp, H., Ching, K.A., Block, D., Zhang, J., Soden, R., Hayakawa, M., Kreiman, G., Cooke, M.P., Walker, J.R., and Hogenesch, J.B. (2004). A gene atlas of the mouse and human protein-encoding transcriptomes. *Proc. Natl. Acad. Sci. U. S. A* 101, 6062-6067.

Taniguchi, C.M., Emanuele, B., and Kahn, C.R. (2006). Critical nodes in signalling pathways: insights into insulin action. *Nat. Rev. Mol. Cell Biol.* 7, 85-96.

Toneatto, J., Guber, S., Charo, N.L., Susperreguy, S., Schwartz, J., Galgiani, M.D., and Piwien-Pilipuk, G. (2013). Dynamic mitochondrial-nuclear redistribution of the immunophilin FKBP51 is regulated by the PKA signaling pathway to control gene expression during adipocyte differentiation. *J. Cell Sci.* 126, 5357-5368.

Tranguch, S., Cheng-Flynn, J., Daikoku, T., Prapapanich, V., Cox, M.B., Xie, H., Wang, H., Das, S.K., Smith, D.F., and Dey, S.K. (2005). Cochaperone immunophilin FKBP52 is critical to uterine receptivity for embryo implantation. *Proc. Natl. Acad. Sci. U. S. A* 102, 14326-14331.

Van Klinken, J.B., van den Berg, S.A., Havekes, L.M., and Willems Van D.K. (2012). Estimation of activity related energy expenditure and resting metabolic rate in freely moving mice from indirect calorimetry data. *PLoS. One*. 7, e36162.

WEIR, J.B. (1949). New methods for calculating metabolic rate with special reference to protein metabolism. *J. Physiol* 109, 1-9.

Zierath, J.R. and Wallberg-Henriksson, H. (2002). From receptor to effector: insulin signal transduction in skeletal muscle from type II diabetic patients. *Ann. N. Y. Acad. Sci.* 967, 120-134.

term (6h) cold exposure. (h) In a separate cohort of animals, a pair-feeding experiment was performed over 6 weeks to assess genotype-dependent effects on food intake. At the experiment onset, all mice were placed on a HF diet. 51KO control and WT ad libitum mice had free access to food, whereas WT PF were pair-fed to the 51KO mice. The WT PF group continued to gain weight despite pair-feeding. (i) At the end of the pair-feeding paradigm 51KO mice weighed significantly less compared to WT control mice. Data are expressed as means  $\pm$  s.e.m. \* $P < 0.05$ , \*\* $P < 0.01$ ; + significant genotype effect.

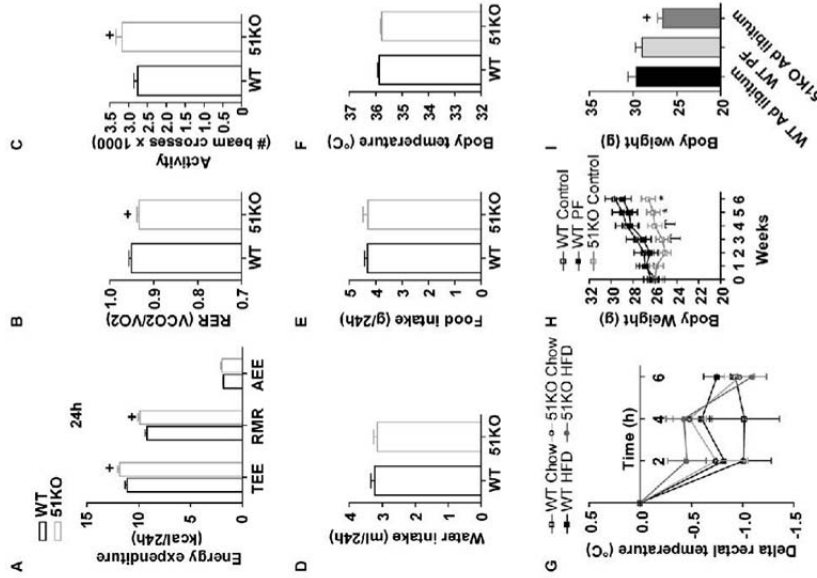


**Figure S2 Metabolic phenotype in 51KO transgenic mice.** Initially metabolic readouts were assessed in WT mice (n = 17) and 51KO mice (n = 16) under chow conditions in CLAMS (Comprehensive Lab Animal Monitor Systems). (a) When bodyweight was held constant, total energy expenditure (TEE) was higher in the chow-fed 51KO animals measured across 24h. Decomposition of TEE into its resting (RMR) and activity-related (AEE) components revealed that the observed TEE difference was due to increased RMR in the 51KO animals measured over 24h. AEE did not differ between genotypes as assessed across 24h. (b) Loss of FKBP51 furthermore decreased the average respiratory exchange ratio (RER) activity and (c) increased the average home-cage assessed across 24h. There was however no effect of genotype on either water consumption (d), food intake (e) or body temperature (f) assessed across 24 h. (g) A separate cohort of mice were examined for cold-induced rectal temperature changes following exposure to 4°C under control and HF diet conditions. Neither genotype nor diet had an effect on body temperature following short-

20

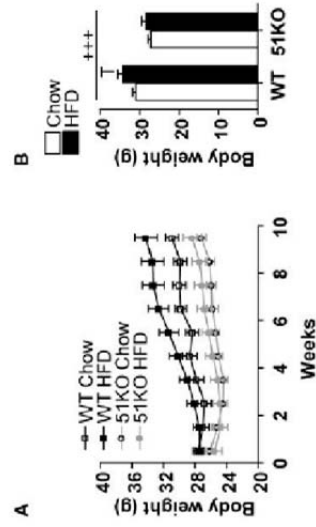


**Figure S3 Genetic ablation of FKBP51 prevents HF diet-induced weight gain observed across 2 independent experiments.** In an independent experiment used to assess glucose and insulin tolerance, 51KO mice presented the same body weight phenotype compared to WT mice as reported in Experiment 1. (a) 51KO mice weighed significantly less than WT mice throughout the 8 week dietary treatment and (b) at the experimental end. Furthermore, a tendency was observed indicating that WT mice were susceptible to HF diet-induced weight gain compared to 51KO mice as interpreted from body weight progression. \* $P < 0.1$ , +  $++P < 0.0001$ ; + significant treatment effect; T significant trend for diet.

21

TABLE LEGENDS

Primary Antibody	Dilution	Phosphorylation site	Company
AKT2	1:1000	/	CST, AKT2 (D5G4) Rabbit mAb #3063
IRS1	1:1000	/	CST, IRS-1 (S938) Rabbit mAb #2390
p70S6K	1:1000	/	CST, p70 S6 Kinase Antibody #9202
pAKT2	1:1000	S473	Ce-ll Signaling # 40758
pIRS1	1:1000	S307	CST, Phospho-IRS-1 (Ser307) Antibody #2381
pp70S6K	1:1000	T389	CST, Phospho-p70 S6 Kinase (Thr389) [108D2] Rabbit mAb #

Table 1 List of all primary antibodies

Measurement	Figure	Experiment	Transformation
24h RER	S2	1 (cohort 1)	Reciprocal
24h Fecal Energy	S2	1 (cohort 1)	Lg10
Final body weight	1	1 (cohort 1)	Lg10
eWAT	1	1 (cohort 1)	Lg10
iWAT	1	1 (cohort 1)	Lg10
Fasted insulin	2	3	Lg10

Table 2 Data transformations used to generate data with homogeneous variance. Data represented in all Figures reflect the non-transformed data.

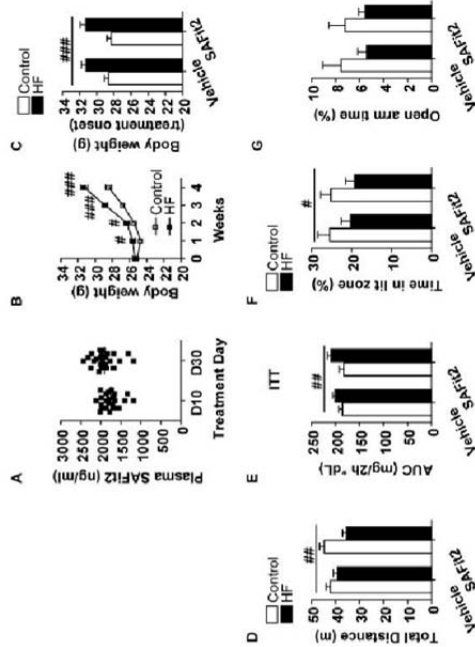


Figure S4 Metabolic phenotypes from pharmacological blockade of FKBP51 using SAFi2

(a) Administration of SAFi2 (twice daily at 20 mg/kg) by intraperitoneal injections resulted in high SAFi2 plasma levels and minimal inter-animal variability on day 10 and day 30 of treatment schedule. (b) 4 weeks before SAFi2 treatment onset, mice were randomly assigned to either the control diet or HF diet group. Exposure to the HF diet resulted in a significant increase in body weight progression (c) At treatment onset, mice were subdivided into treatment groups counterbalanced by body weight, and therefore within each dietary group there was no difference in body weight. (d) SAFi2 treatment had no effect on locomotor activity assessed as total distance traveled in an open field, although HF diet exposure significantly reduced locomotor activity. (e) Although insulin tolerance was significantly impaired by HF diet exposure, there was no improvement on account of SAFi2 treatment, demonstrated by the glucose AUC. (f, g) 30-day administration of SAFi2 had no undesirable behavioural side effects on anxiety-like behavior examined in both the dark-light transition test and the elevated plus maze test. By contrast, exposure to a HF decreased the time spent in the lit compartment of the dark-light test. Data are expressed as means  $\pm$  s.e.m. \* $P < 0.05$ , \*\* $P < 0.01$ ; # significant diet effect.

## B. Research Articles – Publication/Manuscript V

### 6.4. *Manuscript V*

**The FKBP51 antagonist SAFit2 decreases basal ultradian corticosterone secretion in the rat**– manuscript in preparation

(Francesca Spiga, Zidong Zhao, **Xixi Feng**, Felix Hausch, Stafford Lightman)

#### **Summary**

The ultradian rhythmicity of corticosterone secretion in rodents is regulated by feedback/feedforward interactions between pituitary ACTH and the adrenal CORT (corticosterone in rodents; cortisol in human beings), which leads to glucocorticoid receptor (GR) activation. Within this system the regulating role of GR in rats was analyzed by inhibiting FKBP51, a negative regulator of GR, with the FKBP51 selective antagonist SAFit2.

It was shown that SAFit2 treatment led to decreased basal and stress induced CORT secretion. Reduced ultradian CORT pulse amplitudes and inter-pulse intervals were observed after prolonged administration, suggesting that the ultradian rhythmicity is GR-mediated. Since diseases like depression and stress-related depressive disorders have been associated with elevated CORT levels, FKBP51 inhibition, by modulating basal CORT secretion, could be a therapeutic strategy for the treatment.

## B. Research Articles – Publication/Manuscript VI

### 7. Publication/Manuscript VI-VIII: Own publication

#### 7.1. Publication VI

#### Structure–Affinity Relationship Analysis of Selective FKBP51 Ligands

(Xixi Feng, Claudia Sippel, Andreas Bracher, Felix Hausch, *J. Med. Chem.* **2015**, 58, 7796-7806, doi: 10.1021/acs.jmedchem.5b00785)

#### Summary

In order to improve the drug-like properties of SAFit1 and 2 we started with an analysis of the structural requirements for FKBP51 selective ligands. Gaali et. al. discovered a cyclohexylring in the C9 position (Fig.2, Original Publication) as the key feature for high selectivity. We therefore developed a new series of ligands that all contained this moiety and discovered an asymmetric methyl-cyclohexyl group as the smallest possible structural feature for FKBP51 selective binding.

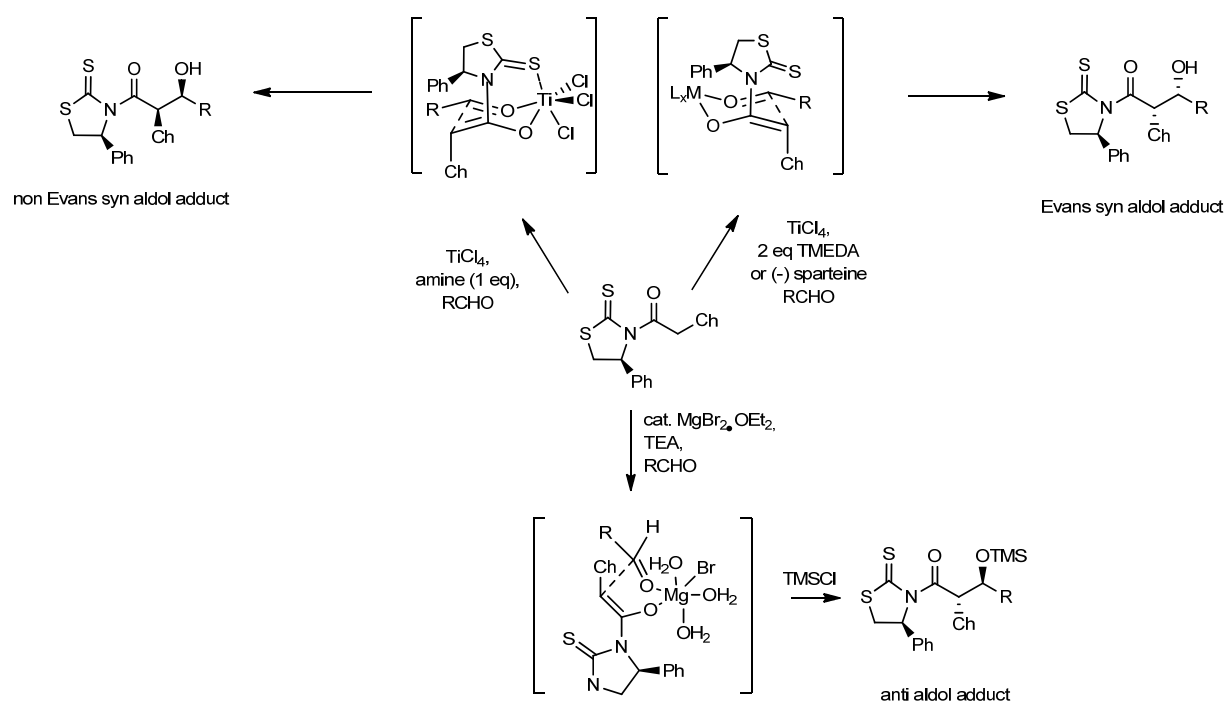
Using this finding as a starting point we introduced a hydroxyl group in the C10 position via an asymmetric aldol reaction and performed a structure affinity relationship analysis. In FK506 and a derived ligand series by Gopalakrishnan et. al. a hydroxyl group in a similar position was engaged in a hydrogen bond with Asp68, which we were trying to reproduce. Unfortunately, the crystal structure of the best ligand in this series didn't confirm this. Instead, we were delighted to discover that we were able to reproduce the induced fit binding mode and that substitution in this position does not influence selective binding, which is a useful finding for further drug optimization.

The publication represents the first structure-affinity relationship analysis on FKBP51 selective ligands after discovery of the induced fit binding mechanism.

## B. Research Articles – Publication/Manuscript VI

### An asymmetric aldol reaction as key synthesis step

The central step in the synthesis of all SAFit-type ligands is the coupling step between the pipercolic acid top group ester (s. abstract) and a carboxylic acid (“Bottom Group”). In order to obtain a carboxylic acid building block that contained the cyclohexyl as well as the hydroxy group in a specific stereochemistry the chiral auxiliary-mediated aldol addition seemed to be the perfect reaction. We chose an Evans type (*S*)-benzylthiazolidinethione auxiliary since high diastereoselectivities can be achieved and the cleavage can be conducted under milder conditions than the classic oxazolidinones auxiliaries.<sup>42</sup>



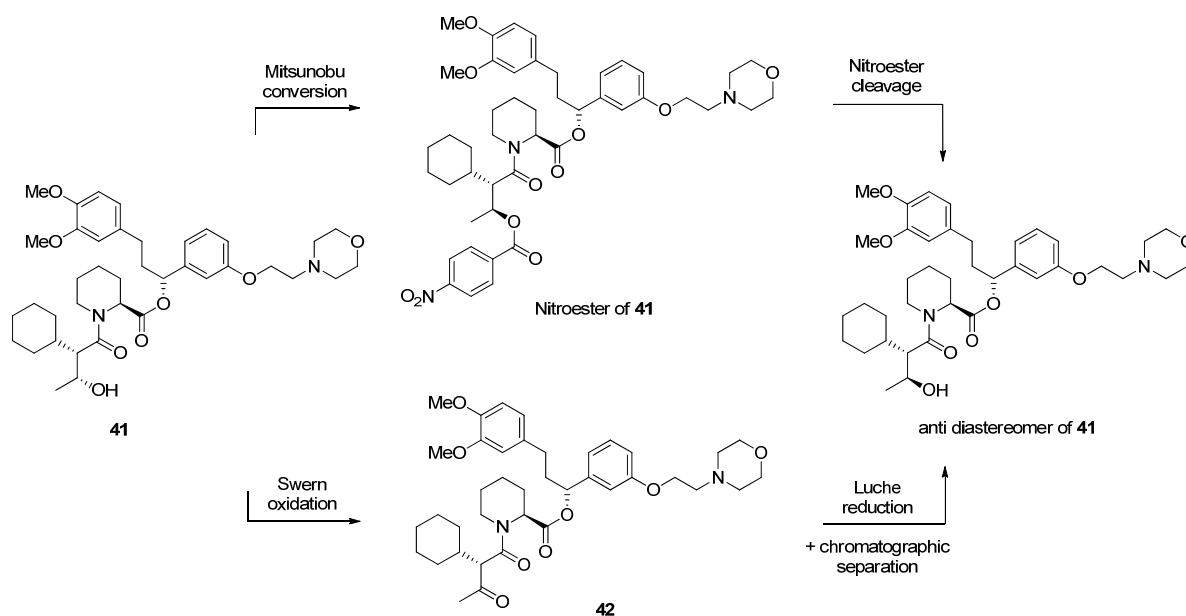
**Scheme 2:** Proposed transition states of the chiral auxiliary-mediated syn and anti aldol reactions. Adapted from Crimmins et al.<sup>42</sup> and Evans et al.<sup>43</sup>.

Scheme 2 shows the versatility of this type of reaction. Starting from the same *n*-acyl thiazolidinethione and aldehyde it is theoretically possible to obtain three specific diastereomers, whereby we were only interested in the Evans syn aldol adduct and the anti aldol adduct, due to the stereochemistry of the cyclohexyl ring. We used different aldehydes and synthesized a series of Evans syn aldol adducts with a method developed by Crimmins et al.<sup>42</sup> In all reactions only one major diastereomer was isolated. By slightly changing the reaction conditions, in fact only the equivalents of the base, it would also be possible to obtain the non Evans aldol adduct. Although the reaction conditions are very similar, the proposed transition states differ significantly. Addition of 2 eq base seems to inhibit the chelation of the

## B. Research Articles – Publication/Manuscript VI

thiocarbonyl, which happens during formation of the non Evans syn aldol adduct. It is supposed that this is caused by the amine coordinating to the titanium. Although direct conversions of thiazolidinethiones to amides are described with primary<sup>42</sup> and secondary<sup>44</sup> amines we observed no reaction when we conducted this step with pipercolic ester **36** (Orig. Publ.). We assume that this is caused by the low nucleophilicity of the pipercole nitrogen and the sterically demanding cyclohexyl group. The latter one is also the reason why a very mild cleavage method<sup>45</sup> with H<sub>2</sub>O and DMAP to obtain the carboxylic acid did not work. In the end, the auxiliary was cleaved with the classic LiOOH method<sup>46</sup>.

Though starting with the same reactants, but different reagents, the anti aldol product is formed via a complete different transition state. It is assumed that the Mg center is not coordinating to the thiocarbonyl and a boat-metal transition structure is suggested. Only this would explain, why a (Z) metal enolate can lead to an anti aldol product. Interestingly, a Mg-catalyzed anti aldol reaction with N-acyloxazolidinones leads to the complementary adducts.<sup>47</sup> In this publication Evans et al.<sup>47</sup> also mention that a current limitation of the procedure is  $\beta$ -branched substituents, which would include our cyclohexylacetyl residue. We hoped we could circumvent this problem by using the thiazolidinethione auxiliary, since it also worked in the syn-aldol series. Unfortunately, this was not the case. No product conversion was observed using the described reaction conditions. Attempts to obtain the desired anti product via a boron enolate, a method described by Walker et al.<sup>48</sup>, were also not successful.



**Scheme 3:** Theoretically proposed synthetic strategies for the synthesis of the anti diastereomer of **41**.

## B. Research Articles – Publication/Manuscript VI

We then decided to use the best syn aldol product from our ligand series (**41**, Orig. Publ.) as starting point to obtain the corresponding anti-diastereomer (Scheme 2). The Mitsunobu reaction was performed with **41** and p-nitrobenzoic acid, since the resulting ester can be cleaved under mild conditions<sup>49</sup>. After the reaction several peaks with the same mass that either corresponded to the p-nitrobenzoic ester or the elimination product were obtained in the LCMS. We assume that the reaction conditions induced deprotonation and thus racemization and elimination of the hydroxyl stereocenter, leading to a mixture of different undesired products. The same problem occurred, when we tried to convert the respective intermediate (**25**, Org. Publ.) that was obtained after aldol reaction.

In our next attempt **42** (Org. Publ.) was reduced under Luche conditions<sup>50</sup> in order to obtain a mixture of the desired compound and **41**. Chromatographic separation should then provide the desired anti-diastereomer. As already suspected the reaction did not lead to a 1:1 mixture of both diastereomers. HPLC analysis showed one major peak and one minor peak (~ 5 %), whereby we assign the syn-diastereomer with the major peak after comparing the retention time. Unfortunately, the defined position of the cyclohexylring seems to only favor the formation of the (*R*)-hydroxy group, leading to the syn-product that we already obtained from the aldol reaction. A formation of the (*S*)-hydroxy group is sterically more hindered since the hydrogen would have to attack from the side the cyclohexyl ring is pointing towards.

In the end, the synthesis of the anti diastereomer of **41** could not be realized and the influence of this single hydroxyl group on the binding affinity still remains an open question.

Reproduced with permission from Journal of Medicinal Chemistry. Copyright 2015 American Chemical Society.

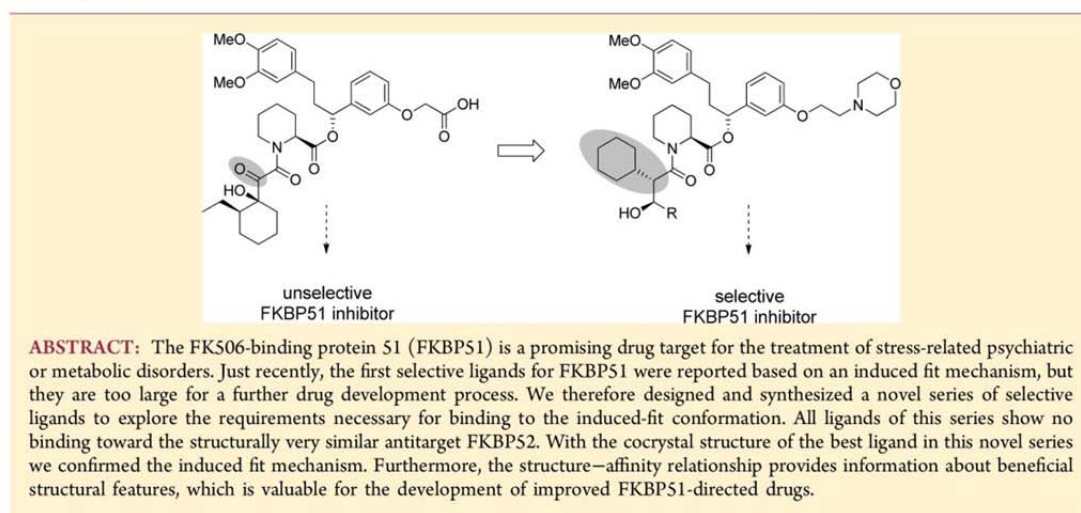
## Structure–Affinity Relationship Analysis of Selective FKBP51 Ligands

Xixi Feng,<sup>†</sup> Claudia Sippel,<sup>†</sup> Andreas Bracher,<sup>‡</sup> and Felix Hausch\*<sup>†</sup>

<sup>†</sup>Department of Translational Research in Psychiatry, Max Planck Institute of Psychiatry, Kraepelinstrasse 2, 80804 Munich, Germany

<sup>‡</sup>Max Planck Institute of Biochemistry, Am Klopferspitz 18, 82152 Martinsried, Germany

### Supporting Information



### INTRODUCTION

FKBP51 plays an important role in stress biology. It is robustly induced by stress, and it regulates stress hormone systems. FKBP51 knockout mice showed enhanced active stress-coping behavior after stress and were protected on the endocrine level from hyperactive stress responses, likely due to an improved feedback regulation of the hypothalamus–pituitary–adrenal axis.<sup>1–4</sup> Also in humans, FKBP51 and its encoding gene FKBP5 have been associated with the stress system, especially with the pathology of stress-related disorders like depression or post-traumatic stress disorder. Genetic variations of FKBP5, leading to an upregulation of FKBP51, were linked to a susceptibility for these diseases.<sup>5,6</sup> FKBP51 is also strongly expressed in adipocytes<sup>7</sup> and in several cancers.<sup>8,9</sup> In line with these results FKBP51 reduction was shown to protect from weight gain after a high fat diet<sup>10</sup> and to reduce chemoresistance in malignant melanoma.<sup>11–13</sup> Pharmacological FKBP51 inhibition could hence be a novel treatment for these diseases, suggesting FKBP51 as a promising drug target.<sup>14–16</sup>

A key issue in FKBP51 drug development is selectivity against its closest homolog FKBP52.<sup>17</sup> Unselective binding must be avoided, since an inhibition of FKBP52 has exactly the opposite effects compared to FKBP51 inhibitors in neuronal cells.<sup>18</sup> Moreover, studies with FKBP52 knockout mice revealed highly undesirable effects of FKBP52 deficiency on the endocrine system.<sup>19,20</sup> Female FKBP52 knockout mice were

complete sterile, and male mice displayed a compromised development of sex organs.<sup>21–24</sup> Notably, the active sites of FKBP51 and FKBP52 are highly homologous<sup>25–27</sup> and all ligands known before 2014,<sup>1,7</sup> such as prototypical FK506 (Figure 1), bind with virtually the same binding affinities to both proteins.

Very recently we discovered that an additional substituent in the C<sup>9</sup>-position of piperolate-based FKBP ligands stabilizes a novel cavity in the binding pocket of FKBP51 (Figure 1).<sup>18</sup> This ligand-induced rearrangement is energetically less favorable in FKBP52 due to sequence differences remote from the primary binding site.

The most advanced ligands of the FKBP51-selective iFit series, SAFit1 and SAFit2, both contained a cyclohexyl group as the additional C<sup>9</sup> substituent. SAFit2 was moderately blood–brain permeable and allowed the first pharmacological studies for FKBP51 in vivo. In several animal models SAFit2 showed clear antidepressant-like<sup>18</sup> and anxiolytic effects.<sup>28</sup> However, SAFit1 and SAFit2 suffered from poor physicochemical properties. Especially the high molecular weight of SAFit1 and SAFit2 (748 and 802 g/mol, respectively) is far outside the typical range of CNS-directed drugs.<sup>29,30</sup>

Received: June 11, 2015

Published: September 30, 2015

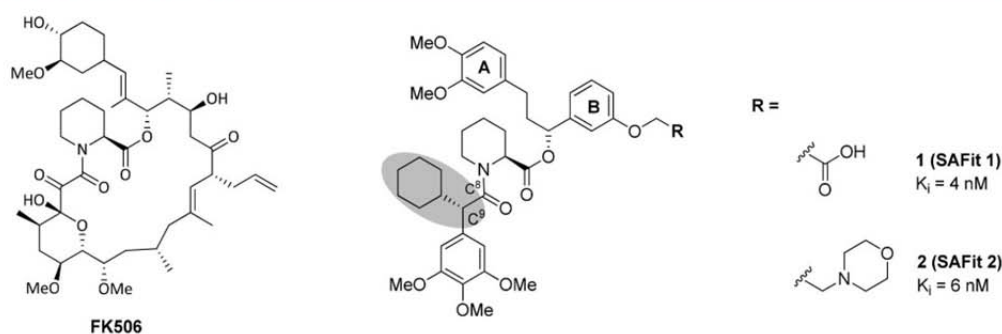
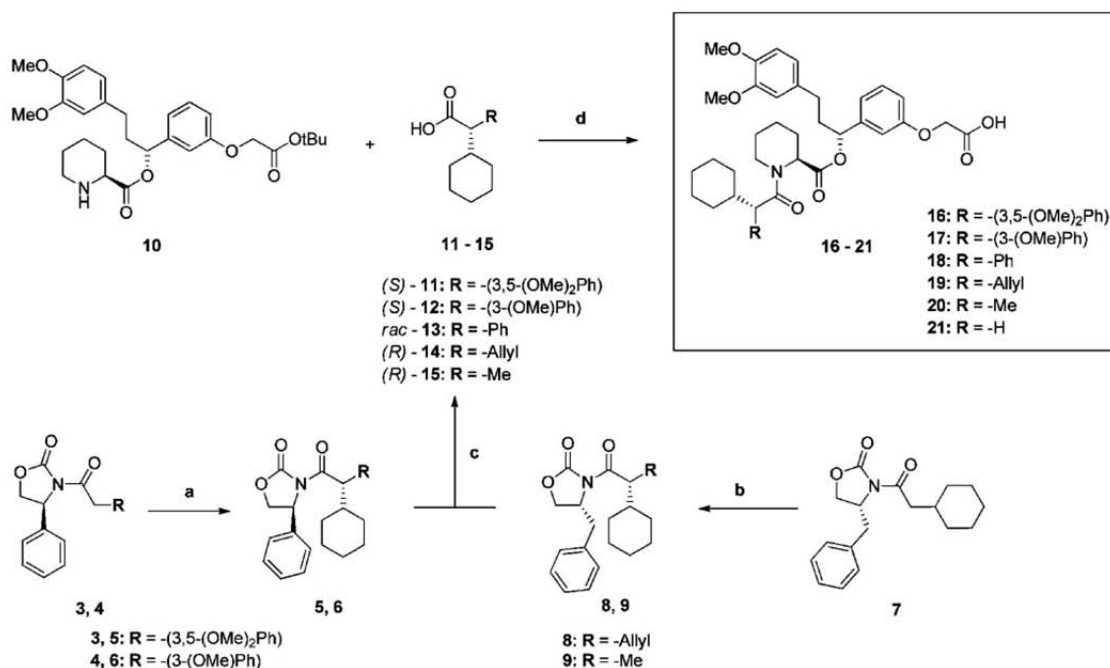


**Figure 1.** Chemical structures of FK506 and of the FKBP51-selective ligands SAFit1 (1), SAFit2 (2), and their binding affinities toward FKBP51. The cyclohexyl moiety in the C<sup>9</sup> position that induces the FKBP51-selective conformation is highlighted as gray shadows.

### Scheme 1. Synthesis of 16–21<sup>a</sup>



<sup>a</sup>Reagents and conditions: (a) NaHMDS, THF, 3-bromocyclohex-1-ene, then Pd–C, H<sub>2</sub>, MeOH; (b) NaHMDS, THF, MeI (for 9) or AllylBr (for 8); (c) LiOH, H<sub>2</sub>O<sub>2</sub>, THF/H<sub>2</sub>O; (d) COMU, DIPEA, DMF, then TFA, DCM.

The aim of this study was to gain better understanding of the FKBP51 binding pocket and the requirements for the induced-fit binding mode in particular. We designed a novel selective ligand series, focusing on a replacement of the trimethoxyaryl substituent of iFit ligands.

## RESULTS AND DISCUSSION

**Structure–Affinity Relationship (SAR) of a New FKBP51-Selective Ligand Series.** During the discovery of SAFit2 the cyclohexyl ring was found to be the most critical structural feature for high selectivity against FKBP52. Replacing it with smaller substituents led to a significant loss of both selectivity and binding affinity. We were therefore interested to see how different substituents in place of the neighboring trimethoxyphenyl ring would influence these properties. In the crystal structure of the SAFit2 analog iFit4 the trimethox-

ylphenyl moiety engages in several van der Waals contacts with FKBP51 as well as in an intramolecular edge-to-face stacking with the B-ring of the 1,3-diarylpropyl ester moiety (PDB code 4TW8<sup>18</sup>).

To perform a systematic structure–affinity relationship analysis of this substituent, we gradually replaced the trimethoxyphenyl ring by smaller residues. The new residues were introduced into the final compounds via the carboxylic acid building blocks 11–15, which were coupled to pipercolic ester 10 followed by <sup>t</sup>Bu deprotection (Scheme 1).

To obtain 18, commercially available racemic 13 was used and 18 was thus tested as a 1:1 diastereomeric mixture. 21 was synthesized by acetylation of the pipercolic ester 10 with cyclohexylacetyl chloride and subsequent deprotection of the <sup>t</sup>Bu group. For the synthesis of 16, 17, 19, 20 the carboxylic acid building blocks 11, 12, 14, 15 were synthesized via

stereoselective alkylation directed by an Evans auxiliary<sup>31</sup> and subsequent cleavage of the auxiliary (Scheme 1).

The affinities of the final compounds to FKBP51, FKBP52, and FKBP12 were determined by a fluorescence polarization (FP) assay (Table 1). The removal of the methoxy group in the

**Table 1.** FKBP Binding Affinities of C<sup>9</sup>-Trimethoxyaryl SAFit1 (1) Analogs

Entry	R	FKBP51 <sup>a</sup> K <sub>i</sub> [μM]	FKBP52 <sup>a</sup> K <sub>i</sub> [μM]	FKBP12 <sup>a</sup> K <sub>i</sub> [μM]
1		0.004 <sup>b,c</sup>	> 50	0.09
16		0.11 <sup>b</sup>	> 50	0.6
17		0.16 <sup>b</sup>	> 100	1.2
18 <sup>d</sup>		0.6	> 500	0.9
19		3.4	> 500	1.0
20	Me	1.2	> 1000	6.8
21	H	4.2	9.7	0.3

<sup>a</sup>K<sub>i</sub> values were determined by a competitive fluorescence polarization assay.<sup>33</sup> <sup>b</sup>iFit-FL<sup>18</sup> was used as tracer; <sup>c</sup>Adapted from Gaali et al.<sup>18</sup> <sup>d</sup>Mixture of C<sup>9</sup>-diastereomers was tested.

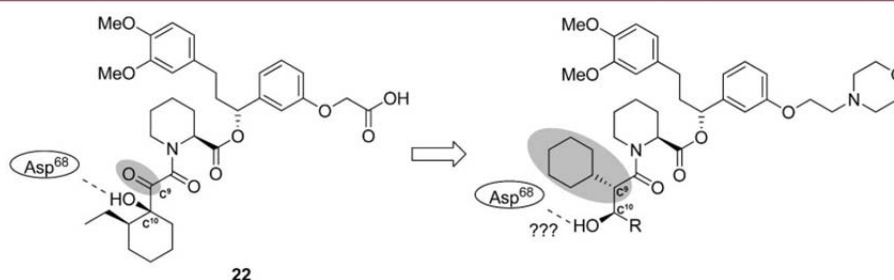
para position led to an almost 30-fold loss in binding affinity (1 → 16) for FKBP51 (K<sub>i</sub> = 0.11 μM) and a 6-fold reduction for FKBP12. This was surprising, since this methoxy group engaged only in moderate van der Waals contacts with Lys121 and intramolecularly with the B ring in cocrystal structures of SAFit1 analogs with FKBP51. When we further removed one meta-methoxy group, leading to the mono-methoxy SAFit1 derivative 17, we observed only a slight reduction of the binding affinity (K<sub>i</sub> = 0.16 μM). This suggests

that one of the meta-methoxy groups contributed comparatively little to the overall binding affinity. In contrast, a removal of all methoxy groups (1 → 18) led to a 100-fold loss in binding affinity for FKBP51 (K<sub>i</sub> = 0.6 μM) and a 10-fold reduction for FKBP12. FKBP12 is the most abundant FKBP isoform in most cells, and discrimination against FKBP12 will likely be important for improved pharmacological studies of FKBP51. Interestingly, removal of the arylmethoxy groups affected the affinity to FKBP12 and FKBP51 to different extents. This suggests that variation of the aryl substituents might be one strategy to fine-tune the selectivity between FKBP12 and FKBP51. As for all previous C<sup>9</sup>-branched analogs, no binding to FKBP52 could be detected.

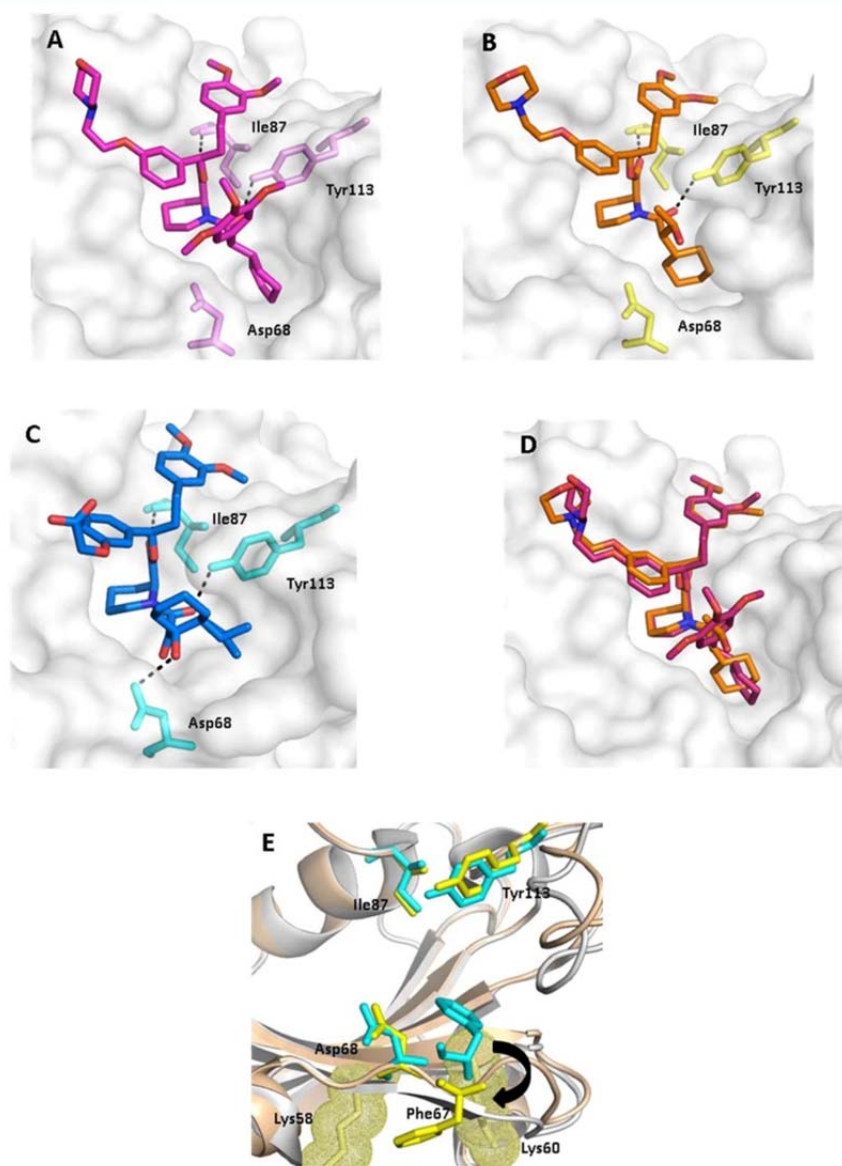
A further reduction of the substituent size to allyl (19) and methyl (20) led to a further decrease of the binding affinities to K<sub>i</sub> = 3.4 μM and K<sub>i</sub> = 1.2 μM, respectively. Interestingly, when we removed the second C<sup>9</sup>-substituent completely, the resulting compound 21 bound with similar affinity to FKBP51 (K<sub>i</sub> = 4.2 μM) and to FKBP52 (K<sub>i</sub> = 9.7 μM). We thus postulate that for compound 21 the cyclohexyl ring adopts a position previously occupied by the trimethoxyphenyl ring (see Figure 3). In this conformation, 21 does not interfere with Phe67 of FKBP51 and FKBP52 and thus can bind to both proteins, as observed previously for cyclohexyl-substituted diketoamide pipercolates.<sup>32</sup> At least a methyl group seems to be necessary at C<sup>9</sup> to direct the cyclohexyl ring into a Phe67-displacing conformation.

On the basis of these encouraging findings, we decided to explore the potential of the pro-(R)-C<sup>9</sup> substituent in more detail. FK506<sup>26,34</sup> and synthetic analogs thereof, such as 22,<sup>32</sup> have a hydroxyl group in the C<sup>10</sup> position, which forms a hydrogen bond with Asp68 of FKBP51 (Figure 2). We were therefore interested to see whether a similar hydrogen bond can form for FKBP51-selective iFit analogs as well.

To introduce the C<sup>10</sup>-hydroxyl group in a stereospecific manner, we employed a Crimmins-type aldol reaction, which yielded exclusively the syn-aldol product (Scheme 2).<sup>35</sup> The resulting hydroxy group was then protected with MOMCl, and the auxiliary was removed. Alternatively, the auxiliary was first cleaved followed by TBS protection of the hydroxyl group. The obtained building blocks 30–34 were then coupled to the pipercolate ester 36<sup>36</sup> to provide the final compounds 37–47 after deprotection and further derivatization. 38 was derivatized by acetylation with acetic anhydride in the presence of a base to provide 39. 42 was obtained by oxidation of 41 under Swern conditions.



**Figure 2.** Framework for novel C<sup>10</sup>-derivatized FKBP51 ligands, inspired by  $\alpha$ -ketoamide 22. The potential hydrogen bond to Asp68 of FKBP51 is indicated as a dotted line. The FK506-derived  $\alpha$ -ketoamide and the FKBP51 selectivity-inducing cyclohexyl moiety at C<sup>9</sup> are highlighted as gray shadows.

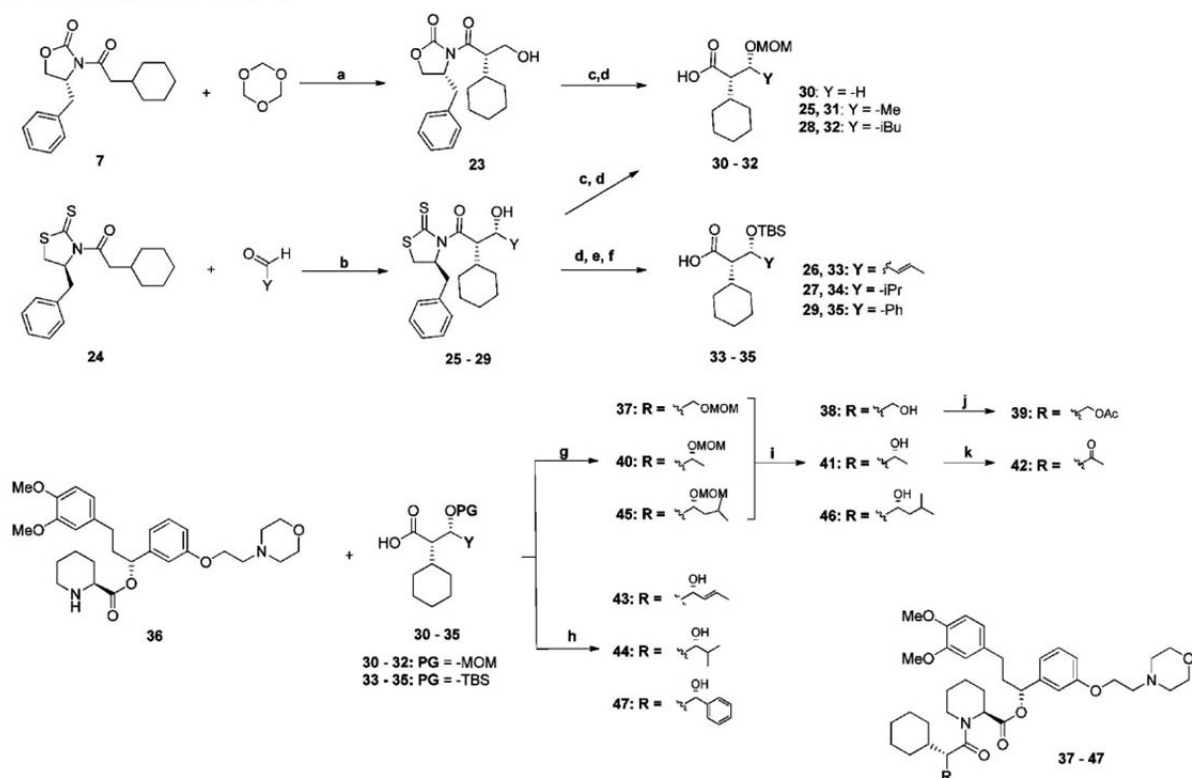


**Figure 3.** X-ray structures of different ligands in complex with the FK506-binding domain of FKBP51. Lys121 is not shown for clarity. Hydrogen bonds to Tyr113, Ile87, and Asp68 are indicated as black dotted lines. (A) Surface representation of FKBP51 in complex with FKBP51-selective iFit4 (magenta; 4TW7). (B) Surface representation of FKBP51 in complex with FKBP51-selective **41** (orange, SDIT). (C) Surface representation of FKBP51 in complex with unselective **22** (dark blue; 4DRN). (D) Surface representation of FKBP51 in complex with **41** (orange). iFit4 bound to FKBP51 is superimposed in magenta. (E) Active site residues in the crystal structures of FKBP51 (yellow; backbone of FKBP51 is shown as light brown cartoon) in complex with **41**. The structure of the FKBP51–**22** complex is superimposed as gray cartoon with the active site residues highlighted in cyan (**41** and **22** not shown for clarity). The flip of Phe67 is indicated by a black arrow. Residues Lys58 and Lys60 that are important for stabilizing the Phe67-out conformation are indicated as dotted yellow envelopes.

The binding assay (Table 2) revealed that a simple hydroxymethyl group (**38**) does not affect the affinity toward FKBP51. Similar results were obtained for the methoxymethyl and acetylated derivatives **37** and **39**, suggesting that the C<sup>10</sup>-hydroxyl group in **38** did not behave as an important hydrogen bond donor. In contrast, compound **41**, containing an additional methyl group at the C<sup>10</sup> position, showed a slightly improved binding affinity of 0.7  $\mu\text{M}$ . However, after removal of the hydrogen bond donor of **41** by methoxymethyl

derivatization (**40**) or by oxidation of the hydroxyl group to a ketone (**42**) this slight increase in affinity was not maintained.

Upon further increasing the size of the C<sup>10</sup>-substituent, we noticed a decrease in binding affinity. While compound **43**, derived from crotonaldehyde, still retained a moderate binding affinity of  $K_i = 1.1 \mu\text{M}$ , the affinities of **44** and **46**, containing an isopropyl and an isobutyl group, respectively, dropped about 10-fold to 13 and 9  $\mu\text{M}$ . Compound **45**, the methoxymethyl derivative of **46**, showed a 2-fold loss of binding affinity

Scheme 2. Synthesis of 37–47<sup>a</sup>

<sup>a</sup>Reagents and conditions: (a)  $\text{TiCl}_4$ , DIPEA, DCM; (b)  $\text{TiCl}_4$ , TMEDA, DCM; (c) MOMCl, DIPEA, DCM; (d) LiOH,  $\text{H}_2\text{O}_2$ , THF/ $\text{H}_2\text{O}$ ; (e) TBSOTf, lutidine, DCM; (f)  $\text{K}_2\text{CO}_3$ , MeOH/ $\text{H}_2\text{O}$ /THF; (g) PyBrop, DIPEA, DCM; (h) PyBrop, DIPEA, DCM, then HCl, EtOH; (i) HCl, EtOH; (j) TEA,  $\text{Ac}_2\text{O}$ ; (k)  $(\text{COCl})_2$ , DMSO, TEA, DCM.

compared to the free alcohol, similar to the trend observed for 38/37 and 41/40. Introduction of a phenyl ring at C<sup>10</sup> as in compound 47 abolished binding to FKBP51, indicating the size limitation of the substituent in this position.

Strikingly, none of the novel FKBP51 ligands showed any detectable binding to FKBP52, indicating that the selectivity for FKBP51 over FKBP52 is not affected by the substitution pattern in the C<sup>10</sup> position.

**Cocrystal Structure of 41.** To elucidate the binding mechanism of this novel series of selective FKBP51 ligands, we solved the cocrystal structure of the ligand 41 in complex with FKBP51 (Figure 3B) and compared it to related FKBP51 structures, the complex with the unselective ligand 22 (Figure 3C)<sup>32</sup> and with the selective ligand iFit4 (Figure 3A).<sup>18</sup>

In the cocrystal structure the common 1,3-diarylpropyl pipercolic ester moiety of 41 adopts nearly the same position as for 22 and iFit4 (Figure 3D). The pipercolate core sits in a conserved hydrophobic pocket formed by Tyr57, Phe77, Val86, Ile87, W90, and Phe130. Two hydrogen bonds between Ile87 and the C<sup>1</sup> carbonyl of 41 and between the C<sup>8</sup>-carbonyl of 41 and Tyr113 are formed. These hydrogen bonds are observed in all FKBP51 complexes with carbonyl pipercolate-based ligands so far.<sup>18,32,36–39</sup> However, a dipolar contact between the C<sup>1</sup> carbonyl and Tyr113, which has been observed for many pipercolate-based FKBP51 ligands, is absent in the complex with 41.

The cyclohexyl ring sits in a hydrophobic pocket formed by Gly59, Lys60, Leu61, Lys66, Asp68, and Ile122. In contrast to iFit4, however, 41 adopts a different conformer by rotation around the C<sup>9</sup>-cyclohexyl bond. As observed for iFit4 the cyclohexyl ring displaces Phe67 compared to the apo structure (Figure 3E), resulting in contacts to Lys58 and Lys60. These two positions differ in sequence between FKBP51 and FKBP52, and these residues have been shown to govern the differential ability to adopt the Phe67-out conformation.<sup>18</sup> As in the FKBP51 complexes with iFit1 and iFit4 the hydrogen bond between the amide of Phe67 to the carbonyl of Gly59, which enables the Phe-in conformation, is replaced by a hydrogen bond between the amide of Asp68 to Gly59, thus continuing the canonical  $\beta$ -strand by one residue. This switch in the hydrogen bonding pattern has been suggested to underlie FKBP51-specific dynamics recently observed by NMR.<sup>40,41</sup> Unlike the FKBP51-iFit4 structure, the carbonyl of Lys66 does not form a hydrogen bond with the amide of Leu61. Instead the remodeled  $\beta 2$ - $\beta 3$  loop matches almost perfectly the conformation observed for in the FKBP51-iFit1 complex (4TW6). The C<sup>10</sup>-methyl group of 41 engages in an intramolecular van der Waals contact with the B-ring of the 1,3-diarylpropyl ester, whereas the chiral hydroxyl group contacts the side chain of Lys121. No hydrogen bond between the hydroxyl group and Asp68 could be observed (measured distance 4.4 Å).

Table 2. FKBP51 Binding Affinities of Aldol Reaction-Derived Products and Derivatives (SAFit2 (2) Analogs)<sup>a</sup>

Entry	R	FKBP51 K <sub>i</sub> [μM]	Entry	R	FKBP51 K <sub>i</sub> [μM]
37		4.1	43		1.1
38		2.0	44		13
39		2.1	45		17
40		2.0	46		9.0
41		0.7	47		> 100 μM
42		2.5			

<sup>a</sup>K<sub>i</sub> values were determined by a competitive fluorescence polarization assay.<sup>33</sup>

## CONCLUSION

During the development of SAFit1 and SAFit2 it was shown that the cyclohexyl substituent is the key structural feature for highly selective FKBP51 ligands. In this study we synthesized a novel series of selective FKBP51 ligands and for the first time performed an investigation on the structure–affinity relationship on compounds containing this structural feature. The methoxy groups of the trimethoxyphenyl group are surprisingly important, whereas the rest of the phenyl ring seems to contribute comparatively less to the binding energy. As little as an additional methyl group at the C<sup>9</sup> position is sufficient to abolish binding to the antitarget FBKP52. A cocrystal structure with the best novel ligand (41) confirmed the induced-fit conformation, which does not seem to be influenced by the substitution pattern in the C<sup>10</sup> position. The latter thus represents a possibility to optimize the FKBP51-selective class of iFit ligands.

## EXPERIMENTAL SECTION

**Chemistry.** Chromatographic separations were performed by manual flash chromatography, automated flash chromatography using an Interchim Puriflash 430 with an UV detector, or preparative HPLC. Merck F-254 (thickness 0.25 mm) commercial plates were used for analytical TLC. <sup>1</sup>H NMR spectra, <sup>13</sup>C NMR spectra, 2D HSQC, HMBC, and COSY of all intermediates were obtained from

the Department of Chemistry and Pharmacy, LMU, on a Bruker Avance III HD 400/800 or a Varian NMR system 300/400/600 at room temperature. Chemical shifts for <sup>1</sup>H or <sup>13</sup>C are given in ppm (δ) downfield from tetramethylsilane using residual protio solvent as an internal standard. The high resolution mass spectrometry was carried out at MPI for Biochemistry (Microchemistry Core Facility) on Bruker Daltonics MicrOTOF. The purity of the compounds was verified by reversed phase HPLC (see Supporting Information for detailed conditions). All of the final compounds synthesized and tested had a purity of >95%.

**2-(3-((R)-1-(((S)-1-((S)-2-Cyclohexyl-2-(3,5-dimethoxyphenyl)acetyl)piperidine-2-carbonyloxy)-3,4-dimethoxyphenyl)propyl)phenoxy)acetic Acid (16).** 11 (26.0 mg, 93 μmol), 10 (48.0 mg, 93 μmol), COMU (60.0 mg, 0.14 mmol), and DIPEA (32.6 μL, 0.19 mmol) were stirred in DMF (1.0 mL) at room temperature for 16 h. The dark red reaction mixture was then diluted with brine and extracted with Et<sub>2</sub>O. The combined organics were dried over MgSO<sub>4</sub>, filtered, and the solvent was removed. In the following step the *tert*-butyl ester was first purified by flash chromatography (gradient 0–20% EtOAc in cyclohexane) and then cleaved at room temperature in DCM/TFA (1.0 mL, 1:1) to obtain the free carboxylic acid. The reaction was quenched with saturated NaHCO<sub>3</sub> solution, and the product was extracted with DCM. The combined organic layers were dried over MgSO<sub>4</sub>, filtered, and purified by flash chromatography (gradient 0–30% EtOAc + 1% HCOOH in hexane) to obtain the title compound (22.8 mg, 31.8 μmol, 34.0%) as a colorless oil.

TLC [EtOAc/cyclohexane, 1:1 + 1% HCOOH]:  $R_f$  = 0.28. HPLC [50–100% solvent B, 20 min]:  $t_R$  = 15.6 min. HRMS: calculated 718.3591 [C<sub>41</sub>H<sub>81</sub>NO<sub>10</sub> + H]<sup>+</sup>, found 718.3584 [M + H]<sup>+</sup>. <sup>1</sup>H NMR (599 MHz, CDCl<sub>3</sub>)  $\delta$  6.98–6.86 (m, 1H), 6.86–6.55 (m, 6H), 6.43–6.25 (m, 3H), 5.53 (dd,  $J$  = 8.8, 5.1 Hz, 1H), 5.48–5.41 (m, 1H), 4.64–4.55 (m, 2H), 3.91 (d,  $J$  = 13.7 Hz, 1H), 3.87–3.83 (m, 6H), 3.57 (s, 6H), 3.37 (d,  $J$  = 9.6 Hz, 1H), 3.14–3.04 (m, 4H), 2.80 (td,  $J$  = 13.4, 3.1 Hz, 1H), 2.59–2.52 (m, 1H), 2.48–2.41 (m, 1H), 2.30 (d,  $J$  = 13.1 Hz, 1H), 2.11–2.01 (m, 2H), 1.72–1.58 (m, 3H), 1.45–1.38 (m, 1H), 1.34–1.26 (m, 3H), 1.23 (dt,  $J$  = 13.4, 3.8 Hz, 1H), 1.16–1.08 (m, 2H), 0.94–0.86 (m, 1H), 0.74 (qd,  $J$  = 12.2, 3.5 Hz, 1H). <sup>13</sup>C NMR (151 MHz, CDCl<sub>3</sub>)  $\delta$  172.64, 171.53, 170.14, 160.49, 157.95, 148.82, 147.27, 142.24, 139.64, 133.47, 129.47, 120.22, 119.25, 114.82, 111.74, 111.26, 106.82, 98.87, 76.00, 65.73, 55.91, 55.85, 55.13, 52.22, 45.54, 43.62, 40.82, 38.08, 32.82, 31.25, 30.59, 27.00, 26.52, 26.18, 25.39, 20.95.

**2-(3-((R)-1-((S)-1-((S)-2-Cyclohexyl-2-(3-methoxyphenyl)acetyl)piperidine-2-carbonyloxy)-3-(3,4-dimethoxyphenyl)propyl)phenoxy)acetic Acid (17)**. 17 was synthesized according to 16 with 12 (50.0 mg, 0.20 mmol), 10 (103 mg, 0.20 mmol), COMU (129 mg, 0.30 mmol), and DIPEA (70.3  $\mu$ L, 0.40 mmol) in DMF (2.0 mL). The *tert*-butyl ester was cleaved in DCM/TFA (2.0 mL, 1:1) to obtain the title compound (49.7 mg, 72.3  $\mu$ mol, 36.0%) as a colorless oil.

TLC [EtOAc/cyclohexane, 1:1 + 1% HCOOH]:  $R_f$  = 0.27. HPLC [50–100% solvent B, 20 min]:  $t_R$  = 15.9 min. HRMS: calculated 688.3486 [C<sub>40</sub>H<sub>49</sub>NO<sub>9</sub> + H]<sup>+</sup>, found 688.43546 [M + H]<sup>+</sup>. <sup>1</sup>H NMR (400 MHz, CDCl<sub>3</sub>)  $\delta$  7.09–7.03 (m, 2H), 6.76–6.69 (m, 5H), 6.60–6.56 (m, 3H), 6.48 (dt,  $J$  = 7.7, 1.2 Hz, 1H), 5.48 (dd,  $J$  = 8.7, 5.1 Hz, 1H), 5.43–5.38 (m, 1H), 4.59–4.51 (m, 2H), 3.88 (d,  $J$  = 13.6 Hz, 1H), 3.78–3.77 (m, 6H), 3.50 (s, 3H), 3.37 (d,  $J$  = 9.7 Hz, 1H), 2.71 (td,  $J$  = 13.4, 3.0 Hz, 1H), 2.55–2.42 (m, 2H), 2.36 (ddd,  $J$  = 13.9, 9.2, 6.7 Hz, 1H), 2.24 (td,  $J$  = 10.9, 5.5 Hz, 1H), 2.08–2.00 (m, 2H), 1.96–1.89 (m, 1H), 1.88–1.71 (m, 2H), 1.63–1.52 (m, 5H), 1.46–1.31 (m, 2H), 1.11–0.98 (m, 3H), 0.84 (qd,  $J$  = 12.3, 3.4 Hz, 1H), 0.73–0.59 (m, 1H). <sup>13</sup>C NMR (101 MHz, CDCl<sub>3</sub>)  $\delta$  172.86, 171.56, 170.23, 159.62, 157.72, 148.86, 147.32, 142.27, 138.99, 133.54, 129.61, 129.22, 121.50, 120.27, 119.73, 114.87, 113.90, 112.68, 111.84, 111.34, 111.27, 75.93, 65.27, 55.94, 55.88, 55.10, 55.02, 52.30, 43.72, 40.98, 37.95, 32.81, 31.24, 30.62, 26.53, 26.16, 25.43, 20.95.

**2-(3-((1R)-1-(((2S)-1-(2-Cyclohexyl-2-phenylacetyl)piperidine-2-carbonyloxy)-3-(3,4-dimethoxyphenyl)propyl)phenoxy)acetic Acid (18)**. 13 (87.8 mg, 0.4 mmol), 10 (50 mg, 0.1 mmol), COMU (94.6 mg, 0.22 mmol), and 2,2,6,6-tetramethylpiperidine (67.8  $\mu$ L, 0.40 mmol) were stirred in DMF (1.5 mL) for 25 h at room temperature. The reaction mixture was directly loaded on silica and purified by flash chromatography (gradient 0–10% EtOAc in cyclohexane). The *tert*-butyl ester was stirred in DCM/TFA (2 mL, 1:1) for 6 h at room temperature and then poured into saturated NaHCO<sub>3</sub>. The free carboxylic acid was extracted with DCM. The combined organic layers were dried over MgSO<sub>4</sub>, filtered, and purified by preparative chromatography (gradient 0–30% EtOAc + 1% HCOOH in cyclohexane) to obtain the title compound (58.4 mg, 88.8  $\mu$ mol, 88.3%) as a colorless oil.

TLC [EtOAc/cyclohexane, 1:1 + 1% HCOOH]:  $R_f$  = 0.33. HPLC [70–80% solvent B, 20 min]:  $t_R$  = 13.4 min. HRMS: calculated 658.3380 [C<sub>39</sub>H<sub>47</sub>NO<sub>8</sub> + H]<sup>+</sup>, found 658.3420 [M + H]<sup>+</sup>. <sup>1</sup>H NMR (599 MHz, CDCl<sub>3</sub>)  $\delta$  7.28–7.25 (m, 2H), 7.23–7.17 (m, 2H), 7.17–7.12 (m, 1H), 7.11–7.06 (m, 1H), 6.93–6.81 (m, 2H), 6.81–6.72 (m, 2H), 6.69–6.61 (m, 2H), 5.56 (dd,  $J$  = 8.6, 5.3 Hz, 1H), 5.52–5.45 (m, 1H), 4.66–4.53 (m, 2H), 4.02–3.92 (m, 1H), 3.84 (s, 3H), 3.83 (s, 3H), 3.46 (d,  $J$  = 9.9 Hz, 1H), 3.24–3.15 (m, 1H), 2.74 (td,  $J$  = 13.6, 3.0 Hz, 1H), 2.62–2.46 (m, 2H), 2.42–2.36 (m, 1H), 2.18–2.09 (m, 1H), 1.95–1.82 (m, 2H), 1.82–1.75 (m, 1H), 1.64–1.51 (m, 4H), 1.50–1.39 (m, 2H), 1.34–1.22 (m, 3H), 1.15–1.06 (m, 2H), 0.93–0.84 (m, 1H), 0.74–0.66 (m, 1H). <sup>13</sup>C NMR (151 MHz, CDCl<sub>3</sub>)  $\delta$  172.64, 171.25, 170.32, 157.64, 148.77, 147.22, 141.97, 138.50, 137.70, 133.58, 129.57, 128.75, 128.46, 128.19, 126.89, 120.20, 119.75, 114.52, 111.99, 111.77, 111.66, 111.27, 111.13, 75.77, 65.16, 55.90, 55.83,

54.94, 52.18, 43.73, 41.11, 37.81, 36.76, 32.72, 31.68, 31.12, 30.61, 29.67, 26.78, 26.50, 26.11, 25.46, 24.86, 20.96

**2-(3-((R)-1-(((S)-1-((R)-2-Cyclohexylpent-4-enoyl)piperidine-2-carbonyloxy)-3-(3,4-dimethoxyphenyl)propyl)phenoxy)acetic Acid (19)**. 10 (141 mg, 0.27 mmol), 14 (50 mg, 0.27 mmol), COMU (176 mg, 0.41 mmol), and DIPEA (96  $\mu$ L, 0.55 mmol) were stirred in DMF (3.0 mL) for 20 h at room temperature. The resulting dark red reaction mixture was directly loaded on silica and purified by flash chromatography (gradient 0–20% EtOAc in cyclohexane). The *tert*-butyl ester was stirred in DCM/TFA (2.0 mL, 1:1) for 1 h at room temperature and then poured into sat. NaHCO<sub>3</sub>. The free carboxylic acid was extracted with DCM. The combined organic layers were dried over MgSO<sub>4</sub>, filtered, and purified by preparative chromatography (gradient 0–10% EtOAc + 1% HCOOH in hexane) to obtain the title compound (13.4 mg, 21.6  $\mu$ mol, 7.8%) as a light yellow oil.

TLC [EtOAc/cyclohexane, 1:1 + 1% HCOOH]:  $R_f$  = 0.19. HPLC [50–100% solvent B, 20 min]:  $t_R$  = 16.0 min. HRMS: calculated 622.3380 [C<sub>36</sub>H<sub>47</sub>NO<sub>8</sub> + H]<sup>+</sup>, found 622.3426 [M + H]<sup>+</sup>. <sup>1</sup>H NMR (599 MHz, DMSO-*d*<sub>6</sub>)  $\delta$  7.31–7.19 (m, 1H), 6.91–6.87 (m, 1H), 6.86–6.77 (m, 3H), 6.75–6.70 (m, 1H), 6.67–6.60 (m, 1H), 5.78–5.68 (m, 1H), 5.67–5.63 (m, 1H), 5.37–5.30 (m, 1H), 5.07–4.90 (m, 2H), 4.85 (d,  $J$  = 10.2 Hz, 1H), 4.63–4.56 (m, 2H), 4.00 (d,  $J$  = 13.4 Hz, 1H), 3.69 (s, 3H), 3.68 (s, 3H), 2.95 (t,  $J$  = 13.1 Hz, 1H), 2.70–2.62 (m, 1H), 2.46–2.38 (m, 1H), 2.27–2.13 (m, 3H), 2.13–1.94 (m, 2H), 1.84–1.73 (m, 1H), 1.68–1.48 (m, 5H), 1.45–1.38 (m, 2H), 1.37–1.24 (m, 2H), 1.20–1.02 (m, 4H), 0.92 (p,  $J$  = 12.7, 11.1 Hz, 2H). <sup>13</sup>C NMR (151 MHz, DMSO-*d*<sub>6</sub>)  $\delta$  174.30, 170.79, 170.58, 158.36, 149.06, 147.47, 142.26, 137.00, 133.67, 129.98, 120.35, 119.12, 116.34, 114.28, 112.73, 112.53, 112.33, 75.77, 66.32, 65.16, 55.92, 55.76, 51.90, 47.41, 45.65, 43.66, 38.15, 34.22, 31.07, 29.91, 27.01, 26.41, 26.35, 25.52, 21.17.

**2-(3-((R)-1-(((S)-1-((R)-2-Cyclohexylpropanoyl)piperidine-2-carbonyloxy)-3-(3,4-dimethoxyphenyl)propyl)phenoxy)acetic Acid (20)**. 10 (49.3 mg, 0.10 mmol), 15 (15 mg, 0.10 mmol), COMU (61.7 mg, 0.14 mmol), and DIPEA (33.5  $\mu$ L, 0.19 mmol) were stirred in DMF (1.0 mL) for 20 h at room temperature. The orange reaction mixture was diluted with Et<sub>2</sub>O and washed with brine. The combined organic layers were dried over MgSO<sub>4</sub>, filtered, and the solvent was removed under reduced pressure. The crude *tert*-butyl ester was stirred in DCM/TFA (2.0 mL, 1:1) for 1 h at room temperature and then poured into saturated NaHCO<sub>3</sub>. The free carboxylic acid was extracted with DCM. The combined organic layers were dried over MgSO<sub>4</sub>, filtered, and purified by flash chromatography (gradient 0–40% EtOAc + 0.5% HCOOH in cyclohexane) to obtain the title compound (44.6 mg, 74.9  $\mu$ mol, 78.0%) as a light yellow oil.

TLC [EtOAc/cyclohexane, 1:1 + 1% HCOOH]:  $R_f$  = 0.16. HPLC [50–100% solvent B, 20 min]:  $t_R$  = 15.0 min. HRMS: calculated 596.3223 [C<sub>34</sub>H<sub>45</sub>NO<sub>8</sub> + H]<sup>+</sup>, found 596.3267 [M + H]<sup>+</sup>. <sup>1</sup>H NMR (300 MHz, CDCl<sub>3</sub>)  $\delta$  7.24–7.18 (m, 1H), 6.89–6.82 (m, 2H), 6.81–6.74 (m, 2H), 6.72–6.61 (m, 2H), 5.66 (dd,  $J$  = 8.7, 4.9 Hz, 1H), 5.53–5.46 (m, 1H), 4.70–4.56 (m, 2H), 3.93–3.87 (m, 1H), 3.85 (s, 3H), 3.84 (s, 3H), 3.37–3.21 (m, 1H), 2.71–2.47 (m, 3H), 2.42–2.31 (m, 1H), 2.26–2.13 (m, 1H), 2.15–2.04 (m, 1H), 1.89–1.46 (m, 10H), 1.44–1.37 (m, 2H), 1.22–1.10 (m, 2H), 1.02 (d,  $J$  = 6.8 Hz, 3H), 0.95–0.78 (m, 2H). <sup>13</sup>C NMR (75 MHz, CDCl<sub>3</sub>)  $\delta$  177.32, 171.32, 170.34, 163.23, 158.01, 148.91, 147.38, 142.08, 133.43, 129.65, 120.18, 119.41, 115.65, 111.71, 111.37, 110.14, 76.35, 65.46, 60.42, 55.91, 55.86, 52.28, 43.51, 41.19, 40.53, 38.03, 31.90, 31.44, 29.51, 27.21, 26.88, 26.38, 26.27, 26.22, 25.50, 21.07, 14.32.

**2-(3-((R)-1-(((S)-1-(2-Cyclohexylacetyl)piperidine-2-carbonyloxy)-3-(3,4-dimethoxyphenyl)propyl)phenoxy)acetic Acid (21)**. 10 (50 mg, 0.10 mmol) and DIPEA (20.4  $\mu$ L, 0.12 mmol) were dissolved in DCM (1.0 mL). Then 2-cyclohexylacetyl chloride (17.9  $\mu$ L, 0.12 mmol) was added, and it was stirred at room temperature for 1 h. TFA (1.0 mL) was then added to the red brown reaction mixture, and the mixture was stirred for 1.5 h at room temperature and then poured into sat. NaHCO<sub>3</sub>. The free carboxylic acid was extracted with DCM. The combined organic layers were washed with H<sub>2</sub>O, dried over MgSO<sub>4</sub>, filtered, and purified by preparative chromatography (gradient 0–40% EtOAc + 1% HCOOH

in hexane) to obtain the title compound (52 mg, 81.5  $\mu\text{mol}$ , 84.1%) as a light yellow oil.

TLC [EtOAc/cyclohexane, 1:1 + 1% HCOOH]:  $R_f$  = 0.15. HPLC [50–100% solvent B, 20 min]:  $t_R$  = 16.0 min. HRMS: calculated 582.3067 [ $\text{C}_{33}\text{H}_{43}\text{NO}_8 + \text{H}$ ]<sup>+</sup>, found 582.3103 [ $\text{M} + \text{H}$ ]<sup>+</sup>. <sup>1</sup>H NMR (300 MHz,  $\text{CDCl}_3$ )  $\delta$  8.23 (s, 1H), 7.24–7.17 (m, 1H), 6.91–6.82 (m, 3H), 6.79–6.73 (m, 1H), 6.70–6.60 (m, 2H), 5.69 (dd,  $J$  = 8.1, 5.5 Hz, 1H), 5.48–5.38 (m, 1H), 4.57–4.52 (m, 2H), 3.84 (s, 3H), 3.82 (s, 3H), 3.80–3.71 (m, 1H), 3.20 (td,  $J$  = 13.0, 3.0 Hz, 1H), 2.59–2.45 (m, 2H), 2.38–2.18 (m, 3H), 2.17–2.05 (m, 1H), 2.07–1.96 (m, 1H), 1.78–1.60 (m, 9H), 1.45–1.26 (m, 3H), 1.19–1.04 (m, 2H), 0.99–0.84 (m, 2H). <sup>13</sup>C NMR (75 MHz,  $\text{CDCl}_3$ )  $\delta$  172.83, 172.62, 170.55, 158.28, 148.85, 147.30, 141.76, 133.51, 129.55, 120.14, 119.22, 114.44, 112.11, 111.72, 111.34, 66.02, 55.90, 55.83, 52.03, 45.41, 43.84, 40.86, 38.09, 35.04, 33.30, 33.24, 31.26, 29.65, 26.82, 26.18, 26.11, 26.09, 25.39, 20.99, 8.37.

**(S)-(R)-3-(3,4-Dimethoxyphenyl)-1-(3-(2-morpholinoethoxy)-phenyl)propyl 1-((S)-2-Cyclohexyl-3-(methoxymethoxy)-propanoyl)piperidine-2-carboxylate (37)**. 36 (71.1 mg, 0.14 mmol), 30 (30.0 mg, 0.14 mmol), COMU (89.0 mg, 0.21 mmol), and DIPEA were stirred in DMF (1.5 mL) at room temperature for 16 h, which resulted in an orange-red solution. The reaction mixture was directly loaded on silica and purified by flash chromatography (0–5% MeOH in DCM) and preparative flash chromatography (gradient 0–40% EtOAc + 2% MeOH + 0.1% TEA in hexane) to obtain the title compound (72.8 mg, 0.10 mmol, 73.5%) as a light yellow oil.

TLC [EtOAc + 2% MeOH + 1% TEA]:  $R_f$  = 0.40. HPLC [50–100% solvent B, 20 min]:  $t_R$  = 16.0 min. HRMS: calculated 711.4221 [ $\text{C}_{40}\text{H}_{58}\text{N}_2\text{O}_9 + \text{H}$ ]<sup>+</sup>, found 711.4274 = [ $\text{M} + \text{H}$ ]<sup>+</sup>. <sup>1</sup>H NMR (599 MHz,  $\text{CDCl}_3$ )  $\delta$  7.24–7.19 (m, 1H), 6.93–6.89 (m, 1H), 6.86–6.83 (m, 1H), 6.82–6.74 (m, 2H), 6.67–6.62 (m, 2H), 5.71 (dd,  $J$  = 8.0, 5.6 Hz, 1H), 5.54–5.48 (m, 1H), 4.48–4.42 (m, 2H), 4.11–4.06 (m, 2H), 3.98–3.91 (m, 1H), 3.85–3.83 (m, 6H), 3.77–3.69 (m, 6H), 3.26–3.21 (m, 1H), 3.19 (s, 3H), 2.92–2.85 (m, 1H), 2.81–2.76 (m, 2H), 2.60–2.55 (m, 5H), 2.53–2.47 (m, 1H), 2.34–2.29 (m, 1H), 2.28–2.23 (m, 1H), 2.20–2.12 (m, 1H), 2.10–1.98 (m, 2H), 1.80–1.76 (m, 1H), 1.71–1.62 (m, 6H), 1.38–1.33 (m, 2H), 1.27–1.19 (m, 2H), 1.17–1.07 (m, 2H), 1.05–0.94 (m, 2H). <sup>13</sup>C NMR (151 MHz,  $\text{CDCl}_3$ )  $\delta$  173.85, 170.62, 158.74, 148.82, 147.26, 141.90, 141.40, 133.61, 129.50, 120.12, 118.83, 113.80, 112.89, 111.72, 111.26, 96.53, 75.87, 68.00, 66.88, 65.74, 65.68, 57.65, 55.90, 55.81, 55.10, 54.07, 52.03, 47.07, 43.67, 39.34, 38.57, 38.29, 31.46, 31.18, 30.68, 27.07, 26.37, 26.30, 25.57, 24.87, 21.09.

**(S)-(R)-3-(3,4-Dimethoxyphenyl)-1-(3-(2-morpholinoethoxy)-phenyl)propyl 1-((S)-2-Cyclohexyl-3-hydroxypropanoyl)-piperidine-2-carboxylate (38)**. 37 (50.0 mg, 70.0  $\mu\text{mol}$ ) was stirred in EtOH (1.88 mL) and conc HCl (120  $\mu\text{L}$ ) at room temperature for 16 h. Since the reaction was not finished, conc HCl (180  $\mu\text{L}$ ) was added and the yellow reaction mixture was further stirred for 8 h at room temperature. It was then poured into sat.  $\text{NaHCO}_3$  solution, and the product was extracted with DCM. The organic layer was dried over  $\text{MgSO}_4$ , filtered, and the solvent was removed under reduced pressure. After preparative flash chromatography (0–60% EtOAc + 2% MeOH + 0.1% TEA in hexane) the title compound (28.4 mg, 42.6  $\mu\text{mol}$ , 60.6%) was obtained as a light yellow oil.

TLC [EtOAc + 2% MeOH + 1% TEA]:  $R_f$  = 0.18. HPLC [50–100% solvent B, 20 min]:  $t_R$  = 16.0 min. HRMS: calculated 667.3958 [ $\text{C}_{38}\text{H}_{54}\text{N}_2\text{O}_8 + \text{H}$ ]<sup>+</sup>, found 667.4021 = [ $\text{M} + \text{H}$ ]<sup>+</sup>. <sup>1</sup>H NMR (599 MHz,  $\text{CDCl}_3$ )  $\delta$  7.24–7.20 (m, 1H), 6.90–6.85 (m, 2H), 6.83–6.80 (m, 1H), 6.79–6.73 (m, 1H), 6.69–6.63 (m, 2H), 5.75 (dd,  $J$  = 7.9, 5.8 Hz, 1H), 5.54–5.51 (m, 1H), 4.13–4.08 (m, 2H), 3.97–3.89 (m, 1H), 3.85–3.82 (m, 7H), 3.77–3.70 (m, 6H), 3.11 (td,  $J$  = 13.2, 2.9 Hz, 2H), 2.84–2.78 (m, 2H), 2.78–2.73 (m, 1H), 2.63–2.58 (m, 4H), 2.57–2.54 (m, 1H), 2.53–2.47 (m, 1H), 2.39–2.34 (m, 1H), 2.23–2.17 (m, 1H), 2.05–2.01 (m, 1H), 1.87–1.81 (m, 1H), 1.76–1.63 (m, 7H), 1.47–1.37 (m, 2H), 1.33 (t,  $J$  = 13.2, 3.3 Hz, 1H), 1.29–1.19 (m, 3H), 1.18–1.04 (m, 2H), 0.96 (qd,  $J$  = 12.3, 4.4 Hz, 1H). <sup>13</sup>C NMR (151 MHz,  $\text{CDCl}_3$ )  $\delta$  175.85, 170.66, 158.76, 148.85, 147.31, 141.36, 133.43, 129.60, 120.09, 119.01, 114.07, 112.98, 111.67, 111.29,

76.53, 66.77, 65.58, 62.16, 57.60, 55.90, 55.83, 54.03, 52.14, 48.52, 44.00, 37.98, 37.00, 31.74, 31.26, 30.30, 26.53, 26.32, 26.16, 25.42, 20.96.

**(S)-(R)-3-(3,4-Dimethoxyphenyl)-1-(3-(2-morpholinoethoxy)-phenyl)propyl 1-((S)-3-Acetoxy-2-cyclohexylpropanoyl)-piperidine-2-carboxylate (39)**. 38 (17.0 mg, 25.0  $\mu\text{mol}$ ) was stirred with DMAP (catalytic amount) and  $\text{Ac}_2\text{O}$  (100  $\mu\text{L}$ , 1.06 mmol) at room temperature for 6 h. The title compound was purified by preparative flash chromatography (0–50% EtOAc + 2% MeOH + 0.1% TEA in hexane) and obtained as colorless oil (7.6 mg, 10.7  $\mu\text{mol}$ , 42.1%).

TLC [EtOAc + 2% MeOH + 1% TEA]:  $R_f$  = 0.28. HPLC [50–100% solvent B, 20 min]:  $t_R$  = 16.0 min. HRMS: calculated 709.4064 [ $\text{C}_{40}\text{H}_{56}\text{N}_2\text{O}_9 + \text{H}$ ]<sup>+</sup>, found 709.4117 = [ $\text{M} + \text{H}$ ]<sup>+</sup>. <sup>1</sup>H NMR (599 MHz,  $\text{CDCl}_3$ )  $\delta$  7.24–7.19 (m, 1H), 6.94–6.84 (m, 2H), 6.83–6.79 (m, 1H), 6.78–6.74 (m, 1H), 6.67–6.63 (m, 2H), 5.72 (dd,  $J$  = 7.9, 5.6 Hz, 1H), 5.54–5.49 (m, 1H), 4.36–4.30 (m, 1H), 4.17 (t,  $J$  = 10.0 Hz, 1H), 4.12–4.08 (m, 2H), 3.92–3.87 (m, 1H), 3.85–3.83 (m, 6H), 3.76–3.70 (m, 4H), 3.32–3.25 (m, 1H), 3.02–2.96 (m, 1H), 2.84–2.76 (m, 2H), 2.58 (td,  $J$  = 11.6, 9.9, 5.3 Hz, 5H), 2.54–2.48 (m, 1H), 2.37–2.31 (m, 1H), 2.23–2.17 (m, 1H), 2.08–2.03 (m, 1H), 1.91 (d,  $J$  = 10.0 Hz, 3H), 1.88 (s, 3H), 1.74–1.63 (m, 6H), 1.44–1.37 (m, 2H), 1.28–1.22 (m, 2H), 1.18–1.06 (m, 2H), 1.05–0.97 (m, 1H). <sup>13</sup>C NMR (151 MHz,  $\text{CDCl}_3$ )  $\delta$  173.20, 171.19, 170.34, 158.76, 148.85, 147.31, 141.64, 133.56, 129.53, 120.11, 118.86, 113.88, 112.80, 111.69, 111.60, 111.28, 75.96, 66.82, 64.80, 57.61, 55.90, 55.82, 54.02, 52.06, 45.62, 43.56, 38.67, 38.23, 31.39, 31.26, 30.38, 27.17, 26.21, 26.14, 25.58, 21.10, 20.77.

**(S)-(R)-3-(3,4-Dimethoxyphenyl)-1-(3-(2-morpholinoethoxy)-phenyl)propyl 1-((2S,3R)-2-Cyclohexyl-3-(methoxymethoxy)-butanoyl)piperidine-2-carboxylate (40)**. 36 (31.2 mg, 0.061 mmol), 31 (14 mg, 0.061 mmol), PyBrop (31.2 mg, 0.067 mmol), and DIPEA (32  $\mu\text{L}$ , 0.18 mmol) were stirred in DCM (1.0 mL) at room temperature for 16 h. The crude product was directly loaded on silica and purified by flash chromatography (0–70% EtOAc + 2% MeOH + 0.1% TEA in cyclohexane) to obtain the title compound as light yellow oil (27 mg, 37.2  $\mu\text{mol}$ , 61.2%).

TLC [EtOAc + 2% MeOH + 0.1% TEA]:  $R_f$  = 0.18. HRMS: calculated 725.4377 [ $\text{C}_{41}\text{H}_{61}\text{N}_2\text{O}_9 + \text{H}$ ]<sup>+</sup>, found 725.4434 [ $\text{M} + \text{H}$ ]<sup>+</sup>. HPLC [30–100% solvent B, 20 min]:  $t_R$  = 14.0 min, purity (220 nm). <sup>1</sup>H NMR (599 MHz,  $\text{CDCl}_3$ )  $\delta$  7.25–7.21 (m, 1H), 6.93–6.89 (m, 1H), 6.86–6.77 (m, 3H), 6.68–6.64 (m, 2H), 5.75 (dd,  $J$  = 8.1, 5.6 Hz, 1H), 5.58–5.51 (m, 1H), 4.72–4.65 (m, 1H), 4.63–4.56 (m, 1H), 4.15–4.05 (m, 3H), 3.89–3.81 (m, 6H), 3.77–3.70 (m, 4H), 3.41–3.34 (m, 3H), 3.21–3.10 (m, 1H), 2.86 (dd,  $J$  = 8.0, 6.1 Hz, 1H), 2.83–2.78 (m, 2H), 2.66–2.57 (m, 5H), 2.54–2.48 (m, 1H), 2.38–2.30 (m, 1H), 2.28–2.15 (m, 2H), 2.05–1.96 (m, 1H), 1.95–1.85 (m, 1H), 1.79–1.57 (m, 10H), 1.44–1.35 (m, 2H), 1.32–1.26 (m, 1H), 1.21–1.15 (m, 4H), 1.08–1.01 (m, 1H). <sup>13</sup>C NMR (151 MHz,  $\text{CDCl}_3$ )  $\delta$  172.41, 170.74, 158.82, 158.73, 148.83, 147.28, 141.76, 133.57, 129.53, 120.14, 118.96, 113.80, 113.14, 111.71, 111.28, 95.20, 76.02, 73.11, 66.85, 57.64, 55.91, 55.82, 55.67, 54.07, 51.69, 44.14, 39.06, 38.06, 37.72, 31.72, 31.25, 29.60, 27.04, 26.74, 26.56, 26.45, 25.60, 21.09, 18.23.

**(S)-(R)-3-(3,4-Dimethoxyphenyl)-1-(3-(2-morpholinoethoxy)-phenyl)propyl 1-((2S,3R)-2-Cyclohexyl-3-hydroxybutanoyl)-piperidine-2-carboxylate (41)**. 40 was stirred in EtOH (940  $\mu\text{L}$ ) and conc HCl (120  $\mu\text{L}$ ) at room temperature for 22 h. The solution was quenched with saturated  $\text{NaHCO}_3$  solution (200  $\mu\text{L}$ ). The crude product was directly loaded on silica and purified by flash chromatography (0–70% EtOAc + 2% MeOH + 0.1% TEA in cyclohexane), giving the title compound as colorless solid after lyophilization (15.8 mg, 23.2  $\mu\text{mol}$ , 62.2%).

TLC [EtOAc + 5% MeOH + 1% TEA]:  $R_f$  = 0.27. HRMS: calculated 681.4115 [ $\text{C}_{39}\text{H}_{56}\text{N}_2\text{O}_8 + \text{H}$ ]<sup>+</sup>, found 681.4149 [ $\text{M} + \text{H}$ ]<sup>+</sup>. HPLC [0–100% solvent B, 20 min]:  $t_R$  = 16.4 min. <sup>1</sup>H NMR (599 MHz,  $\text{CDCl}_3$ )  $\delta$  7.26–7.22 (m, 1H), 6.92–6.86 (m, 2H), 6.84–6.81 (m, 1H), 6.79–6.76 (m, 1H), 6.69–6.64 (m, 2H), 5.77 (dd,  $J$  = 7.9, 5.6 Hz, 1H), 5.60–5.56 (m, 1H), 4.19 (s, 2H), 4.12–4.05 (m, 2H), 3.87–3.84 (m, 6H), 3.83–3.76 (m, 4H), 3.14–3.06 (m, 1H), 2.93–

2.85 (m, 3H), 2.78–2.63 (m, 4H), 2.61–2.56 (m, 1H), 2.54–2.50 (m, 1H), 2.41–2.34 (m, 1H), 2.27–2.18 (m, 1H), 2.11–1.99 (m, 2H), 1.87–1.79 (m, 1H), 1.77–1.72 (m, 3H), 1.69–1.64 (m, 3H), 1.44–1.39 (m, 1H), 1.34 (tt,  $J = 13.0, 3.5$  Hz, 1H), 1.29–1.23 (m, 2H), 1.23–1.20 (m, 1H), 1.18 (d,  $J = 6.4$  Hz, 3H), 1.15–1.10 (m, 1H), 1.03 (qd,  $J = 13.5, 12.9, 4.0$  Hz, 1H), 0.98–0.89 (m, 1H).  $^{13}\text{C}$  NMR (151 MHz,  $\text{CDCl}_3$ )  $\delta$  173.72, 171.24, 158.56, 148.87, 147.34, 141.40, 133.42, 129.63, 120.12, 119.24, 114.17, 112.86, 111.68, 111.31, 76.55, 68.18, 57.54, 57.49, 56.66, 55.92, 55.84, 53.93, 53.86, 52.23, 52.13, 44.63, 37.96, 36.94, 31.54, 31.29, 26.57, 26.43, 26.35, 26.26, 25.57, 21.17, 19.88.

**(S)-(R)-3-(3,4-Dimethoxyphenyl)-1-(3-(2-morpholinoethoxy)-phenyl)propyl 1-((S)-2-Cyclohexyl-3-oxobutanoyl)piperidine-2-carboxylate (42).** DMSO (56.3  $\mu\text{L}$ , 0.79 mmol) was added at  $-78^\circ\text{C}$  to a solution of oxalyl chloride (198  $\mu\text{L}$ , 0.40 mmol, 2 M in DCM) in DCM (2.0 mL). The mixture was stirred at that temperature for 30 min, then **41** (177 mg, 0.26 mmol) was added and stirring was continued for 45 min. TEA (0.55 mL, 3.97 mmol) was added to the reaction mixture, and it was allowed to warm to room temperature. The reaction was diluted with DCM and washed with water and brine. Then the organic layer was dried over  $\text{MgSO}_4$  and the solvent was removed. The crude product was purified by preparative flash chromatography (0–50% EtOAc + 2% MeOH + 0.1% TEA in hexane) to obtain the title compound as a light yellow oil (150 mg, 0.22 mmol, 83.8%).

TLC [EtOAc + 2% MeOH + 1% TEA]:  $R_f = 0.27$ . HPLC [30–100% solvent B, 20 min]:  $t_R = 15.0$  min. HRMS: calculated 679.3958 [ $\text{C}_{39}\text{H}_{44}\text{N}_2\text{O}_8 + \text{H}$ ] $^+$ , found 679.4052 [ $\text{M} + \text{H}$ ] $^+$ .  $^1\text{H}$  NMR (599 MHz,  $\text{CDCl}_3$ )  $\delta$  7.24–7.21 (m, 1H), 6.88–6.83 (m, 1H), 6.83–6.80 (m, 2H), 6.79–6.74 (m, 1H), 6.68–6.61 (m, 2H), 5.73 (dd,  $J = 8.0, 5.8$  Hz, 1H), 5.44–5.40 (m, 1H), 4.13–4.06 (m, 2H), 3.96–3.91 (m, 1H), 3.83 (s, 3H), 3.75–3.70 (m, 4H), 3.35 (d,  $J = 10.2$  Hz, 1H), 3.06–2.96 (m, 1H), 2.84–2.75 (m, 2H), 2.62–2.54 (m, 5H), 2.51–2.43 (m, 1H), 2.35–2.29 (m, 1H), 2.28–2.22 (m, 1H), 2.20–2.13 (m, 1H), 2.11–2.09 (m, 3H), 2.06–1.97 (m, 1H), 1.82–1.74 (m, 1H), 1.74–1.68 (m, 2H), 1.67–1.60 (m, 4H), 1.55–1.47 (m, 1H), 1.41–1.34 (m, 1H), 1.32–1.22 (m, 3H), 1.13 (qt,  $J = 12.6, 3.9$  Hz, 1H), 0.95 (qd,  $J = 12.6, 3.6$  Hz, 1H), 0.87–0.73 (m, 1H).  $^{13}\text{C}$  NMR (151 MHz,  $\text{CDCl}_3$ )  $\delta$  204.91, 170.24, 168.01, 158.89, 158.80, 148.84, 147.32, 141.34, 133.39, 129.61, 120.09, 118.96, 114.13, 112.90, 111.66, 111.28, 76.78, 76.29, 66.90, 57.64, 55.90, 55.82, 54.08, 52.50, 43.73, 37.93, 37.85, 31.57, 31.46, 31.22, 30.65, 26.94, 26.72, 26.15, 25.93, 25.30, 20.99.

**(S)-(R)-3-(3,4-Dimethoxyphenyl)-1-(3-(2-morpholinoethoxy)-phenyl)propyl 1-((2S,3R,E)-2-Cyclohexyl-3-hydroxyhex-4-enoyl)piperidine-2-carboxylate (43).** **36** (34.5 mg, 0.067 mmol), **33** (20 mg, 0.061 mmol), PyBrop (42.8 mg, 0.092 mmol), and DIPEA (32.1  $\mu\text{L}$ , 0.18 mmol) were stirred in DCM (1.0 mL) at room temperature for 16 h. The coupling product was purified by flash chromatography (0–100% EtOAc + 2% MeOH + 0.1% TEA in cyclohexane) and then dissolved in EtOH (940  $\mu\text{L}$ ). Then conc HCl (60.0  $\mu\text{L}$ ) was added and stirred at room temperature for 20 h. The crude product was directly loaded on silica and purified by flash chromatography (0–100% EtOAc + 2% MeOH + 0.1% TEA in cyclohexane). The title compound was obtained as colorless oil (3.9 mg, 5.52  $\mu\text{mol}$ , 9.05%).

TLC [EtOAc + 2% MeOH + 1% TEA]:  $R_f = 0.59$ . HPLC [0–100% solvent B, 20 min]:  $t_R = 17.1$  min. HRMS: calculated 707.4271 [ $\text{C}_{41}\text{H}_{58}\text{N}_2\text{O}_8 + \text{H}$ ] $^+$ , found 707.4303 [ $\text{M} + \text{H}$ ] $^+$ .  $^1\text{H}$  NMR (599 MHz,  $\text{DMSO}-d_6$ )  $\delta$  7.30–7.25 (m, 1H), 6.94–6.83 (m, 4H), 6.79–6.76 (m, 1H), 6.72–6.67 (m, 1H), 5.64–5.55 (m, 2H), 5.44–5.32 (m, 1H), 5.26–5.19 (m, 1H), 4.71–4.61 (m, 1H), 4.11–4.07 (m, 2H), 4.06–4.02 (m, 1H), 3.75–3.72 (m, 6H), 3.62–3.56 (m, 4H), 2.70 (t,  $J = 5.8$  Hz, 2H), 2.50–2.47 (m, 4H), 2.22–1.90 (m, 4H), 1.75–1.53 (m, 8H), 1.27–1.24 (m, 6H), 1.22–1.14 (m, 3H), 1.06 (dd,  $J = 12.4, 6.4$  Hz, 3H), 0.88–0.86 (m, 2H).  $^{13}\text{C}$  NMR (151 MHz,  $\text{DMSO}-d_6$ )  $\delta$  173.72, 171.24, 158.56, 148.87, 147.34, 141.40, 135.61, 133.42, 129.63, 129.33, 120.12, 119.24, 114.17, 112.86, 111.68, 111.31, 76.55, 68.18, 57.54, 57.49, 56.66, 55.92, 55.84, 53.93, 53.86, 52.23, 52.13, 44.63, 37.96, 36.94, 31.54, 31.29, 26.57, 26.43, 26.35, 26.26, 25.57, 21.17, 19.88.

**(S)-(R)-3-(3,4-Dimethoxyphenyl)-1-(3-(2-morpholinoethoxy)-phenyl)propyl 1-((2R,3R)-2-Cyclohexyl-3-hydroxy-4-methylpentanoyl)piperidine-2-carboxylate (44).** **44** was synthesized according to **43** with **34** (18 mg, 0.055 mmol), **36** (30.9 mg, 0.060 mmol), PyBrop (38.3 mg, 0.082 mmol), and DIPEA (28.7  $\mu\text{L}$ , 0.164 mmol) in DCM (1 mL) to afford the TBS-protected compound as colorless oil (37.1 mg, 45.1  $\mu\text{mol}$ , 81.9%). Subsequent TBS deprotection in EtOH (940  $\mu\text{L}$ ) and conc HCl (60.0  $\mu\text{L}$ ) afforded the title compound as light yellow solid (11 mg, 15.5  $\mu\text{mol}$ , 34.5%).

TLC [EtOAc + 10% MeOH + 1% TEA]:  $R_f = 0.49$ . HPLC [0–100% solvent B, 20 min]:  $t_R = 19.2$  min. HRMS: calculated 709.4428 [ $\text{C}_{41}\text{H}_{58}\text{N}_2\text{O}_8 + \text{H}$ ] $^+$ , found 709.4466 [ $\text{M} + \text{H}$ ] $^+$ .  $^1\text{H}$  NMR (599 MHz,  $\text{DMSO}-d_6$ )  $\delta$  7.26 (t,  $J = 7.9$  Hz, 1H), 6.89–6.80 (m, 4H), 6.74 (d,  $J = 1.9$  Hz, 1H), 6.66 (dd,  $J = 8.2, 2.0$  Hz, 1H), 5.69–5.65 (m, 1H), 5.38–5.34 (m, 1H), 4.51 (d,  $J = 9.3$  Hz, 1H), 4.06 (t,  $J = 5.6$  Hz, 2H), 3.70 (d,  $J = 9.9$  Hz, 7H), 3.55 (t,  $J = 4.6$  Hz, 5H), 3.01–2.93 (m, 1H), 2.86 (dd,  $J = 8.9, 3.7$  Hz, 1H), 2.68–2.65 (m, 2H), 2.46–2.43 (m, 4H), 2.23–2.17 (m, 1H), 2.16–2.10 (m, 1H), 2.05–1.99 (m, 2H), 1.88–1.83 (m, 1H), 1.77–1.71 (m, 2H), 1.69–1.63 (m, 3H), 1.58–1.54 (m, 4H), 1.42–1.37 (m, 1H), 1.23–1.20 (m, 3H), 1.10–1.06 (m, 3H), 0.88 (d,  $J = 6.5$  Hz, 3H), 0.84 (d,  $J = 6.7$  Hz, 3H).  $^{13}\text{C}$  NMR (151 MHz,  $\text{DMSO}-d_6$ )  $\delta$  176.21, 170.51, 158.94, 149.07, 147.51, 142.30, 133.64, 130.12, 120.41, 118.70, 114.45, 112.60, 112.36, 76.03, 74.89, 73.27, 66.63, 65.77, 57.43, 55.95, 55.76, 55.74, 54.08, 51.87, 46.70, 44.38, 40.51, 38.69, 38.08, 36.67, 32.57, 31.37, 31.06, 30.55, 30.34, 29.43, 26.56, 26.48, 26.39, 25.55, 21.12, 20.31, 20.01, 19.41.

**(S)-(R)-3-(3,4-Dimethoxyphenyl)-1-(3-(2-morpholinoethoxy)-phenyl)propyl 1-((2S,3R)-2-Cyclohexyl-3-(methoxymethoxy)-5-methylhexanoyl)piperidine-2-carboxylate (45).** **45** was synthesized according to **40** with **32** (30 mg, 0.110 mmol), **36** (62.1 mg, 0.121 mmol), PyBrop (77 mg, 0.165 mmol), and DIPEA (57.7  $\mu\text{L}$ , 0.330 mmol) in DCM (dry, 3 mL) to afford the title compound as colorless oil (19 mg, 0.025 mmol, 22.6%).

TLC [EtOAc + 2% MeOH + 1% TEA]:  $R_f = 0.37$ . HPLC [0–100% solvent B, 20 min]:  $t_R = 20.1$  min. HRMS: calculated 767.4847 [ $\text{C}_{44}\text{H}_{66}\text{N}_2\text{O}_9 + \text{H}$ ] $^+$ , found 767.4818 [ $\text{M} + \text{H}$ ] $^+$ .  $^1\text{H}$  NMR (400 MHz,  $\text{DMSO}-d_6$ )  $\delta$  7.33–7.22 (m, 1H), 7.02–6.82 (m, 3H), 6.86–6.76 (m, 1H), 6.76–6.67 (m, 1H), 6.68–6.57 (m, 1H), 5.71–5.59 (m, 1H), 5.33–5.20 (m, 1H), 4.72–4.65 (m, 1H), 4.63–4.56 (m, 1H), 4.42–4.32 (m, 2H), 4.08 (d,  $J = 13.6$  Hz, 1H), 3.95–3.87 (m, 1H), 3.84–3.73 (m, 2H), 3.72–3.61 (m, 6H), 3.53–3.38 (m, 6H), 3.33–3.24 (m, 4H), 3.20–3.11 (m, 2H), 3.03–2.95 (m, 1H), 2.73 (t,  $J = 6.9$  Hz, 1H), 2.60–2.48 (m, 2H), 2.19–2.05 (m, 2H), 1.70–1.39 (m, 8H), 1.24–1.15 (m, 4H), 1.08–0.92 (m, 5H), 0.87–0.70 (m, 5H), 0.65 (dd,  $J = 16.8, 6.6$  Hz, 3H).  $^{13}\text{C}$  NMR (101 MHz,  $\text{DMSO}$ )  $\delta$  173.04, 170.82, 157.59, 149.06, 147.48, 142.59, 133.61, 130.06, 120.39, 112.66, 112.37, 75.45, 68.09, 63.61, 60.14, 55.95, 55.79, 52.01, 51.53, 43.96, 38.83, 37.80, 37.74, 31.09, 29.32, 27.05, 26.81, 26.61, 24.59, 24.43, 24.24, 24.04, 21.55, 21.46, 21.13, 21.07, 14.45.

**(S)-(R)-3-(3,4-Dimethoxyphenyl)-1-(3-(2-morpholinoethoxy)-phenyl)propyl 1-((2S,3R)-2-Cyclohexyl-3-hydroxy-5-methylhexanoyl)piperidine-2-carboxylate (46).** **46** was stirred in EtOH (940  $\mu\text{L}$ ) and conc HCl (60.0  $\mu\text{L}$ ) at room temperature for 44 h. The crude product was directly loaded on silica and purified by flash chromatography (0–100% EtOAc + 2% MeOH + 0.1% TEA in cyclohexane). The title compound was obtained as light yellow oil (11.2 mg, 15.5  $\mu\text{mol}$ , 62.6%).

TLC [EtOAc + 5% MeOH + 1% TEA]:  $R_f = 0.59$ . HPLC [0–100% solvent B, 20 min]:  $t_R = 17.3$  min. HRMS: calculated 723.4584 [ $\text{C}_{42}\text{H}_{62}\text{N}_2\text{O}_8 + \text{H}$ ] $^+$ , found 723.4632 [ $\text{M} + \text{H}$ ] $^+$ .  $^1\text{H}$  NMR (400 MHz,  $\text{DMSO}-d_6$ )  $\delta$  7.33–7.22 (m, 1H), 7.02–6.82 (m, 3H), 6.86–6.76 (m, 1H), 6.76–6.67 (m, 1H), 6.68–6.57 (m, 1H), 5.71–5.59 (m, 1H), 5.33–5.20 (m, 1H), 4.42–4.32 (m, 2H), 4.08 (d,  $J = 13.6$  Hz, 1H), 3.95–3.87 (m, 1H), 3.84–3.73 (m, 2H), 3.72–3.61 (m, 6H), 3.53–3.38 (m, 3H), 3.33–3.24 (m, 4H), 3.20–3.11 (m, 2H), 3.03–2.95 (m, 1H), 2.73 (t,  $J = 6.9$  Hz, 1H), 2.60–2.48 (m, 2H), 2.19–2.05 (m, 2H), 1.70–1.39 (m, 8H), 1.24–1.15 (m, 4H), 1.08–0.92 (m, 5H), 0.87–0.70 (m, 5H), 0.65 (dd,  $J = 16.8, 6.6$  Hz, 3H).  $^{13}\text{C}$  NMR (101 MHz,  $\text{DMSO}$ )  $\delta$  173.04, 170.82, 157.59, 149.06, 147.48, 142.59, 133.61, 130.06, 120.39, 112.66, 112.37, 75.45, 68.09, 63.61, 60.14, 55.95,

55.79, 52.01, 51.53, 43.96, 38.83, 37.80, 37.74, 31.09, 29.32, 27.05, 26.81, 26.61, 24.59, 24.43, 24.24, 24.04, 21.55, 21.46, 21.13, 21.07, 14.45.

(S)-(R)-3-(3,4-Dimethoxyphenyl)-1-(3-(2-morpholinoethoxy)-phenyl)propyl 1-((2R,3S)-2-Cyclohexyl-3-hydroxy-3-phenylpropanoyl)piperidine-2-carboxylate (**47**). **36** (107 mg, 0.21 mmol), **35** (73.1 mg, 0.20 mmol), PyBrop (141 mg, 0.30 mmol) and DIPEA (106  $\mu$ L, 0.61 mmol) were stirred in DCM (2.0 mL) at room temperature for 4 h. The coupling product was purified by flash chromatography (0–100% EtOAc + 2% MeOH + 0.1% TEA in cyclohexane) and then dissolved in EtOH (970  $\mu$ L). Then conc HCl (60.0  $\mu$ L) was added and stirred at room temperature for 24 h. The crude product was directly loaded on silica and purified by flash chromatography (0–100% EtOAc + 2% MeOH + 0.1% TEA in cyclohexane). The title compound was obtained as colorless oil (34.2 mg, 46.0  $\mu$ mol, 21.9%).

TLC [EtOAc + 5% MeOH + 1% TEA]:  $R_f$  = 0.62. HPLC [0–100% solvent B, 20 min]:  $t_R$  = 16.8 min. HRMS: calculated 743.4271 [C<sub>44</sub>H<sub>58</sub>N<sub>2</sub>O<sub>8</sub> + H]<sup>+</sup>, found 743.4306 [M + H]<sup>+</sup>. <sup>1</sup>H NMR (599 MHz, CDCl<sub>3</sub>)  $\delta$  7.39–7.29 (m, 2H), 7.27–7.22 (m, 3H), 7.22–7.16 (m, 1H), 6.91–6.86 (m, 2H), 6.85–6.81 (m, 1H), 6.79–6.75 (m, 1H), 6.69–6.59 (m, 2H), 5.76–5.68 (m, 1H), 5.54–5.50 (m, 1H), 5.05 (d,  $J$  = 3.2 Hz, 1H), 4.60 (s<sub>br</sub>, 1H), 4.20–4.07 (m, 2H), 3.99–3.89 (m, 1H), 3.86–3.83 (m, 5H), 3.80–3.70 (m, 4H), 3.18 (td,  $J$  = 13.1, 3.0 Hz, 1H), 2.99 (dd,  $J$  = 6.0, 3.3 Hz, 1H), 2.73–2.46 (m, 4H), 2.39–2.31 (m, 1H), 2.27–2.14 (m, 1H), 2.09–1.98 (m, 1H), 1.97–1.86 (m, 1H), 1.85–1.80 (m, 1H), 1.78–1.61 (m, 5H), 1.60–1.55 (m, 1H), 1.54–1.16 (m, 6H), 1.14–0.93 (m, 4H), 0.91–0.76 (m, 2H). <sup>13</sup>C NMR (151 MHz, CDCl<sub>3</sub>)  $\delta$  175.28, 170.41, 158.72, 148.87, 147.31, 142.32, 141.61, 133.44, 129.63, 128.03, 126.91, 125.87, 120.11, 118.98, 113.98, 112.89, 111.68, 111.30, 76.32, 73.28, 57.51, 55.91, 55.83, 54.00, 53.94, 51.74, 44.05, 37.99, 35.65, 33.14, 31.32, 31.06, 26.76, 26.59, 26.51, 26.21, 25.30, 20.71.

## ■ ASSOCIATED CONTENT

### 📄 Supporting Information

The Supporting Information is available free of charge on the ACS Publications website at DOI: 10.1021/acs.jmedchem.5b00785.

Full characterization and synthetic procedures of all intermediates and crystallography information (PDF)  
Molecular formula strings (CSV)

## ■ AUTHOR INFORMATION

### Corresponding Author

\*E-mail: hausch@psych.mpg.de. Phone: +49 (0) 89-30622-640.

### Author Contributions

All authors have given approval to the final version of the manuscript.

### Notes

The authors declare no competing financial interest.

## ■ ACKNOWLEDGMENTS

This work was supported by the M4 award 2011 to F.H. We are indebted to Claudia Dubler (Ludwig-Maximilians-University, München, Germany) and Elisabeth Weyher (Max Planck Institute of Biochemistry, Martinsried, Germany) for measurement of the NMR spectra and high-resolution mass spectra, respectively. We thank the JSBG staff at the European Synchrotron Radiation Facility (ESRF) in Grenoble, France.

## ■ ABBREVIATIONS USED

FKBP, FK506-binding protein; CNS, central nervous system; FP, fluorescence polarization

## ■ REFERENCES

- (1) Albu, S.; Romanowski, C. P.; Letizia Curzi, M.; Jakubcakova, V.; Flachskamm, C.; Gassen, N. C.; Hartmann, J.; Schmidt, M. V.; Schmidt, U.; Rein, T.; Holsboer, F.; Hausch, F.; Paez-Pereda, M.; Kimura, M. Deficiency of FK506-binding protein (FKBP) 51 alters sleep architecture and recovery sleep responses to stress in mice. *J. Sleep Res.* **2014**, *23* (2), 176–85.
- (2) Hartmann, J.; Wagner, K. V.; Liebl, C.; Scharf, S. H.; Wang, X.-D.; Wolf, M.; Hausch, F.; Rein, T.; Schmidt, U.; Touma, C.; Cheung-Flynn, J.; Cox, M. B.; Smith, D. F.; Holsboer, F.; Müller, M. B.; Schmidt, M. V. The involvement of FK506-binding protein 51 (FKBP5) in the behavioral and neuroendocrine effects of chronic social defeat stress. *Neuropharmacology* **2012**, *62* (1), 332–339.
- (3) Hoeijmakers, L.; Harbich, D.; Schmid, B.; Lucassen, P. J.; Wagner, K. V.; Schmidt, M. V.; Hartmann, J. Depletion of FKBP51 in female mice shapes HPA axis activity. *PLoS One* **2014**, *9* (4), e95796.
- (4) O'Leary, J. C., 3rd; Dharia, S.; Blair, L. J.; Brady, S.; Johnson, A. G.; Peters, M.; Cheung-Flynn, J.; Cox, M. B.; de Erausquin, G.; Weeber, E. J.; Jinwal, U. K.; Dickey, C. A. A new anti-depressive strategy for the elderly: ablation of FKBP5/FKBP51. *PLoS One* **2011**, *6* (9), e24840.
- (5) Klengel, T.; Mehta, D.; Anacker, C.; Rex-Haffner, M.; Pruessner, J. C.; Pariante, C. M.; Pace, T. W. W.; Mercer, K. B.; Mayberg, H. S.; Bradley, B.; Nemeroff, C. B.; Holsboer, F.; Heim, C. M.; Ressler, K. J.; Rein, T.; Binder, E. B. Allele-specific FKBP5 DNA demethylation mediates gene-childhood trauma interactions. *Nat. Neurosci.* **2013**, *16* (1), 33–41.
- (6) Zannas, A. S.; Binder, E. B. Gene–environment interactions at the FKBP5 locus: sensitive periods, mechanisms and pleiotropism. *Genes, Brain and Behavior* **2014**, *13* (1), 25–37.
- (7) Yeh, W.; Li, T.; Bierer, B. E.; McKnight, S. L. Identification and Characterization of an Immunophilin Expressed During the Clonal Expansion Phase to Adipocyte Differentiation. *Proc. Natl. Acad. Sci. U. S. A.* **1995**, *92* (24), 11081–11085.
- (8) Romano, S.; Mallardo, M.; Romano, M. F. FKBP51 and the NF-kappaB regulatory pathway in cancer. *Curr. Opin. Pharmacol.* **2011**, *11*, 288–93.
- (9) Romano, S.; Sorrentino, A.; Di Pace, A. L.; Nappo, G.; Mercogliano, C.; Romano, M. F. The emerging role of large immunophilin FK506 binding protein 51 in cancer. *Curr. Med. Chem.* **2011**, *18* (35), 5424–9.
- (10) Warrior, M. Role of Fkbp51 and Fkbp52 in Glucocorticoid Receptor Regulated Metabolism. Ph.D. Thesis, University of Toledo, OH, 2008.
- (11) Romano, S.; D'Angelillo, A.; Pacelli, R.; Staibano, S.; De Luna, E.; Bisogni, R.; Eskelinen, E. L.; Mascolo, M.; Cali, G.; Arra, C.; Romano, M. F. Role of FK506-binding protein 51 in the control of apoptosis of irradiated melanoma cells. *Cell Death Differ.* **2010**, *17*, 145–157.
- (12) Romano, S.; Staibano, S.; Greco, A.; Brunetti, A.; Nappo, G.; Iardi, G.; Martinelli, R.; Sorrentino, A.; Di Pace, A.; Mascolo, M.; Bisogni, R.; Scalvenzi, M.; Alfano, B.; Romano, M. F. FK506 binding protein 51 positively regulates melanoma stemness and metastatic potential. *Cell Death Dis.* **2013**, *4*, e578.
- (13) Srivastava, S. K.; Bhardwaj, A.; Arora, S.; Tyagi, N.; Singh, A. P.; Carter, J. E.; Scammell, J. G.; Fodstad, O.; Singh, S. Interleukin-8 is a key mediator of FKBP51-induced melanoma growth, angiogenesis and metastasis. *Br. J. Cancer* **2015**, *112*, 1772.
- (14) Gaali, S.; Gopalakrishnan, R.; Wang, Y.; Kozany, C.; Hausch, F. The chemical biology of immunophilin ligands. *Curr. Med. Chem.* **2011**, *18* (35), 5355–79.
- (15) Schmidt, M. V.; Paez-Pereda, M.; Holsboer, F.; Hausch, F. The Prospect of FKBP51 as a Drug Target. *ChemMedChem* **2012**, *7* (8), 1351–9.
- (16) Hausch, F. FKBP5 and their role in neuronal signaling. *Biochim. Biophys. Acta, Gen. Subj.* **2015**, *1850*, 2035–40.
- (17) Blackburn, E. A.; Walkinshaw, M. D. Targeting FKBP isoforms with small-molecule ligands. *Curr. Opin. Pharmacol.* **2011**, *11* (4), 365–371.

- (18) Gaali, S.; Kirschner, A.; Cuboni, S.; Hartmann, J.; Kozany, C.; Balsevich, G.; Namendorf, C.; Fernandez-Vizorra, P.; Sippel, C.; Zannas, A. S.; Draenert, R.; Binder, E. B.; Almeida, O. F. X.; Rühler, G.; Uhr, M.; Schmidt, M. V.; Touma, C.; Bracher, A.; Hausch, F. Selective inhibitors of the FK506-binding protein 51 by induced fit. *Nat. Chem. Biol.* **2015**, *11* (1), 33–37.
- (19) Hartmann, J.; Wagner, K. V.; Dedic, N.; Marinescu, D.; Scharf, S. H.; Wang, X. D.; Deussing, J. M.; Hausch, F.; Rein, T.; Schmidt, U.; Holsboer, F.; Müller, M. B.; Schmidt, M. V. Fkbp52 heterozygosity alters behavioral, endocrine and neurogenetic parameters under basal and chronic stress conditions in mice. *Psychoneuroendocrinology* **2012**, *37* (12), 2009–21.
- (20) Warriar, M.; Hinds, T. D., Jr.; Ledford, K. J.; Cash, H. A.; Patel, P. R.; Bowman, T. A.; Stechschulte, L. A.; Yong, W.; Shou, W.; Najjar, S. M.; Sanchez, E. R. Susceptibility to diet-induced hepatic steatosis and glucocorticoid resistance in FK506-binding protein 52-deficient mice. *Endocrinology* **2010**, *151* (7), 3225–36.
- (21) Cheung-Flynn, J.; Prapapanich, V.; Cox, M. B.; Riggs, D. L.; Suarez-Quian, C.; Smith, D. F. Physiological role for the cochaperone FKBP52 in androgen receptor signaling. *Mol. Endocrinol.* **2005**, *19* (6), 1654–66.
- (22) Tranguch, S.; Cheung-Flynn, J.; Daikoku, T.; Prapapanich, V.; Cox, M. B.; Xie, H.; Wang, H.; Das, S. K.; Smith, D. F.; Dey, S. K. From The Cover: Cochaperone immunophilin FKBP52 is critical to uterine receptivity for embryo implantation. *Proc. Natl. Acad. Sci. U. S. A.* **2005**, *102* (40), 14326–14331.
- (23) Yang, Z.; Wolf, I. M.; Chen, H.; Periyasamy, S.; Chen, Z.; Yong, W.; Shi, S.; Zhao, W.; Xu, J.; Srivastava, A.; Sanchez, E. R.; Shou, W. FK506-Binding Protein 52 Is Essential to Uterine Reproductive Physiology Controlled by the Progesterone Receptor A Isoform. *Mol. Endocrinol.* **2006**, *20* (11), 2682–2694.
- (24) Yong, W.; Yang, Z.; Periyasamy, S.; Chen, H.; Yucel, S.; Li, W.; Lin, L. Y.; Wolf, I. M.; Cohn, M. J.; Baskin, L. S.; Sanchez, E. R.; Shou, W. Essential Role for Co-chaperone Fkbp52 but Not Fkbp51 in Androgen Receptor-mediated Signaling and Physiology. *J. Biol. Chem.* **2007**, *282* (7), 5026–5036.
- (25) Bracher, A.; Kozany, C.; Hähle, A.; Wild, P.; Zacharias, M.; Hausch, F. Crystal Structures of the Free and Ligand-Bound FK1-FK2 Domain Segment of FKBP52 Reveal a Flexible Inter-Domain Hinge. *J. Mol. Biol.* **2013**, *425* (22), 4134–4144.
- (26) Bracher, A.; Kozany, C.; Thost, A. K.; Hausch, F. Structural characterization of the PPLase domain of FKBP51, a cochaperone of human Hsp90. *Acta Crystallogr., Sect. D: Biol. Crystallogr.* **2011**, *67* (6), 549–59.
- (27) Marz, A. M.; Fabian, A.-K.; Kozany, C.; Bracher, A.; Hausch, F. Large FK506-Binding Proteins Shape the Pharmacology of Rapamycin. *Mol. Cell. Biol.* **2013**, *33* (7), 1357–1367.
- (28) Hartmann, J.; Wagner, K. V.; Gaali, S.; Kirschner, A.; Kozany, C.; Rühler, G.; Hoeijmakers, L.; Westerholz, S.; Uhr, M.; Chen, A.; Holsboer, F.; Hausch, F.; Schmidt, M. V. Pharmacological inhibition of the psychiatric risk factor FKBP51 has anxiolytic properties. *J. Neurosci.* **2015**, *35*, 9007–16.
- (29) Rankovic, Z. CNS Drug Design: Balancing Physicochemical Properties for Optimal Brain Exposure. *J. Med. Chem.* **2015**, *58* (6), 2584–2608.
- (30) Wager, T. T.; Chandrasekaran, R. Y.; Hou, X.; Troutman, M. D.; Verhoest, P. R.; Villalobos, A.; Will, Y. Defining desirable central nervous system drug space through the alignment of molecular properties, in vitro ADME, and safety attributes. *ACS Chem. Neurosci.* **2010**, *1* (6), 420–34.
- (31) Evans, D. A.; Ennis, M. D.; Le, T.; Mandel, N.; Mandel, G. Asymmetric acylation reactions of chiral imide enolates. The first direct approach to the construction of chiral.β-dicarbonyl synthons. *J. Am. Chem. Soc.* **1984**, *106* (4), 1154–1156.
- (32) Gopalakrishnan, R.; Kozany, C.; Gaali, S.; Kress, C.; Hoogeland, B.; Bracher, A.; Hausch, F. Evaluation of Synthetic FK506 Analogues as Ligands for the FK506-Binding Proteins 51 and 52. *J. Med. Chem.* **2012**, *55* (9), 4114–22.
- (33) Kozany, C.; März, A.; Kress, C.; Hausch, F. Fluorescent Probes to Characterise FK506-Binding Proteins. *ChemBioChem* **2009**, *10* (8), 1402–1410.
- (34) Van Duyne, G. D.; Standaert, R. F.; Karplus, P. A.; Schreiber, S. L.; Clardy, J. Atomic structure of FKBP-FK506, an immunophilin-immunosuppressant complex. *Science* **1991**, *252* (5007), 839–42.
- (35) Crimmins, M. T.; Chaudhary, K. Titanium Enolates of Thiazolidinethione Chiral Auxiliaries: Versatile Tools for Asymmetric Aldol Additions. *Org. Lett.* **2000**, *2* (6), 775–777.
- (36) Gopalakrishnan, R.; Kozany, C.; Wang, Y.; Schneider, S.; Hoogeland, B.; Bracher, A.; Hausch, F. Exploration of Pipecolate Sulfonamides as Binders of the FK506-Binding Proteins 51 and 52. *J. Med. Chem.* **2012**, *55* (9), 4123–31.
- (37) Bischoff, M.; Sippel, C.; Bracher, A.; Hausch, F. Stereoselective Construction of the 5-Hydroxy Diazabicyclo[4.3.1]decane-2-one Scaffold, a Privileged Motif for FK506-Binding Proteins. *Org. Lett.* **2014**, *16*, 5254–7.
- (38) Pomplun, S.; Wang, Y.; Kirschner, A.; Kozany, C.; Bracher, A.; Hausch, F. Rational Design and Asymmetric Synthesis of Potent and Neurotrophic Ligands for FK506-Binding Proteins (FKBPs). *Angew. Chem., Int. Ed.* **2015**, *54*, 345–8.
- (39) Wang, Y.; Kirschner, A.; Fabian, A. K.; Gopalakrishnan, R.; Kress, C.; Hoogeland, B.; Koch, U.; Kozany, C.; Bracher, A.; Hausch, F. Increasing the Efficiency of Ligands for FK506-Binding Protein 51 by Conformational Control. *J. Med. Chem.* **2013**, *56* (10), 3922–35.
- (40) LeMaster, D. M.; Mustafi, S. M.; Brecher, M.; Zhang, J.; Heroux, A.; Li, H.; Hernandez, G. Coupling of conformational transitions in the N-terminal domain of the 51 kDa FK506-binding protein (FKBP51) near its site of interaction with the steroid receptor proteins. *J. Biol. Chem.* **2015**, *16*, 5254–7.
- (41) Mustafi, S. M.; Lemaster, D. M.; Hernandez, G. Differential conformational dynamics in the closely homologous FK506-binding domains of FKBP51 and FKBP52. *Biochem. J.* **2014**, *461* (1), 115–23.

## B. Research Articles – Publication/Manuscript VI

### SUPPORTING INFORMATION

#### **Structure-activity relationship analysis of selective FKBP51 ligands**

Xixi Feng\*, Claudia Sippel\*, Andreas Bracher<sup>#</sup>, Felix Hausch\*

\* Max Planck Institute of Psychiatry, Dept. Translational Research in Psychiatry, Kraepelinstrasse 2, 80804 Munich, Germany

<sup>#</sup> Max Planck Institute of Biochemistry, Am Klopferspitz 18, 82152 Martinsried, Germany

#### **Table of contents**

I. Crystallography	S2
II. Chemistry	S3
III. References	S16

**I. Crystallography**

<b>Dataset</b>	<b>FKBP51·41</b>
Space group	$P2_12_12_1$
Cell dimensions	
a, b, c (Å)	43.37, 50.22, 61.81
$\alpha, \beta, \gamma$ (°)	90, 90, 90
Wavelength (Å)	0.97895
Resolution (Å)	43.37- 2.25 (2.32 - 2.25)*
$R_{\text{merge}}$	0.093 (0.599)
$I/\sigma I$	10.4 (2.4)
Completeness (%)	99.4 (95.9)
Redundancy	5.2 (5.3)
<b>Refinement</b>	
Resolution (Å)	30 - 2.25
No reflections	6454
$R_{\text{work}} / R_{\text{free}}$	0.211 / 0.284
Number of atoms	
Protein	986
Ligand/ion	49
Water	55
<i>B</i> -factors	
Protein	39.71
Ligand/ion	42.14
Water	41.11
R.m.s. deviations	
Bond length (Å)	0.007
Bond angles (°)	1.437

\* Values in parenthesis for outer shell.

**Table 1** | *Data Collection and Refinement Statistics*

*Crystallization*

The complexes were prepared by mixing FKBP51 (16-140)-A19T protein at 1.75 mM with 29 mM **41** dissolved in DMSO in 9:1 ratio. Crystallization was performed at 20 °C using the hanging drop vapor-diffusion method, equilibrating mixtures of 1  $\mu$ l protein complex and 1  $\mu$ l reservoir against 500  $\mu$ l reservoir solution. Crystals were obtained with reservoir solution containing 22 % PEG-3350, 0.2 M  $\text{NH}_4$ -acetate and 0.1 M HEPES-NaOH pH 7.5.

*Structure Solution and Refinement*

The diffraction data were collected at beamline ID29 of the European Synchrotron Radiation Facility (ESRF) in Grenoble, France. Diffraction data were integrated with XDS<sup>1</sup> and further processed with Aimless and Ctruncate<sup>2</sup>, as implemented in the CCP4i interface<sup>3, 4</sup>. The crystal structures were solved by molecular replacement employing the program Molrep<sup>5</sup>.

## B. Research Articles – Publication/Manuscript VI

Iterative model improvement and refinement were performed with Coot<sup>6</sup> and Refmac5<sup>7</sup>. The dictionaries for the compounds were generated with the PRODRG server<sup>8</sup>. Residues facing solvent channels without detectable side chain density were modeled as alanines. Molecular graphics figures were generated with the program Pymol<sup>9</sup>.

### II. Chemistry

Chromatographic separations were performed either by manual flash chromatography or automated flash chromatography using an Interchim Puriflash 430 with an UV detector.

Merck F-254 (thickness 0.25 mm) commercial plates were used for analytical TLC. <sup>1</sup>H NMR spectra, <sup>13</sup>C NMR spectra, 2D HSQC, HMBC, and COSY of all intermediates were obtained from the Department of Chemistry and Pharmacy, LMU, on a Bruker AC 300, a Bruker XL 400, or a Bruker AMX 600 at room temperature. Chemical shifts for <sup>1</sup>H or <sup>13</sup>C are given in ppm ( $\delta$ ) downfield from tetramethylsilane using residual protio solvent as an internal standard.

Mass spectra (m/z) were recorded on a Thermo Finnigan LCQ DECA XP Plus mass spectrometer at the Max Planck Institute of Psychiatry, while the high resolution mass spectrometry was carried out at MPI for Biochemistry (Microchemistry Core Facility) on Bruker Daltonics MicrOTOF.

The purity of the compounds was verified by reversed phase HPLC. All gradients were started after 1 min of equilibration with starting percentage of solvent mixture.

#### Analytical HPLC:

**Pump:** Beckman System Gold 125S Solvent Module  
**Detector:** Beckman System Gold Diode Array Detector Module 168  
**Column:** Phenomenex Jupiter 4 $\mu$  Proteo 90Å, 250 x 4.6 mm 4 micron

**Solvent A:** 95% H<sub>2</sub>O, 5% MeCN, 0.1% TFA

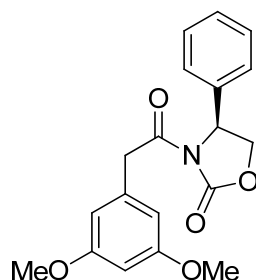
**Solvent B:** 95% MeCN, 5% H<sub>2</sub>O, 0.1% TFA

**Methods:** Described for the specific compound

#### Preparative HPLC:

**Pump:** Beckman System Gold Programmable Solvent Module 126 NMP  
**Detector:** Beckman Programmable Detector Module 166  
**Column:** Phenomenex Jupiter 10 $\mu$  Proteo 90 Å, 250 x 21.2 mm 10 micron

**Methods:** Described for the specific compound

**(S)-3-(2-(3,5-dimethoxyphenyl)acetyl)-4-phenyloxazolidin-2-one****3**

DIPEA (0.49 mL, 2.80 mmol) and pivaloyl chloride (0.35 mL, 2.80 mmol) were added to a solution of 2-(3,5-dimethoxyphenyl)acetic acid (620 mg, 3.16 mmol) in DCM (5.0 mL) at 0 °C. The reaction mixture was stirred at that temperature for 30 min and at RT for 1 h. Then it was quenched by the addition of saturated NH<sub>4</sub>Cl and the product was extracted with DCM. The combined organics were dried over MgSO<sub>4</sub>, filtered and the solvent was removed to obtain the pivalic acid mixed anhydride as light yellow oil, which was used without further purification.

In the meantime n-BuLi (1.22 mL, 3.06 mmol, 2.5 M) was added to a solution of (S)-4-phenyloxazolidin-2-one (457 mg, 2.80 mmol) in THF (8.0 mL) at -78 °C and stirred at that temperature for 1 h. The pivalic acid mixed anhydride, dissolved in DCM, was added and the reaction mixture was stirred for 16 h, whereby it was allowed to warm to RT. The reaction mixture was then quenched by the addition of saturated NH<sub>4</sub>Cl and the product was extracted with Et<sub>2</sub>O. The combined organics were dried over MgSO<sub>4</sub>, filtered and the solvent was removed. After purification by flash chromatography (gradient 0-20 % EtOAc in cyclohexane) the title compound was obtained as light yellow oil (588 mg, 1.72 mmol, 67.7 %).

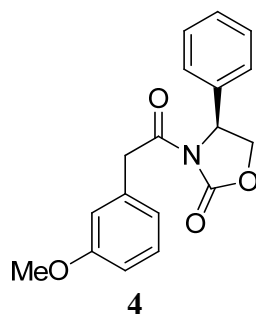
**TLC** [EtOAc/cyclohexane, 4:6]: R<sub>f</sub> = 0.38.

**Mass:** (ESI<sup>+</sup>), calculated 342.13 [C<sub>19</sub>H<sub>19</sub>NO<sub>5</sub>+H]<sup>+</sup>, found 341.99 [M+H]<sup>+</sup>.

**<sup>1</sup>H NMR** (300 MHz, CDCl<sub>3</sub>) δ 7.36 – 7.29 (m, 3H), 7.24 – 7.18 (m, 2H), 6.40 – 6.37 (m, 2H), 6.37 – 6.34 (m, 1H), 5.42 (dd, J = 8.8, 3.9 Hz, 1H), 4.67 (t, J = 8.8 Hz, 1H), 4.28 – 4.23 (m, 1H), 4.23 – 4.20 (m, 2H), 3.75 – 3.69 (m, 6H).

**<sup>13</sup>C NMR** (75 MHz, CDCl<sub>3</sub>) δ 170.27, 160.72, 153.54, 138.72, 135.29, 129.07, 128.67, 125.97, 107.57, 107.43, 99.59, 69.85, 57.75, 55.30, 55.25, 41.75.

**(S)-3-(2-(3-methoxyphenyl)acetyl)-4-phenyloxazolidin-2-one**



**4** was synthesized according to **3** with DIPEA (0.58 mL, 3.31 mmol), pivaloyl chloride (407  $\mu$ l, 3.31 mmol), 2-(3-methoxyphenyl)acetic acid (500 mg, 3.01 mmol) in DCM (6.0 mL) and n-BuLi (1.44 mL, 3.61 mmol, 2.5 M), (*S*)-4-phenyloxazolidin-2-one (540 mg, 3.31 mmol) in THF (9.0 mL). After purification by flash chromatography (gradient 0-10 % EtOAc in cyclohexane) the title compound was obtained as light yellow oil (655 mg, 2.11 mmol, 70.0 %).

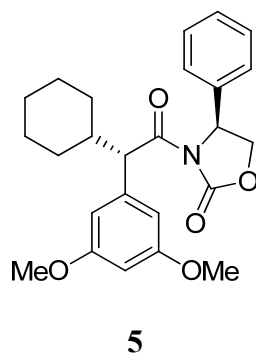
**TLC** [EtOAc/cyclohexane, 2:8]:  $R_f$  = 0.18.

**Mass:** (ESI<sup>+</sup>), calculated 312.12 [C<sub>18</sub>H<sub>17</sub>NO<sub>4</sub>+H]<sup>+</sup>, found 311.97 [M+H]<sup>+</sup>.

**<sup>1</sup>H NMR** (400 MHz, CDCl<sub>3</sub>)  $\delta$  7.30 – 7.23 (m, 3H), 7.16 – 7.10 (m, 3H), 6.78 – 6.69 (m, 3H), 5.36 (dd,  $J$  = 8.8, 3.9 Hz, 1H), 4.61 (t,  $J$  = 8.9 Hz, 1H), 4.20 (s, 3H), 3.68 (s, 3H).

**<sup>13</sup>C NMR** (101 MHz, CDCl<sub>3</sub>)  $\delta$  170.54, 159.76, 153.72, 138.90, 134.81, 129.57, 129.24, 128.82, 126.10, 122.19, 115.18, 113.12, 77.16, 70.01, 57.89, 55.28, 41.76.

**(S)-3-((S)-2-cyclohexyl-2-(3,5-dimethoxyphenyl)acetyl)-4-phenyloxazolidin-2-one**



NaHMDS (2.58 mL, 2.58 mmol, 1.0 M) was added to a solution of **3** (588 mg, 1.72 mmol) in THF (20.0 mL) at -78 °C. After stirring at -78 °C for 1h 3-bromocyclohex-1-ene (991  $\mu$ l, 8.61 mmol) was added drop wise. The reaction mixture was stirred at that temperature for 1 h and then at 4 °C for 16 h. Then it was quenched by the addition of saturated NH<sub>4</sub>Cl and the product was extracted with Et<sub>2</sub>O. The combined organics were dried over MgSO<sub>4</sub>, filtered and the solvent was removed. The crude product was purified and separated from the minor diastereomer by flash chromatography (gradient 0-5 % EtOAc in cyclohexane).

The major alkylation product was dissolved in MeOH (10.0 mL) and the solution was degassed with argon. Then Pd-C (40.4 mg, 38  $\mu$ mol, 10 % wt) was added. In the following step H<sub>2</sub> was bubbled through the reaction mixture for 5 min. The reaction was then stirred

## B. Research Articles – Publication/Manuscript VI

under H<sub>2</sub> atmosphere for 16 h. After that time the dark suspension was filtered through celite and the solvent was removed under reduced pressure. After purification by flash chromatography (gradient 0-20 % EtOAc in cyclohexane) the title compound was obtained as colourless oil (144 mg, 0.34 mmol, 19.8 %).

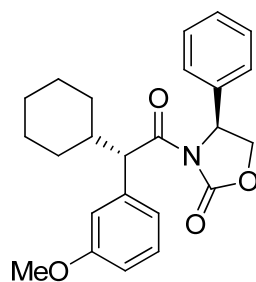
**TLC** [EtOAc/cyclohexane, 2:8]: R<sub>f</sub> = 0.32.

**Mass:** (ESI<sup>+</sup>), calculated 424.21 [C<sub>25</sub>H<sub>29</sub>NO<sub>5</sub>+H]<sup>+</sup>, found 424.05 [M+H]<sup>+</sup>.

**<sup>1</sup>H NMR** (800 MHz, CDCl<sub>3</sub>) δ 7.43 – 7.40 (m, 2H), 7.38 – 7.35 (m, 1H), 7.34 – 7.32 (m, 2H), 6.61 (d, *J* = 2.3 Hz, 2H), 6.38 (t, *J* = 2.3 Hz, 1H), 5.37 (dd, *J* = 8.7, 3.4 Hz, 1H), 4.84 (d, *J* = 10.7 Hz, 1H), 4.57 (t, *J* = 8.8 Hz, 1H), 4.22 (dd, *J* = 8.9, 3.5 Hz, 1H), 3.79 (s, 6H), 2.03 (qt, *J* = 11.0, 3.4 Hz, 1H), 1.62 – 1.54 (m, 2H), 1.46 – 1.40 (m, 3H), 1.15 – 1.05 (m, 3H), 1.00 – 0.93 (m, 1H), 0.86 – 0.80 (m, 1H).

**<sup>13</sup>C NMR** (201 MHz, CDCl<sub>3</sub>) δ 175.53, 162.55, 155.37, 141.68, 141.38, 131.09, 130.63, 127.80, 126.27, 125.08, 109.15, 101.42, 71.33, 60.07, 57.27, 43.70, 33.40, 32.14, 28.86, 28.20, 27.79, 27.73, 24.70, 19.73.

### (*S*)-3-((*S*)-2-cyclohexyl-2-(3-methoxyphenyl)acetyl)-4-phenyloxazolidin-2-one



6

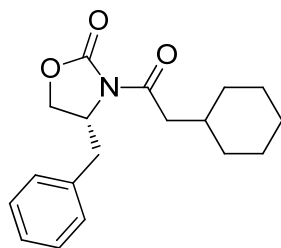
**6** was synthesized according to **5** with NaHMDS (1.88 mL, 1.88 mmol, 1.0 M), **4** (390mg, 1.25 mmol), 3-bromocyclohex-1-ene (720 μL, 6.26 mmol) in THF (15.0 mL) and Pd-C (37.5 mg, 35 μmol, 10 % wt) in MeOH (10.0 mL) to obtain the title compound as colourless oil (130 mg, 0.33 mmol, 26.4 %).

**TLC** [EtOAc/cyclohexane, 3:7]: R<sub>f</sub> = 0.47.

**Mass:** (ESI<sup>+</sup>), calculated 394.20 [C<sub>24</sub>H<sub>27</sub>NO<sub>4</sub>+H]<sup>+</sup>, found 394.01 [M+H]<sup>+</sup>.

**<sup>1</sup>H NMR** (400 MHz, CDCl<sub>3</sub>) δ 7.37 – 7.22 (m, 5H), 7.17 – 7.10 (m, 1H), 6.95 – 6.89 (m, 2H), 6.72 (ddd, *J* = 8.2, 2.6, 1.0 Hz, 1H), 5.27 (dd, *J* = 8.7, 3.5 Hz, 1H), 4.79 (d, *J* = 10.7 Hz, 1H), 4.47 (t, *J* = 8.8 Hz, 1H), 4.12 (dd, *J* = 8.9, 3.5 Hz, 1H), 3.72 (s, 3H), 2.01 – 1.89 (m, 1H), 1.57 – 1.43 (m, 1H), 1.29 (d, *J* = 12.5 Hz, 1H), 1.23 – 1.12 (m, 2H), 1.08 – 0.97 (m, 3H), 0.95 – 0.84 (m, 1H), 0.80 – 0.68 (m, 2H).

**<sup>13</sup>C NMR** (101 MHz, CDCl<sub>3</sub>) δ 173.74, 159.62, 153.44, 139.44, 139.00, 129.27, 129.14, 128.70, 125.89, 121.87, 114.63, 112.92, 69.40, 58.12, 55.21, 54.59, 41.82, 31.50, 30.23, 26.93, 26.26, 25.85, 25.80.

**(R)-4-benzyl-3-(2-cyclohexylacetyl)oxazolidin-2-one**

7

To a solution of (*R*)-4-benzylloxazolidin-2-one (500 mg, 2.82 mmol) in THF (25.0 mL) was added *n*-BuLi (1.7 mL, 4.23 mmol, 2.5 M) at  $-78\text{ }^{\circ}\text{C}$  and the resulting mixture was stirred at that temperature for 1.5 h, whereby it turned into an orange solution. To the resulting mixture was added 2-cyclohexylacetyl chloride (0.65 mL, 4.23 mmol) at  $-78\text{ }^{\circ}\text{C}$ . The reaction was stirred at that temperature for 2.5 h and was then slowly warmed to RT.

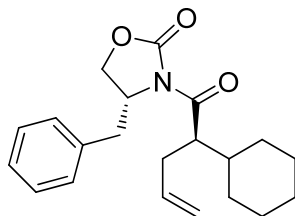
After stirring at 16 h, the colorless reaction mixture was quenched with sat.  $\text{NH}_4\text{Cl}$  solution. The aqueous layer was extracted with  $\text{Et}_2\text{O}$ . The combined organic layers were washed with brine, dried over  $\text{MgSO}_4$ , filtrated, and concentrated under reduced pressure. The crude product was purified by flash chromatography (gradient 0-10 % EtOAc in cyclohexane) to yield the title compound (850 mg, 2.82 mmol, quant.) as a colorless solid.

**TLC** [EtOAc/cyclohexane, 2:8]:  $R_f = 0.30$ .

**Mass:** ( $\text{ESI}^+$ ), calculated 302.18 [ $\text{C}_{18}\text{H}_{23}\text{NO}_3+\text{H}$ ] $^+$ , found 302.14 [ $\text{M}+\text{H}$ ] $^+$ .

**$^1\text{H}$  NMR** (599 MHz,  $\text{CDCl}_3$ )  $\delta$  7.35 – 7.31 (m, 2H), 7.29 – 7.26 (m, 1H), 7.23 – 7.20 (m, 2H), 4.70 – 4.65 (m, 1H), 4.21 – 4.14 (m, 2H), 3.31 (dd,  $J = 13.4, 3.4$  Hz, 1H), 2.90 – 2.86 (m, 1H), 2.81 – 2.73 (m, 2H), 1.94 – 1.87 (m, 1H), 1.81 – 1.64 (m, 5H), 1.35 – 1.24 (m, 2H), 1.17 (qt,  $J = 12.7, 3.5$  Hz, 1H), 1.09 – 0.99 (m, 2H).

**$^{13}\text{C}$  NMR** (151 MHz,  $\text{CDCl}_3$ )  $\delta$  172.59, 153.40, 135.33, 129.39, 128.92, 128.90, 127.30, 66.05, 55.19, 42.65, 37.99, 34.29, 33.11, 33.06, 26.19, 26.12, 26.10.

**(R)-4-benzyl-3-((R)-2-cyclohexylpent-4-enoyl)oxazolidin-2-one**

8

NaHMDS (1.5 mL, 1.5 mmol, 1.0 M in THF) was added to a solution of **7** (300 mg, 1.0 mmol) in THF (2.0 mL) at  $-78\text{ }^{\circ}\text{C}$  and stirred for 1 h, whereby it turned into a light yellow solution. Allyl bromide (129  $\mu\text{L}$ , 1.5 mmol) was then added dropwise. The reaction was stirred for 1 h at  $-78\text{ }^{\circ}\text{C}$  and then for 16 h at  $4\text{ }^{\circ}\text{C}$ .

## B. Research Articles – Publication/Manuscript VI

The reaction mixture was quenched with saturated  $\text{NH}_4\text{Cl}$  solution and the aqueous layer was extracted with  $\text{Et}_2\text{O}$ . The combined organic layers were washed with brine, dried over  $\text{MgSO}_4$ , filtrated, and concentrated under reduced pressure. The crude product was purified by flash chromatography (gradient 0-5 %  $\text{EtOAc}$  in cyclohexane) to yield the title compound (249 mg, 0.72 mmol, 73.2 %) as a colorless solid.

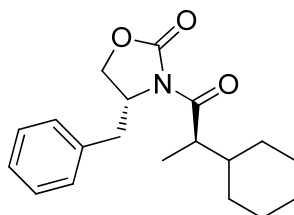
**TLC** [ $\text{EtOAc}/\text{cyclohexane}$ , 2:8]:  $R_f = 0.43$ .

**Mass:** ( $\text{ESI}^+$ ), calculated 342.21 [ $\text{C}_{21}\text{H}_{27}\text{NO}_3+\text{H}$ ] $^+$ , found 342.27 [ $\text{M}+\text{H}$ ] $^+$ .

**$^1\text{H}$  NMR** (599 MHz,  $\text{CDCl}_3$ )  $\delta$  7.47 – 6.99 (m, 5H), 5.90 – 5.71 (m, 1H), 5.07 (dq,  $J = 17.0$ , 1.5 Hz, 1H), 5.02 – 4.98 (m, 1H), 4.67 (ddt,  $J = 10.3$ , 6.7, 3.2 Hz, 1H), 4.17 – 4.05 (m, 2H), 3.90 (ddd,  $J = 9.6$ , 7.6, 4.4 Hz, 1H), 3.30 (dd,  $J = 13.4$ , 3.3 Hz, 1H), 2.62 (dd,  $J = 13.4$ , 10.1 Hz, 1H), 2.51 – 2.32 (m, 2H), 1.87 – 1.79 (m, 1H), 1.77 – 1.58 (m, 4H), 1.30 – 1.15 (m, 3H), 1.17 – 1.04 (m, 2H), 1.00 (qd,  $J = 12.4$ , 3.6 Hz, 1H).

**$^{13}\text{C}$  NMR** (151 MHz,  $\text{CDCl}_3$ )  $\delta$  175.83, 153.22, 135.64, 135.55, 129.38, 128.88, 127.22, 116.88, 65.69, 55.64, 47.40, 40.05, 38.06, 33.78, 31.17, 29.66, 26.28.

### (R)-4-benzyl-3-((R)-2-cyclohexylpropanoyl)oxazolidin-2-one



9

$\text{NaHMDS}$  (1.0 mL, 1.0 mmol, 1.0 M in THF) was added to a solution of **7** (200 mg, 0.66 mmol) in THF (2.0 mL) at  $-78\text{ }^\circ\text{C}$  and stirred for 1 h, whereby it turned into a light yellow solution. Iodomethane (415  $\mu\text{L}$ , 6.64 mmol) was then added dropwise. The reaction was stirred for 2.5 h at  $-78\text{ }^\circ\text{C}$  and then for 16 h at  $4\text{ }^\circ\text{C}$ .

The reaction mixture was quenched with saturated  $\text{NH}_4\text{Cl}$  solution and the aqueous layer was extracted with  $\text{Et}_2\text{O}$ . The combined organic layers were washed with brine, dried over  $\text{MgSO}_4$ , filtrated, and concentrated under reduced pressure. The crude product was purified by flash chromatography (gradient 0-5 %  $\text{EtOAc}$  in cyclohexane) to yield the title compound (163 mg, 0.52 mmol, 78.0 %) as a colorless solid.

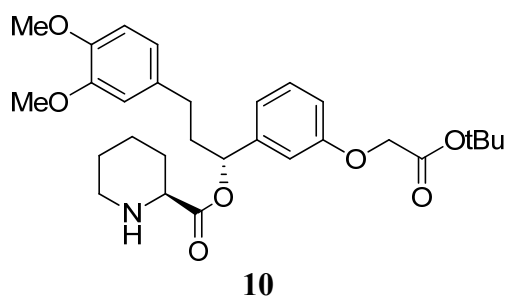
**TLC** [ $\text{EtOAc}/\text{cyclohexane}$ , 2:8]:  $R_f = 0.43$ .

**Mass:** ( $\text{ESI}^+$ ), calculated 316.19 [ $\text{C}_{19}\text{H}_{25}\text{NO}_3+\text{H}$ ] $^+$ , found 316.03 [ $\text{M}+\text{H}$ ] $^+$ .

**$^1\text{H}$  NMR** (300 MHz,  $\text{CDCl}_3$ )  $\delta$  7.48 – 7.10 (m, 5H), 4.66 (ddt,  $J = 10.0$ , 6.6, 3.3 Hz, 1H), 4.22 – 4.11 (m, 2H), 3.64 (p,  $J = 7.0$  Hz, 1H), 3.28 (dd,  $J = 13.2$ , 3.2 Hz, 1H), 2.75 (dd,  $J = 13.3$ , 9.6 Hz, 1H), 1.79 – 1.53 (m, 6H), 1.29 – 0.89 (m, 8H).

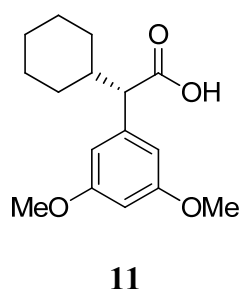
**$^{13}\text{C}$  NMR** (75 MHz,  $\text{CDCl}_3$ )  $\delta$  177.16, 153.12, 135.38, 129.40, 128.89, 127.27, 65.88, 55.44, 42.62, 40.47, 37.89, 31.47, 29.03, 26.30, 26.25, 14.16.

**(S)-(R)-3-(3,4-dimethoxyphenyl)-1-(3-(2-oxopropoxy)phenyl)propyl piperidine-2-carboxylate**



Synthesized as previously described <sup>10</sup>.

**(S)-2-cyclohexyl-2-(3,5-dimethoxyphenyl)acetic acid**



LiOH (34.4 mg, 1.43 mmol) and H<sub>2</sub>O<sub>2</sub> (163 μL, 1.59 mmol, 30 % wt) were added to a solution of **5** (135 mg, 0.32 mmol) in THF/H<sub>2</sub>O (6.5 mL, 8:5) at 0 °C. The reaction mixture was stirred at RT for 16 h and then it was quenched with saturated Na<sub>2</sub>SO<sub>3</sub> solution. The aqueous layer was extracted with DCM and, in the following step, acidified with concentrated HCl. Then the aqueous layer was again extracted with DCM. These layers were combined, dried over MgSO<sub>4</sub> and filtered. The solvent was then removed to obtain the title compound without any further purification as colorless oil (36.1 mg, 0.13 mmol, 40.7 %).

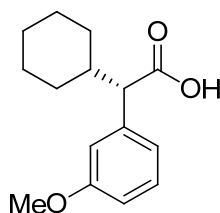
**TLC** [EtOAc/cyclohexane, 1:1]: R<sub>f</sub> = 0.46.

**Mass:** (ESI<sup>+</sup>), calculated 279.16 [C<sub>16</sub>H<sub>22</sub>O<sub>4</sub>+H]<sup>+</sup>, found 279.02 [M+H]<sup>+</sup>.

**<sup>1</sup>H NMR** (800 MHz, CDCl<sub>3</sub>) δ 6.51 (d, J = 2.3 Hz, 2H), 6.38 (t, J = 2.2 Hz, 1H), 3.80 (s, 6H), 3.16 (d, J = 10.7 Hz, 1H), 1.98 (qt, J = 11.1, 3.4 Hz, 1H), 1.92 – 1.89 (m, 1H), 1.79 – 1.72 (m, 1H), 1.68 – 1.60 (m, 2H), 1.43 – 1.37 (m, 1H), 1.35 – 1.30 (m, 1H), 1.19 – 1.13 (m, 2H), 1.11 – 1.03 (m, 1H), 0.81 – 0.72 (m, 1H).

**<sup>13</sup>C NMR** (201 MHz, CDCl<sub>3</sub>) δ 178.74, 160.73, 139.54, 106.80, 99.19, 58.85, 55.32, 40.63, 31.93, 30.27, 26.26, 25.95, 25.93.

**(S)-2-cyclohexyl-2-(3-methoxyphenyl)acetic acid**



**12**

**12** was synthesized according to **11** with LiOH (32.9 mg, 1.37 mmol), H<sub>2</sub>O<sub>2</sub> (156 μl, 1.53 mmol, 30 % wt) and **6** (120mg, 0.31 mmol) in THF/H<sub>2</sub>O (6.5 mL, 8:5) to obtain the title compound as colorless oil (54.5 mg, 0.22 mmol, 71.7 %).

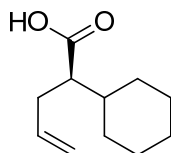
**TLC** [EtOAc/cyclohexane, 1:1]: R<sub>f</sub> = 0.48.

**Mass:** (ESI<sup>+</sup>), calculated 249.15 [C<sub>15</sub>H<sub>20</sub>O<sub>3</sub>+H]<sup>+</sup>, found 248.94 [M+H]<sup>+</sup>.

**<sup>1</sup>H NMR** (599 MHz, CDCl<sub>3</sub>) δ 7.22 (t, *J* = 7.8 Hz, 1H), 6.92 – 6.88 (m, 2H), 6.82 – 6.79 (m, 1H), 3.80 (s, 3H), 3.68 – 3.61 (m, 1H), 3.11 – 3.04 (m, 1H), 1.99 (qt, *J* = 11.0, 3.4 Hz, 1H), 1.93 – 1.87 (m, 1H), 1.77 – 1.71 (m, 1H), 1.67 – 1.58 (m, 2H), 1.40 – 1.23 (m, 2H), 1.18 – 1.12 (m, 1H), 1.10 – 1.02 (m, 1H), 0.75 (qd, *J* = 12.0, 3.9 Hz, 1H).

**<sup>13</sup>C NMR** (151 MHz, CDCl<sub>3</sub>) δ 178.34, 159.93, 139.22, 129.96, 121.48, 114.70, 113.01, 77.16, 58.91, 55.52, 54.07, 42.62, 40.99, 32.26, 30.63, 26.57, 26.39, 19.00, 17.73.

**(R)-2-cyclohexylpent-4-enoic acid**



**14**

LiOH (72.6 mg, 3.03 mmol) and H<sub>2</sub>O<sub>2</sub> (344 μl, 2.38 mmol, 30 % wt) were added to a solution of **8** (230 mg, 0.67 mmol) in THF/H<sub>2</sub>O (13.0 mL, 8:5). The resulting turbid solution was stirred at RT for 4.5 h. Then the reaction mixture was quenched with saturated Na<sub>2</sub>SO<sub>3</sub> solution and it was extracted with DCM. The organic layers were discarded. Then the aqueous layer was acidified with concentrated HCl to pH = 1 and extracted with DCM. The organic layers were combined, dried over MgSO<sub>4</sub> and the solvent was removed. The title compound (80.0 mg, 0.44 mmol, 65.7 %) was obtained without further purification as a colorless oil.

**TLC** [EtOAc/cyclohexane, 1:1]: R<sub>f</sub> = 0.56.

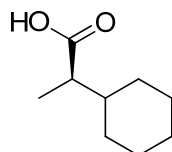
**Mass:** (ESI<sup>+</sup>), calculated 183.14 [C<sub>11</sub>H<sub>18</sub>O<sub>2</sub>+H]<sup>+</sup>, found 183.14 [M+H]<sup>+</sup>.

**<sup>1</sup>H NMR** (400 MHz, CDCl<sub>3</sub>) δ 4.81 – 4.52 (m, 2H), 4.07 – 3.94 (m, 1H), 3.37 (s, 3H), 2.49 (dd, *J* = 7.8, 6.9 Hz, 1H), 1.83 – 1.58 (m, 6H), 1.25 (d, *J* = 6.3 Hz, 3H), 1.24 – 0.98 (m, 5H).

## B. Research Articles – Publication/Manuscript VI

$^{13}\text{C}$  NMR (75 MHz,  $\text{CDCl}_3$ )  $\delta$  181.42, 135.64, 116.59, 51.59, 39.57, 33.30, 30.76, 30.38, 26.26, 26.25, 26.21.

### (R)-2-cyclohexylpropanoic acid



15

LiOH (51.3 mg, 2.14 mmol) and  $\text{H}_2\text{O}_2$  (243  $\mu\text{l}$ , 2.38 mmol, 30 % wt) were added to a solution of **9** (150 mg, 0.48 mmol) in THF/ $\text{H}_2\text{O}$  (6.5 mL, 8:5) at 0 °C. The resulting turbid solution was stirred at that temperature for 1.5 h and at RT for 1.5 h.

Then the reaction mixture was quenched with saturated  $\text{Na}_2\text{SO}_3$  solution at 0°C and it was extracted with DCM. The aqueous layer was acidified with concentrated HCl to pH = 1 and extracted with DCM. These layers were combined, dried over  $\text{MgSO}_4$  and the solvent was removed. The title compound (74.3 mg, 0.48 mmol, quant.) was obtained without further purification as a colorless oil.

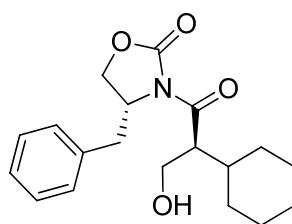
TLC [EtOAc/cyclohexane, 4:6]:  $R_f$  = 0.44.

Mass: (ESI<sup>+</sup>), calculated 157.12 [ $\text{C}_9\text{H}_{16}\text{O}_2+\text{H}$ ]<sup>+</sup>, found 157.08 [M+H]<sup>+</sup>.

$^1\text{H}$  NMR (300 MHz,  $\text{CDCl}_3$ )  $\delta$  2.27 (p,  $J$  = 7.1 Hz, 1H), 1.84 – 1.42 (m, 6H), 1.38 – 0.76 (m, 8H).

$^{13}\text{C}$  NMR (75 MHz,  $\text{CDCl}_3$ )  $\delta$  182.63, 45.25, 40.44, 31.12, 29.37, 26.26, 26.25, 26.21, 13.64.

### (R)-4-benzyl-3-((S)-2-cyclohexyl-3-hydroxypropanoyl)oxazolidin-2-one



23

**7** (200 mg, 0.66 mmol) in DCM (3.0 mL) was cooled to 0 °C and  $\text{TiCl}_4$  (730  $\mu\text{l}$ , 0.73 mmol, 1.0 M in DCM) was added drop wise. It was stirred for 10 min then DIPEA (139  $\mu\text{l}$ , 0.80 mmol) was added. The dark red enolate was stirred for 45 min at 0 °C. Then 1,3,5-Trioxane (90.0 mg, 1.0 mmol), dissolved in DCM (0.5 mL) and precooled, and afterward an additional equivalent of  $\text{TiCl}_4$  (1.0 M in DCM) were added drop wise. It was stirred for 2.5 h at 0 °C.

The brown reaction mixture was quenched with half-saturated  $\text{NH}_4\text{Cl}$  solution. The layers were separated and the organic layer was dried over  $\text{MgSO}_4$ , filtrated and concentrated under reduced pressure. The crude product was purified by flash chromatography (0 – 20 % EtOAc

## B. Research Articles – Publication/Manuscript VI

in cyclohexane) to afford the title compound as a colorless solid (171 mg, 0.52 mmol, 77.7 %).

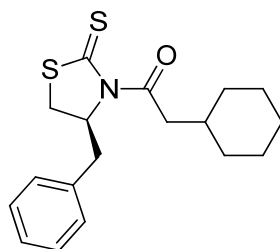
**TLC** [EtOAc/cyclohexane, 4:6]:  $R_f = 0.39$ .

**Mass:** (ESI<sup>+</sup>), calculated 332.19 [C<sub>19</sub>H<sub>25</sub>NO<sub>4</sub> + H]<sup>+</sup>, found = 331.94 [M+H]<sup>+</sup>.

**<sup>1</sup>H NMR** (300 MHz, CDCl<sub>3</sub>)  $\delta$  7.47 – 7.06 (m, 5H), 4.70 (ddt,  $J = 9.9, 6.6, 3.4$  Hz, 1H), 4.27 – 4.07 (m, 2H), 4.04 – 3.78 (m, 3H), 3.30 (dd,  $J = 13.5, 3.4$  Hz, 1H), 2.81 (dd,  $J = 13.5, 9.3$  Hz, 1H), 1.92 – 1.50 (m, 6H), 1.34 – 0.94 (m, 5H).

**<sup>13</sup>C NMR** (75 MHz, CDCl<sub>3</sub>)  $\delta$  176.04, 153.55, 135.21, 129.45, 128.90, 127.32, 66.00, 62.04, 55.54, 50.51, 37.84, 37.61, 31.29, 29.91, 26.22, 26.15.

**(S)-1-(4-benzyl-2-thioxothiazolidin-3-yl)-2-cyclohexylethanone**



**24**

To a solution of (S)-4-benzylthiazolidine-2-thione (1 g, 4.78 mmol) in THF (dry, 50 mL) was added n-BuLi (2.87 mL, 7.17 mmol, 2.5 M) at  $-78$  °C. The resulting mixture was stirred at that temperature for 1.5 h, then 2-cyclohexylacetyl chloride (1.10 ml, 7.17 mmol) was added. The temperature was maintained at  $-78$  °C for 2.5 h. Then the reaction mixture was allowed to warm to RT and stirred for 16 h. After an aqueous work up with saturated NH<sub>4</sub>Cl solution the crude product was purified by flash chromatography (cyclohexane) to afford the title compound as a yellow crystalline solid (1.48 g, 4.45 mmol, 93 %).

**TLC** [cyclohexane/EtOAc, 8:2]:  $R_f = 0.60$ .

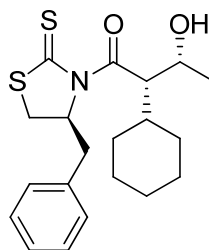
**Mass:** (ESI<sup>+</sup>), calculated 333.12 [C<sub>18</sub>H<sub>23</sub>NOS<sub>2</sub> + H]<sup>+</sup>, found = 334.04 [M+H]<sup>+</sup>

**<sup>1</sup>H NMR** (599 MHz, CDCl<sub>3</sub>)  $\delta$  7.35 – 7.30 (m, 2H), 7.30 – 7.24 (m, 3H), 5.39 – 5.30 (m, 1H), 3.36 (ddd,  $J = 11.5, 7.2, 1.0$  Hz, 1H), 3.23 – 3.09 (m, 3H), 3.03 (dd,  $J = 13.2, 10.6$  Hz, 1H), 2.88 – 2.84 (m, 1H), 1.97 – 1.88 (m, 1H), 1.78 – 1.62 (m, 5H), 1.30 – 1.22 (m, 3H), 1.15 (qt,  $J = 12.7, 3.3$  Hz, 3H), 1.08 – 0.92 (m, 2H).

**<sup>13</sup>C NMR** (151 MHz, CDCl<sub>3</sub>)  $\delta$  201.08, 173.27, 136.58, 129.42, 128.85, 127.15, 68.67, 45.41, 36.79, 34.54, 33.16, 32.91, 31.87, 26.22, 26.13, 26.04.

## B. Research Articles – Publication/Manuscript VI

### (2*S*,3*R*)-1-((*S*)-4-benzyl-2-thioxothiazolidin-3-yl)-2-cyclohexyl-3-hydroxybutan-1-one



**25**

**24** (200 mg, 0.60 mmol) in DCM (dry, 2 mL) was cooled to 0 °C. Then TiCl<sub>4</sub> (660 μl, 0.66 mmol, 1 M) was added dropwise. After 5 min TMEDA (226 μl, 1.50 mmol) was added and the resulting dark red enolate was stirred for 20 min at 0 °C. Then acetaldehyde (0.10 mL, 1.80 mmol) was then added dropwise and it was stirred for 4 h at 0 °C.

After an aqueous work up with half-saturated NH<sub>4</sub>Cl solution the crude product was purified by flash chromatography (0 – 100 % DCM in cyclohexane) to afford the title compound as a yellow oil (116.6 mg, 0.31 mmol, 52 %).

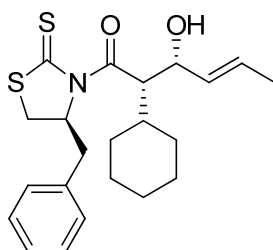
TLC [DCM]: R<sub>f</sub> = 0.19.

**Mass:** (ESI<sup>+</sup>), calculated 378.57 [C<sub>20</sub>H<sub>27</sub>NO<sub>2</sub>S<sub>2</sub> + H]<sup>+</sup>, found = 377.88 [M+H]<sup>+</sup>

**<sup>1</sup>H NMR** (599 MHz, CDCl<sub>3</sub>) δ 7.34 – 7.26 (m, 5H), 5.51 – 5.38 (m, 1H), 5.27 (dd, *J* = 9.1, 5.8 Hz, 1H), 4.25 (q, *J* = 6.2 Hz, 1H), 3.33 (ddd, *J* = 11.4, 7.2, 1.1 Hz, 1H), 3.21 (dd, *J* = 13.2, 3.9 Hz, 1H), 3.04 (dd, *J* = 13.2, 10.6 Hz, 1H), 2.80 (dd, *J* = 11.4, 0.7 Hz, 1H), 1.87 (dddd, *J* = 12.4, 11.2, 6.5, 3.3 Hz, 1H), 1.82 – 1.76 (m, 2H), 1.74 – 1.66 (m, 2H), 1.66 – 1.62 (m, 2H), 1.30 – 1.24 (m, 2H), 1.20 (d, *J* = 6.3 Hz, 3H), 1.18 – 1.06 (m, 2H).

**<sup>13</sup>C NMR** (151 MHz, CDCl<sub>3</sub>) δ 203.00, 175.26, 136.51, 129.41, 128.86, 127.17, 69.30, 68.17, 53.61, 38.47, 37.00, 31.66, 31.58, 30.12, 26.34, 26.29, 26.18, 18.49.

### (2*S*,3*R*,*E*)-1-((*S*)-4-benzyl-2-thioxothiazolidin-3-yl)-2-cyclohexyl-3-hydroxyhex-4-en-1-one



**26**

**26** was synthesized according to **25** with (*E*)-but-2-enal (0.15 mL, 1.80 mmol) to afford the title compound as yellow solid (171 mg, 0.43 mmol, 71 %).

TLC [DCM]: R<sub>f</sub> = 0.39.

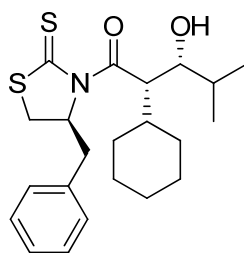
**Mass:** (ESI<sup>+</sup>), calculated 404.17 [C<sub>22</sub>H<sub>29</sub>NO<sub>2</sub>S<sub>2</sub> + H]<sup>+</sup>, found = 404.01 [M+H]<sup>+</sup>.

## B. Research Articles – Publication/Manuscript VI

**<sup>1</sup>H NMR** (400 MHz, CDCl<sub>3</sub>) δ 7.39 – 7.22 (m, 5H), 5.78 – 5.58 (m, 2H), 5.43 – 5.29 (m, 1H), 5.20 (dd, *J* = 8.5, 6.5 Hz, 1H), 4.43 (t, *J* = 6.8 Hz, 1H), 3.30 (ddd, *J* = 11.3, 7.1, 1.0 Hz, 1H), 3.22 (dd, *J* = 13.2, 4.0 Hz, 1H), 3.05 (dd, *J* = 13.2, 10.6 Hz, 1H), 2.81 (d, *J* = 11.4 Hz, 1H), 1.92 – 1.75 (m, 2H), 1.72 (d, 3H), 1.70 – 1.55 (m, 6H), 1.43 – 1.32 (m, 1H), 1.29 – 1.04 (m, 3H).

**<sup>13</sup>C NMR** (101 MHz, CDCl<sub>3</sub>) δ 202.39, 175.27, 136.59, 130.22, 129.45, 129.39, 128.85, 127.14, 73.61, 69.29, 52.80, 38.49, 36.95, 31.81, 31.03, 30.07, 26.44, 26.38, 26.27, 17.86.

### (2*S*,3*R*)-1-((*S*)-4-benzyl-2-thioxothiazolidin-3-yl)-2-cyclohexyl-3-hydroxy-4-methylpentan-1-one



27

**27** was synthesized according to **25** with TiCl<sub>4</sub> (1.12 mL, 1.12 mmol, 1 M), TMEDA (385 μL, 2.55 mmol) and isobutyraldehyde (279 μL, 3.06 mmol) in DCM (3.4 mL). The title compound (86.8 mg, 0.21 mmol, 21.0 %) was obtained as yellow oil.

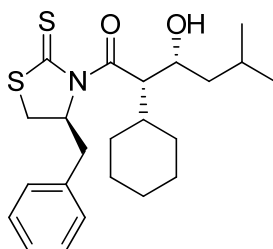
**TLC** [DCM]: R<sub>f</sub> = 0.60.

**Mass:** (ESI<sup>+</sup>), calculated 406.19 [C<sub>22</sub>H<sub>31</sub>NO<sub>2</sub>S<sub>2</sub> + H]<sup>+</sup>, found = 406.17 [M+H]<sup>+</sup>.

**<sup>1</sup>H NMR** (300 MHz, CDCl<sub>3</sub>) δ 7.38 – 7.28 (m, 5H), 5.45 – 5.35 (m, 1H), 5.05 (t, *J* = 6.2 Hz, 1H), 3.72 (dd, *J* = 6.0, 4.9 Hz, 1H), 3.35 – 3.20 (m, 2H), 3.06 (dd, *J* = 13.2, 10.6 Hz, 1H), 2.92 – 2.81 (m, 1H), 1.88 – 1.79 (m, 2H), 1.77 – 1.69 (m, 3H), 1.65 (d, *J* = 10.7 Hz, 2H), 1.35 – 1.09 (m, 6H), 0.99 (d, *J* = 6.8 Hz, 3H), 0.95 (d, *J* = 6.7 Hz, 3H).

**<sup>13</sup>C NMR** (75 MHz, CDCl<sub>3</sub>) δ 202.40, 177.33, 136.40, 129.42, 128.90, 127.24, 76.47, 69.00, 50.01, 39.96, 36.68, 31.81, 31.62, 31.30, 29.20, 26.90, 26.63, 26.57, 26.20, 20.13, 16.98.

### (2*S*,3*R*)-1-((*S*)-4-benzyl-2-thioxothiazolidin-3-yl)-2-cyclohexyl-3-hydroxy-5-methylhexan-1-one



28

## B. Research Articles – Publication/Manuscript VI

**28** was synthesized according to **25** with 3-methylbutanal (0.19 mL, 1.80 mmol) to afford the title compound as yellow solid (172 mg, 0.41 mmol, 68.3 %).

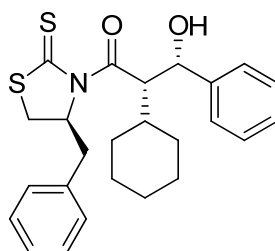
**TLC** [DCM]:  $R_f = 0.52$ .

**Mass:** (ESI<sup>+</sup>), calculated 420.20 [C<sub>23</sub>H<sub>33</sub>NO<sub>2</sub>S<sub>2</sub> + H]<sup>+</sup>, found = 420.04 [M+H]<sup>+</sup>.

<sup>1</sup>H NMR (300 MHz, CDCl<sub>3</sub>)  $\delta$  7.47 – 7.22 (m, 5H), 5.56 – 5.39 (m, 1H), 5.36 – 5.21 (m, 1H), 4.13 (ddd,  $J = 10.4, 5.7, 2.2$  Hz, 1H), 3.34 (ddd,  $J = 11.5, 7.2, 1.0$  Hz, 1H), 3.21 (dd,  $J = 13.2, 3.9$  Hz, 1H), 3.08 – 2.96 (m, 1H), 2.91 – 2.72 (m, 1H), 1.84 – 1.60 (m, 7H), 1.33 – 1.14 (m, 6H), 0.96 – 0.93 (m, 4H), 0.90 (d,  $J = 6.6$  Hz, 4H).

<sup>13</sup>C NMR (75 MHz, CDCl<sub>3</sub>)  $\delta$  203.01, 175.63, 136.52, 129.43, 128.85, 127.17, 70.06, 69.25, 53.27, 41.18, 38.19, 37.01, 31.67, 31.50, 30.14, 26.89, 26.36, 26.33, 26.22, 24.51, 23.93, 21.35.

**(2*S*,3*S*)-1-((*S*)-4-benzyl-2-thioxothiazolidin-3-yl)-2-cyclohexyl-3-hydroxy-3-phenylpropan-1-one**



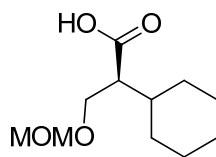
**29**

**29** was synthesized according to **25** with TiCl<sub>4</sub> (0.63 mL, 0.63 mmol, 1 M), TMEDA (226  $\mu$ L, 1.50 mmol) and benzaldehyde (91.0  $\mu$ L, 0.90 mmol) in DCM (4.0 mL). After flash chromatography (0-50 % DCM in cyclohexane) the title compound (74 mg, 0.17 mmol, 28.0 %) was obtained as yellow oil.

**TLC** [DCM/cyclohexane, 1:1]:  $R_f = 0.09$ .

**Mass:**(ESI<sup>+</sup>), calculated 440.17 [C<sub>25</sub>H<sub>29</sub>NO<sub>2</sub>S<sub>2</sub> + H]<sup>+</sup>, found = 439.82 [M+H]<sup>+</sup>.

<sup>1</sup>H NMR (599 MHz, CDCl<sub>3</sub>)  $\delta$  7.39 – 7.35 (m, 2H), 7.32 – 7.28 (m, 4H), 7.26 – 7.22 (m, 2H), 7.20 – 7.17 (m, 2H), 5.17 (dd,  $J = 8.9, 5.4$  Hz, 1H), 4.92 (d,  $J = 8.9$  Hz, 1H), 4.61 – 4.55 (m, 1H), 3.05 (dd,  $J = 13.3, 4.2$  Hz, 1H), 2.86 (dd,  $J = 13.3, 10.5$  Hz, 1H), 2.46 (dd,  $J = 11.1, 0.7$  Hz, 1H), 2.31 (ddd,  $J = 11.1, 6.9, 1.0$  Hz, 1H), 2.25 – 2.18 (m, 1H), 2.11 – 2.05 (m, 1H), 1.92 – 1.64 (m, 5H), 1.34 – 1.15 (m, 5H).

**(S)-2-cyclohexyl-3-(methoxymethoxy)propanoic acid****30**

**23** (160 mg, 0.48 mmol) was dissolved in DCM (1.0 mL) and DIPEA (253  $\mu$ L, 1.45 mmol) was added. The solution was cooled to 0 °C and MOM-Cl (110  $\mu$ l, 1.45 mmol) was added and it was stirred 2.5 h at 0°C. The reaction mixture was diluted with DCM and washed with half saturated  $\text{NH}_4\text{Cl}$  solution and half saturated  $\text{NaHCO}_3$  solution. The organic layer was dried over  $\text{MgSO}_4$  and the solvent was removed under reduced pressure. After this the residue was dissolved in THF/ $\text{H}_2\text{O}$  (6.5 mL, 8:5) followed by the addition of LiOH (52.0 mg, 2.17 mmol) and  $\text{H}_2\text{O}_2$  (247  $\mu$ l, 2.41 mmol, 30% wt) at 0 °C. The reaction mixture was stirred at that temperature for 1.5 h and at RT for 1.5h.

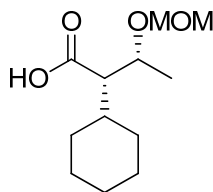
Then the reaction mixture was quenched with sat.  $\text{Na}_2\text{SO}_3$  solution at 0°C. It was extracted with DCM and the combined organic layers were discarded. Then the aqueous layer was acidified with conc. HCl to pH = 1 and extracted with DCM. At this step the organic layers were combined, dried over  $\text{MgSO}_4$  and the solvent was removed under reduced pressure to yield the title compound (104 mg, 0.48 mmol, quant) without further purification as a colorless oil.

**TLC** [EtOAc/cyclohexane, 4:6]:  $R_f = 0.26$ .

**Mass:** (ESI<sup>+</sup>), calculated 217.14 [ $\text{C}_{11}\text{H}_{20}\text{O}_4 + \text{H}$ ]<sup>+</sup>, found = 216.86 [M+H]<sup>+</sup>.

**<sup>1</sup>H NMR** (300 MHz,  $\text{CDCl}_3$ )  $\delta$  4.60 (s, 2H), 3.83 – 3.62 (m, 2H), 3.34 (s, 3H), 2.60 – 2.47 (m, 1H), 1.86 – 1.51 (m, 6H), 1.35 – 0.89 (m, 5H).

**<sup>13</sup>C NMR** (75 MHz,  $\text{CDCl}_3$ )  $\delta$  179.20, 96.48, 66.67, 55.29, 51.87, 37.55, 30.87, 30.64, 26.16, 26.13.

**(2S,3R)-2-cyclohexyl-3-(methoxymethoxy)butanoic acid****31**

The title compound was synthesized according to **30** with **25** (360 mg, 0.95 mmol), DIPEA (0.50 mL, 2.86 mmol) and MOM-Cl (0.72 mL, 9.53 mmol) in DCM (1.0 mL). The auxiliary was cleaved with LiOH (103 mg, 4.29 mmol),  $\text{H}_2\text{O}_2$  (0.24 mL, 2.38 mmol, 30 % wt) in THF/ $\text{H}_2\text{O}$  (8:5, 13.0 mL) at RT.

The product (150 mg, 0.65 mmol, 68.2 %) was obtained after flash chromatography (0 – 20 % EtOAc in cyclohexane) as colorless oil.

## B. Research Articles – Publication/Manuscript VI

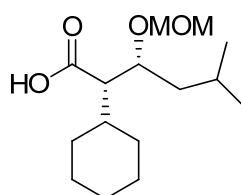
**TLC** [EtOAc/cyclohexane, 1:1]:  $R_f = 0.34$ .

**Mass:** (ESI<sup>+</sup>), calculated 231.16 [C<sub>12</sub>H<sub>22</sub>O<sub>4</sub> + H]<sup>+</sup>, found = 230.78 [M+H]<sup>+</sup>.

**<sup>1</sup>H NMR** (300 MHz, CDCl<sub>3</sub>)  $\delta$  4.60 (s, 2H), 3.83 – 3.62 (m, 2H), 3.34 (s, 3H), 2.60 – 2.47 (m, 1H), 1.86 – 1.51 (m, 6H), 1.35 – 0.89 (m, 5H).

**<sup>13</sup>C NMR** (101 MHz, CDCl<sub>3</sub>)  $\delta$  177.89, 94.92, 71.12, 56.46, 55.61, 36.60, 30.93, 30.43, 26.28, 26.26, 26.12, 16.70.

### (2S,3R)-2-cyclohexyl-3-(methoxymethoxy)-5-methylhexanoic acid



**32**

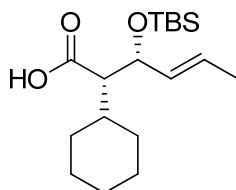
**26** (170 mg, 0.41 mmol) and DIPEA (213  $\mu$ l, 1.22 mmol) were dissolved in DCM (dry, 0.5 mL) and cooled to 0 °C. Then MOM-Cl (155  $\mu$ l, 2.04 mmol) was added and it was stirred at RT for 2.5 h. The reaction mixture was diluted with DCM and washed with half-saturated NH<sub>4</sub>Cl solution and a half-saturated NaHCO<sub>3</sub> solution. The organic layer was dried over MgSO<sub>4</sub>, filtrated and the solvent was removed under vacuum. Then the residue was dissolved in THF/H<sub>2</sub>O (8:5, 1.3 mL) followed by the addition of LiOH (43.9 mg, 1.83 mmol) and H<sub>2</sub>O<sub>2</sub> (104  $\mu$ l, 1.02 mmol, 30 % wt). The reaction mixture was stirred at RT for 2 h and then quenched with Na<sub>2</sub>SO<sub>3</sub> solution (1.5 M) and it was extracted with DCM, whereby the organic layer was discarded. The aqueous layer was acidified and the product was extracted several times with DCM. The combined organics were dried over anhydrous MgSO<sub>4</sub> filtrated and concentrated to afford the title compound (46 mg, 0.17 mmol, 41 %) as colorless oil.

**TLC** [EtOAc/cyclohexane, 1:1]:  $R_f = 0.45$ .

**<sup>1</sup>H NMR** (300 MHz, CDCl<sub>3</sub>)  $\delta$  4.77 (d,  $J = 7.0$  Hz, 1H), 4.61 (d,  $J = 7.1$  Hz, 1H), 3.94 (ddd,  $J = 10.7, 5.6, 2.1$  Hz, 1H), 3.42 (s, 3H), 2.61 (dd,  $J = 9.5, 5.5$  Hz, 1H), 1.87 – 1.81 (m, 1H), 1.75 – 1.66 (m, 6H), 1.29 – 1.14 (m, 5H), 1.03 (d,  $J = 10.4$  Hz, 2H), 0.96 – 0.90 (m, 6H).

**<sup>13</sup>C NMR** (75 MHz, CDCl<sub>3</sub>)  $\delta$  178.16, 129.00, 95.86, 74.20, 56.03, 55.01, 39.29, 36.56, 31.75, 30.20, 26.29, 26.02, 25.94, 24.22, 24.04, 21.14.

### (2S,3R,E)-3-((tert-butyldimethylsilyl)oxy)-2-cyclohexylhex-4-enoic acid



**33**

## B. Research Articles – Publication/Manuscript VI

LiOH (32.0 mg, 1.34 mmol) and H<sub>2</sub>O<sub>2</sub> (76 μL, 0.74 mmol, 30 % wt) were added to a solution of **26** (120 mg, 0.297 mmol) in THF/H<sub>2</sub>O (6.5 mL, 8:5). The reaction mixture was stirred at RT for 2 h. Then the reaction was quenched with 1.5 M Na<sub>2</sub>SO<sub>3</sub> solution and it was extracted with DCM. The combined organic layers were discarded. In the following step the aqueous layer was acidified with conc. HCl to pH = 1 and again extracted with DCM. At this step the organic layers were combined, dried over MgSO<sub>4</sub> and the solvent was removed under reduced pressure to yield the free carboxylic acid.

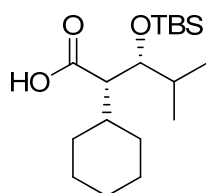
The protection group was introduced at – 78 °C via drop wise addition of TBSOTf (162 μL, 0.71 mmol) to a solution of the carboxylic acid in 2,6-Lutidine (137 μL, 1.18 mmol) and DCM (2.0 mL). The reaction was stirred for 2 h and then quenched with sat. NaHCO<sub>3</sub> solution. The layers were separated and it was extracted with Et<sub>2</sub>O. Then the combined organic layers were washed with sat. NH<sub>4</sub>Cl and brine, dried over MgSO<sub>4</sub> and filtered. After the solvent was removed under reduced pressure the residue was dissolved in MeOH/THF (2.0 mL, 1:1) and a solution of K<sub>2</sub>CO<sub>3</sub> (71.6 mg, 0.52 mmol) in H<sub>2</sub>O (0.40 mL) was added. The reaction was stirred at RT for 1 h and then diluted with 1 N NaOH. It was extracted with DCM and the organic layers were discarded. Subsequently, the aqueous layer was acidified and the product was extracted with DCM. The combined organic layers were dried over MgSO<sub>4</sub>, filtered and the solvent was removed under reduced pressure to obtain the title compound without further purification as colorless oil (22.0 mg, 67.4 μmol, 29.0 %).

TLC [EtOAc/cyclohexane, 1:1]: R<sub>f</sub> = 0.65.

<sup>1</sup>H NMR (400 MHz, CDCl<sub>3</sub>) δ 5.63 – 5.49 (m, 2H), 4.30 (t, *J* = 7.4 Hz, 1H), 2.45 – 2.34 (m, 1H), 2.26 – 2.17 (m, 1H), 1.74 – 1.68 (m, 5H), 1.67 – 1.65 (m, 3H), 1.26 – 1.13 (m, 5H), 0.85 (s, 9H), 0.04 (s, 3H), -0.00 (s, 3H).

<sup>13</sup>C NMR (101 MHz, CDCl<sub>3</sub>) δ 178.02, 131.19, 128.08, 72.24, 58.36, 41.78, 36.18, 34.61, 32.93, 31.26, 29.71, 26.45, 26.36, 26.17, 26.06, 25.96, 25.75, 25.67, 18.04, 17.62, -3.98, -5.03.

### (2*S*,3*R*)-3-((*tert*-butyldimethylsilyl)oxy)-2-cyclohexyl-4-methylpentanoic acid



**34**

**34** was synthesized according to **33** with **27** (85 mg, 0.21 mmol). The Evans auxiliary was cleaved with LiOH (22.6 mg, 0.94 mmol), H<sub>2</sub>O<sub>2</sub> (0.54 mL, 0.52 mmol, 30 % wt) in THF/H<sub>2</sub>O (8:5, 6.5 mL). The TBS protected alcohol was obtained by treatment with TBSOTf (142 μL, 0.62 mmol), 2,6-Lutidine (120 μL, 1.03 mmol) in DCM (2.0 mL) and K<sub>2</sub>CO<sub>3</sub> (62.4 mg, 0.45 mmol) in MeOH/THF (2 mL, 1:1).

In the following step the organic solvent was removed, it was extracted with DCM and the combined organic layers were discarded. Then the aqueous layer was acidified with conc. HCl to pH = 1 and again extracted with DCM. At this step the organic layers were combined, dried over MgSO<sub>4</sub> and the solvent was removed under reduced pressure. After flash chromatography (0-20 % EtOAc in cyclohexane) the title compound (33.0 mg, 0.10 mmol, 48.9 %) was obtained as colorless crystalline solid.

## B. Research Articles – Publication/Manuscript VI

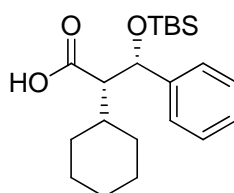
**TLC** [EtOAc/cyclohexane, 1:1]:  $R_f = 0.72$ .

**Mass:** (ESI<sup>+</sup>), calculated 329.25 [C<sub>12</sub>H<sub>22</sub>O<sub>4</sub> + H]<sup>+</sup>, found = 329.09 [M+H]<sup>+</sup>.

**<sup>1</sup>H NMR** (400 MHz, CDCl<sub>3</sub>)  $\delta$  3.87 (dd,  $J = 5.1, 1.6$  Hz, 1H), 3.82 (d,  $J = 2.9$  Hz, 1H), 2.22 (dd,  $J = 9.5, 1.6$  Hz, 1H), 1.93 – 1.86 (m, 1H), 1.83 – 1.63 (m, 5H), 1.25 – 1.09 (m, 5H), 0.94 (s, 12H), 0.91 (d,  $J = 7.0$  Hz, 3H), 0.17 (s, 3H), 0.16 (s, 3H).

**<sup>13</sup>C NMR** (101 MHz, CDCl<sub>3</sub>)  $\delta$  174.18, 75.96, 52.19, 36.69, 33.85, 31.63, 30.92, 26.10, 26.08, 26.05, 25.81, 19.14, 18.13, 16.52, -4.01, -4.66.

### (2*S*,3*S*)-3-((*tert*-butyldimethylsilyloxy)-2-cyclohexyl-3-phenylpropanoic acid



**35**

**35** was synthesized according to **33** with **29** (197 mg, 0.45 mmol). The auxiliary was cleaved with LiOH (49.0 mg, 2.05 mmol), H<sub>2</sub>O<sub>2</sub> (0.30 mL, 2.94 mmol, 30 % wt) in THF/H<sub>2</sub>O (8:5, 19.5 mL). The TBS protected alcohol was obtained with TBSOTf (314  $\mu$ L, 1.37 mmol), 2,6-Lutidine (265  $\mu$ L, 2.28 mmol) in DCM (4.5 mL) and K<sub>2</sub>CO<sub>3</sub> (138 mg, 1.0 mmol) in MeOH/THF (3 mL, 1:1).

In the following step the organic solvent was removed, it was extracted with DCM and the combined organic layers were discarded. Then the aqueous layer was acidified with conc. HCl to pH = 1 and again extracted with DCM. At this step the organic layers were combined, dried over MgSO<sub>4</sub> and the solvent was removed under reduced pressure to yield the title compound (69.8 mg, 0.19 mmol, 42.3 %) without further purification as a colorless crystalline solid.

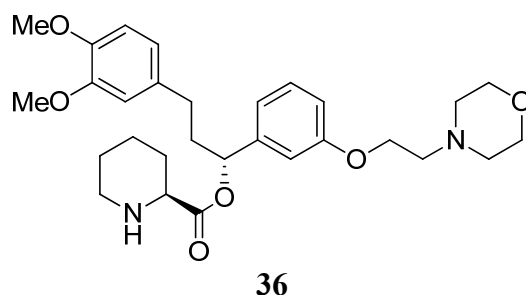
**TLC** [EtOAc/cyclohexane, 1:1]:  $R_f = 0.65$ .

**<sup>1</sup>H NMR**  $\delta$  7.33 – 7.18 (m, 5H), 4.82 (d,  $J = 9.7$  Hz, 1H), 2.66 (dd,  $J = 9.7, 4.1$  Hz, 1H), 2.13 – 1.97 (m, 1H), 1.91 – 1.61 (m, 5H), 1.43 – 1.02 (m, 5H), 0.83 (s, 9H), 0.02 (s, 3H), -0.35 (s, 3H).

**<sup>13</sup>C NMR** (101 MHz, CDCl<sub>3</sub>)  $\delta$  177.77, 143.45, 128.53, 128.24, 127.89, 73.66, 60.88, 37.19, 33.01, 28.47, 27.59, 27.11, 26.99, 26.33, 18.66, -3.92, -4.61.

## B. Research Articles – Publication/Manuscript VI

### (S)-(R)-3-(3,4-dimethoxyphenyl)-1-(3-(2-morpholinoethoxy)phenyl)propyl piperidine-2-carboxylate



Synthesized as previously described<sup>10</sup>.

### References

1. Collaborative Computational Project, N. (1994). The CCP4 suite: programs for protein crystallography. *Acta Crystallogr. D Biol. Crystallogr.* *50*, 760-763.
2. DeLano, W.L. (2002). The PyMOL Molecular Graphics System.
3. Emsley, P., and Cowtan, K. (2004). Coot: model-building tools for molecular graphics. *Acta Crystallogr. D Biol. Crystallogr.* *60*, 2126-2132.
4. Evans, P.R. (1997). Scala. *Joint CCP4 and ESF-EACBM Newsletter* *33*, 22-24.
5. French, G.S., and Wilson, K.S. (1978). On the treatment of negative intensity observations. *Acta Crystallogr. A* *34*, 517-525.
6. Kabsch, W. (2010). XDS. *Acta Crystallogr. D Biol. Crystallogr.* *66*, 125-132.
7. Potterton, E., Briggs, P., Turkenburg, M., and Dodson, E. (2003). A graphical user interface to the CCP4 program suite. *Acta crystallographica* *59*, 1131-1137.
8. Schüttelkopf, A.W., and van Aalten, D.M. (2004). PRODRG: a tool for high-throughput crystallography of protein-ligand complexes. *Acta Crystallogr. D Biol. Crystallogr.* *60*, 1355-1363.
9. Vagin, A.A., and Isupov, M.N. (2001). Spherically averaged phased translation function and its application to the search for molecules and fragments in electron-density maps. *Acta Crystallogr. D Biol. Crystallogr.* *57*, 1451-1456.
10. Gopalakrishnan R, Kozany C, Gaali S, Kress C, Hoogeland B, Bracher A, Hausch F: Evaluation of Synthetic FK506 Analogues as Ligands for the FK506-Binding Proteins 51 and 52. *J. Med. Chem.* 2012, *55*:4114-4122.

## B. Research Articles – Publication/Manuscript VII

### 7.2. *Manuscript VII*

**A novel decalin-based bicyclic scaffold for FKBP51-selective ligands** – manuscript in preparation

(**Xixi Feng**, Claudia Sippel, Andreas Bracher, Felix Hausch)

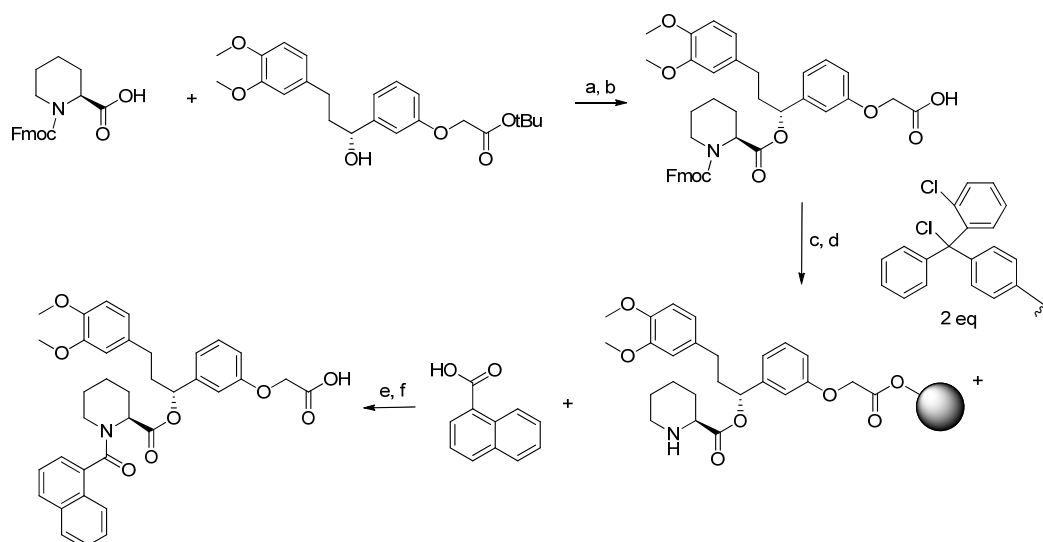
#### **Summary**

In the second “Bottom Group” series a novel bicyclic scaffold was designed and its usability as lead structure for further FKBP51 ligand development was tested. The crystal structure-based model indicated that this type of chemical structure, in fact a trans decalin, could pre-shape the cyclohexyl ring to its binding conformation. One ring of the bicycle is supposed to serve as a bridge, leading to a more stabilized conformation, less entropy loss during binding and thus higher binding affinities.

A synthesis with an asymmetric intramolecular Diels-Alder cyclization as key synthetic step was developed that also allowed ring substitutions to perform structure affinity relationship analysis. None of the ligands from the decalin series showed any binding towards FKBP52. The best ligand of this series exhibited a  $K_i$  of 0.23  $\mu\text{M}$  and contained a carbonyl group in the 4-position. A cocrystal structure was solved to analyze the binding mode. We were delighted to see that our model was confirmed and that one of the bicyclic rings promoted an induced fit in FKBP51, exactly like the cyclohexyl ring in the previous series. This series also indicates that the rigidification itself is beneficial for the binding affinity. These findings, together with the possibility to further modify the bicycles make the decalin-series a promising lead structure for future ligand optimization.

### Prescreening of bicyclic aromating scaffolds

The discovery of a bicyclic structure as promising new scaffold led us to the idea to perform a rapid prescreening with commercially available aromatic, bicyclic carboxylic acids (Scheme 4, exemplified on 1-naphthoic acid). The compounds were synthesized based on a solid phase-assisted method developed by Gopalakrishnan et al.<sup>21</sup> (Scheme 4) and tested in a fluorescence polarization assay (Orig. Publ).



**Scheme 4:** Synthesis of the aromatic bicycle series exemplified on 1-naphthoic acid. Reagents and conditions: (a) DCC, DMAP. (b) TFA, DCM (c) DIPEA (d) 4-methyl-piperidine, DCM. (e) HATU, DIPEA, DCM (f) TFA, DCM.

Unfortunately, none of the compounds showed any binding towards FKBP51 which we attribute to the partially planar structure of the aromatic bicycles. Thereupon, we focused on the synthesis of the trans-decalin scaffold we obtained from the computer model.

### An asymmetric intramolecular Diels-Alder (IMDA) reaction as key synthesis step

The trans-decalin scaffold we aimed to include in our ligands is a motif occurring in several natural products like tetrodecamycin, (-)-Himgaline and (-)-GB13 (Fig.9).

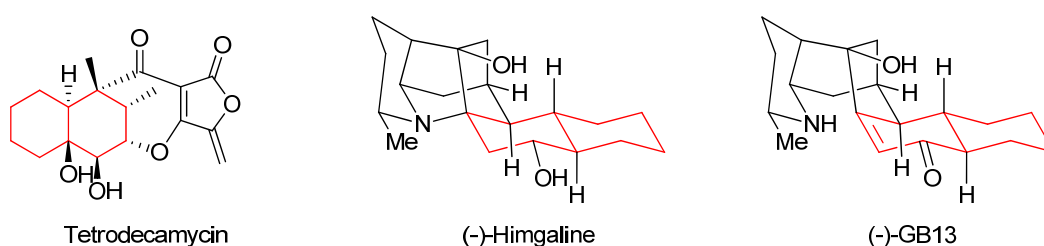


**Fig. 9:** Examples of natural products containing a trans-decalin motif (red).

## B. Research Articles – Publication/Manuscript VII

Paintner et al.<sup>51</sup> carried out an asymmetric intramolecular Diels-Alder reaction as core step for the synthesis of the bicyclic portion of tetrodecamycin. Evans et al.<sup>52</sup> conducted a similar step during the synthesis of *ent*-Himgaline and *ent*-GB 13. The stereochemical outcome of the cyclization is mediated, similarly to our asymmetric aldol-reaction (see 7.1.), by an Evans oxazolidinone auxiliary but also electronic factors of the precursor. As in the aldol series the oxazolidinone auxiliary can be directly converted to a carboxylic acid and immediately coupled with the pipercolic esters to obtain the final compounds. The cyclization of a triene with a benzyloxazolidinone auxiliary, promoted by DMAC, (dimethylaluminium chloride) exhibits high diastereoselectivity and high endo selectivity.<sup>53</sup> It is supposed that the formation of the exo product is disfavored since interactions between the diene and the chain linking the diene and the dienophile destabilize the resulting transition state and the bonding geometries are more difficult attained. Therefore, the formation of trans-fused products is favored.<sup>54</sup> The suggested transition state is shown in Fig. 10. Additionally, it is assumed that a “ $\pi$ -stacking interaction” or charge-transfer occurs between the benzyl group and the dienophile.<sup>53</sup>

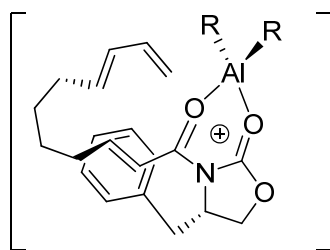


**Fig. 10:** Proposed transition state for the chiral auxiliary-mediated intramolecular Diels-Alder cyclization. Adapted from Evans et al.<sup>53</sup> and Roush et al.<sup>54</sup>.

Together with steric effects, one diastereoface is selectively shielded, which leads to a high diastereoselective conversion. The Lewis acid DMAC promotes the reaction by chelating the imide carbonyls.<sup>54</sup>

Also during our synthesis of the bicyclic ligand series we observed only the formation of one major product after the intramolecular cyclization step. Although we partly synthesized structures that were already described by Evans et al.<sup>54</sup> our synthesis differs slightly. The described synthetic procedures, e.g. those for the natural products shown in Fig. 9, are optimized and adapted to the respective chemical scaffolds. Since we planned to perform a structure-affinity-relationship analysis on the bicyclic scaffold we designed the new synthesis in a way that it is both shorter and more versatile than the previous published procedure. With our synthesis we are able to introduce substituents on the terminal double bond via a Wittig reaction (Scheme 1, manuscript). Also the double bond, that is a leftover of the cyclization,

## B. Research Articles – Publication/Manuscript VII

gives possibilities to chemically modify the bicyclic scaffold. The modifications we performed are summarized by Table 1 (manuscript). The stereochemical outcome of the dihydroxylation step that was conducted for the synthesis of intermediate **9d** (and compounds **23** and **24**) is deviated from the dihydroxylation reaction conducted by Evans et al.<sup>52</sup> during the synthesis of *ent*-Himgaline and *ent*-GB 13.

With the aldol series (chapter 7.1.) we aimed to reproduce a hydrogen bond that was observed between FK506 and Asp68 and also in the ligand series developed by Gopalakrishnan et al.<sup>20</sup>. Unfortunately, the cocrystal structure of a representative ligand of the series didn't show the expected hydrogen bond. Therefore we hoped we could be more successful with our new scaffold and tried to introduce a hydroxyl group in the position corresponding to the position of the hydroxyl group in the aldol series.

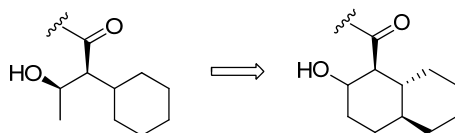
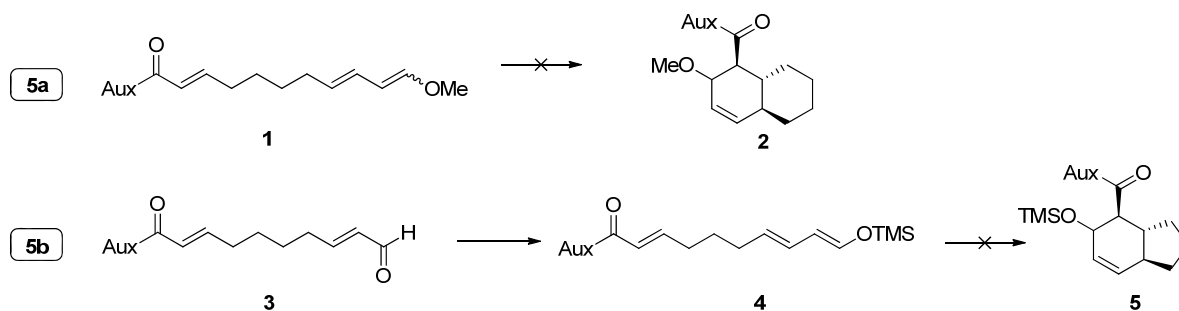


**Fig. 11:** Transferring the hydroxyl group from the aldol series to the new bicyclic scaffold.

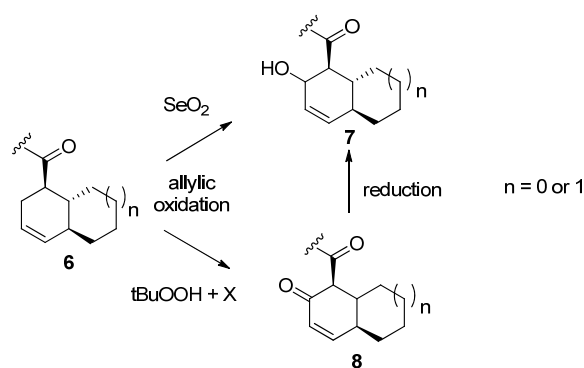
First, we utilized our new versatile synthesis and introduced a methyl vinyl ether group (**1**) via a Wittig reaction with (Methoxymethyl)triphenylphosphonium chloride. Cyclization of the linear precursor should provide the bicycle with a methoxy substituent (**2**), which represents a direct precursor of our desired structure (Scheme 5a). As suspected the labile methyl vinyl ether function did not survive the cyclization reaction. Directly after addition of DMAC to the linear precursor the reaction solution turned brown (usually light yellow). TLC control indicated an inseparable and unclear mixture. The same thing happened with a trimethylsilyl enol ether as functional group that was obtained by enolization of an  $\alpha,\beta$ -unsaturated aldehyde (**3**->**4**) with TMSBr after a method developed by Iqbal et al.<sup>55</sup> (Scheme 5b). Attempts to replace the labile TMS ether by more stable silyl ethers failed since the enolization step did not work. Due to synthetic reasons this step was first conducted with a precursor leading to the 9-membered bicycle.

## B. Research Articles – Publication/Manuscript VII



**Scheme 5:** Unsuccessful intramolecular Diels-Alder cyclizations. (Aux = Evans auxiliary)

We then tried to use a more straightforward step and tested conditions to obtain the hydroxyl-decalin from **6**, the direct cyclization product, by allylic oxidations (Scheme 6).



**Scheme 6:** Theoretically proposed allylic oxidation of the IMDA cyclization product.

First attempts to introduce the alcohol via oxidation of the allylic methylene group (**7**) with  $\text{SeO}_2$ <sup>56</sup> did not work since no clear conversion could be observed. We then changed our focus and tried to introduce a keto group (**8**), since it is more versatile for further chemical modifications and the hydroxy group could theoretically be obtained by simple reduction of the carbonyl. We tried several  $t\text{BuOOH}$ -based methods: in combination with sodium chlorite ( $\text{NaClO}_2$ )<sup>57</sup>, with diacetoxyiodobenzene<sup>58</sup> or with dirhodium(II) caprolactamate<sup>59</sup>. But none of the promising conditions led to a successful conversion of the reactant both with the 9- and the 10-membered bicycles as reactants.

Within the decalin-series this issue is still an ongoing project and it is aimed to work on conditions that could lead to the desired moiety (see C-Outlook).

## B. Research Articles – Publication/Manuscript VII

### ORIGINAL MANUSCRIPT

#### A novel decalin-based bicyclic scaffold for FKBP51-selective ligands

Xixi Feng\*, Claudia Sippel\*, Andreas Bracher#, Felix Hausch\*

\* Max Planck Institute of Psychiatry, Dept. Translational Research in Psychiatry,  
Kraepelinstrasse 2, 80804 Munich, Germany

# Max Planck Institute of Biochemistry, Am Klopferspitz 18, 82152 Martinsried, Germany

#### Abstract

Selective inhibition of FKBP51 has emerged as possible novel treatment for diseases like major depressive disorders or obesity. However, the physicochemical properties of the current FKBP51 inhibitors are outside the range of drug-like molecules and therefore have to be further optimized. Using a rigidification strategy we hereby report the structure-based design and synthesis of a novel promising bicyclic scaffold for FKBP51 ligands. With the cocrystal structure of the best ligand in this novel series we show, how the cyclization locks the ligand in a conformation typical for FKBP51-selective binding.

#### Introduction

The important role of the FK506-binding protein 51 (FKBP51) has been shown in several diseases and pathologic states. It has been reported that FKBP51 is involved in the development of obese conditions by activating adipocyte differentiation.<sup>1</sup> FKBP51 knockout mice were protected from weight gain after a high fat diet and in general exhibited reduced weight.<sup>2,3</sup> FKBP51 influences have also been genetically associated with the severity of pain symptoms experienced after trauma.<sup>4</sup> FKBP51 is also involved in the development of stress-related psychiatric disorders, which is supposed to be its most prominent function.<sup>5</sup> It is assumed that overactive FKBP51 leads to an impaired feedback in the stress regulation system, most notably the hypothalamus-pituitary-adrenal axis. In accordance with this, a knockout of the gene FKBP5 in mice resulted in improved stress-coping behavior.<sup>2</sup> In humans, polymorphisms in the FKBP51-encoding gene (FKBP5) were linked to an enhanced susceptibility for stress-related disorders.<sup>5</sup> In all these diseases FKBP51 was therefore considered as promising drug target.<sup>6</sup>

## B. Research Articles – Publication/Manuscript VII

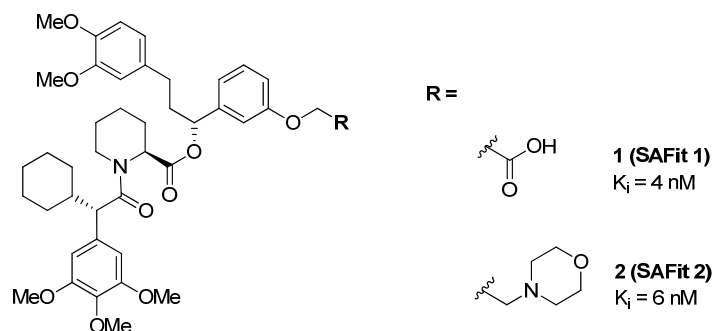


**Figure 1:** Chemical structures of the FKBP51-selective ligands SAFit1 (1), SAFit2 (2) and their binding affinities towards FKBP51.

A key problem in FKBP51 drug discovery is to achieve selectivity over its close homolog FKBP52. Due to the high structural analogy between these proteins, all ligands derived from FK506 exhibit similar binding affinities to both proteins.<sup>7</sup> Concomitant binding, however, has to be avoided since both proteins have opposing effects, e.g. in neuronal cells.<sup>8</sup> An inhibition of FKBP52 is even supposed to have toxic effects, since a knockout of this protein in mice led to severe impairment of the reproduction system.<sup>9-12</sup> In contrast to that, an inhibition of FKBP51 is well tolerated since no adverse phenotypes were observed in FKBP51 knockout mice.<sup>9</sup>

With the discovery of SAFit2, a highly selective, potent and blood-brain permeable FKBP51 inhibitor, it was possible to perform first studies to test the effects of FKBP51 inhibition in vivo. It was shown that SAFit2 has clear antidepressant-like effects.<sup>8</sup> Additionally, mice that were treated with SAFit2 for 30 days showed a reduced body weight under control and high fat diet conditions.<sup>15</sup> These data confirmed FKBP51 as a promising drug target and selective FKBP51 ligands as a possible novel treatment for obesity or major depression.

However, SAFit1 and SAFit2 are unsuitable as drug candidates. Especially their high molecular weight (748 g/mol and 802 g/mol respectively) is far outside the typical range of CNS-directed drugs and further optimization is needed. In our previous structure-affinity-relationship studies it became clear that an improved scaffold would be necessary to achieve drug-like selective FKBP51 inhibitors. The aim of this study was to explore decalin-based SAFit analogs as improved selective FKBP51 inhibitors. A similar approach has already been very effective in substantially increasing the ligand efficiencies of pan-selective FKBP inhibitors.<sup>16-18</sup>

### Results and Discussion

#### *Rigidification for improving binding affinity*

During the discovery of SAFit2 the cyclohexyl ring was found to be the most critical structural feature for high selectivity against FKBP52. Replacing it with smaller substituents led to a significant loss of both selectivity and binding affinity.<sup>8</sup> In contrast the trimethoxyphenyl ring was shown to be important for high binding affinity but not for selectivity. Replacing it by different aliphatic substituents and alcohols retained a FKBP51-

## B. Research Articles – Publication/Manuscript VII

preferring, induced fit-like binding mode.<sup>19</sup> In order to improve the affinity of the FKBP51-selective ligands, we set out to explore a preorganization strategy.

A closer inspection of the cocrystal structures of the SAFit1-analog SG623<sup>20</sup>, revealed that the trimethoxyphenyl ring as well as the cyclohexyl ring are positioned in a way that suggested a possible cyclization by an ethylene linker (Fig.2).

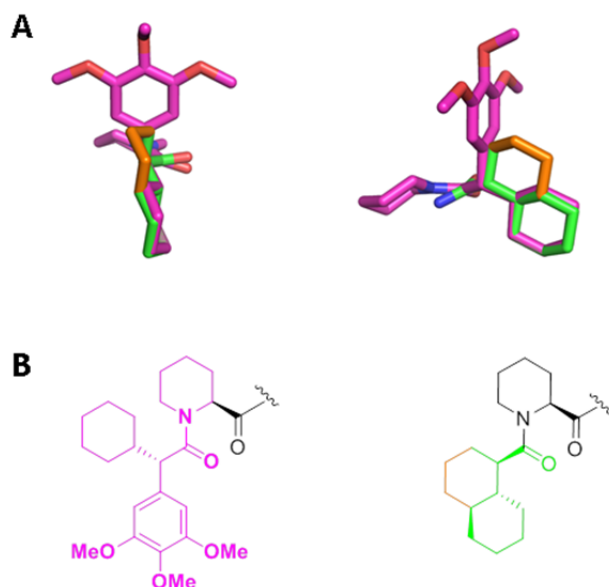


**Figure 2:** A rigidification strategy to increase binding affinity. (a) SG623 is shown as stick (magenta) in its active conformation bound to FKBP51 (pipercolic ester amide is not shown for clarity). The decalin-derived scaffold is superimposed (green sticks). The ethylene linker is highlighted in orange. (b) The chemical structures of the respective stick representations.

We first started with a screening of synthetic ligands that contained a bicyclic aromatic moiety instead of the trimethoxyphenyl-cyclohexyl group of SAFit1 (Fig. 3). All compounds were synthesized by solid phase-assisted synthesis<sup>21</sup>. Unfortunately, no binding towards FKBP51 was observed in a fluorescence polarization assay<sup>22</sup>. We attributed this to the planar geometry of the aromatic bicycles, which may not fit to the shape of the FKBP51 binding pocket. We therefore set out to synthesize exactly the saturated bicyclic structure derived from our modelling studies. Although this decalin structure contains three stereocenters, we were happy to find out that they can be all generated in a single step by an intramolecular Diels-Alder cyclization.

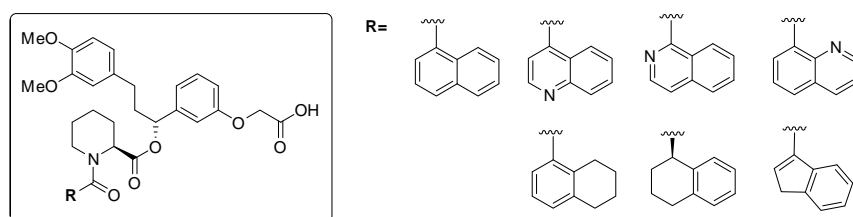
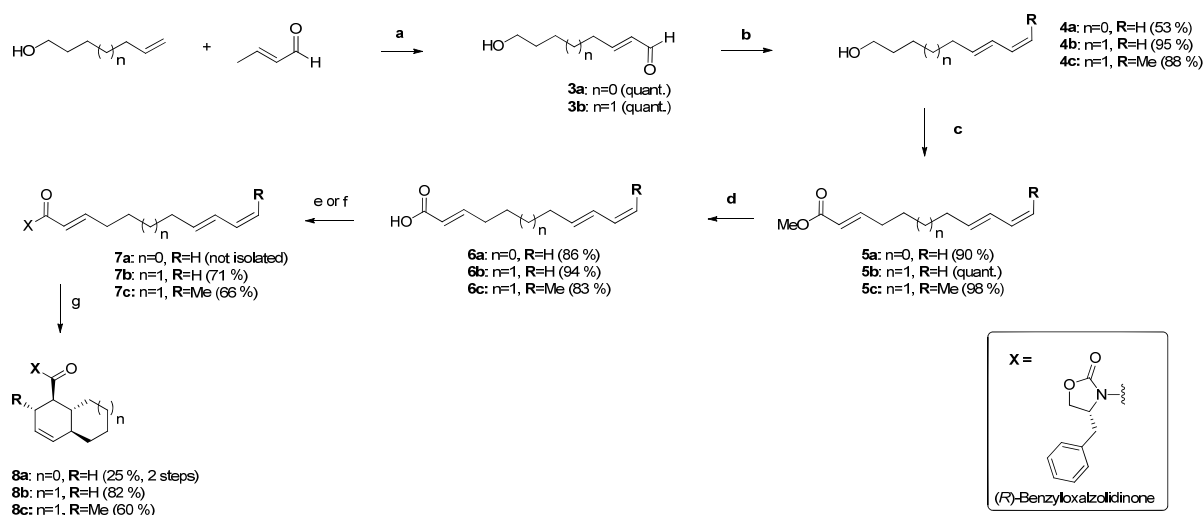


**Figure 3:** Chemical structures of synthetic ligands that contain an aromatic bicycle, instead of the trimethoxyphenyl-cyclohexyl group of SAFit1.

## B. Research Articles – Publication/Manuscript VII

### Synthesis of a novel bicyclic FKBP51 ligand series

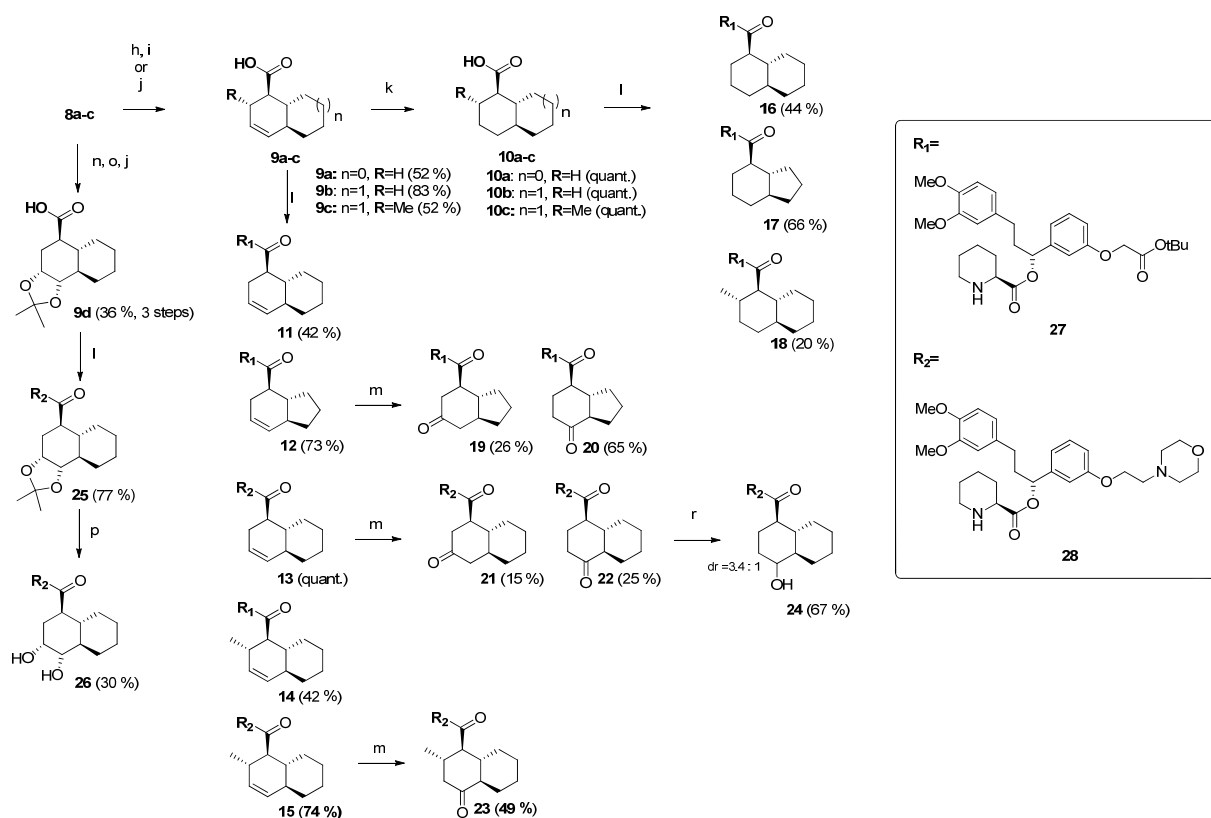
The key step of the decalin synthesis is a dimethylaluminium chloride-promoted (DMAC) cyclization of trienimides **7a-c**, whereby the stereochemistry is directed by an Evans auxiliary (Scheme 1). To obtain the trienimides for cyclization we developed a synthesis that is significantly shorter than Evans<sup>23</sup> synthetic procedure (3 steps instead of 6 to synthesize the methyltrienoates). Additionally, our synthesis is more adjustable for the introduction of substituents.



**Scheme 1:** Reagents and conditions. (a) Grubbs 2<sup>nd</sup> gen., DCM (b) ethyltriphenylphosphonium bromide (for **4a+b**); methyltriphenylphosphonium iodide (for **4c**), KOtBu, THF (c) 1. (COCl)<sub>2</sub>, DMSO, DIPEA, DCM; 2. Methyl(triphenylphosphoranylidene) acetate (d) NaOH, THF/H<sub>2</sub>O (e) 1. (COCl)<sub>2</sub>, DMF, DCM; 2. nBuLi, THF, (R)-4-Benzyl-2-oxazolidinone (f) DCC, DMAP, (R)-4-Benzyl-2-oxazolidinone (g) dimethylaluminium chloride, DCM. Yields stated in parentheses.

The synthesis of the triene-chain starts with a cross metathesis between an alkenol and trans-crotonaldehyde<sup>24</sup> to exclusively yield the (*E*)-products **3a** and **3b**. In the following step the  $\alpha,\beta$ -unsaturated aldehydes are converted by a Wittig reaction to the dienols **4a-c**. Due to the wide range of commercially available Wittig reagents it is possible to introduce different ring moieties in this step that will result in a substituent in 2-position of the cyclized decalins. To further extend the chain at the opposite end the alcohols **4a-c** were first converted under Swern conditions to aldehydes and elongated by adding Methyl(triphenylphosphoranylidene) acetate directly to the reaction mixture. Also this step mainly provided the *E*-isomers **5a-c**. The small amounts of the formed *Z*-isomers (~ 5 %) can easily be separated from the desired trienoate by flash chromatography. To obtain the free carboxylic acids **6a-c** the methyl esters were cleaved in a mixture of 2 M NaOH and THF respectively. The Evans auxiliary was introduced to the trienoic acids by acetylation with the respective acid chlorides of **6a-c** or directly with a coupling reagent. The following DMAC-promoted cyclization steps of the trienimides proceeds smoothly, yielding the desired *trans*-cycloadducts as single diastereomers **8a-c**.

## B. Research Articles – Publication/Manuscript VII



**Scheme 2:** (h) BuLi, EtSH, THF (i) Hg(CF<sub>3</sub>COO)<sub>2</sub>, THF/H<sub>2</sub>O (j) LiOH, H<sub>2</sub>O<sub>2</sub>, THF/H<sub>2</sub>O (k) H<sub>2</sub>, Pd(C), MeOH (l) **27**: 1. COMU/HATU/PyBrop, DIPEA, DMF; 2. TFA/DCM; **28**: COMU, DIPEA, DMF (m) p-benzoquinone, Pd(AcO)<sub>2</sub>, HBF<sub>4</sub>, MeCN/H<sub>2</sub>O (n) OsO<sub>4</sub>, NMO, acetone (o) 2,2-dimethoxypropane, pTsoH, acetone (p) HCl, MeOH (r) NaBH<sub>4</sub>, CeCl<sub>3</sub>, MeOH. Yields stated in parentheses.

After cyclization, the chiral auxiliary (Scheme 2) of the unsubstituted bicycles **8a** and **8b** was cleaved with LiOOH to obtain the free carboxylic acids **9a** and **9b** respectively. Bicycle **8c** that is substituted in the 2-position was first converted to the respective thioester and then hydrolyzed with mercury (II) trifluoroacetate<sup>25</sup> (**9c**). Hydrogenation catalyzed by Pd/C provided the respective saturated bicycles **10a-c**.

The free carboxylic acids were coupled to **27** or **28** with HATU or COMU as coupling reagent to obtain the final compounds as SAFit1 (after tBu deprotection) or SAFit2 derivatives respectively. **12** and **13** were oxidized under Wacker conditions<sup>27</sup> to obtain the 3-keto (**18**, **20**) and the 4-keto (**19**, **21**) compounds in a 1:2.5 ratio, which can be easily separated by flash chromatography. In contrast, oxidation of **15** only provided the respective 4-keto compound **23**. To obtain **24** (dr = 3.4:1) the carbonyl group of **22** was reduced via Luche reduction.<sup>26</sup>

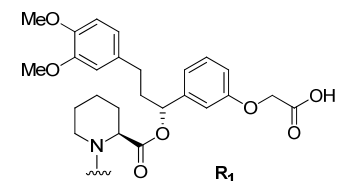
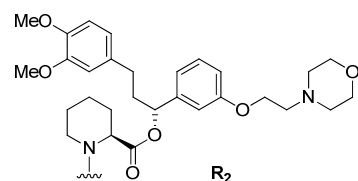
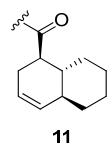
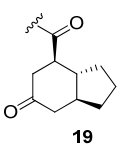
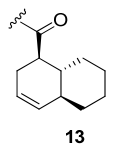
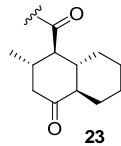
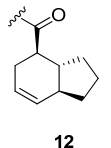
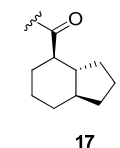
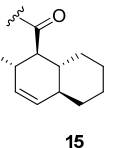
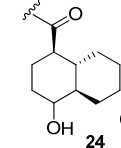
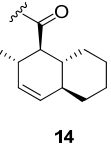
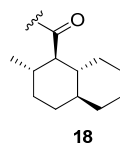
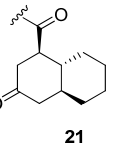
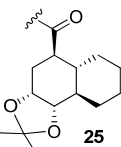
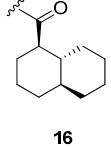
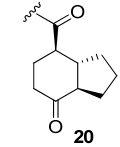
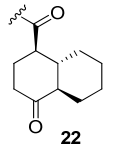
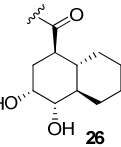
To obtain **9d** a dihydroxylation step was conducted with OsO<sub>4</sub> and **8a**. After protection of the hydroxyl groups the minor diastereomer was removed by flash chromatography. Then the auxiliary was cleaved and the free carboxylic acid was coupled to **28** to obtain **24**. The dihydroxy compound **26** was obtained after treatment of **25** under acidic conditions.

## B. Research Articles – Publication/Manuscript VII

### Structure-Affinity Relationship (SAR) of a new FKBP51-selective ligand series

**11-26** were tested in a competitive fluorescence polarization assay for binding to FKBP51 and FKBP52. All bicycles showed binding towards FKBP51 but almost no binding towards FKBP52 was observed. This is in agreement with our modelling studies that one of the bicyclic rings corresponds to the cyclohexyl substituent that was previously reported to be important for FKBP51 selective ligands.<sup>19,20</sup>

In general we observed that the [4.3.0] bicycles, containing octahydro-indene and derivatives, show lower binding affinities towards FKBP51 than their corresponding decalin-compounds. Additionally, all decalin-like compounds showed no binding towards FKBP52, whereas one octahydro-indene derivative (**20**) showed low binding towards FKBP52. In all cases a saturation of the double bond, a leftover of the intramolecular Diels-Alder cyclization, resulted in a significant increase in binding affinity (compare **11/15**, **12/17**, **14/18**). Also the addition of a methyl group in the 2-position of the saturated decalins (**18**), led to a 2-fold increase in affinity.

 R <sub>1</sub>		 R <sub>2</sub>					
Entry	K <sub>i</sub>	Entry	K <sub>i</sub>	Entry	K <sub>i</sub>	Entry	K <sub>i</sub>
	2.4		28		2.6		0.33
	7.8		2.6		1.9		0.65 (d <sub>r</sub> = 3.4:1)
	2.0		0.49		1.3		8.2
	0.81		3.1		0.23		0.28

**Table 1.** FKBP binding affinities bicyclic SAFit1 (**1**) and SAFit2 (**2**) analogs; K<sub>i</sub> values were determined by a competitive fluorescence polarization assay<sup>22</sup>; **22** was tested as diastereomeric mixture (3.4:1).

## B. Research Articles – Publication/Manuscript VII

The introduction of polar groups to the ring system had interesting effects on the binding affinity. Carbonyl groups in the in the 3-position either had no effect or a negative effect on the binding affinity (**19** and **21**). A hydroxyl group in the 4-position improved binding to  $K_i = 0.65 \mu\text{M}$  (**24**). A carbonyl group in the 4-position even improved the  $K_i$  of **22** and **23** to  $0.23 \mu\text{M}$  and  $0.33 \mu\text{M}$ , respectively. Also the dihydroxylated derivative **26** shows a similar binding affinity of  $K_i = 0.28 \mu\text{M}$ , whereby alkylation of the hydroxy groups (**25**) significantly decreases the binding affinity.

### *Cocrystal structure of 22*

**22** represents the best ligand in our bicyclic FKBP51-selective ligand series. We therefore solved a cocrystal structure of **22** with FKBP51 to elucidate its binding mechanism (Fig. 4). The X-ray structure revealed a binding conformation that is in agreement with previously described FKBP ligands. The piperidic ester is centered in a hydrophobic pocket. The prominent hydrogen bonds to Ile87 and Tyr113, which until now have been observed in all FKBP51 complexes with carbonyl pipercolate-based ligands<sup>19,20,28</sup> are also present (Fig. 4a). We were happy to see that also in this series selective binding to FKBP51 was accompanied by an induced fit-like binding mode, which is indicated by the position of Phe67 (Fig. 3a). One of the bicyclic rings is deeply buried in the enlarged binding pocket, similar to the cyclohexyl substituent known FKBP51-selective ligands. No clear interactions between the protein and the keto group were observed.

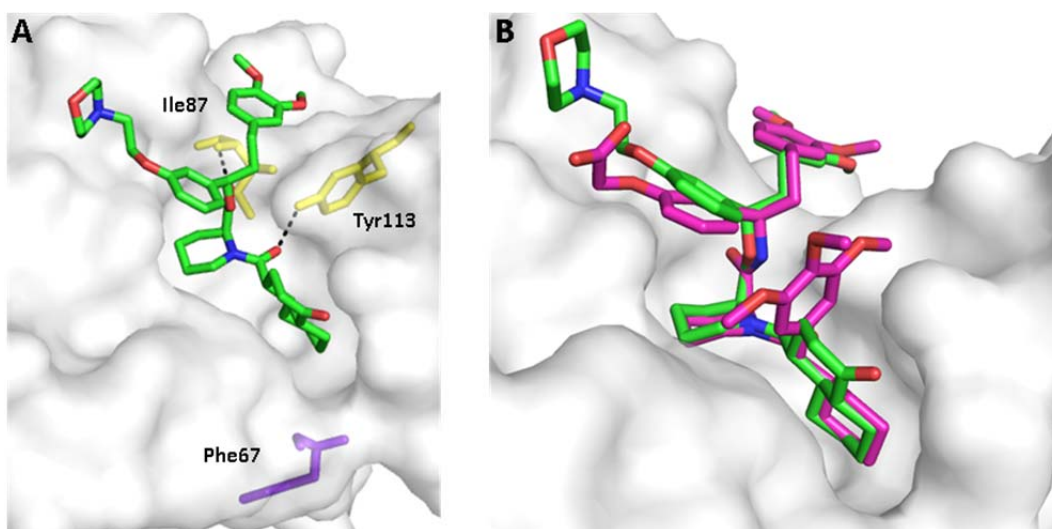


**Figure 4:** X-ray structures of **22** in complex with the FK506-binding domain of FKBP51; Lys121 is not shown for clarity (a) Surface representation of FKBP51 in complex with **22** (green) Hydrogen bonds to Tyr113 (yellow) and Ile87 (yellow) are indicated as black dotted lines. Phe67 is shown as purple sticks. (b) Surface representation of FKBP51 in complex with **22** (green). SG623 bound to FKBP51 is superimposed in magenta.

When we superimposed **22** with SG623 (Fig. 4b), a close analog of SAFit1, we were excited to see that the decalin-derivative virtually showed exactly the same conformation as SG623. The distal cyclohexyl ring completely correlates to the cyclohexyl ring of SG623, whereas the other serves as additional bridge to stabilize the spatial conformation. This allows introducing substituents in positions that cannot be achieved with open-chained analogs, which is in the crystal structures exemplified by the location of the carbonyl group.

## B. Research Articles – Publication/Manuscript VII

### Conclusion

In order to improve the properties of selective FKBP51 antagonists, we used a rigidification strategy to design a novel scaffold for new FKBP51 ligands. The binding affinities of the resulting bicyclic structure and derivatives, in comparison with the corresponding open-chained structure, confirmed our aim to increase binding affinity. Additionally we could show that despite of the clearly different structure of the bicyclic ligand series, the compound still exhibit the induced fit binding mechanism as previously published for FKBP51-selective ligands. The bicyclic structure also enables novel substitution patterns that are not possible with open-chained analogs. The decalin scaffold therefore serves as useful lead structure and scaffold for future FKBP51 drug development.

### References

1. Yeh, W.; Li, T.; Bierer, B. E.; McKnight, S. L., Identification and Characterization of an Immunophilin Expressed During the Clonal Expansion Phase to Adipocyte Differentiation. *PNAS* 1995, 92, (24), 11081-11085.
2. Hartmann, J.; Wagner, K. V.; Liebl, C.; Scharf, S. H.; Wang, X.-D.; Wolf, M.; Hausch, F.; Rein, T.; Schmidt, U.; Touma, C.; Cheung-Flynn, J.; Cox, M. B.; Smith, D. F.; Holsboer, F.; Müller, M. B.; Schmidt, M. V., The involvement of FK506-binding protein 51 (FKBP5) in the behavioral and neuroendocrine effects of chronic social defeat stress. *Neuropharmacology* 2012, 62, (1), 332-339.
3. Warriar, M., Role of Fkbp51 and Fkbp52 in Glucocorticoid Receptor Regulated Metabolism. Thesis, University of Toledo 2008.
4. A. V. Bortsov, J. E. Smith, L. Diatchenko, A. C. Soward, J. C. Ulirsch, C. Rossi, R. A. Swor, W. E. Hauda, D. A. Peak, J. S. Jones, D. Holbrook, N. K. Rathlev, K. A. Foley, D. C. Lee, R. Collette, R. M. Domeier, P. L. Hendry, S. A. McLean, Polymorphisms in the glucocorticoid receptor co-chaperone FKBP5 predict persistent musculoskeletal pain after traumatic stress exposure. *Pain* 154, 1419–1426 (2013).
5. Zannas AS, Binder EB: Gene–environment interactions at the FKBP5 locus: sensitive periods, mechanisms and pleiotropism. *Genes, Brain and Behavior* 2014, 13:25-37.
6. Feng, X., Pomplun S., Hausch F., Recent progress in FKBP ligand development. *Current molecular pharmacology* (2015).
7. Blackburn, E. A.; Walkinshaw, M. D. Targeting FKBP isoforms with small-molecule ligands. *Curr. Opin. Pharmacol.* 2011, 11 (4), 365–371.
8. Gaali, S.; Kirschner, A.; Cuboni, S.; Hartmann, J.; Kozany, C.; Balsevich, G.; Namendorf, C.; Fernandez-Vizarra, P.; Sippel, C.; Zannas, A. S.; Draenert, R.; Binder, E. B.; Almeida, O. F. X.; Rühler, G.; Uhr, M.; Schmidt, M. V.; Touma, C.; Bracher, A.; Hausch, F. Selective inhibitors of the FK506-binding protein 51 by induced fit. *Nat. Chem. Biol.* 2015, 11 (1), 33–37.
9. Hartmann, J.; Wagner, K. V.; Dedic, N.; Marinescu, D.; Scharf, S. H.; Wang, X. D.; Deussing, J. M.; Hausch, F.; Rein, T.; Schmidt, U.; Holsboer, F.; Muller, M. B.; Schmidt, M. V. Fkbp52 heterozygosity alters behavioral, endocrine and neurogenetic parameters under basal and chronic stress conditions in mice. *Psychoneuroendocrinology* 2012, 37 (12), 2009–21.
10. Warriar, M.; Hinds, T. D., Jr.; Ledford, K. J.; Cash, H. A.; Patel, P. R.; Bowman, T. A.; Stechschulte, L. A.; Yong, W.; Shou, W.; Najjar, S. M.; Sanchez, E. R. Susceptibility to diet-induced hepatic steatosis and glucocorticoid resistance in FK506-binding protein 52-deficient mice. *Endocrinology* 2010, 151 (7), 3225–36.

## B. Research Articles – Publication/Manuscript VII

11. Cheung-Flynn, J.; Prapapanich, V.; Cox, M. B.; Riggs, D. L.; Suarez-Quian, C.; Smith, D. F. Physiological role for the cochaperone FKBP52 in androgen receptor signaling. *Mol. Endocrinol.* 2005, 19 (6), 1654–66.
12. Tranguch, S.; Cheung-Flynn, J.; Daikoku, T.; Prapapanich, V.; Cox, M. B.; Xie, H.; Wang, H.; Das, S. K.; Smith, D. F.; Dey, S. K. From The Cover: Cochaperone immunophilin FKBP52 is critical to uterine receptivity for embryo implantation. *Proc. Natl. Acad. Sci. U. S.A.* 2005, 102 (40), 14326–14331.
13. Yang, Z.; Wolf, I. M.; Chen, H.; Periyasamy, S.; Chen, Z.; Yong, W.; Shi, S.; Zhao, W.; Xu, J.; Srivastava, A.; Sanchez, E. R.; Shou, W. FK506-Binding Protein 52 Is Essential to Uterine Reproductive Physiology Controlled by the Progesterone Receptor A Isoform. *Mol. Endocrinol.* 2006, 20 (11), 2682–2694.
14. Yong, W.; Yang, Z.; Periyasamy, S.; Chen, H.; Yucel, S.; Li, W.; Lin, L. Y.; Wolf, I. M.; Cohn, M. J.; Baskin, L. S.; Sanchez, E. R.; Shou, W. Essential Role for Co-chaperone Fkbp52 but Not Fkbp51 in Androgen Receptor-mediated Signaling and Physiology. *J. Biol. Chem.* 2007, 282 (7), 5026–5036.
15. Balsevich, G.; Gassen, N. C.; Häusl, A.; Feng, X.; Meyer, C. W.; Karamihalev, S.; Dournes, C.; Uribe, A.; Santarelli, S.; Hafner, K.; Theodoropoulou, M.; Namendorf, C.; Uhr, M.; Paez-Pereda, M.; Hausch, F.; Chen, A.; Tschöp, M. H.; Rein, T.; Schmidt, M. V. Loss or inhibition of FKBP51 protects against diet-induced metabolic disorders by shaping insulin signaling. (manuscript in preparation)
16. Pomplun, S., Wang, Y., Kirschner, A., Kozany, C., Bracher, A., & Hausch, F. (2015). Rational Design and Asymmetric Synthesis of Potent and Neurotrophic Ligands for FK506-Binding Proteins (FKBPs). *Angewandte Chemie International Edition*, 54(1), 345-348.
17. Wang Y, Kirschner A, Fabian AK, Gopalakrishnan R, Kress C, Hoogeland B, Koch U, Kozany C, Bracher A, Hausch F: Increasing the Efficiency of Ligands for FK506-Binding Protein 51 by Conformational Control. *J Med Chem* 2013, 56:3922-3935.
18. Bischoff M, Sippel C, Bracher A, Hausch F: Stereoselective Construction of the 5-Hydroxy Diazabicyclo[4.3.1]decane-2-one Scaffold, a Privileged Motif for FK506-Binding Proteins. *Organic Letters* 2014, 16:5254–5257.
19. Feng, X., Sippel, C., Bracher, A., Hausch, F., Structure–Affinity Relationship Analysis of Selective FKBP51 Ligands. *J. Med. Chem.*, 2015, 58, 7796-7806.
20. Gaali, S., Feng, X., Sippel, C., Bracher, A., Hausch, F., Rapid, structure-based exploration of pipercolic acid amides as novel selective antagonists of the FK506-binding protein 51. *J. Med. Chem.* (submitted manuscript)
21. Gopalakrishnan, R., Kozany, C., Wang, Y., Schneider, S., Hoogeland, B., Bracher, A., & Hausch, F. (2012). Exploration of pipercolate sulfonamides as binders of the FK506-binding proteins 51 and 52. *Journal of medicinal chemistry*, 55(9), 4123-4131.
22. Kozany, C., März, A., Kress, C., & Hausch, F. (2009). Fluorescent Probes to Characterise FK506-Binding Proteins. *ChemBioChem*, 10(8), 1402-1410.
23. Evans, D. A., Chapman, K. T., Bisaha, J., Asymmetric Diels-Alder cycloaddition reactions with chiral alpha-, beta-unsaturated N-acyloxazolidinones. *JACS*, 1988, 110(4), 1238-1256.
24. Biannic, B., & Aponick, A. (2011). Gold-Catalyzed Dehydrative Transformations of Unsaturated Alcohols. *European Journal of Organic Chemistry*, 2011(33), 6605-6617.
25. van der Knaap, M., Basalan, F., van de Mei, H. C., Busscher, H. J., van der Marel, G. A., Overkleeft, H. S., & Overhand, M. (2012). Synthesis and Biological Evaluation of Gramicidin S-Inspired Cyclic Mixed  $\alpha/\beta$ -Peptides. *Chemistry & biodiversity*, 9(11), 2494-2506.
26. Laube, T., Beil, W., & Seifert, K. (2005). Total synthesis of two 12-nordrimanes and the pharmacological active sesquiterpene hydroquinone yahazunol. *Tetrahedron*, 61(5), 1141-1148.

## B. Research Articles – Publication/Manuscript VII

27. Morandi B., Wickens Z., Grubbs R., Regioselective Wacker Oxidation of Internal Alkenes: Rapid Access to Functionalized Ketones Facilitated by Cross-Metathesis. *Angew. Chem.*, 2013, 125, 9933 –9936.

28. Gopalakrishnan R, Kozany C, Gaali S, Kress C, Hoogeland B, Bracher A, Hausch F: Evaluation of Synthetic FK506 Analogues as Ligands for the FK506-Binding Proteins 51 and 52. *J Med Chem* 2012, 55:4114-4122.

## B. Research Articles – Publication/Manuscript VII

### SUPPORTING INFORMATION

#### **A novel decalin-based bicyclic scaffold for FKBP51-selective ligands**

Xixi Feng\*, Claudia Sippel\*, Andreas Bracher#, Felix Hausch\*

\* Max Planck Institute of Psychiatry, Dept. Translational Research in Psychiatry,  
Kraepelinstrasse 2, 80804 Munich, Germany

# Max Planck Institute of Biochemistry, Am Klopferspitz 18, 82152 Martinsried, Germany

#### **Table of contents**

- I. Crystallography
- II. Chemistry
- III. References

## B. Research Articles – Publication/Manuscript VII

### I. Crystallography

Dataset	FKBP51-22
Space group	$P2_12_12_1$
Cell dimensions	
a, b, c (Å)	42.56, 50.33, 62.78
$\alpha$ , $\beta$ , $\gamma$ (°)	90, 90, 90
Wavelength (Å)	0.97857
Resolution (Å)	50.33- 2.05 (2.16 - 2.05)*
$R_{\text{merge}}$	0.065 (0.597)
$I/\sigma I$	13.3 (2.5)
Completeness (%)	99.7 (99.6)
Redundancy	5.3 (5.4)
<b>Refinement</b>	
Resolution (Å)	30 - 2.05
No reflections	8432
$R_{\text{work}} / R_{\text{free}}$	0.2137 / 0.2870
Number of atoms	
Protein	975
Ligand/ion	50
Water	74
<i>B</i> -factors	
Protein	47.80
Ligand/ion	53.08
Water	59.08
R.m.s. deviations	
Bond length (Å)	0.011
Bond angles (°)	1.625

\* Values in parenthesis for outer shell.

**Table 1** | *Data Collection and Refinement Statistics*

#### *Crystallization*

The complexes were prepared by mixing FKBP51 (16-140)-A19T protein at 1.75 mM with 50 mM **22** dissolved in DMSO in 16:1 ratio. Crystallization was performed at 20 °C using the hanging drop vapor-diffusion method, equilibrating mixtures of 1  $\mu$ l protein complex and 1  $\mu$ l reservoir against 500  $\mu$ l reservoir solution. Crystals were obtained with reservoir solution containing 28 % PEG-3350, 0.2 M  $\text{NH}_4$ -acetate and 0.1 M HEPES-NaOH pH 7.5.

## B. Research Articles – Publication/Manuscript VII

### *Structure Solution and Refinement*

The diffraction data were collected at beamline ID29 of the European Synchrotron Radiation Facility (ESRF) in Grenoble, France. Diffraction data were integrated with XDS<sup>1</sup> and further processed with Scala and Ctruncate<sup>2</sup>, as implemented in the CCP4i interface<sup>3,4</sup>. The crystal structures were solved by molecular replacement employing the program Molrep<sup>5</sup>. Iterative model improvement and refinement were performed with Coot<sup>6</sup> and Refmac5<sup>7</sup>. The dictionaries for the compounds were generated with the PRODRG server<sup>8</sup>. Residues facing solvent channels without detectable side chain density were modeled as alanines.

Molecular graphics figures were generated with the program Pymol<sup>9</sup>.

### **II. Chemistry**

All dry reactions were performed under argon atmosphere and with commercially available dry solvents

Chromatographic separations were performed either by manual flash chromatography or automated flash chromatography using an Interchim Puriflash 430 with an UV detector.

Merck F-254 (thickness 0.25 mm) commercial plates were used for analytical TLC. <sup>1</sup>H NMR spectra, <sup>13</sup>C NMR spectra, 2D HSQC, HMBC, and COSY of all intermediates were obtained from the Department of Chemistry and Pharmacy, LMU, on a Bruker Avance III HD 400/800 or a Varian NMR system 300/400/600 at room temperature. Chemical shifts for <sup>1</sup>H or <sup>13</sup>C are given in ppm ( $\delta$ ) downfield from tetramethylsilane using residual protio solvent as an internal standard.

Mass spectra (m/z) were recorded on a Thermo Finnigan LCQ DECA XP Plus mass spectrometer at the Max Planck Institute of Psychiatry, while the high resolution mass spectrometry was carried out at MPI for Biochemistry (Microchemistry Core Facility) on Bruker Daltonics MicrOTOF.

The purity of the compounds was verified by reversed phase HPLC. All gradients were started after 1 min of equilibration with starting percentage of solvent mixture. All of the final compounds synthesized and tested have a purity of more than 95%.

#### **Analytical HPLC:**

**Pump:** Beckman System Gold 125S Solvent Module  
**Detector:** Beckman System Gold Diode Array Detector Module 168  
**Column:** Phenomenex Jupiter 4 $\mu$  Proteo 90Å, 250 x 4.6 mm 4 micron

**Solvent A:** 95% H<sub>2</sub>O, 5% MeCN, 0.1% TFA

**Solvent B:** 95% MeCN, 5% H<sub>2</sub>O, 0.1% TFA

**Methods:** Described for the specific compound

#### **Preparative HPLC:**

**Pump:** Beckman System Gold Programmable Solvent Module 126 NMP

**Detector:** Beckman Programmable Detector Module 166

**Column:** Phenomenex Jupiter 10 $\mu$  Proteo 90 Å, 250 x 21.2 mm 10 micron

**Solvent A:** 95% H<sub>2</sub>O, 5% MeOH, 0.1% TFA

**Solvent B:** 95% MeOH, 5% H<sub>2</sub>O, 0.1% TFA

**Methods:** Described for the specific compound

## B. Research Articles – Publication/Manuscript VII

### *General procedure A – Wittig olefination*

To a suspension of the Wittig salt (2.4 eq) in THF (0.2 M) was added dropwise K<sup>+</sup>OtBu (2.6 eq, 1 M in THF) at 0 °C. The solution was stirred at RT for 1 h and then again cooled to 0 °C. The aldehyde (1 eq) dissolved in some THF (1 M) was then added dropwise and the mixture was stirred at 4 °C for 16 h. After warming to RT the reaction was quenched by the addition of a saturated NH<sub>4</sub>Cl solution and the product was extracted several times with Et<sub>2</sub>O. The combined organics were dried over MgSO<sub>4</sub>, filtered and the solvent was removed under reduced pressure. The crude product was purified by flash chromatography to obtain the title compounds as light yellow oils.

### *General procedure B– Swern Oxidation and subsequent Wittig olefination*

DMSO (3 eq) was added to a solution of oxalyl chloride (2 M in DCM, 1.5 eq) in DCM (0.1 M related to alcohol) at -78 °C and stirred at that temperature for 30 min. Then the alcohol (1 eq), dissolved in DCM (1 M) was added and the reaction mixture was stirred for further 60 min at -78 °C. In the following step TEA (10 eq) was added and the slurry was allowed to warm to RT. methyl 2-(triphenylphosphoranylidene)acetate (1.1 eq) was added in one portion and the slurry was stirred at RT for 16 h. If necessary, the reaction mixture was diluted with some DCM to maintain adequate stirring. The reaction mixture was then washed with H<sub>2</sub>O and saturated NH<sub>4</sub>Cl solution. The organic layer was then dried over MgSO<sub>4</sub>, filtered and the solvent was removed under reduced pressure. The product was obtained after purification by flash chromatography.

### *General procedure C – Methyl ester cleavage*

The methyl ester was dissolved in THF/1.5-2 M NaOH (1.5:1, 0.1 M) and stirred at 70 °C until the reaction was finished. After cooling to RT the reaction mixture was extracted with Et<sub>2</sub>O. The organic layer was removed and the aqueous layer acidified with concentrated HCl. Then free carboxylic acid was extracted several times with DCM. The combined organic solvents were dried over MgSO<sub>4</sub>, filtered and the solvent was removed under reduced pressure to obtain the product without further purification.

### *General procedure D – N-Acylation of the Evans auxiliary*

The carboxylic acid (1 eq) was dissolved in DCM (1 M) and oxalyl chloride (2 M in DCM, 2 eq) with a catalytic amount of DMF (a few drops) was added to convert the acid into an acid chloride. The reaction mixture was stirred at RT for 2. Then the solvent was removed and the carboxylic acid chloride was used without further purification. In the meantime n-BuLi (1.1 eq, 2.5 M in hexane) was added to (*R*)-4-benzyloxazolidin-2-one (1.0 eq) in THF (0.2 M) at -78 °C and the reaction mixture was stirred at that temperature for 1 h. Then the acid chloride, dissolved in some DCM, was added to the deprotonated auxiliary and the mixture was allowed to warm to RT. The reaction was quenched by the addition of saturated NH<sub>4</sub>Cl and the product was extracted with Et<sub>2</sub>O. The combined organics were then dried over MgSO<sub>4</sub>, filtered and the solvent was removed under reduced pressure. The product was obtained after purification by flash chromatography.

## B. Research Articles – Publication/Manuscript VII

### *General procedure E – Intramolecular Diels Alder cyclization*

The acylated Evans auxiliary was dissolved in DCM (0.025 M) and cooled to -78 °C. DMAC (1.5 eq, 1 M in hexane) was added and the reaction mixture was stirred for 16 h, whereby it slowly warmed to RT. Then the mixture was quenched with 1 N HCl and the product extracted with DCM. The combined organics were then dried over MgSO<sub>4</sub>, filtered and the solvent was removed under reduced pressure. The product was obtained after purification by flash chromatography.

### *General procedure F – Evans auxiliary cleavage*

To cleave the Evans auxiliary the reactant (1 eq) was dissolved in THF/H<sub>2</sub>O (0.075 M, 8:5) followed by the addition of LiOH (4.5 eq) and H<sub>2</sub>O<sub>2</sub> (5 eq, 30 % wt). The reaction mixture was stirred at RT for 2.5 h and then quenched by adding a half-saturated Na<sub>2</sub>SO<sub>3</sub> solution. It was extracted with DCM and the organic layers were removed. Then the aqueous layer was acidified with concentrated HCl and the product was extracted with DCM. The combined organics were dried over MgSO<sub>4</sub>, filtered and the solvent was removed under reduced pressure to obtain the title compound without further purification.

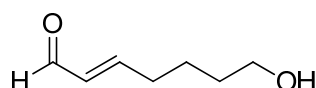
### *General procedure G – Double bond hydrogenation*

The reactant, containing the unsaturated double bond, was dissolved in MeOH (0.05 M) and the solution was degassed with argon. Then Pd/C (0.1 eq, 10 % wt) was added. In the following step H<sub>2</sub> was bubbled through the reaction mixture for 5 min. The reaction was then stirred under H<sub>2</sub> atmosphere for 16 h. After that time the dark suspension was filtered through celite and the solvent was removed under reduced pressure to obtain the title compound without further purification.

### *General procedure H – Coupling reaction with 34*

The carboxylic acid, **27** (1.0 eq), COMU (1.5 eq) and DIPEA (2.0 eq) were stirred in DMF (0.1 M) at RT for 16 h and the tBu-ester was isolated after flash chromatography (0-20 % EtOAc in cyclohexane). To obtain the free carboxylic acid the tBu-ester was cleaved in DCM/TFA (0.1 M) for 1 h at RT. The reaction mixture was quenched with saturated NaHCO<sub>3</sub> and the product was extracted with DCM. The combined organics were dried over MgSO<sub>4</sub>, filtered and the solvent was removed under reduced pressure to obtain the title compound, after purification.

### **(E)-7-hydroxyhept-2-enal (3a)**



**3a**

To a solution of Hoveyda-Grubbs 2<sup>nd</sup> generation catalyst (47.0 mg, 75.0 μmol) in DCM (35.0 mL) was added hex-5-en-1-ol (0.75 g, 7.50 mmol) and crotonaldehyde (3.11 mL, 37.5 mmol). The reaction mixture was heated to reflux for 2 h (oil bath was preheated to 50 °C). After

## B. Research Articles – Publication/Manuscript VII

completion of the reaction the mixture was cooled to RT. Some silica gel was added to the flask and the resulting slurry was stirred open to air for 30 min. The solvent was removed and the crude product was purified by flash chromatography (0-40 % EtOAc in cyclohexane) to obtain the title compound as light brown oil (quantitative yield).

**TLC** [EtOAc/cyclohexane, 1:1]:  $R_f = 0.16$

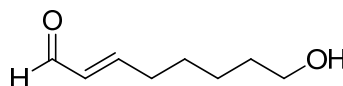
**Mass:** (ESI<sup>+</sup>), calculated 129.09 [C<sub>7</sub>H<sub>12</sub>O<sub>2</sub>+H]<sup>+</sup>, found 129.87 [M+H]<sup>+</sup>.

**<sup>1</sup>H NMR** (300 MHz, CDCl<sub>3</sub>)  $\delta$  9.49 (d,  $J = 7.8$  Hz, 1H), 6.84 (dt,  $J = 15.6, 6.7$  Hz, 1H), 6.12 (ddt,  $J = 15.6, 7.9, 1.5$  Hz, 1H), 3.70 – 3.59 (m, 2H), 2.47 – 2.24 (m, 2H), 1.70 – 1.53 (m, 4H).

**<sup>13</sup>C NMR** (75 MHz, CDCl<sub>3</sub>)  $\delta$  193.98, 158.21, 133.13, 62.34, 32.37, 32.00, 24.10.

Analytical data in accordance with Biannic et al.<sup>10</sup>

### (E)-8-hydroxyoct-2-enal (**3b**)



**3b**

To a solution of Grubbs 2<sup>nd</sup> generation catalyst (85.0 mg, 100  $\mu$ mol) in DCM (50.0 mL) was added hept-6-en-1-ol (1.35 mL, 10.0 mmol,  $d = 0.85$  g/mL) and crotonaldehyde (4.14 mL, 50.0 mmol,  $d = 0.85$  g/mL). The reaction mixture was heated to reflux for 2 h (oil bath was preheated to 50 °C). After completion of the reaction the mixture was cooled to RT. Some silica gel was added to the flask and the resulting slurry was stirred open to air for 30 min. The solvent was removed and the crude product was purified by flash chromatography (0-40 % EtOAc in cyclohexane) to obtain the title compound as light brown oil (quantitative yield)

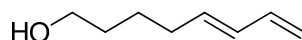
**TLC** [EtOAc/cyclohexane, 1:1]:  $R_f = 0.32$

**Mass:** (ESI<sup>+</sup>), calculated 165.09 [C<sub>8</sub>H<sub>14</sub>O<sub>2</sub>+Na]<sup>+</sup>, found 164.08 [M+Na]<sup>+</sup>.

**<sup>1</sup>H NMR** (599 MHz, CDCl<sub>3</sub>)  $\delta$  9.49 (d,  $J = 7.9$  Hz, 1H), 6.83 (dt,  $J = 15.6, 6.8$  Hz, 1H), 6.10 (ddt,  $J = 15.6, 7.9, 1.5$  Hz, 1H), 3.64 (t,  $J = 6.5$  Hz, 2H), 2.38 – 2.30 (m, 2H), 1.61 – 1.56 (m, 2H), 1.55 – 1.50 (m, 2H), 1.44 – 1.38 (m, 2H).

**<sup>13</sup>C NMR** (151 MHz, CDCl<sub>3</sub>)  $\delta$  194.07, 158.54, 133.04, 62.63, 32.63, 32.36, 27.61, 25.32.

### (E)-octa-5,7-dien-1-ol (**4a**)



**4a**

General procedure A was used with **3a** (963 mg, 7.51 mmol) and methyltriphenylphosphonium iodide to obtain the title compound after purification by flash

## B. Research Articles – Publication/Manuscript VII

chromatography (0-40 % EtOAc in cyclohexane) as a light yellow oil (500 mg, 3.96 mmol, 52.7 %).

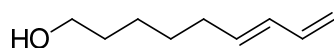
TLC [EtOAc/cyclohexane, 1:1]:  $R_f = 0.43$

$^1\text{H NMR}$  (300 MHz,  $\text{CDCl}_3$ )  $\delta$  6.30 (dt,  $J = 16.9, 10.2$  Hz, 0H), 6.17 – 5.96 (m, 1H), 5.79 – 5.59 (m, 1H), 5.18 – 4.87 (m, 2H), 3.64 (t,  $J = 6.4$  Hz, 2H), 2.18 – 2.03 (m, 1H), 1.65 – 1.40 (m, 4H), 1.30 – 1.19 (m, 1H).

$^{13}\text{C NMR}$  (75 MHz,  $\text{CDCl}_3$ )  $\delta$  137.16, 137.15, 134.82, 131.24, 114.86, 77.39, 77.18, 76.97, 76.55, 62.78, 32.21, 32.17, 25.26.

Analytical data in accordance with Craig et al.<sup>11</sup>

### (E)-nona-6,8-dien-1-ol (4b)



**4b**

General procedure A was used with **3b** (1.07 g, 7.50 mmol) and methyltriphenylphosphonium iodide to obtain the title compound after purification by flash chromatography (0-40 % EtOAc in cyclohexane) as a yellow oil (1.0g, 7.14 mmol, 95.1 %).

TLC [EtOAc/cyclohexane, 1:1]:  $R_f = 0.51$

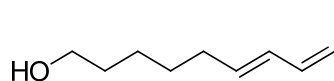
**Mass:** (ESI<sup>+</sup>), calculated 141.23 [ $\text{C}_9\text{H}_{16}\text{O}+\text{H}$ ]<sup>+</sup>, found 140.90 [ $\text{M}+\text{H}$ ]<sup>+</sup>.

$^1\text{H NMR}$  (300 MHz,  $\text{CDCl}_3$ )  $\delta$  6.31 (dt,  $J = 16.9, 10.2$  Hz, 1H), 6.12 – 5.99 (m, 1H), 5.70 (dt,  $J = 14.6, 6.9$  Hz, 1H), 5.14 – 5.04 (m, 1H), 4.99 – 4.92 (m, 1H), 3.64 (t,  $J = 6.6$  Hz, 2H), 2.18 – 2.00 (m, 2H), 1.68 – 1.49 (m, 2H), 1.47 – 1.32 (m, 5H).

$^{13}\text{C NMR}$  (75 MHz,  $\text{CDCl}_3$ )  $\delta$  137.23, 135.12, 131.07, 114.73, 62.92, 32.61, 32.44, 28.94, 25.29.

Analytical data in accordance with Craig et al.<sup>11</sup>

### (6E, 8Z)-deca-6,8-dien-1-ol (4c)



**4c**

General procedure A was used with **3c** (711 mg, 5.0 mmol) and ethyltriphenylphosphonium bromide to obtain the title compound (containing ~20% 8E-isomer) after purification by flash chromatography (0-20 % EtOAc in cyclohexane) as a light yellow oil (680 mg, 4.41 mmol, 88.2 %).

## B. Research Articles – Publication/Manuscript VII

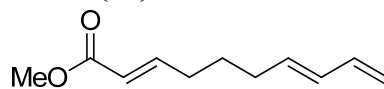
TLC [EtOAc/cyclohexane, 1:1]:  $R_f = 0.46$

$^1\text{H NMR}$  (300 MHz,  $\text{CDCl}_3$ )  $\delta$  6.44 – 6.24 (m, 1H), 6.09 – 5.88 (m, 1H), 5.71 – 5.59 (m, 1H), 5.44 – 5.31 (m, 1H), 3.68 – 3.60 (m, 2H), 2.18 – 2.02 (m, 2H), 1.73 (dd,  $J = 7.1, 1.7$  Hz, 3H), 1.56 (dd,  $J = 15.7, 8.5$  Hz, 3H), 1.48 – 1.30 (m, 4H).

$^{13}\text{C NMR}$  (75 MHz,  $\text{CDCl}_3$ )  $\delta$  134.12, 129.43, 125.52, 124.01, 62.94, 32.79, 32.62, 29.17, 25.31, 13.25.

Analytical data in accordance with Larson et al.<sup>12</sup>

### (2E, 7E)-methyl deca-2,7,9-trienoate (5a)



**5a**

General procedure B was used with **4a** (490 mg, 3.88 mmol) and the title compound was obtained after purification by flash chromatography (0-5 % EtOAc in cyclohexane) as yellow oil (630 mg, 90.1 %, 3.50 mmol).

TLC [EtOAc/cyclohexane, 2:8]:  $R_f = 0.53$

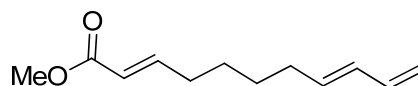
**Mass:** ( $\text{ESI}^+$ ), calculated 181.12 [ $\text{C}_{11}\text{H}_{16}\text{O}_2 + \text{H}$ ] $^+$ , found 181.00 [ $\text{M} + \text{H}$ ] $^+$ .

$^1\text{H NMR}$  (300 MHz,  $\text{CDCl}_3$ )  $\delta$  6.95 (dt,  $J = 15.7, 7.0$  Hz, 1H), 6.39 – 6.21 (m, 1H), 6.12 – 5.98 (m, 1H), 5.82 (dt,  $J = 15.6, 1.6$  Hz, 1H), 5.72 – 5.59 (m, 1H), 5.15 – 5.04 (m, 1H), 5.03 – 4.91 (m, 1H), 3.72 (s, 3H), 2.28 – 2.16 (m, 2H), 2.11 (q,  $J = 7.0$  Hz, 2H), 1.64 – 1.48 (m, 2H).

$^{13}\text{C NMR}$  (75 MHz,  $\text{CDCl}_3$ )  $\delta$  167.05, 149.09, 137.00, 134.05, 131.66, 121.14, 115.16, 51.36, 31.80, 31.53, 27.42.

Analytical data in accordance with Roush et al.<sup>13</sup>

### (2E,8E)-methyl undeca-2,8,10-trienoate (5b)



**5b**

General procedure B was used with **4b** (700 mg, 4.99 mmol) and the title compound was obtained after purification by flash chromatography (0-5 % EtOAc in cyclohexane) as yellow oil (quantitative yield).

TLC [EtOAc/cyclohexane, 1:9]:  $R_f = 0.48$

**Mass:** ( $\text{ESI}^+$ ), calculated 195.14 [ $\text{C}_{12}\text{H}_{18}\text{O}_2 + \text{H}$ ] $^+$ , found 195.01 [ $\text{M} + \text{H}$ ] $^+$ .

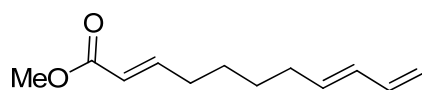
## B. Research Articles – Publication/Manuscript VII

**<sup>1</sup>H NMR** (400 MHz, CDCl<sub>3</sub>) δ 6.95 (dt, *J* = 15.7, 7.0 Hz, 1H), 6.42 – 6.19 (m, 1H), 6.13 – 5.97 (m, 1H), 5.81 (dt, *J* = 15.6, 1.6 Hz, 1H), 5.75 – 5.58 (m, 1H), 5.15 – 5.03 (m, 1H), 5.03 – 4.86 (m, 1H), 3.72 (s, 3H), 2.20 (qd, *J* = 7.0, 1.6 Hz, 2H), 2.12 – 2.01 (m, 2H), 1.52 – 1.36 (m, 4H).

**<sup>13</sup>C NMR** (101 MHz, CDCl<sub>3</sub>) δ 167.11, 149.41, 137.13, 134.71, 131.25, 120.97, 114.92, 51.37, 32.20, 32.00, 28.57, 27.48, 26.89.

Analytical data in accordance with Roush et al.<sup>13</sup>

### (2E,8E,10Z)-methyl dodeca-2,8,10-trienoate (**5c**)



**5c**

General procedure B was used with **4c** (680 mg, 4.41 mmol) and the title compound (containing ~20% 10E-isomer) was obtained, after purification by flash chromatography (0-5 % EtOAc in cyclohexane) as colorless oil (904 mg, 4.34 mmol, 98.1 %).

**TLC** [EtOAc/cyclohexane, 1:9]: *R<sub>f</sub>* = 0.41

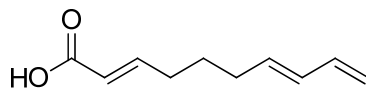
**Mass:** (ESI<sup>+</sup>), calculated 209.30 [C<sub>13</sub>H<sub>20</sub>O<sub>2</sub>+H]<sup>+</sup>, found 208.99 [M+H]<sup>+</sup>.

**<sup>1</sup>H NMR** (599 MHz, CDCl<sub>3</sub>) δ 6.96 (dt, *J* = 15.6, 7.0 Hz, 1H), 6.32 (ddq, *J* = 15.1, 11.0, 1.4 Hz, 1H), 5.99 – 5.93 (m, 1H), 5.85 – 5.78 (m, 1H), 5.66 – 5.59 (m, 1H), 5.44 – 5.32 (m, 1H), 3.74 – 3.71 (m, 3H), 2.21 (qd, *J* = 7.1, 1.6 Hz, 2H), 2.15 – 2.08 (m, 2H), 1.75 – 1.71 (m, 3H), 1.50 – 1.39 (m, 4H).

**<sup>13</sup>C NMR** (151 MHz, CDCl<sub>3</sub>) δ 167.12, 149.47, 133.71, 129.33, 125.72, 124.20, 120.94, 51.37, 32.56, 32.04, 28.83, 27.53, 13.27.

Analytical data in accordance with Lygo et al.<sup>14</sup>

### (2E, 7E)- deca-2,7,9-trienoic acid (**6a**)



**6a**

General procedure C was used with **5a** (620 mg, 3.44 mmol) to obtain the title compound as light brown oil (493 mg, 2.97 mmol, 86.2 %).

**TLC** [EtOAc/cyclohexane, 1:1]: *R<sub>f</sub>* = 0.36

## B. Research Articles – Publication/Manuscript VII

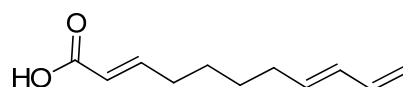
**Mass:** (ESI<sup>+</sup>), calculated 167.11 [C<sub>10</sub>H<sub>14</sub>O<sub>2</sub>+H]<sup>+</sup>, found 167.01 [M+H]<sup>+</sup>.

**<sup>1</sup>H NMR** (300 MHz, CDCl<sub>3</sub>) δ 6.95 (dt, *J* = 15.7, 7.0 Hz, 1H), 6.39 – 6.21 (m, 1H), 6.12 – 5.98 (m, 1H), 5.82 (dt, *J* = 15.6, 1.6 Hz, 1H), 5.72 – 5.59 (m, 1H), 5.15 – 5.04 (m, 1H), 5.03 – 4.91 (m, 1H), 2.28 – 2.16 (m, 2H), 2.11 (q, *J* = 7.0 Hz, 2H), 1.64 – 1.48 (m, 2H).

**<sup>13</sup>C NMR** (75 MHz, CDCl<sub>3</sub>) δ 167.05, 149.09, 137.00, 134.05, 131.66, 121.14, 115.16, 31.80, 31.53, 27.42.

Analytical data in accordance with Evans et al.<sup>15</sup>

### (2E, 8E)- undeca-2,8,10-trienoic acid (**6b**)



**6b**

General procedure C was used with **5b** (680 mg, 3.50 mmol) to obtain the title compound as light yellow oil (595 mg, 3.30 mmol, 94.3 %).

**TLC** [EtOAc/cyclohexane, 1:1]: R<sub>f</sub> = 0.48

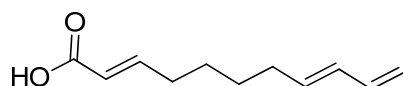
**Mass:** (ESI<sup>+</sup>), calculated 181.12 [C<sub>11</sub>H<sub>16</sub>O<sub>2</sub>+H]<sup>+</sup>, found 181.00 [M+H]<sup>+</sup>.

**<sup>1</sup>H NMR** (400 MHz, CDCl<sub>3</sub>) δ 7.07 (dt, *J* = 15.6, 7.0 Hz, 1H), 6.30 (dtd, *J* = 17.0, 10.2, 0.7 Hz, 1H), 6.21 – 5.92 (m, 1H), 5.82 (dt, *J* = 15.6, 1.6 Hz, 1H), 5.78 – 5.55 (m, 1H), 5.15 – 5.05 (m, 1H), 5.05 – 4.85 (m, 1H), 2.23 (qd, *J* = 6.9, 1.6 Hz, 2H), 2.18 – 2.03 (m, 2H), 1.62 – 1.30 (m, 4H).

**<sup>13</sup>C NMR** (101 MHz, CDCl<sub>3</sub>) δ 171.79, 152.04, 137.11, 134.63, 131.30, 120.71, 114.96, 32.19, 32.11, 28.59, 27.34.

Analytical data in accordance with Evans et al.<sup>15</sup>

### (2E,8E,10Z)-dodeca-2,8,10-trienoic acid (**6c**)



**6c**

General procedure C was used with **5c** (890 mg, 4.27 mmol) to obtain the title compound (containing ~20% 10E-isomer) as light yellow oil (688 mg, 3.54 mmol, 82.9 %).

**TLC** [EtOAc/cyclohexane, 1:1]: R<sub>f</sub> = 0.44

## B. Research Articles – Publication/Manuscript VII

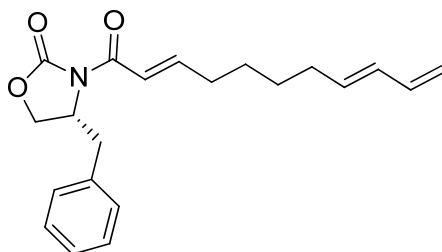
**Mass:** (ESI<sup>+</sup>), calculated 195.14 [C<sub>12</sub>H<sub>18</sub>O<sub>2</sub>+H]<sup>+</sup>, found 195.00 [M+H]<sup>+</sup>.

**<sup>1</sup>H NMR** (599 MHz, CDCl<sub>3</sub>) δ 7.08 (dt, *J* = 15.6, 7.0 Hz, 1H), 6.33 (ddq, *J* = 15.1, 10.9, 1.3 Hz, 1H), 6.02 – 5.93 (m, 1H), 5.83 (dt, *J* = 15.6, 1.6 Hz, 1H), 5.67 – 5.59 (m, 1H), 5.44 – 5.33 (m, 1H), 2.25 (qd, *J* = 7.1, 1.6 Hz, 2H), 2.15 – 2.10 (m, 2H), 1.76 – 1.72 (m, 3H), 1.53 – 1.47 (m, 2H), 1.46 – 1.40 (m, 2H).

**<sup>13</sup>C NMR** (151 MHz, CDCl<sub>3</sub>) δ 171.70, 152.14, 133.63, 129.32, 125.77, 124.25, 120.64, 32.54, 32.15, 28.84, 27.39, 13.28.

Analytical data in accordance with Lygo et al.<sup>14</sup>

### (*R*)-4-benzyl-3-((2*E*,8*E*)-undeca-2,8,10-trienoyl)oxazolidin-2-one (**7b**)



**7b**

General procedure D was used with **6b** (900 mg, 4.99 mmol) and the title compound was obtained after purification by flash chromatography (0-10 % EtOAc in cyclohexane) as yellow oil (1.21 g, 3.55 mmol, 71.1 %).

**TLC** [EtOAc/cyclohexane, 2:8]: *R<sub>f</sub>* = 0.40

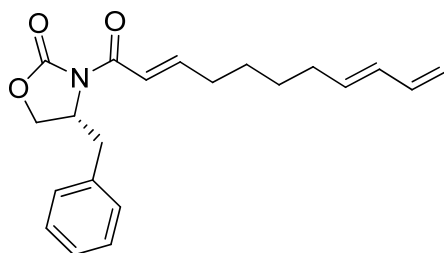
**Mass:** (ESI<sup>+</sup>), calculated 340.19 [C<sub>21</sub>H<sub>25</sub>NO<sub>3</sub>+H]<sup>+</sup>, found 340.28 [M+H]<sup>+</sup>.

**<sup>1</sup>H NMR** (599 MHz, CDCl<sub>3</sub>) δ 7.34 – 7.30 (m, 2H), 7.26 – 7.16 (m, 5H), 6.30 (dtd, *J* = 17.1, 10.3, 0.8 Hz, 1H), 6.15 – 5.98 (m, 1H), 5.68 (dtd, *J* = 15.0, 7.0, 0.8 Hz, 1H), 5.15 – 5.03 (m, 1H), 5.02 – 4.88 (m, 1H), 4.82 – 4.64 (m, 1H), 4.26 – 4.11 (m, 2H), 3.33 (dd, *J* = 13.4, 3.3 Hz, 1H), 2.78 (dd, *J* = 13.4, 9.6 Hz, 1H), 2.30 (qd, *J* = 6.9, 1.2 Hz, 2H), 2.10 (qd, *J* = 7.2, 1.4 Hz, 2H), 1.55 – 1.49 (m, 2H), 1.48 – 1.43 (m, 2H).

**<sup>13</sup>C NMR** (101 MHz, CDCl<sub>3</sub>) δ 165.06, 153.42, 151.64, 137.17, 135.37, 134.80, 131.24, 129.44, 128.93, 127.29, 120.45, 114.92, 66.10, 55.32, 37.89, 32.53, 32.24, 28.67, 27.59, 26.90.

## B. Research Articles – Publication/Manuscript VII

### (*R*)-4-benzyl-3-((2*E*,8*E*,10*Z*)-dodeca-2,8,10-trienoyl)oxazolidin-2-one (**7c**)



**7c**

General procedure D was used with **6c** (611 mg, 3.45 mmol) and the title compound (containing ~20% 10*E*-isomer) was obtained, after purification by flash chromatography (0-5 % EtOAc in cyclohexane) as yellow oil (800 mg, 2.26 mmol, 65.6 %).

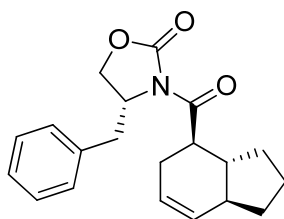
TLC [EtOAc/cyclohexane, 2:8]:  $R_f = 0.42$

**Mass:** (ESI<sup>+</sup>), calculated 354.21 [C<sub>22</sub>H<sub>27</sub>NO<sub>3</sub>+H]<sup>+</sup>, found 354.08 [M+H]<sup>+</sup>.

**<sup>1</sup>H NMR** (599 MHz, CDCl<sub>3</sub>)  $\delta$  7.36 – 7.31 (m, 2H), 7.29 – 7.26 (m, 2H), 7.25 – 7.20 (m, 3H), 6.34 (ddq,  $J = 15.1, 11.0, 1.4$  Hz, 1H), 6.02 – 5.90 (m, 1H), 5.71 – 5.59 (m, 1H), 5.43 – 5.35 (m, 1H), 4.78 – 4.68 (m, 1H), 4.28 – 4.13 (m, 2H), 3.34 (dd,  $J = 13.4, 3.3$  Hz, 1H), 2.80 (dd,  $J = 13.4, 9.6$  Hz, 1H), 2.39 – 2.24 (m, 2H), 2.18 – 2.10 (m, 2H), 1.78 – 1.68 (m, 3H), 1.57 – 1.51 (m, 2H), 1.50 – 1.40 (m, 2H).

**<sup>13</sup>C NMR** (151 MHz, CDCl<sub>3</sub>)  $\delta$  165.07, 153.41, 151.67, 135.39, 133.77, 129.43, 129.37, 128.93, 127.28, 125.72, 124.18, 120.45, 66.10, 55.32, 37.91, 32.57, 28.92, 27.64, 13.28.

### (*R*)-4-benzyl-3-((3*aR*,4*R*,7*aS*)-2,3,3*a*,4,5,7*a*-hexahydro-1*H*-indene-4-carbonyl)oxazolidin-2-one (**8a**)



**8a**

To a suspension of (*R*)-4-benzyl-oxazolidin-2-one (665 mg, 3.75 mmol), DMAP (70.6 mg) and **6a** (480 mg, 2.89 mmol) in DCM (6.0 mL) was added DCC (596 mg, 2.89 mmol) at -78 °C. The reaction was stirred at that temperature for 1 h and then at 0 °C for 20 h. Purification by flash chromatography (0-10 % EtOAc in cyclohexane) provided the product as inseparable mixture of the title compound and the *N*-acylurea byproduct. To a solution of this mixture (490 mg) in DCM (50.0 mL) was added DMAC (2.26 mL, 2.26 mmol, 1 M in hexane) at -78 °C. The solution was stirred for 16 h, whereby it was slowly warmed to RT. Then 1 N HCl was added and the product was extracted with DCM. The combined organics were dried over

## B. Research Articles – Publication/Manuscript VII

MgSO<sub>4</sub>, filtered and the solvent was removed under reduced pressure. Purification by flash chromatography provided the title compound as colorless oil (304 mg, 0.93 mmol, 24.9 % after 2 steps).

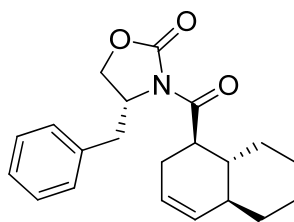
TLC [EtOAc/cyclohexane, 1:9]: R<sub>f</sub> = 0.26

Mass: (ESI<sup>+</sup>), calculated 326.18 [C<sub>20</sub>H<sub>23</sub>NO<sub>3</sub>+H]<sup>+</sup>, found 326.14 [M+H]<sup>+</sup>.

<sup>1</sup>H NMR (300 MHz, CDCl<sub>3</sub>) δ 7.44 – 7.02 (m, 5H), 5.85 (dq, *J* = 9.7, 2.0 Hz, 1H), 5.64 – 5.53 (m, 1H), 4.79 – 4.57 (m, 1H), 4.29 – 4.02 (m, 2H), 3.86 (td, *J* = 10.7, 6.2 Hz, 1H), 3.25 (dd, *J* = 13.1, 3.2 Hz, 1H), 2.76 (dd, *J* = 13.4, 9.5 Hz, 1H), 2.67 – 2.45 (m, 1H), 2.36 – 2.11 (m, 1H), 2.03 – 1.95 (m, 1H), 1.92 – 1.78 (m, 2H), 1.81 – 1.62 (m, 3H), 1.25 – 1.06 (m, 2H).

<sup>13</sup>C NMR (75 MHz, CDCl<sub>3</sub>) δ 175.83, 153.13, 135.26, 129.86, 129.40, 128.90, 127.32, 125.29, 66.07, 55.28, 45.45, 43.60, 43.40, 37.96, 30.27, 28.90, 27.67, 21.83.

**(R)-4-benzyl-3-((1R,4aS,8aR)-1,2,4a,5,6,7,8,8a-octahydronaphthalene-1-carbonyl)oxazolidin-2-one (8b)**



**8b**

General procedure E was used with **7b** (140 mg, 0.41 mmol) and the title compound was obtained after purification by flash chromatography (0-10 % EtOAc in cyclohexane) as colorless oil (115 mg, 0.34 mmol, 82.1 %).

TLC [EtOAc/cyclohexane, 2:8]: R<sub>f</sub> = 0.43

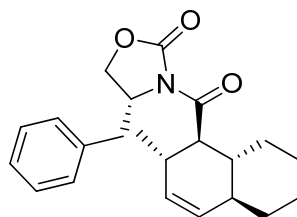
Mass: (ESI<sup>+</sup>), calculated 340.19 [C<sub>21</sub>H<sub>25</sub>NO<sub>3</sub>+H]<sup>+</sup>, found 340.11 [M+H]<sup>+</sup>.

<sup>1</sup>H NMR (599 MHz, CDCl<sub>3</sub>) δ 7.35 – 7.30 (m, 2H), 7.28 – 7.25 (m, 1H), 7.22 – 7.18 (m, 2H), 5.64 – 5.60 (m, 1H), 5.49 – 5.41 (m, 1H), 4.72 – 4.67 (m, 1H), 4.21 – 4.14 (m, 2H), 3.87 (td, *J* = 10.8, 5.7 Hz, 1H), 3.25 (dd, *J* = 13.4, 3.3 Hz, 1H), 2.77 (dd, *J* = 13.4, 9.5 Hz, 1H), 2.41 – 2.35 (m, 1H), 2.32 – 2.24 (m, 1H), 1.88 – 1.81 (m, 1H), 1.79 – 1.68 (m, 3H), 1.69 – 1.62 (m, 1H), 1.61 – 1.49 (m, 1H), 1.34 – 1.28 (m, 2H), 1.12 – 0.99 (m, 2H).

<sup>13</sup>C NMR (151 MHz, CDCl<sub>3</sub>) δ 176.37, 153.12, 135.24, 132.09, 129.41, 128.90, 127.32, 123.96, 65.96, 55.29, 43.13, 42.46, 41.09, 37.96, 32.99, 29.95, 29.83, 26.62, 26.44.

## B. Research Articles – Publication/Manuscript VII

### (*R*)-4-benzyl-3-((1*R*,2*S*,4*aS*,8*aR*)-2-methyl-1,2,4*a*,5,6,7,8,8*a*-octahydronaphthalene-1-carbonyl)oxazolidin-2-one (**8c**)



**8c**

General procedure E was used with **7c** (790 mg, 2.24 mmol) and the title compound was obtained after purification by flash chromatography (0-20 % DCM in cyclohexane) as a colorless oil (470 mg, 1.33 mmol, 59.5 %).

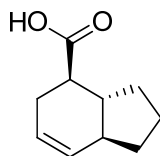
TLC [DCM/cyclohexane, 1:1]:  $R_f = 0.23$

Mass: (ESI<sup>+</sup>), calculated 354.21 [C<sub>22</sub>H<sub>27</sub>NO<sub>3</sub>+H]<sup>+</sup>, found 354.02 [M+H]<sup>+</sup>.

<sup>1</sup>H NMR (800 MHz, CDCl<sub>3</sub>)  $\delta$  7.38 – 7.33 (m, 2H), 7.30 – 7.26 (m, 3H), 5.60 (ddd,  $J = 9.8, 4.6, 2.5$  Hz, 1H), 5.43 (dt,  $J = 9.9, 1.7$  Hz, 1H), 4.76 – 4.71 (m, 1H), 4.21 – 4.11 (m, 2H), 3.84 (dd,  $J = 11.4, 5.9$  Hz, 1H), 3.44 (dd,  $J = 13.2, 3.4$  Hz, 1H), 2.87 – 2.78 (m, 1H), 2.65 (dd,  $J = 13.2, 10.5$  Hz, 1H), 1.96 – 1.89 (m, 1H), 1.82 – 1.74 (m, 3H), 1.65 – 1.56 (m, 2H), 1.45 – 1.38 (m, 1H), 1.34 (qt,  $J = 14.1, 3.9$  Hz, 1H), 1.18 – 1.10 (m, 1H), 0.98 (d,  $J = 7.2$  Hz, 3H), 0.93 – 0.85 (m, 1H).

<sup>13</sup>C NMR (201 MHz, CDCl<sub>3</sub>)  $\delta$  173.62, 153.06, 135.51, 130.83, 130.70, 129.34, 128.99, 127.32, 66.03, 55.37, 47.67, 41.89, 38.29, 36.59, 33.17, 30.91, 30.09, 26.70, 26.59, 17.77.

### (3*aR*,4*R*,7*aS*)-2,3,3*a*,4,5,7*a*-hexahydro-1*H*-indene-4-carboxylic acid (**9a**)



**9a**

General procedure F was used with **8a** (290 mg, 0.89 mmol) to obtain the title compound without further purification as a colorless solid (77 mg, 0.46 mmol, 52.1 %).

TLC [EtOAc/cyclohexane, 1:9]:  $R_f = 0.26$ .

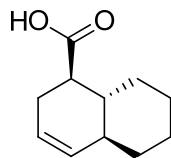
<sup>1</sup>H NMR (599 MHz, CDCl<sub>3</sub>)  $\delta$  5.88 – 5.79 (m, 1H), 5.64 – 5.50 (m, 1H), 2.59 – 2.49 (m, 1H), 2.48 – 2.28 (m, 2H), 1.98 – 1.80 (m, 3H), 1.79 – 1.64 (m, 2H), 1.56 (qd,  $J = 11.3, 6.4$  Hz, 1H), 1.32 – 1.23 (m, 1H), 1.23 – 1.14 (m, 1H).

## B. Research Articles – Publication/Manuscript VII

$^{13}\text{C}$  NMR (151 MHz,  $\text{CDCl}_3$ )  $\delta$  181.57, 129.77, 125.21, 45.54, 45.12, 44.11, 29.78, 28.97, 28.08, 21.79.

Analytical data in accordance with Clive et al.<sup>16</sup>

### (1*R*,4*aS*,8*aR*)-1,2,4*a*,5,6,7,8,8*a*-octahydronaphthalene-1-carboxylic acid (**9b**)



**9b**

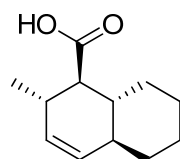
General procedure F was used with **8b** (43 mg, 0.13 mmol) to obtain the title compound without further purification as a colorless solid (19 mg, 0.11 mmol, 83.2 %).

TLC [EtOAc/cyclohexane, 2:8]:  $R_f$  = 0.12

$^1\text{H}$  NMR (300 MHz,  $\text{CDCl}_3$ )  $\delta$  5.65 – 5.57 (m, 1H), 5.45 (dq,  $J$  = 9.9, 1.9 Hz, 1H), 2.48 – 2.39 (m, 1H), 2.38 – 2.29 (m, 2H), 1.87 – 1.71 (m, 4H), 1.68 – 1.21 (m, 4H), 1.19 – 0.99 (m, 2H).

$^{13}\text{C}$  NMR (75 MHz,  $\text{CDCl}_3$ )  $\delta$  181.95, 132.09, 123.79, 46.17, 42.12, 41.33, 32.94, 30.31, 29.47, 26.58, 26.36.

### (1*R*,2*S*,4*aS*,8*aR*)-2-methyl-1,2,4*a*,5,6,7,8,8*a*-octahydronaphthalene-1-carboxylic acid (**9c**)



**9c**

*n*-Buli (0.42 mL, 1.06 mmol, 2.5 M) was added to a solution of ethanethiol (94  $\mu\text{L}$ , 1.27 mmol,  $d$  = 0.84 g/mol) in THF (4.5 mL) at  $-78$   $^\circ\text{C}$  and stirred for 10 min. The reaction mixture was transferred to an ice bath and **8c** (150 mg, 0.42 mmol), dissolved in THF (0.5 mL), was added. The solution was stirred at  $0$   $^\circ\text{C}$  for 1 h, then quenched with saturated  $\text{NH}_4\text{Cl}$  solution and extracted with  $\text{Et}_2\text{O}$ . The organics were combined, dried over  $\text{MgSO}_4$ , filtered and concentrated in vacuo.

After purification (quantitative yield) by flash chromatography (0-5 % EtOAc in cyclohexane) the thioester (80.0 mg, 0.34 mmol) was dissolved in THF/ $\text{H}_2\text{O}$  (1.8 mL, 5:1) followed by addition of mercury(II)trifluoroacetate (215 mg, 0.5 mmol). The reaction mixture was stirred at  $60$   $^\circ\text{C}$  for 2 h and the title compound was obtained after purification by flash

## B. Research Articles – Publication/Manuscript VII

chromatography (0-20 % EtOAc in cyclohexane) as colorless solid (33.9 mg, 0.17 mmol, 52.0 %).

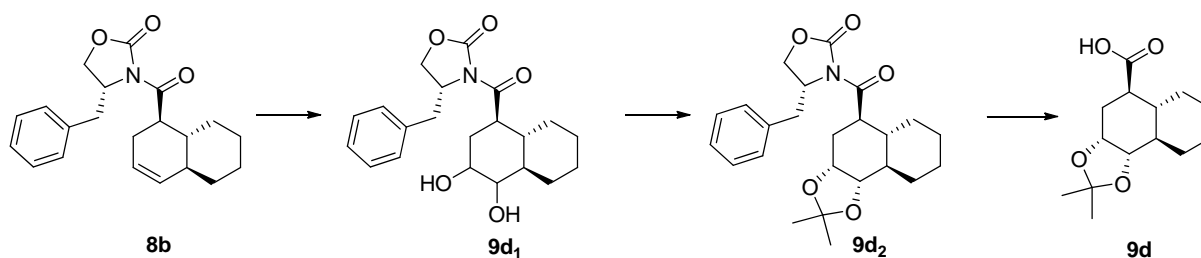
**TLC** [EtOAc/cyclohexane, 3:7]:  $R_f = 0.42$ .

**Mass:** (ESI<sup>+</sup>), calculated 195.14 [C<sub>12</sub>H<sub>18</sub>O<sub>2</sub>+H]<sup>+</sup>, found 195.01 [M+H]<sup>+</sup>.

**<sup>1</sup>H NMR** (599 MHz, CDCl<sub>3</sub>)  $\delta$  5.55 (ddd,  $J = 9.9, 4.0, 2.7$  Hz, 1H), 5.39 (dq,  $J = 9.8, 0.9$  Hz, 1H), 2.64 – 2.55 (m, 2H), 2.05 – 1.98 (m, 1H), 1.80 – 1.74 (m, 2H), 1.72 – 1.66 (m, 1H), 1.43 – 1.38 (m, 1H), 1.38 – 1.34 (m, 1H), 1.35 – 1.32 (m, 1H), 1.32 – 1.27 (m, 1H), 1.12 – 1.05 (m, 1H), 1.00 – 0.97 (m, 3H), 0.96 – 0.88 (m, 1H).

**<sup>13</sup>C NMR** (151 MHz, CDCl<sub>3</sub>)  $\delta$  179.77, 130.95, 130.52, 49.32, 42.01, 36.26, 33.01, 32.14, 30.04, 26.63, 26.47, 17.61.

### (3*aR*,5*R*,5*aR*,9*aR*,9*bS*)-2,2-dimethyldecahydronaphtho[1,2-*d*][1,3]dioxole-5-carboxylic acid (**9d**)



**8b** (80 mg, 0.26 mmol) was dissolved in acetone (1.0 mL) and H<sub>2</sub>O (0.5 mL). Then 4-methylmorpholine-4-oxide (55 mg, 0.47 mmol) and osmium tetroxide (118  $\mu$ L, 9.4  $\mu$ mol, 2.5 % wt in tBuOH) were added and the mixture was stirred at RT for 16 h. The crude product was directly loaded on silica and purified by flash chromatography (0-50 % [EtOAc + 2 % MeOH] in cyclohexane) to obtain **9d<sub>1</sub>** as a diastereomeric mixture (dr = 4:1, quant. yield). **9d<sub>1</sub>** was dissolved in acetone and 2,2-dimethoxypropane (1:1, 1.4 mL) and PTSA (0.02 eq) was added. The reaction was stirred for 24 h and then purified by flash chromatography (0-5 % EtOAc in cyclohexane), whereby the minor diastereomer was separated, to obtain **9d<sub>2</sub>**. Then general procedure F was used to obtain **9d** without further purification as colorless oil (24 mg, 9.4  $\mu$ mol, 36.3 % from **8b**).

**TLC** [EtOAc/cyclohexane, 1:1]:  $R_f = 0.20$ .

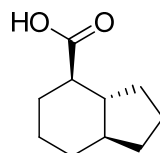
**Mass:** (ESI<sup>+</sup>), calculated 255.16 [C<sub>14</sub>H<sub>22</sub>O<sub>4</sub>+H]<sup>+</sup>, found 255.02 [M+H]<sup>+</sup>.

**<sup>1</sup>H NMR** (400 MHz, CDCl<sub>3</sub>)  $\delta$  4.28 – 4.20 (m, 1H), 3.60 (dd,  $J = 8.6, 4.9$  Hz, 1H), 2.46 – 2.36 (m, 1H), 2.32 (ddd,  $J = 14.9, 4.0, 2.6$  Hz, 1H), 2.13 – 2.04 (m, 1H), 1.96 (ddd,  $J = 14.8, 12.1, 4.0$  Hz, 1H), 1.84 – 1.64 (m, 3H), 1.48 (s, 3H), 1.34 (s, 3H), 1.26 – 1.14 (m, 4H), 1.02 (dt,  $J = 10.9, 6.1$  Hz, 1H), 0.97 – 0.87 (m, 1H).

## B. Research Articles – Publication/Manuscript VII

$^{13}\text{C}$  NMR (101 MHz,  $\text{CDCl}_3$ )  $\delta$  181.15, 108.31, 79.53, 72.31, 44.28, 43.73, 40.16, 30.73, 30.12, 29.67, 28.53, 26.38, 25.77, 25.59.

### (3a*R*,4*R*,7a*S*)-octahydro-1*H*-indene-4-carboxylic acid (**10a**)



**10a**

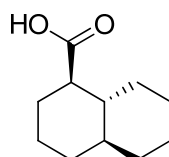
General procedure G was used with **9a** (15 mg, 90  $\mu\text{mol}$ ) to obtain the title compound (quantitative yield) as colorless oil.

TLC [EtOAc/cyclohexane, 1:9]:  $R_f$  = 0.45

$^1\text{H}$  NMR (599 MHz,  $\text{CDCl}_3$ )  $\delta$  2.14 – 2.03 (m, 1H), 1.95 (d,  $J$  = 12.9 Hz, 1H), 1.92 – 1.76 (m, 3H), 1.79 – 1.71 (m, 1H), 1.69 – 1.47 (m, 2H), 1.40 (qd,  $J$  = 12.9, 12.4, 3.5 Hz, 1H), 1.31 – 1.04 (m, 5H), 1.00 (qd,  $J$  = 12.2, 3.3 Hz, 1H).

$^{13}\text{C}$  NMR (151 MHz,  $\text{CDCl}_3$ )  $\delta$  182.17, 48.91, 47.60, 45.52, 30.96, 30.81, 29.67, 29.57, 29.39, 25.74, 21.31.

### (1*R*,4a*S*,8a*R*)-decahydronaphthalene-1-carboxylic acid (**10b**)



**10b**

General procedure G was used with **9b** (24 mg, 0.133 mmol) to obtain the title compound (quantitative yield) as colorless solid.

TLC [EtOAc/cyclohexane, 2:8]:  $R_f$  = 0.24

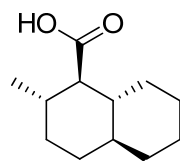
**Mass:** (ESI $^+$ ), calculated 183.14 [ $\text{C}_{11}\text{H}_{18}\text{O}_2 + \text{H}$ ] $^+$ , found 183.14 [ $\text{M} + \text{H}$ ] $^+$ .

$^1\text{H}$  NMR (400 MHz,  $\text{CDCl}_3$ )  $\delta$  2.04 (ddd,  $J$  = 12.2, 10.7, 3.5 Hz, 1H), 1.94 (dq,  $J$  = 12.7, 3.4, 1.6 Hz, 1H), 1.78 (dq,  $J$  = 13.2, 3.1 Hz, 1H), 1.74 – 1.71 (m, 1H), 1.71 – 1.66 (m, 2H), 1.64 – 1.56 (m, 2H), 1.55 – 1.44 (m, 2H), 1.39 – 1.26 (m, 2H), 1.26 – 1.17 (m, 2H), 1.09 – 0.90 (m, 3H).

$^{13}\text{C}$  NMR (75 MHz,  $\text{CDCl}_3$ )  $\delta$  182.36, 50.11, 44.21, 41.80, 34.00, 33.39, 31.30, 30.22, 26.38, 26.29, 25.29.

## B. Research Articles – Publication/Manuscript VII

### (1*R*,2*S*,4*aS*,8*aR*)-2-methyldecahydronaphthalene-1-carboxylic acid (**10c**)



**10c**

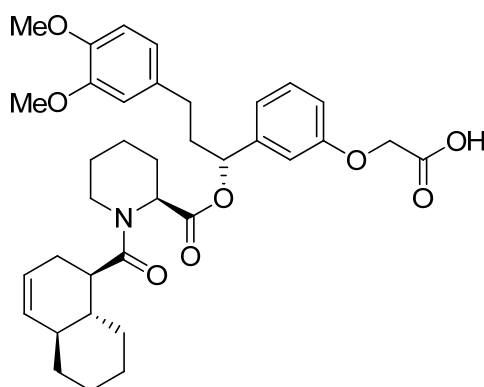
General procedure G was used with **9c** (10 mg, 0.05 mmol) to obtain the title compound (quantitative yield) as colorless oil.

TLC [EtOAc/cyclohexane, 2:8]:  $R_f = 0.27$ .

$^1\text{H NMR}$  (400 MHz,  $\text{CDCl}_3$ )  $\delta$  2.32 – 2.21 (m, 2H), 1.85 – 1.77 (m, 1H), 1.71 – 1.53 (m, 5H), 1.46 – 1.18 (m, 5H), 1.08 – 1.00 (m, 1H), 0.97 (d,  $J = 6.9$  Hz, 3H), 0.95 – 0.92 (m, 1H), 0.88 – 0.78 (m, 1H).

$^{13}\text{C NMR}$  (151 MHz,  $\text{CDCl}_3$ )  $\delta$  180.47, 52.59, 42.65, 37.54, 33.89, 32.68, 31.58, 31.07, 27.38, 26.55, 26.42, 26.20, 14.36.

### 2-(3-((*R*)-3-(3,4-dimethoxyphenyl)-1-(((*S*)-1-((1*R*,4*aS*,8*aR*)-1,2,4*a*,5,6,7,8,8*a*-octahydronaphthalene-1-carbonyl)piperidine-2-carbonyl)oxy)propyl)phenoxy)acetic acid (**11**)



**11**

**9a** (20.0 mg, 0.11 mmol), **27** (57.0 mg, 0.11 mmol), PyBrop (77.0 mg, 0.17 mmol) and DIPEA (58.0  $\mu\text{L}$ , 0.33 mmol) were stirred in DCM (1.5 mL) at RT for 16 h. The tBu-ester was obtained after purification (0-20 % EtOAc in cyclohexane). To obtain the free carboxylic acid the tBu-ester was cleaved in DCM (3.0 mL) and TFA (300  $\mu\text{L}$ ) for 16 h at RT. The title compound was obtained after preparative HPLC (64-75 % B) as colorless solid (43.3 mg, 69.9  $\mu\text{mol}$ , 42.1 %).

TLC [EtOAc/cyclohexane, 1:1 + 1 % HCOOH]:  $R_f = 0.18$ .

HPLC [50-100% Solvent B, 20 min]:  $R_t = 15.8$  min.

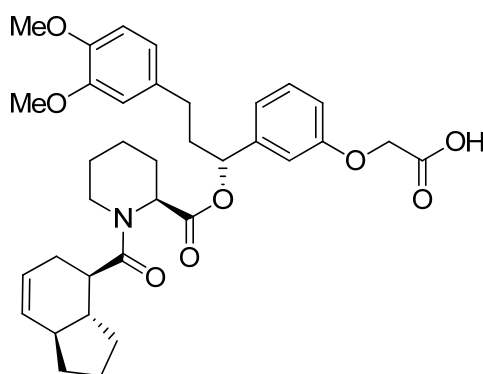
## B. Research Articles – Publication/Manuscript VII

**HRMS:** calculated 620.3223 [C<sub>36</sub>H<sub>45</sub>NO<sub>8</sub>+H]<sup>+</sup>, found 620.3210 [M+H]<sup>+</sup>.

**<sup>1</sup>H NMR** (599 MHz, CDCl<sub>3</sub>) δ 7.22 (t, *J* = 8.1 Hz, 1H), 6.89 – 6.74 (m, 4H), 6.70 – 6.61 (m, 2H), 5.72 – 5.63 (m, 1H), 5.61 – 5.49 (m, 2H), 5.47 – 5.36 (m, 1H), 4.66 – 4.52 (m, 2H), 4.01 – 3.93 (m, 1H), 3.87 – 3.75 (m, 6H), 3.34 (t, *J* = 10.7 Hz, 1H), 2.86 – 2.72 (m, 1H), 2.66 – 2.51 (m, 2H), 2.39 – 2.23 (m, 1H), 2.22 – 2.15 (m, 1H), 2.12 – 2.01 (m, 2H), 1.93 – 1.85 (m, 2H), 1.77 – 1.67 (m, 4H), 1.60 – 1.54 (m, 2H), 1.36 – 1.23 (m, 4H), 1.18 – 1.10 (m, 2H), 1.11 – 1.00 (m, 1H), 0.91 – 0.80 (m, 1H).

**<sup>13</sup>C NMR** (151 MHz, CDCl<sub>3</sub>) δ 175.89, 171.85, 170.28, 158.02, 148.84, 147.30, 142.02, 133.41, 131.99, 129.65, 124.55, 120.16, 119.97, 115.21, 114.78, 112.03, 111.64, 110.87, 76.34, 65.40, 55.89, 52.31, 49.72, 43.60, 42.25, 41.77, 38.06, 33.39, 32.96, 31.38, 30.46, 29.55, 27.13, 26.42, 25.51, 24.74, 21.09.

### 2-(3-((*R*)-3-(3,4-dimethoxyphenyl)-1-(((*S*)-1-((3*aR*,4*R*,7*aS*)-2,3,3*a*,4,5,7*a*-hexahydro-1*H*-indene-4-carbonyl)piperidine-2-carbonyloxy)propyl)phenoxy)acetic acid (12)



### 12

General procedure H was used with **9a** (20.0 mg, 0.12 mmol) and the title compound was obtained after flash chromatography (0-30 % [EtOAc + 1 % HCOOH] in hexane) as colorless solid (53.2 mg, 87.8 μmol, 73.0 %).

**TLC** [EtOAc/cyclohexane, 1:1 + 1 % HCOOH]: R<sub>f</sub> = 0.22.

**HPLC** [50-100% Solvent B, 20 min]: R<sub>t</sub> = 13.9 min.

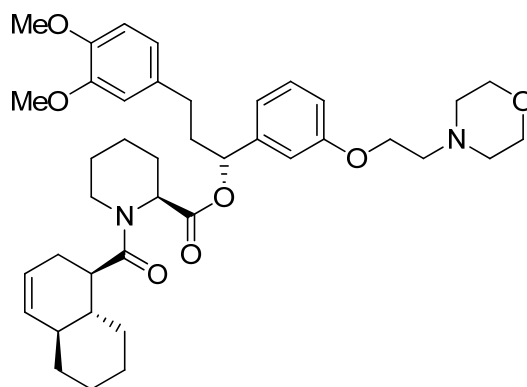
**HRMS:** calculated 606.3067 [C<sub>35</sub>H<sub>43</sub>NO<sub>8</sub>+H]<sup>+</sup>, found 606.3107 [M+H]<sup>+</sup>.

**<sup>1</sup>H NMR** (599 MHz, CDCl<sub>3</sub>) δ 7.24 – 7.19 (m, 1H), 6.89 – 6.83 (m, 2H), 6.81 – 6.75 (m, 2H), 6.70 – 6.62 (m, 2H), 5.83 – 5.77 (m, 1H), 5.65 (dd, *J* = 8.8, 5.0 Hz, 1H), 5.55 – 5.50 (m, 1H), 5.50 – 5.44 (m, 1H), 4.60 (q, *J* = 16.5 Hz, 2H), 3.94 (d, *J* = 13.2 Hz, 1H), 3.88 – 3.79 (m, 6H), 3.28 (td, *J* = 13.1, 2.7 Hz, 1H), 3.06 (q, *J* = 7.6 Hz, 1H), 2.86 – 2.79 (m, 1H), 2.69 – 2.58 (m, 1H), 2.59 – 2.47 (m, 1H), 2.41 – 2.32 (m, 1H), 2.27 – 2.14 (m, 3H), 2.08 – 2.03 (m, 1H), 1.90 – 1.80 (m, 2H), 1.76 – 1.62 (m, 5H), 1.53 – 1.39 (m, 1H), 1.39 – 1.30 (m, 1H), 1.23 – 1.13 (m, 2H), 1.04 (p, *J* = 10.7 Hz, 1H).

## B. Research Articles – Publication/Manuscript VII

$^{13}\text{C}$  NMR (151 MHz,  $\text{CDCl}_3$ )  $\delta$  175.73, 171.69, 170.30, 158.12, 148.88, 147.35, 141.97, 133.42, 129.69, 129.62, 125.68, 120.15, 119.28, 115.40, 111.66, 111.32, 110.48, 76.38, 65.67, 55.91, 55.84, 52.31, 45.66, 45.43, 43.85, 43.44, 41.88, 38.07, 31.43, 29.97, 28.95, 28.22, 27.07, 25.47, 21.75, 21.11, 14.17, 8.39.

**(S)-(R)-3-(3,4-dimethoxyphenyl)-1-(3-(2-morpholinoethoxy)phenyl)propyl 1-((1S,4aS,8aR)-1,2,4a,5,6,7,8,8a-octahydronaphthalene-1-carbonyl) piperidine-2-carboxylate (13)**



13

**9b** (40.0 mg, 0.22 mmol), **28** (125 mg, 0.24 mmol), HATU (127 mg, 0.33 mmol) and DIPEA (86.0 mg, 0.67 mmol) were stirred in DMF (4.0 mL) at RT for 16 h. The reaction mixture was loaded on silica and purified by flash chromatography (0-100 % [EtOAc + 2 % MeOH + 0.1 % TEA] in cyclohexane) to obtain the title compound as light yellow oil (quantitative yield).

**TLC** [EtOAc + 2 % MeOH + 1 % TEA]:  $R_f$  = 0.32.

**HPLC** [30-100% Solvent B, 20 min]:  $R_t$  = 14.5 min.

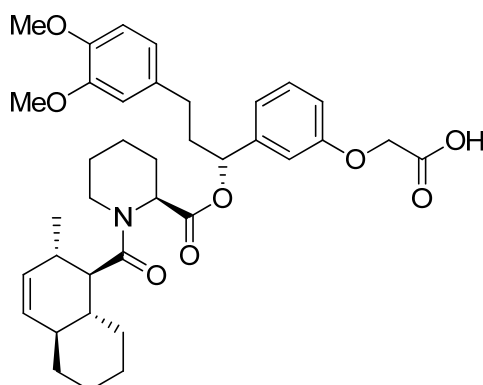
**HRMS**: calculated 675.4009  $[\text{C}_{40}\text{H}_{54}\text{N}_2\text{O}_7+\text{H}]^+$ , found 675.3999  $[\text{M}+\text{H}]^+$ .

$^1\text{H}$  NMR (599 MHz,  $\text{DMSO-d}_6$ )  $\delta$  7.26 – 7.21 (m, 1H), 6.88 – 6.80 (m, 4H), 6.75 – 6.70 (m, 1H), 6.67 – 6.62 (m, 1H), 5.59 (dd,  $J$  = 8.8, 4.7 Hz, 1H), 5.56 – 5.50 (m, 2H), 5.41 – 5.33 (m, 2H), 5.27 – 5.23 (m, 1H), 3.71 – 3.66 (m, 6H), 3.59 – 3.52 (m, 4H), 2.53 – 2.48 (m, 2H), 2.44 – 2.38 (m, 3H), 2.20 – 2.14 (m, 2H), 2.11 – 2.05 (m, 3H), 1.83 – 1.76 (m, 1H), 1.72 – 1.56 (m, 7H), 1.54 – 1.48 (m, 3H), 1.36 – 1.20 (m, 5H), 1.06 – 1.01 (m, 2H), 0.98 – 0.93 (m, 2H), 0.91 – 0.85 (m, 1H).

$^{13}\text{C}$  NMR (151 MHz,  $\text{CDCl}_3$ )  $\delta$  179.56, 177.17, 175.45, 167.31, 163.49, 153.81, 152.20, 147.22, 138.31, 136.98, 134.77, 129.69, 125.10, 123.27, 118.96, 117.35, 116.96, 80.59, 71.20, 70.25, 64.78, 62.12, 60.68, 60.40, 58.75, 56.65, 48.13, 47.26, 45.54, 42.66, 40.94, 37.71, 35.78, 34.45, 31.29, 30.14, 26.21, 19.23.

## B. Research Articles – Publication/Manuscript VII

### 2-(3-((*R*)-3-(3,4-dimethoxyphenyl)-1-(((*S*)-1-((1*R*,2*S*,4*aS*,8*aR*)-2-methyl-1,2,4*a*,5,6,7,8,8*a*-octahydronaphthalene-1-carbonyl)piperidine-2-carbonyloxy)propyl)phenoxy)acetic acid (14)



14

General procedure H was used with **9c** (10.0 mg, 0.05 mmol) and the title compound was obtained after purification by flash chromatography (0-30 % [EtOAc + 0.1 % HCOOH] in hexane) as colorless oil (13.8 mg, 20.0  $\mu$ mol, 42.3 %).

**TLC** [EtOAc/cyclohexane, 1:1 + 1 % HCOOH]:  $R_f$  = 0.29.

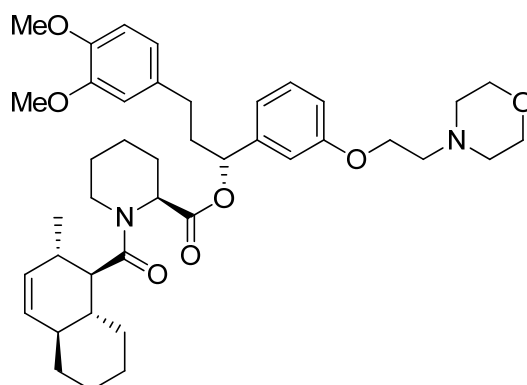
**HPLC** [50-100% Solvent B, 20 min]:  $R_t$  = 15.5 min.

**HRMS**: 634.3380 [ $C_{37}H_{47}NO_8+H$ ] $^+$ , found 634.3383 [ $M+H$ ] $^+$ .

**$^1H$  NMR** (599 MHz,  $CDCl_3$ )  $\delta$  7.24 – 7.19 (m, 1H), 6.89 – 6.84 (m, 2H), 6.81 – 6.76 (m, 2H), 6.72 – 6.62 (m, 2H), 5.68 (dd,  $J$  = 8.8, 4.8 Hz, 1H), 5.51 – 5.46 (m, 2H), 5.35 (dt,  $J$  = 9.9, 1.5 Hz, 1H), 4.65 – 4.59 (m, 1H), 3.91 (d,  $J$  = 14.8 Hz, 1H), 3.89 – 3.83 (m, 6H), 3.34 – 3.26 (m, 1H), 2.79 (dd,  $J$  = 10.9, 6.0 Hz, 1H), 2.72 – 2.64 (m, 1H), 2.63 – 2.53 (m, 2H), 2.45 – 2.33 (m, 2H), 2.27 – 2.18 (m, 2H), 2.10 – 2.05 (m, 1H), 2.00 – 1.93 (m, 1H), 1.79 – 1.66 (m, 6H), 1.53 – 1.47 (m, 1H), 1.46 – 1.33 (m, 3H), 1.31 – 1.28 (m, 1H), 1.09 (qd,  $J$  = 12.1, 3.2 Hz, 1H), 0.80 – 0.69 (m, 4H).

**$^{13}C$  NMR** (151 MHz,  $CDCl_3$ )  $\delta$  173.56, 171.19, 170.49, 163.04, 158.00, 148.90, 147.38, 142.04, 133.42, 130.88, 130.82, 129.59, 120.16, 119.44, 115.71, 111.65, 111.33, 109.68, 76.36, 65.57, 60.42, 55.92, 55.86, 52.05, 45.92, 43.21, 42.34, 38.09, 36.87, 33.11, 31.52, 31.00, 30.37, 27.29, 26.81, 26.46, 25.58, 21.19, 17.51, 14.18.

**(S)-(R)-3-(3,4-dimethoxyphenyl)-1-(3-(2-morpholinoethoxy)phenyl)propyl  
 ((1R,2S,4aS,8aR)-2-methyl-1,2,4a,5,6,7,8,8a-octahydronaphthalene-1-  
 carbonyl)piperidine-2-carboxylate (15)** 1-



15

**9c** (45.0 mg, 0.23 mmol), **28** (119 mg, 0.23 mmol), COMU (149 mg, 0.35 mmol) and DIPEA (81.0  $\mu$ L, 0.46 mmol,  $d = 0.74$  g/mL) were stirred in DMF (3.0 mL) at RT for 16 h. The resulting orange solution was diluted with Et<sub>2</sub>O and washed with brine. Then the organic layer was dried over MgSO<sub>4</sub>, filtered and the solvent was removed under vacuo. After purification by flash chromatography (0-60 % [EtOAc + 2 % MeOH + 0.1 % TEA] in cyclohexane) the title compound was obtained as light yellow oil (118 mg, 0.17 mmol, 74.0 %).

**TLC** [EtOAc + 2 % MeOH + 0.1 % TEA]:  $R_f = 0.28$ .

**HPLC** [0-100% Solvent B, 20 min]:  $R_t = 18.2$  min.

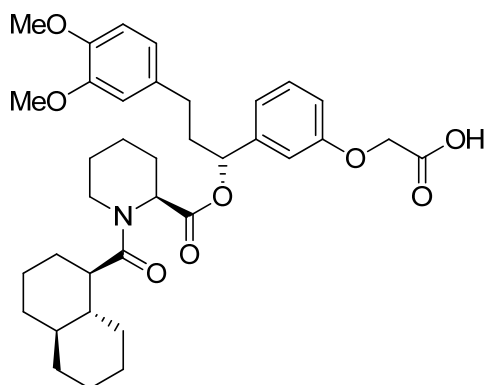
**Mass:** (ESI<sup>+</sup>), calculated 689.42 [C<sub>41</sub>H<sub>56</sub>N<sub>2</sub>O<sub>7</sub>+H]<sup>+</sup>, found 689.21 [M+H]<sup>+</sup>.

**<sup>1</sup>H NMR** (599 MHz, CDCl<sub>3</sub>)  $\delta$  7.24 – 7.19 (m, 1H), 6.92 – 6.87 (m, 1H), 6.84 – 6.74 (m, 3H), 6.67 – 6.61 (m, 2H), 5.75 (dd,  $J = 8.2, 5.5$  Hz, 1H), 5.51 – 5.48 (m, 1H), 5.41 – 5.35 (m, 1H), 4.19 – 4.14 (m, 2H), 3.90 – 3.85 (m, 1H), 3.85 – 3.81 (m, 6H), 3.82 – 3.76 (m, 4H), 3.18 – 3.09 (m, 1H), 3.00 – 2.96 (m, 2H), 2.80 – 2.75 (m, 4H), 2.64 – 2.55 (m, 2H), 2.54 – 2.48 (m, 1H), 2.44 – 2.37 (m, 1H), 2.35 – 2.28 (m, 1H), 2.24 – 2.18 (m, 1H), 2.06 – 1.98 (m, 2H), 1.94 (dd,  $J = 12.4, 3.2$  Hz, 1H), 1.74 – 1.59 (m, 6H), 1.54 – 1.49 (m, 1H), 1.43 – 1.32 (m, 4H), 1.14 – 1.04 (m, 2H), 0.91 – 0.85 (m, 3H), 0.78 – 0.69 (m, 1H).

**<sup>13</sup>C NMR** (151 MHz, CDCl<sub>3</sub>)  $\delta$  172.38, 171.01, 162.60, 158.36, 148.84, 147.30, 141.81, 133.52, 131.01, 130.92, 129.62, 120.11, 119.20, 113.90, 112.75, 111.66, 111.27, 76.03, 66.02, 64.73, 57.34, 55.90, 55.82, 53.76, 53.71, 51.46, 45.61, 43.19, 42.37, 38.06, 37.03, 36.50, 33.18, 31.44, 31.35, 31.01, 30.43, 26.96, 26.83, 26.52, 25.73, 21.20, 17.88.

## B. Research Articles – Publication/Manuscript VII

### 2-(3-((*R*)-1-(((*S*)-1-((1*R*,4*aS*,8*aR*)-decahydronaphthalene-1-carbonyl)piperidine-2-carbonyloxy)-3-(3,4-dimethoxyphenyl)propyl)phenoxy)acetic acid (**16**)



#### 16

**10b** (20.0 mg, 0.11 mmol), **27** (67.6 mg, 0.13 mmol), HATU (62.6 mg, 0.17 mmol) and DIPEA (57.5  $\mu$ L, 0.33 mmol) were stirred in DMF (2.0 mL) at 40 °C for 16 h. The tBu-ester was purified by flash chromatography (0-10 % EtOAc in cyclohexane). To obtain the free carboxylic acid the tBu-ester was cleaved in DCM (3.0 mL) and TFA (300  $\mu$ L) for 16 h at RT. The title compound was obtained after flash chromatography (0-20 % [EtOAc + 2 % MeOH + 0.1 % TFA] in hexane) as colorless solid (30.3 mg, 48.7  $\mu$ mol, 44.3 %).

**TLC** [EtOAc/cyclohexane, 1:1 + 1 % HCOOH]:  $R_f$  = 0.11

**HRMS**: calculated 622.3380 [ $C_{36}H_{47}NO_8+H$ ]<sup>+</sup>, found 622.3360 [ $M+H$ ]<sup>+</sup>.

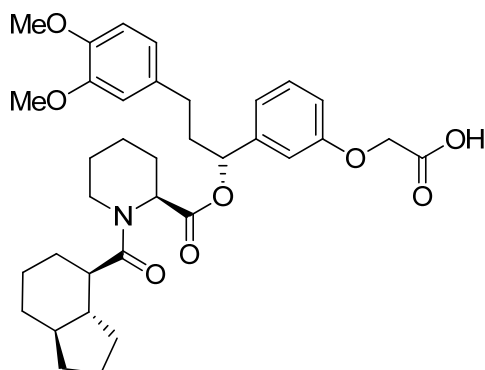
**HPLC** [50-100% Solvent B, 20 min]:  $R_t$  = 15.4 min.

**<sup>1</sup>H NMR** (599 MHz, CDCl<sub>3</sub>)  $\delta$  7.21 (t,  $J$  = 7.8 Hz, 1H), 6.92 – 6.80 (m, 3H), 6.79 – 6.73 (m, 1H), 6.70 – 6.58 (m, 2H), 5.67 – 5.62 (m, 1H), 5.50 – 5.45 (m, 1H), 4.64 – 4.57 (m, 2H), 3.92 (d,  $J$  = 13.8 Hz, 1H), 3.88 – 3.76 (m, 6H), 3.24 – 3.17 (m, 1H), 2.64 – 2.58 (m, 1H), 2.55 – 2.49 (m, 1H), 2.39 – 2.28 (m, 2H), 2.21 – 2.13 (m, 1H), 2.06 – 1.96 (m, 2H), 1.75 – 1.70 (m, 2H), 1.67 – 1.60 (m, 5H), 1.58 – 1.47 (m, 3H), 1.43 – 1.34 (m, 4H), 1.24 – 1.16 (m, 3H), 1.03 – 0.94 (m, 2H), 0.81 – 0.71 (m, 1H).

**<sup>13</sup>C NMR** (151 MHz, CDCl<sub>3</sub>)  $\delta$  170.50, 158.10, 148.84, 147.29, 141.97, 133.46, 129.59, 120.15, 119.37, 114.82, 111.66, 111.39, 111.29, 76.17, 65.45, 55.89, 55.82, 44.33, 43.37, 42.20, 38.10, 34.04, 33.40, 31.42, 31.32, 29.80, 27.08, 26.53, 26.35, 25.56, 25.52, 21.18.

## B. Research Articles – Publication/Manuscript VII

### 2-(3-((*R*)-3-(3,4-dimethoxyphenyl)-1-(((*S*)-1-((3*aR*,4*R*,7*aS*)-octahydro-1*H*-indene-4-carbonyl)piperidine-2-carbonyl)oxy)propyl)phenoxy)acetic acid (17)



17

General procedure H was used with **10a** (15.0 mg, 89.0  $\mu\text{mol}$ ) and the title compound was obtained after flash chromatography (0-20 % [EtOAc + 1 % HCOOH] in hexane) as colorless oil (35.9 mg, 59.1  $\mu\text{mol}$ , 66.2 %).

**TLC** [EtOAc/cyclohexane, 1:1 + 1 % HCOOH]:  $R_f = 0.20$ .

**HPLC** [50-100% Solvent B, 20 min]:  $R_t = 15.0$  min.

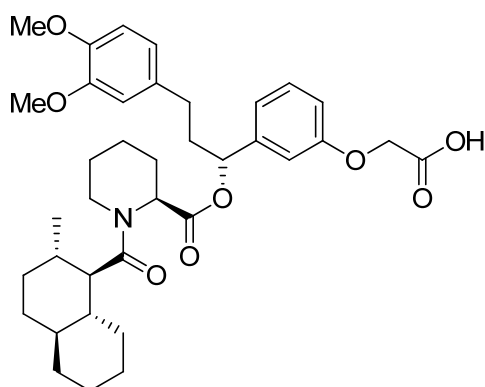
**HRMS**: calculated 608.3223 [ $\text{C}_{35}\text{H}_{45}\text{NO}_8 + \text{H}$ ] $^+$ , found 608.3257 [ $\text{M} + \text{H}$ ] $^+$ .

**$^1\text{H}$  NMR** (599 MHz,  $\text{CDCl}_3$ )  $\delta$  7.24 – 7.19 (m, 1H), 6.88 – 6.81 (m, 2H), 6.79 – 6.75 (m, 2H), 6.71 – 6.66 (m, 2H), 5.63 (dd,  $J = 8.9, 4.8$  Hz, 1H), 5.48 (d,  $J = 5.8$  Hz, 1H), 4.69 – 4.58 (m, 2H), 3.91 (d,  $J = 13.6$  Hz, 1H), 3.89 – 3.80 (m, 6H), 3.30 (t,  $J = 12.7$  Hz, 1H), 2.71 – 2.61 (m, 1H), 2.60 – 2.52 (m, 1H), 2.47 – 2.32 (m, 2H), 2.24 – 2.17 (m, 1H), 2.08 – 2.04 (m, 2H), 1.88 – 1.80 (m, 2H), 1.79 – 1.69 (m, 4H), 1.61 – 1.51 (m, 2H), 1.45 – 1.31 (m, 4H), 1.28 – 1.23 (m, 2H), 1.16 – 1.05 (m, 2H), 1.04 – 0.93 (m, 2H).

**$^{13}\text{C}$  NMR** (151 MHz,  $\text{CDCl}_3$ )  $\delta$  176.06, 171.17, 170.30, 158.05, 148.89, 147.36, 142.11, 133.41, 129.61, 120.17, 119.31, 115.75, 111.66, 111.32, 109.83, 76.34, 65.53, 60.39, 55.91, 55.85, 52.24, 47.64, 45.47, 43.35, 38.06, 31.47, 30.97, 30.77, 29.53, 29.21, 27.17, 25.97, 25.48, 21.31, 21.13, 14.17.

## B. Research Articles – Publication/Manuscript VII

### 2-(3-((*R*)-3-(3,4-dimethoxyphenyl)-1-(((*S*)-1-((1*R*,2*S*,4*aS*,8*aR*)-2-methyldecahydronaphthalene-1-carbonyl)piperidine-2-carbonyloxy)propyl)phenoxy)acetic acid (18)



18

General procedure H was used with **10c** (20.0 mg, 0.10 mmol) and the title compound was obtained after purification by flash chromatography (0-30 % [EtOAc + 0.1 % HCOOH] in hexane) as colorless oil (12.7 mg, 20.0  $\mu$ mol, 19.6 %).

**TLC** [EtOAc/cyclohexane, 1:1 + 1 % HCOOH]:  $R_f$  = 0.28.

**HPLC** [50-100% Solvent B, 20 min]:  $R_t$  = 16.8 min.

**HRMS**: calculated 636.3536 [C<sub>37</sub>H<sub>49</sub>NO<sub>8</sub>+H]<sup>+</sup>, found 636.3545 [M+H]<sup>+</sup>.

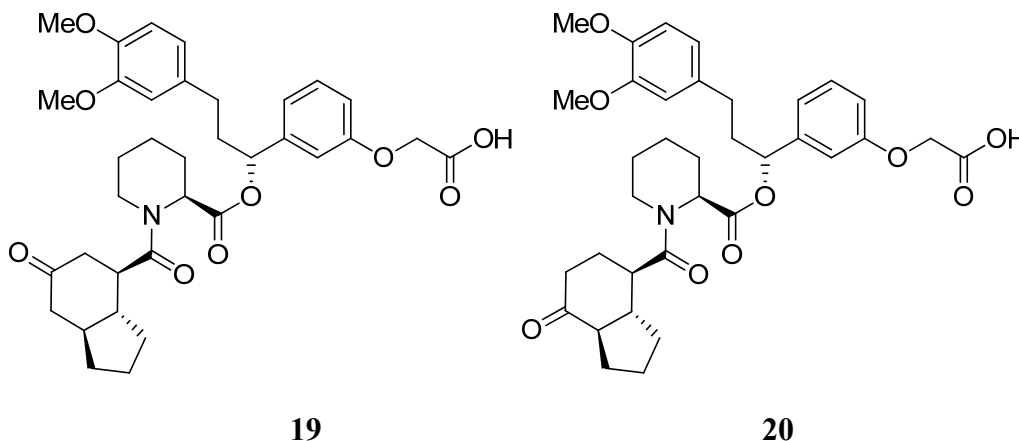
**<sup>1</sup>H NMR** (599 MHz, CDCl<sub>3</sub>)  $\delta$  7.24 – 7.19 (m, 1H), 6.90 – 6.84 (m, 2H), 6.80 – 6.76 (m, 2H), 6.71 – 6.65 (m, 2H), 5.66 (dd,  $J$  = 8.8, 4.8 Hz, 1H), 5.52 – 5.46 (m, 1H), 3.89 – 3.83 (m, 7H), 3.32 – 3.24 (m, 1H), 2.71 – 2.65 (m, 1H), 2.63 – 2.55 (m, 1H), 2.44 (dd,  $J$  = 10.7, 4.2 Hz, 1H), 2.39 – 2.33 (m, 1H), 2.25 – 2.19 (m, 1H), 2.10 – 2.05 (m, 2H), 1.79 (dt,  $J$  = 12.8, 3.3 Hz, 1H), 1.74 – 1.61 (m, 5H), 1.58 – 1.50 (m, 5H), 1.45 – 1.35 (m, 2H), 1.31 – 1.26 (m, 2H), 1.24 – 1.17 (m, 2H), 1.09 – 1.01 (m, 1H), 0.95 – 0.91 (m, 2H), 0.74 (d,  $J$  = 7.1 Hz, 3H), 0.65 (tdd,  $J$  = 12.4, 10.9, 3.4 Hz, 1H).

**<sup>13</sup>C NMR** (151 MHz, CDCl<sub>3</sub>)  $\delta$  173.56, 171.19, 170.49, 163.04, 158.00, 148.90, 147.38, 142.04, 133.42, 130.88, 130.82, 129.59, 120.16, 119.44, 115.71, 111.65, 111.33, 109.68, 76.36, 65.57, 60.42, 55.92, 55.86, 52.05, 45.92, 43.21, 42.34, 38.09, 36.87, 33.11, 31.52, 31.00, 30.37, 27.29, 26.81, 26.46, 25.58, 21.19, 17.51, 14.18.

## B. Research Articles – Publication/Manuscript VII

**2-(3-((R)-3-(3,4-dimethoxyphenyl)-1-(((S)-1-((3aR,4R,7aS)-6-oxooctahydro-1H-indene-4-carbonyl)piperidine-2-carbonyl)oxy)propyl)phenoxy)acetic acid (19)**

**2-(3-((R)-3-(3,4-dimethoxyphenyl)-1-(((S)-1-((3aR,4R,7aR)-7-oxooctahydro-1H-indene-4-carbonyl)piperidine-2-carbonyl)oxy)propyl)phenoxy)acetic acid (20)**



A solution of tetrafluoroboric acid (17  $\mu\text{L}$ , 0.11 mmol, 48 % wt in  $\text{H}_2\text{O}$ ) was added to a solution of palladium(II) acetate (0.89 mg, 3.96  $\mu\text{mol}$ ) and p-benzoquinone (8.57 mg, 79  $\mu\text{mol}$ ) in MeCN (0.45 mL) and  $\text{H}_2\text{O}$  (0.60 mL). This mixture was added to **12** (48.0 mg, 79  $\mu\text{mol}$ ) and it was stirred at RT for 16 h. The reaction mixture was directly loaded on silica and purified by flash chromatography, whereby both products can easily be separated, to obtain title compounds **19** (13.0 mg, 20.9  $\mu\text{mol}$ , 26.4 %) and **20** (31.8 mg, 51.1  $\mu\text{mol}$ , 64.5 %) as colorless oils.

**TLC** [EtOAc + 1 % HCOOH]:  $R_f = 0.39$  (**19**),  $R_f = 0.31$  (**20**)

**HPLC** [30-100% Solvent B, 20 min]:  $R_t = 15.5$  min (**19**),  $R_t = 15.0$  min (**20**).

**HRMS**: calculated 622.3016 [ $\text{C}_{35}\text{H}_{44}\text{NO}_9 + \text{H}$ ] $^+$ , found 622.3036 [ $\text{M}(\mathbf{19}) + \text{H}$ ] $^+$ , 622.3050 [ $\text{M}(\mathbf{20}) + \text{H}$ ] $^+$ .

**(19):  $^1\text{H}$  NMR** (599 MHz,  $\text{CDCl}_3$ )  $\delta$  7.24 – 7.15 (m, 1H), 6.97 – 6.80 (m, 2H), 6.85 – 6.70 (m, 2H), 6.73 – 6.60 (m, 2H), 5.81 – 5.68 (m, 1H), 5.45 (d,  $J = 5.3$  Hz, 1H), 4.69 – 4.63 (m, 1H), 4.59 – 4.54 (m, 1H), 3.89 – 3.77 (m, 6H), 3.08 (q,  $J = 7.3$  Hz, 1H), 2.98 – 2.87 (m, 2H), 2.63 – 2.56 (m, 2H), 2.57 – 2.50 (m, 1H), 2.51 – 2.45 (m, 1H), 2.38 – 2.28 (m, 1H), 2.27 – 2.12 (m, 2H), 2.08 – 1.97 (m, 2H), 1.97 – 1.90 (m, 1H), 1.90 – 1.82 (m, 1H), 1.82 – 1.67 (m, 2H), 1.67 – 1.56 (m, 2H), 1.38 – 1.28 (m, 2H), 1.27 – 1.22 (m, 3H), 1.12 – 1.02 (m, 1H), 0.90 – 0.78 (m, 1H).

**(19):  $^{13}\text{C}$  NMR** (151 MHz,  $\text{CDCl}_3$ )  $\delta$  212.73, 172.69, 171.32, 170.04, 158.45, 148.87, 147.36, 141.33, 133.32, 129.66, 120.62, 120.17, 116.66, 111.70, 111.31, 109.99, 76.15, 65.78, 55.90, 55.84, 52.37, 47.01, 46.87, 45.53, 45.36, 43.70, 43.07, 42.80, 37.35, 31.29, 31.04, 29.67, 28.32, 26.70, 25.45, 22.63, 20.93, 8.43.

**(20):  $^1\text{H}$  NMR** (599 MHz,  $\text{CDCl}_3$ )  $\delta$  8.07 (s, 1H), 7.26 – 7.18 (m, 1H), 6.88 – 6.81 (m, 2H), 6.81 – 6.73 (m, 2H), 6.70 – 6.58 (m, 2H), 5.70 – 5.62 (m, 1H), 5.46 (d,  $J = 6.0$  Hz, 1H), 4.69

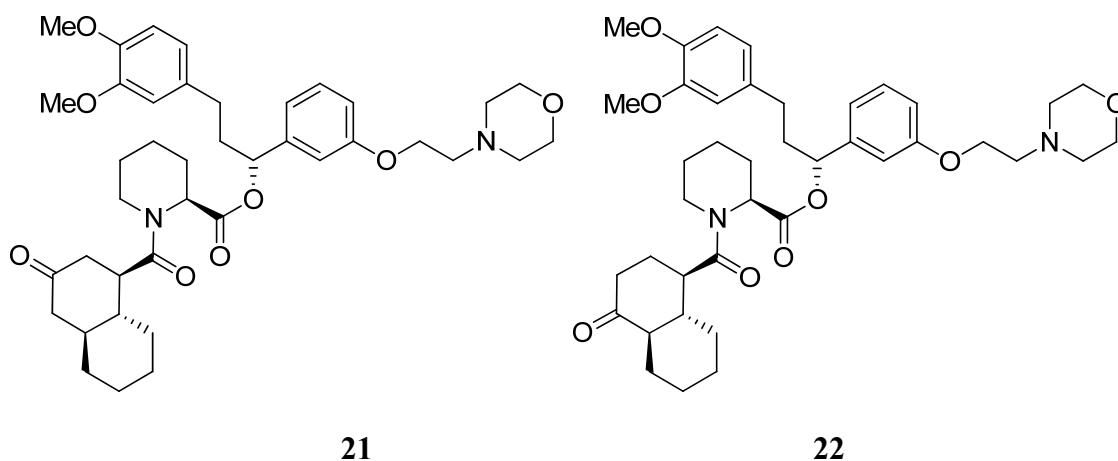
## B. Research Articles – Publication/Manuscript VII

– 4.52 (m, 2H), 4.10 (qd,  $J = 7.2, 1.7$  Hz, 1H), 3.96 (d,  $J = 12.6$  Hz, 1H), 3.89 – 3.74 (m, 6H), 3.36 – 3.25 (m, 1H), 2.93 – 2.83 (m, 1H), 2.62 – 2.49 (m, 2H), 2.42 – 2.33 (m, 2H), 2.28 (dd,  $J = 13.4, 4.6$  Hz, 1H), 2.22 – 2.10 (m, 2H), 2.02 – 1.92 (m, 2H), 1.86 (ddd,  $J = 11.5, 7.8, 5.7$  Hz, 1H), 1.82 – 1.72 (m, 3H), 1.67 – 1.59 (m, 2H), 1.56 – 1.35 (m, 3H), 1.21 – 1.09 (m, 2H), 0.93 – 0.82 (m, 1H).

**(20):**  $^{13}\text{C}$  NMR (151 MHz,  $\text{CDCl}_3$ )  $\delta$  209.86, 174.10, 171.69, 170.14, 163.87, 158.03, 148.89, 147.37, 141.82, 133.32, 129.68, 120.15, 119.48, 115.19, 111.66, 111.34, 110.83, 65.46, 60.42, 55.91, 55.85, 52.38, 49.90, 45.60, 44.21, 43.59, 40.38, 37.95, 31.37, 30.87, 30.28, 29.67, 26.95, 25.48, 22.31, 21.11, 21.03, 14.16, 8.41.

**(S)-(R)-3-(3,4-dimethoxyphenyl)-1-(3-(2-morpholinoethoxy)phenyl)propyl** 1-  
**((1R,4aS,8aR)-3-oxodecahydronaphthalene-1-carbonyl)piperidine-2-carboxylate (21)**

**(S)-(R)-3-(3,4-dimethoxyphenyl)-1-(3-(2-morpholinoethoxy)phenyl)propyl** 1-  
**((1R,4aR,8aR)-4-oxodecahydronaphthalene-1-carbonyl)piperidine-2-carboxylate (22)**



A solution of tetrafluoroboric acid (16  $\mu\text{L}$ , 0.10 mmol, 48 % wt in  $\text{H}_2\text{O}$ ) and **13** were added to a solution of palladium(II) acetate (0.83 mg, 3.70  $\mu\text{mol}$ ) and p-benzoquinone (8.01 mg, 74  $\mu\text{mol}$ ) in MeCN (0.45 mL) and  $\text{H}_2\text{O}$  (0.60 mL). The reaction mixture was stirred at RT for 16 h and then directly loaded on silica for purification by flash chromatography (0-50 % [EtOAc + 2 % MeOH + 0.1 % TEA] in hexane), whereby both products can easily be separated, to obtain title compounds **21** (11.4 mg, 20.9  $\mu\text{mol}$ , 14.8 %) and **22** (19.0 mg, 51.1  $\mu\text{mol}$ , 24.7 %) as colorless oils.

**TLC** [EtOAc + 2 % MeOH + 2 % TEA]:  $R_f = 0.25$ .

**HPLC** [0-100% Solvent B, 20 min]:  $R_t = 15.9$  min (**21**),  $R_t = 15.7$  min (**22**).

**HRMS**: calculated 691.3958 [ $\text{C}_{40}\text{H}_{54}\text{N}_2\text{O}_8 + \text{H}$ ] $^+$ , found 691.4118 [ $\text{M}(\mathbf{20}) + \text{H}$ ] $^+$ , 691.3991 [ $\text{M}(\mathbf{21}) + \text{H}$ ] $^+$ .

**(21):**  $^1\text{H}$  NMR (599 MHz,  $\text{CDCl}_3$ )  $\delta$  7.25 – 7.22 (m, 1H), 6.90 – 6.80 (m, 3H), 6.79 – 6.75 (m, 1H), 6.69 – 6.60 (m, 2H), 5.76 – 5.67 (m, 1H), 5.46 (d,  $J = 4.8$  Hz, 0H), 4.12 – 4.04 (m,

## B. Research Articles – Publication/Manuscript VII

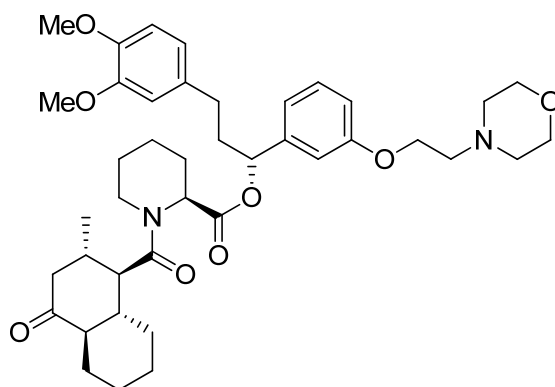
2H), 3.86 (s<sub>br</sub>, 1H), 3.86 – 3.83 (m, 6H), 3.73 (t,  $J = 4.6$  Hz, 3H), 3.11 (td,  $J = 13.2, 12.3, 2.2$  Hz, 1H), 2.86 – 2.76 (m, 3H), 2.64 – 2.53 (m, 5H), 2.52 – 2.44 (m, 1H), 2.42 – 2.27 (m, 3H), 2.27 – 2.13 (m, 3H), 2.07 – 2.00 (m, 1H), 1.86 – 1.77 (m, 2H), 1.76 – 1.57 (m, 7H), 1.51 – 1.35 (m, 2H), 1.36 – 1.27 (m, 2H), 1.27 – 1.22 (m, 1H), 1.22 – 1.07 (m, 2H), 0.91 – 0.79 (m, 1H).

**(21):**  $^{13}\text{C}$  NMR (151 MHz,  $\text{CDCl}_3$ )  $\delta$  209.51, 172.74, 170.25, 158.80, 148.82, 147.29, 141.40, 133.37, 129.66, 120.13, 118.91, 113.97, 113.13, 111.67, 111.26, 76.21, 66.90, 65.75, 57.62, 55.89, 55.82, 54.08, 52.26, 48.38, 45.47, 44.14, 43.58, 43.48, 42.17, 37.83, 34.29, 31.17, 30.52, 26.77, 25.84, 25.73, 25.49, 21.01.

**(22):**  $^1\text{H}$  NMR (599 MHz,  $\text{CDCl}_3$ )  $\delta$  7.24 – 7.21 (m, 1H), 6.95 – 6.74 (m, 4H), 6.68 – 6.62 (m, 2H), 5.74 – 5.68 (m, 1H), 5.48 (d,  $J = 4.9$  Hz, 1H), 4.15 – 4.04 (m, 2H), 3.97 (d,  $J = 13.5$  Hz, 1H), 3.89 – 3.79 (m, 6H), 3.79 – 3.67 (m, 4H), 3.21 (td,  $J = 13.1, 2.8$  Hz, 1H), 2.85 (dt,  $J = 11.9, 5.3$  Hz, 1H), 2.82 – 2.75 (m, 2H), 2.65 – 2.52 (m, 5H), 2.52 – 2.45 (m, 1H), 2.42 – 2.33 (m, 3H), 2.24 – 2.16 (m, 1H), 2.13 – 1.59 (m, 11H), 1.51 – 1.42 (m, 1H), 1.41 – 1.32 (m, 1H), 1.32 – 1.09 (m, 4H), 0.99 (qd,  $J = 12.3, 3.6$  Hz, 1H).

**(22):**  $^{13}\text{C}$  NMR (151 MHz,  $\text{CDCl}_3$ )  $\delta$  210.44, 173.52, 170.47, 158.80, 148.84, 147.32, 141.40, 133.40, 129.60, 120.10, 118.92, 113.84, 113.20, 111.66, 111.27, 76.24, 66.87, 57.64, 55.90, 55.82, 54.08, 53.16, 52.06, 45.67, 44.50, 43.51, 40.36, 37.93, 32.29, 31.22, 29.40, 26.82, 25.61, 25.42, 25.30, 25.14, 21.11.

**(S)-(R)-3-(3,4-dimethoxyphenyl)-1-(3-(2-morpholinoethoxy)phenyl)propyl** **1-**  
**((1R,2S,4aR,8aR)-2-methyl-4-oxodecahydronaphthalene-1-carbonyl)piperidine-2-**  
**carboxylate (23)**



**23**

Tetrafluoroboric acid (31.5  $\mu\text{L}$ , 0.20 mmol, 48 % wt in  $\text{H}_2\text{O}$ ) was added to a solution of palladium(II) acetate (1.63 mg, 7.26  $\mu\text{mol}$ ) and p-benzoquinone (15.7 mg, 0.15  $\mu\text{mol}$ ) in MeCN (0.9 mL) and  $\text{H}_2\text{O}$  (0.12 mL). This mixture was added to **15** (100 mg, 0.15 mmol) and it was stirred at RT for 16 h. The reaction mixture was directly loaded on silica and purified by flash chromatography to obtain title compounds as colorless solid (40.1 mg, 56.9  $\mu\text{mol}$ , 49.1 %) after lyophilization.

**TLC** [DCM + 5 % MeOH]:  $R_f = 0.48$ .

## B. Research Articles – Publication/Manuscript VII

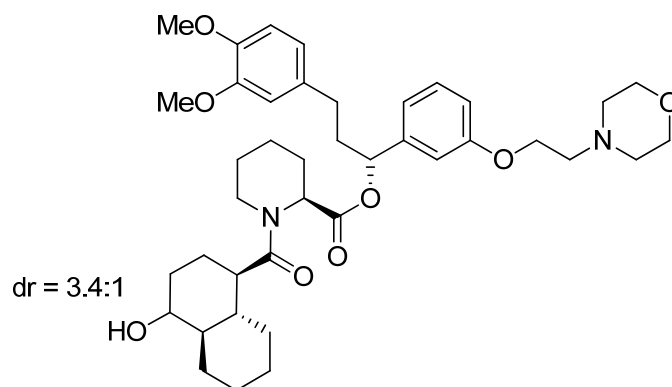
**HPLC** [0-100% Solvent B, 20 min]: Rt = 16.1 min.

**HRMS**: calculated 727.3934 [C<sub>41</sub>H<sub>56</sub>N<sub>2</sub>O<sub>8</sub>+H]<sup>+</sup>, found 727.3950 [M+H]<sup>+</sup>.

**<sup>1</sup>H NMR** (800 MHz, CDCl<sub>3</sub>) δ 7.26 (t, *J* = 7.9 Hz, 1H), 6.91 – 6.82 (m, 3H), 6.82 – 6.77 (m, 1H), 6.68 – 6.64 (m, 2H), 5.77 (dd, *J* = 7.9, 5.8 Hz, 1H), 5.56 – 5.52 (m, 1H), 4.17 – 4.10 (m, 2H), 3.94 – 3.90 (m, 1H), 3.87 (s, 6H), 3.79 – 3.75 (m, 4H), 3.20 (td, *J* = 13.2, 2.9 Hz, 1H), 2.98 (dd, *J* = 10.6, 4.1 Hz, 1H), 2.64 – 2.59 (m, 5H), 2.54 – 2.50 (m, 2H), 2.38 – 2.35 (m, 1H), 2.29 – 2.27 (m, 1H), 2.25 – 2.20 (m, 1H), 2.14 – 2.06 (m, 2H), 2.00 – 1.91 (m, 2H), 1.84 – 1.81 (m, 2H), 1.80 – 1.76 (m, 1H), 1.73 – 1.66 (m, 4H), 1.50 – 1.45 (m, 1H), 1.42 – 1.39 (m, 1H), 1.30 – 1.26 (m, 2H), 1.22 – 1.18 (m, 1H), 0.98 – 0.94 (m, 1H), 0.88 (d, *J* = 7.1 Hz, 3H).

**<sup>13</sup>C NMR** (201 MHz, CDCl<sub>3</sub>) δ 210.66, 171.69, 170.76, 148.87, 147.35, 141.48, 133.45, 129.64, 120.11, 113.93, 111.66, 111.28, 76.26, 55.93, 55.84, 54.05, 53.76, 51.73, 48.06, 48.03, 43.46, 40.76, 37.90, 32.63, 32.25, 31.33, 26.83, 25.78, 25.59, 25.52, 25.07, 21.17, 15.40.

**(2*S*)-(R)-3-(3,4-dimethoxyphenyl)-1-(3-(2-morpholinoethoxy)phenyl)propyl** **1-**  
**((1*R*,4*aR*,8*aR*)-4-hydroxydecahydronaphthalene-1-carbonyl)piperidine-2-carboxylate**  
**(24)**



**24**

Cerium(III) chloride heptahydrate (92 mg, 0.25 mmol) was added to a solution of **22** (17 mg, 25 μmol) in THF/MeOH (2:1, 0.9 mL). It was stirred at RT for 15 min, then NaBH<sub>4</sub> (4.7 mg, 0.12 mmol) was added and it was stirred at RT for 30 min. The reaction mixture was quenched with H<sub>2</sub>O and alkalized with 1 N NaOH. The product was extracted with Et<sub>2</sub>O. Then the combined layers were dried over MgSO<sub>4</sub>, filtered and the solvent was removed under reduced pressure. Purification by flash chromatography (0-100 % [EtOAc + 2 % MeOH + 0.1 % TEA] in cyclohexane) and following lyophilization provided the title compound as colorless solid (11.4 mg, 16.5 μmol, 66.9 %).

**TLC** [EtOAc + 2 % MeOH + 2 % TEA]: R<sub>f</sub> = 0.20.

**HPLC** [0-100% Solvent B, 20 min]: Rt = 15.2-16.4 min.

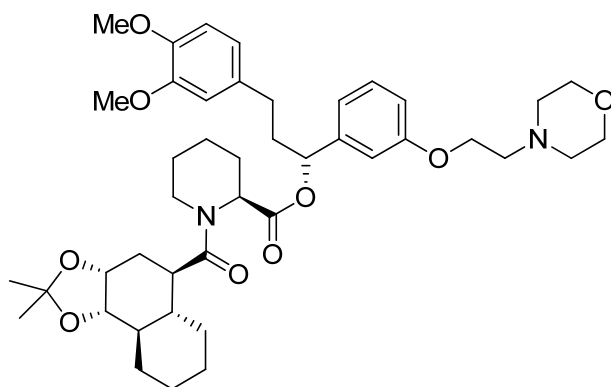
**HRMS**: calculated 693.4115 [C<sub>40</sub>H<sub>56</sub>N<sub>2</sub>O<sub>8</sub>+H]<sup>+</sup>, found 693.4138 [M+H]<sup>+</sup>.

## B. Research Articles – Publication/Manuscript VII

**<sup>1</sup>H NMR** (599 MHz, CDCl<sub>3</sub>) δ 7.24 – 7.20 (m, 1H), 6.89 – 6.85 (m, 1H), 6.85 – 6.80 (m, 2H), 6.79 – 6.73 (m, 1H), 6.68 – 6.61 (m, 2H), 5.72 (ddd, *J* = 20.7, 8.0, 5.9 Hz, 1H), 5.51 – 5.46 (m, 1H), 4.13 – 4.06 (m, 2H), 3.90 (d, *J* = 12.4 Hz, 1H), 3.85 – 3.83 (m, 6H), 3.74 – 3.71 (m, 4H), 3.28 (ddd, *J* = 10.9, 9.4, 4.4 Hz, 1H), 3.14 (td, *J* = 13.2, 2.9 Hz, 1H), 2.82 – 2.75 (m, 2H), 2.61 – 2.55 (m, 5H), 2.52 – 2.45 (m, 1H), 2.39 – 2.28 (m, 2H), 2.22 – 2.10 (m, 2H), 2.04 – 1.97 (m, 2H), 1.81 – 1.74 (m, 2H), 1.71 – 1.63 (m, 6H), 1.57 – 1.51 (m, 2H), 1.44 – 1.40 (m, 1H), 1.35 – 1.31 (m, 1H), 1.23 – 1.13 (m, 2H), 1.04 – 0.91 (m, 2H), 0.87 – 0.78 (m, 1H).

**<sup>13</sup>C NMR** (151 MHz, CDCl<sub>3</sub>) δ 174.79, 170.67, 158.78, 148.83, 147.29, 141.57, 133.51, 129.57, 120.12, 118.93, 113.86, 113.11, 111.72, 111.27, 76.04, 73.77, 66.88, 66.79, 65.70, 57.65, 55.90, 55.83, 54.07, 51.92, 49.06, 44.96, 43.38, 42.33, 37.98, 34.57, 31.25, 31.20, 28.86, 27.37, 26.83, 25.90, 25.60, 21.16.

**(2*S*)-(R)-3-(3,4-dimethoxyphenyl)-1-(3-(2-morpholinoethoxy)phenyl)propyl 1-((5*R*,5*aR*,9*aR*)-2,2-dimethyldecahydronaphtho[1,2-*d*][1,3]dioxole-5-carbonyl)piperidine-2-carboxylate (25)**



**25**

**9d** (20.0 mg, 0.08 mmol), **28** (44.3 mg, 0.09 mmol), HATU (44.9 mg, 0.12 mmol) and DIPEA (30.5 mg, 0.236 mmol) were stirred in DMF (2.0 mL) at RT for 18 h. The orange reaction mixture was loaded on silica and purified by flash chromatography (0-100 % [EtOAc + 2 % MeOH + 0.1 % TEA] in cyclohexane) to obtain the title compound as light yellow oil (45.5 mg, 0.06 mmol, 77.2 %).

**TLC** [EtOAc + 2 % MeOH + 1 % TEA]: *R<sub>f</sub>* = 0.19.

**HPLC** [0-100% Solvent B, 20 min]: *R<sub>t</sub>* = 16.7 min.

**HRMS**: calculated 749.4377 [C<sub>43</sub>H<sub>60</sub>N<sub>2</sub>O<sub>9</sub>+H]<sup>+</sup>, found 749.4380 [M+H]<sup>+</sup>.

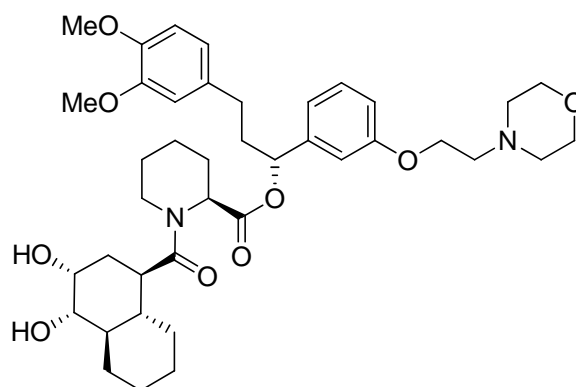
**<sup>1</sup>H NMR** (599 MHz, DMSO-*d*<sub>6</sub>) δ 7.28 – 7.20 (m, 1H), 6.88 – 6.79 (m, 4H), 6.75 – 6.71 (m, 1H), 6.67 – 6.60 (m, 1H), 5.58 (dd, *J* = 8.8, 4.7 Hz, 1H), 5.21 (d, *J* = 6.0 Hz, 0H), 4.20 (d, *J* = 6.7 Hz, 1H), 4.14 – 4.02 (m, 3H), 3.93 (d, *J* = 13.4 Hz, 1H), 3.72 – 3.64 (m, 6H), 3.60 – 3.52 (m, 4H), 3.09 – 2.99 (m, 1H), 2.98 – 2.91 (m, 1H), 2.87 – 2.75 (m, 0H), 2.71 – 2.66 (m, 2H), 2.43 (ddd, *J* = 13.7, 8.3, 4.6 Hz, 1H), 2.19 – 2.12 (m, 2H), 2.09 – 2.01 (m, 2H), 1.98 – 1.95

## B. Research Articles – Publication/Manuscript VII

(m, 2H), 1.77 – 1.48 (m, 8H), 1.44 – 1.31 (m, 5H), 1.29 – 1.04 (m, 8H), 1.02 – 0.66 (m, 4H), 0.30 – 0.20 (m, 1H).

<sup>13</sup>C NMR (151 MHz, DMSO-*d*<sub>6</sub>) δ 174.96, 170.87, 158.85, 149.02, 147.46, 142.43, 133.64, 130.04, 120.38, 120.33, 118.68, 114.34, 112.59, 112.32, 75.86, 74.86, 68.72, 66.47, 65.58, 57.36, 55.93, 55.78, 53.98, 51.88 38.45, 38.06, 34.59, 31.05, 30.85, 29.45, 29.37, 26.90, 26.77, 26.26, 26.13, 25.39, 22.53, 21.18.

**(*S*)-(*R*)-3-(3,4-dimethoxyphenyl)-1-(3-(2-morpholinoethoxy)phenyl)propyl  
((1*R*,3*R*,4*S*,4*aR*,8*aR*)-3,4-dihydroxydecahydronaphthalene-1-carbonyl)piperidine-2-  
carboxylate (**26**)** 1-



**26**

**25** (40 mg, 53 μmol) was stirred in MeOH (1.86 mL) and concentrated HCl (0.14 mL) for 1.5 h at RT. The title compound (11.5 mg, 16.2 μmol, 30.3 %) was obtained after purification by preparative HPLC (40-50 % solvent B).

**TLC** [EtOAc + 5 % MeOH + 1 % TEA]: R<sub>f</sub> = 0.15.

**HPLC** [0-100% Solvent B, 20 min]: R<sub>t</sub> = 14.2 min.

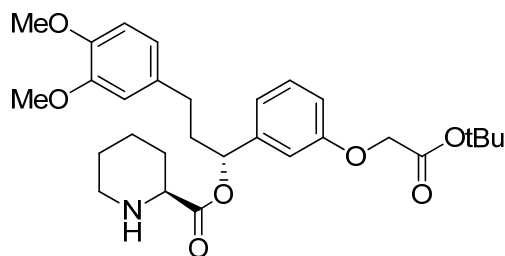
**HRMS**: calculated 709.4064 [C<sub>40</sub>H<sub>56</sub>N<sub>2</sub>O<sub>9</sub>+H]<sup>+</sup>, found 709.4089 [M+H]<sup>+</sup>.

<sup>1</sup>H NMR (599 MHz, DMSO-*d*<sub>6</sub>) δ 7.26 – 7.22 (m, 1H), 6.88 – 6.83 (m, 3H), 6.82 – 6.79 (m, 1H), 6.74 – 6.71 (m, 1H), 6.66 – 6.62 (m, 1H), 5.58 (dd, *J* = 8.8, 4.7 Hz, 1H), 5.23 (d, *J* = 6.1 Hz, 1H), 4.11 – 4.00 (m, 3H), 3.95 (d, *J* = 13.2 Hz, 1H), 3.69 (d, *J* = 11.7 Hz, 6H), 3.57 – 3.52 (m, 4H), 3.49 (td, *J* = 8.8, 4.8 Hz, 1H), 3.06 (td, *J* = 13.1, 2.9 Hz, 1H), 2.76 – 2.69 (m, 1H), 2.65 (q, *J* = 7.6, 6.5 Hz, 2H), 2.43 (tt, *J* = 9.2, 4.3 Hz, 4H), 2.18 – 2.12 (m, 1H), 2.11 – 2.05 (m, 1H), 2.02 – 1.93 (m, 2H), 1.92 – 1.86 (m, 1H), 1.76 – 1.69 (m, 1H), 1.68 – 1.60 (m, 3H), 1.59 – 1.46 (m, 3H), 1.36 – 1.28 (m, 2H), 1.24 – 1.16 (m, 3H), 1.14 – 1.03 (m, 3H), 0.88 – 0.76 (m, 2H).

<sup>13</sup>C NMR (151 MHz, DMSO-*d*<sub>6</sub>) δ 174.49, 170.79, 158.87, 149.04, 147.49, 142.36, 133.60, 130.00, 120.38, 118.76, 114.33, 112.57, 112.31, 107.78, 79.10, 75.90, 72.55, 66.60, 57.42, 55.92, 55.78, 54.05, 52.01, 43.48, 43.35, 37.91, 31.03, 30.34, 30.19, 29.60, 29.05, 26.87, 25.96, 25.85, 25.38, 21.06.

## B. Research Articles – Publication/Manuscript VII

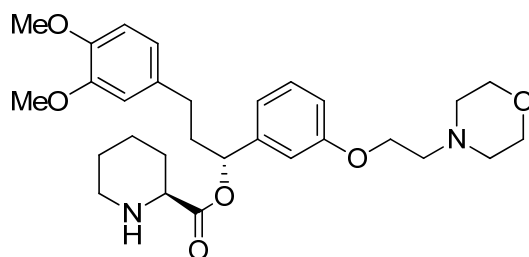
**(S)-(R)-3-(3,4-dimethoxyphenyl)-1-(3-(2-oxopropoxy)phenyl)propyl piperidine-2-carboxylate (27)**



27

Synthesized as previously described.<sup>17</sup>

**(S)-(R)-3-(3,4-dimethoxyphenyl)-1-(3-(2-morpholinoethoxy)phenyl)propyl piperidine-2-carboxylate (28)**



28

Synthesized as previously described.<sup>17</sup>

## B. Research Articles – Publication/Manuscript VII

### III. References

1. Kabsch, W. (2010). XDS. *Acta Crystallogr. D Biol. Crystallogr.* *66*, 125-132.
2. French, G.S., and Wilson, K.S. (1978). On the treatment of negative intensity observations. *Acta Crystallogr. A* *34*, 517-525.
3. Collaborative Computational Project, N. (1994). The CCP4 suite: programs for protein crystallography. *Acta Crystallogr. D Biol. Crystallogr.* *50*, 760-763.
4. Potterton, E., Briggs, P., Turkenburg, M., and Dodson, E. (2003). A graphical user interface to the CCP4 program suite. *Acta crystallographica* *59*, 1131-1137.
5. Vagin, A.A., and Isupov, M.N. (2001). Spherically averaged phased translation function and its application to the search for molecules and fragments in electron-density maps. *Acta Crystallogr. D Biol. Crystallogr.* *57*, 1451-1456.
6. Emsley, P., and Cowtan, K. (2004). Coot: model-building tools for molecular graphics. *Acta Crystallogr. D Biol. Crystallogr.* *60*, 2126-2132.
7. Evans, P.R. (1997). Scala. *Joint CCP4 and ESF-EACBM Newsletter* *33*, 22-24.
8. DeLano, W.L. (2002). The PyMOL Molecular Graphics System.
9. Schüttelkopf, A.W., and van Aalten, D.M. (2004). PRODRG: a tool for high-throughput crystallography of protein-ligand complexes. *Acta Crystallogr. D Biol. Crystallogr.* *60*, 1355-1363.
10. Biannic, B., & Aponick, A. (2011). Gold-Catalyzed Dehydrative Transformations of Unsaturated Alcohols. *European Journal of Organic Chemistry*, 2011(33), 6605-6617.
11. Craig, D., & Geach, N. J. (1991). Asymmetric intramolecular Diels-Alder reaction of a sulphoximine-substituted triene. *Tetrahedron: Asymmetry*, *2*(12), 1177-1180.
12. Larsen, S. D., & Grieco, P. A. (1985). Aza Diels-Alder reactions in aqueous solution: cyclocondensation of dienes with simple iminium salts generated under Mannich conditions. *Journal of the American Chemical Society*, *107*(6), 1768-1769.
13. Roush, W. R., Gillis, H. R., & Ko, A. I. (1982). Stereochemical aspects of the intramolecular Diels-Alder reactions of deca-2, 7, 9-trienoate esters. 3. Thermal, Lewis acid catalyzed, and asymmetric cyclizations. *Journal of the American Chemical Society*, *104*(8), 2269-2283.
14. Lygo, B., Bhatia, M., Cooke, J. W., & Hirst, D. J. (2003). Synthesis of (±)-solanapyrones A and B. *Tetrahedron letters*, *44*(12), 2529-2532.
15. Evans, D. A., Chapman, K. T., Bisaha, J., Asymmetric Diels-Alder cycloaddition reactions with chiral alpha-, beta-unsaturated N-acyloxazolidinones. *JACS*, 1988, *110*(4), 1238-1256.
16. Clive, D. L., & Fletcher, S. P. (2002). Synthesis of the bicyclic dienone core of the antitumor agent ottelione B. *Chemical Communications*, (17), 1940-1941.
17. Gopalakrishnan R, Kozany C, Gaali S, Kress C, Hoogeland B, Bracher A, Hausch F: Evaluation of Synthetic FK506 Analogues as Ligands for the FK506-Binding Proteins 51 and 52. *J. Med. Chem.* 2012, *55*:4114-4122.

## B. Research Articles – Publication/Manuscript VIII

### 7.3. Manuscript VIII

**Rapid, structure-based exploration of pipercolic acid amides as novel selective antagonists of the FK506-binding protein 51** – submitted manuscript

(Steffen Gaali, **Xixi Feng**, Claudia Sippel, Andreas Bracher, Felix Hausch, *J. Med. Chem.*)

#### Summary

With a molecular weight of ~350-400 g/mol the “Top Group” (TG) of SAFit1 and 2 represents a large proportion of the total molecular weight. Additionally, the biological labile ester linkage is not ideal. In order to improve drug-likeness of FKBP51 ligands these two problems were addressed in the presented study.

The pipercolic esters of the SAFit compounds were systematically replaced by various smaller pipercolic acid amides. An efficient, solid phase-assisted method was developed to screen a series of amino acids as TGs. It was shown that none of the 37 ligands showed binding towards FKBP52, suggesting that the TG does not affect the selective binding mode. The best ligand of the series, containing a geminally substituted cyclopentyl ring as key feature, did not only exhibit a high binding affinity of  $K_i = 100$  nM, but even a significantly reduced molecular weight (34% lower than SAFit2). A cocrystal structure was solved to understand the binding mode. The study represents the first systematic TG screening of FKBP ligands. Together with the findings of the “Bottom Group” series this series provides important complementing information for the further development of FKBP51-selective ligands.

Steffen Gaali and I contributed equally to the synthesis of the ligands as well as the preparation of the manuscript.

## B. Research Articles – Publication/Manuscript VIII

### ORIGINAL MANUSCRIPT

Reproduced with permission from Journal of Medicinal Chemistry, submitted for publication.  
Unpublished work copyright 2015 American Chemical Society.

#### **Rapid, structure-based exploration of pipercolic acid amides as novel selective antagonists of the FK506-binding protein 51**

Steffen Gaali\*, Xixi Feng\*, Claudia Sippel\*, Andreas Bracher<sup>#</sup>, Felix Hausch\*

\* Max Planck Institute of Psychiatry, Dept. Translational Research in Psychiatry, Kraepelinstrasse 2, 80804 Munich, Germany

<sup>#</sup> Max Planck Institute of Biochemistry, Am Klopferspitz 18, 82152 Martinsried, Germany

#### **Abstract**

The FK506-binding protein 51 (FKBP51) is a key regulator of stress hormone receptors and an established risk factor for stress-related disorders. Drug development for FKBP51 has been impaired by the structurally similar but functionally opposing homologue FKBP52. High selectivity between FKBP51 and FKBP52 can be achieved by ligands that stabilize a recently discovered FKBP51-favoring conformation. However, drug-like parameters for these ligands remained unfavourable. In the present study, we replaced the potentially labile pipercolic ester group of previous FKBP51 ligands by various low molecular weight amides. This resulted in the first series of pipercolic acid amides, which had much lower MWs without affecting FKBP51 selectivity. We discovered a geminally substituted cyclopentyl amide as a preferred FKBP51-binding motif and elucidated its binding mode to provide a new lead structure for future drug optimization.

#### **Introduction**

The FK506-binding protein 51 (FKBP51) plays an important role in the pathogenesis of depression and other stress-related diseases. It inhibits signaling of the glucocorticoid receptor, a key receptor for the stress hormone cortisol, and its upregulation in the brain causes depression-like behaviors.<sup>1-3</sup> In animal models of anxiety and depression, depletion of FKBP51 led to improved stress hormone signaling and stress-coping behavior.<sup>4-6</sup> Moreover, in humans FKBP51 has repeatedly been

## B. Research Articles – Publication/Manuscript VIII

associated genetically with psychiatric endophenotypes and diseases.<sup>7, 8</sup> Taken together, FKBP51 has emerged as a compelling target for stress-related disorders.<sup>9, 10</sup> Ligands for FKBP51 have been traditionally derived from the natural product FK506 (Fig. 1a) through structure-based design.<sup>11-15</sup> For FKBP51 drug discovery, the key challenge is to achieve selectivity over its closest homologue FKBP52, which is the functional counter-player of FKBP51 and has opposing effects on the endocrine system and on behaviour.<sup>1-3</sup> The active site residues of FKBP51 and FKBP52 are strictly conserved<sup>16-22</sup> and almost all ligands tested so far did not discriminate between these two proteins.<sup>23-27</sup>

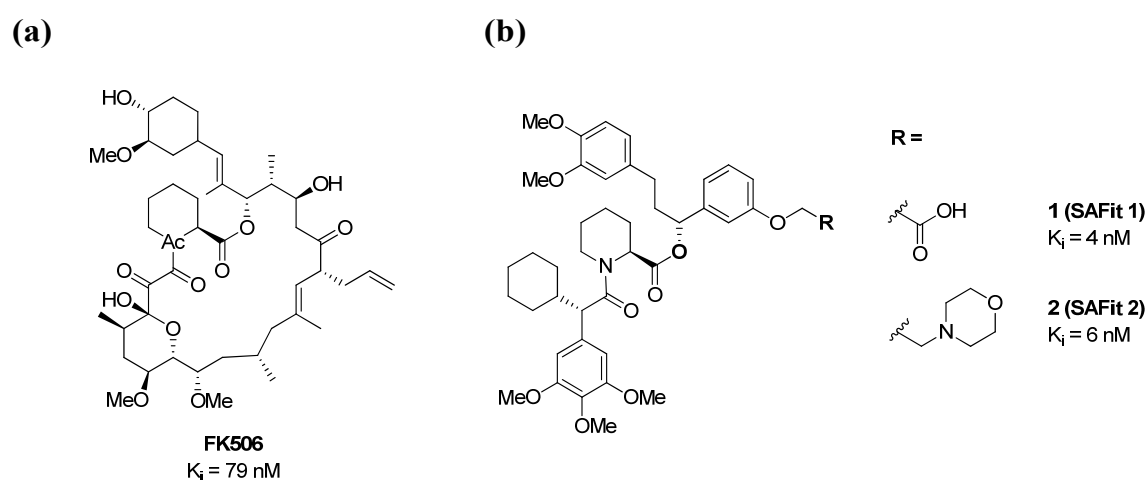


**Fig. 1:** Chemical structures of (a) FK506 and (b) the FKBP51-selective ligands SAFit1 (**1**), SAFit2 (**2**) and their binding affinities towards FKBP51.

Recently, we discovered the first FKBP51-selective ligands based on a novel, FKBP51-specific binding mode.<sup>28</sup> The resulting tool compounds, SAFit1 (**1**) and SAFit2 (**2**) (Fig. 1b), for the first time allowed to pharmacologically probe the role of FKBP51. This enabled the proof-of-concept that inhibition of FKBP51 is neuritrophic, enhances stress hormone regulation, has anxiolytic and antidepressant-like effects, and suppresses NF- $\kappa$ B signalling, a key pathway in melanoma cancers.<sup>28-30</sup> Despite these encouraging findings, it is currently unclear if drug-like FKBP51-selective inhibitors can be developed. SAFit1 and 2 deviate substantially from the physicochemical properties required for CNS-directed drugs.<sup>31</sup> Clearly, the molecular weight (748 and 803 g/mol, compared to 426 g/mol for 90 % of CNS drugs), lipophilicity ( $\text{clogD} = 3.5$  and  $7.1$ , vs.  $<3.8$  for CNS drugs), polar surface area (139 and  $114 \text{ \AA}^2$ , vs.  $<86$  for CNS drugs), and hydrogen bond acceptors ( $\text{HA} = 14$  and  $12$ ) are

## B. Research Articles – Publication/Manuscript VIII

much too high, while the ligand efficiency is too low ( $LE = 0.21$  and  $0.19$ ). Furthermore, there are biological stability issues that require attention. Therefore, we set out to identify improved lead structures that are better suited for further FKBP51 drug development.

### Results and Discussion

#### Cocrystal Structure of **3**

Replacing a labile ester linkage with a metabolically more stable amide group is a common strategy to enhance bioavailability. When we replaced the pipercolic ester moiety of SAFit1 by the analogous amide we were delighted to see that the SAFit1 amide analog **3** retained high-affinity binding towards FKBP51 ( $K_i = 39$  nM, Fig. 2a). No binding towards FKBP52 could be observed, in agreement with a SAFit-like FKBP51-selective binding mode.

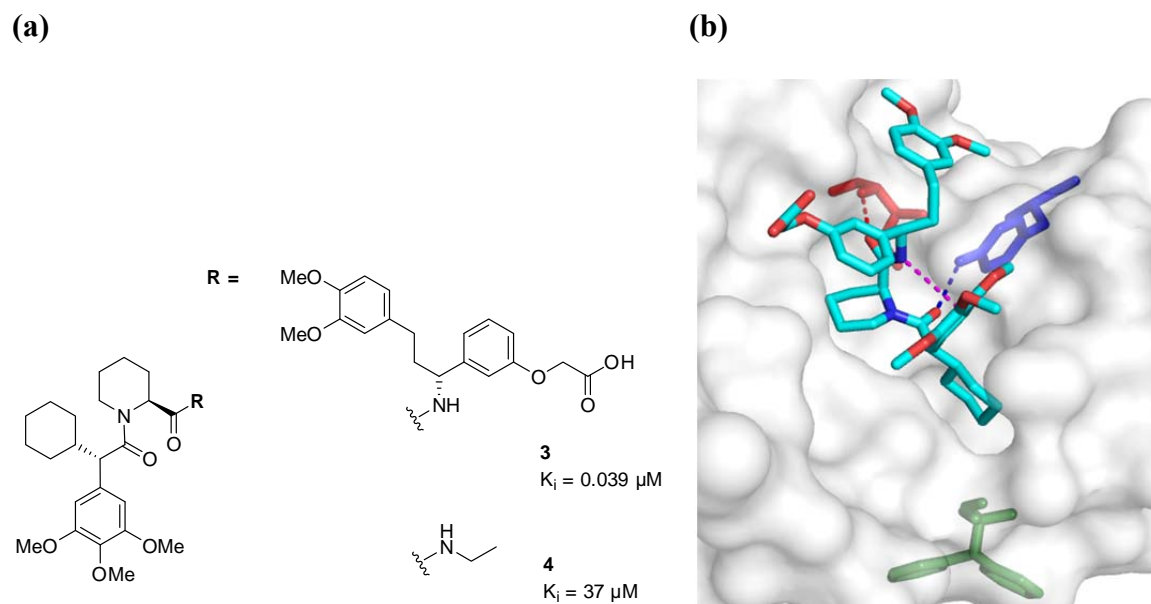


**Fig. 2:** (a) Chemical structures of the SAFit1 amide analog **3** and ethyl amide analog **4** and their binding affinities towards FKBP51. (b) X-ray structure of **3** (cyan) in complex with the FK506-binding domain of FKBP51 (pdb: 5DIU). The hydrogen bonds to Tyr113 (blue), Ile 87 (red) and the intramolecular NH-C<sub>ar</sub> interaction (magenta) are indicated as dotted lines. Phe67 (green) has been displaced by the cyclohexyl moiety upon binding of **3** and adopts two rotamers.

We solved the co-crystal structure of **3** and FKBP51 to confirm this assumption (Fig. 2b). The binding mode of **3** is virtually identical to the previously determined iFit1 and iFit4-FKBP51 complexes, including the key conformational rearrangement of Phe67 that is responsible for the strict selectivity over FKBP52.<sup>28</sup> The important hydrogen bonds to Tyr113 (red) and Ile 87

## B. Research Articles – Publication/Manuscript VIII

(blue) are preserved. Moreover, the conformation of the cyclohexyl ring conformation is similar to the cyclohexenyl moiety of iFit4. It is buried in the subpocket that is generated by the displacement of Phe67. The pipecolate amide of **3** points to the face of the trimethoxy phenyl ring but does not change its conformation.

Encouraged by this finding we started a systematic exploration of pipecolic acid amide substituents, starting with the small ethyl amide analog **4**. As expected, the replacement of the large amide substituent of **3** by the simple ethyl group in **4** caused a substantial loss of binding affinity, resulting in a  $K_i$  value of 37  $\mu\text{M}$ . Nevertheless **4** represented a suitable starting point for further derivatization.

### *An efficient synthetic strategy for pipecolic acid amide screening*

During the investigation on selective FKBP51 ligands, the carboxylic acid **5** proved to be the best building block, regarding binding affinity and selectivity.<sup>28</sup> We therefore developed an efficient, solid phase-assisted method (Fig. 3) to couple **5** with a variety of pipecolic acid dipeptides. The synthesis started with the coupling of an Fmoc protected amino acid to the Sieber amide resin.<sup>32</sup> Then Fmoc-pipecolic acid and subsequently the carboxylic acid **5** were coupled to the free amines after Fmoc deprotection, respectively. Cleavage from the resin provided a variety of pipecolic acid amides in 20-90 % overall yield and excellent purities (> 90 % for crude products).

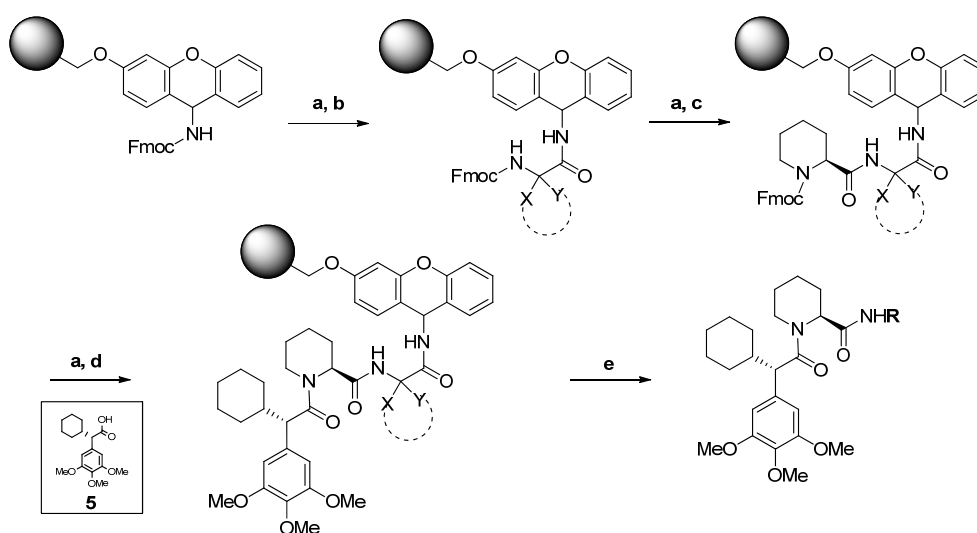


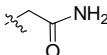
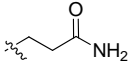
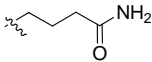
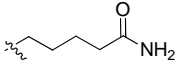
**Fig. 3:** Solid phase synthesis for the pipecolic acid amide series; Reagents and conditions: (a) 20 % 4-Methylpiperidine/DCM, (b) 4.8 eq. HBTU, 4.8 eq. HOBt, 10 eq. DIEA, 5 eq. Fmoc-amino acid (X,Y = different substituents). (c) 3.8 eq. HBTU, 3.8eq HOBt, 8 eq. DIEA, Fmoc-pipecolic acid. (d) 2 eq. HATU, 4 eq. DIEA, 2 eq. **5**. (e) 1% TFA/1% TIS/98% DCM.

## B. Research Articles – Publication/Manuscript VIII

This approach allowed rapid incorporation and testing of a large variety of commercially available amino acid building blocks. Altogether, an FKBP51-focused library of 37 compounds was synthesized by this method (Table 1-5). None of the ligands from this novel pipecolic acid amide series showed any binding to FKBP52.

### *Structure-Affinity Relationship (SAR) of the Amide Substituent*

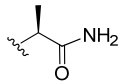
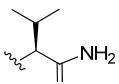
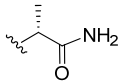
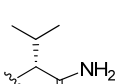
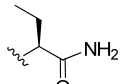
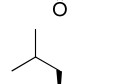
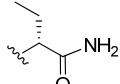
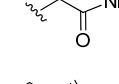
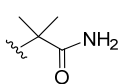
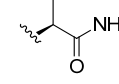
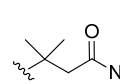
To perform a systematic investigation on the different amide substituents, we started our screening with simple unbranched side chains (Table 1). Entry **6**, which derives from the simplest amino acid glycine, bound to FKBP51 in the same affinity range as the ethyl amide analog **5** (35 and 37  $\mu\text{M}$  respectively). A significant affinity increase to 5.6  $\mu\text{M}$  (**7**) was observed when an additional methylene group was added to the chain. Further prolongation of the chain, however, only resulted in a slight increase of the binding affinity (compounds **8** and **9**).

Entry	R	$K_i$ [ $\mu\text{M}$ ]
<b>6</b>		35
<b>7</b>		5.6
<b>8</b>		4.7
<b>9</b>		3.3

**Table 1:** FKBP51 affinities of amide analogs with unbranched amide substituents;  $K_i$  values were determined by competitive fluorescence polarization assay.<sup>33</sup>

In the next series we assessed, whether branching with additional aliphatic groups would improve the binding affinity (Table 2). The addition of a methyl group (**10a & b**) increased the binding affinity irrespective of the configuration, compared to the linear analog **6**. Further enlargement of the branched side chains resulted only in a slight increase of the binding affinity (**11a & b**, **14a & b**, **15**, **16a & b**). Interestingly, compounds with branched side chains with (*R*)-configuration showed higher binding affinities than their corresponding diastereomers with (*S*)-configuration (**14b** > **14a**, **16b** > **16a**). A clear improvement of the  $K_i$  value was observed when a geminally di-substituted amide was introduced (**12**, **13**).

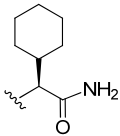
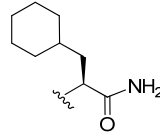
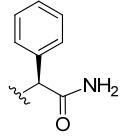
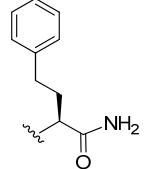
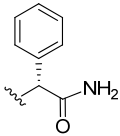
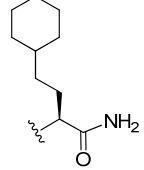
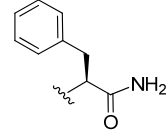
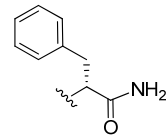
## B. Research Articles – Publication/Manuscript VIII

Entry	R	K <sub>i</sub> [μM]	Entry	R	K <sub>i</sub> [μM]
10a		12	14a		24
10b		10	14b		5
11a		7	15		7
11b		7	16a		7
12		2.3	16b		3
13		2.8			

**Table 2:** FKBP51 binding affinities of amide analogs with branched aliphatic side chain; K<sub>i</sub> values were determined by competitive fluorescence polarization assay.<sup>33</sup>

We hypothesized that additional hydrophobic interactions might be beneficial for the binding to FKBP51 and therefore analyzed the effects of phenyl- and cyclohexyl rings branching off the linear precursor (Table 3). In general, compounds containing an aromatic ring showed better binding affinities than their aliphatic analog (e.g. **19a** vs. **20**). Also shorter linkers tended to result in better affinities towards the protein. As observed in the previous series, ligands with the side chain in (*R*)-configuration were better than their corresponding diastereomers in (*S*)-configuration (**18b** > **18a** and **19b** > **19a**).

## B. Research Articles – Publication/Manuscript VIII

Entry	R	K <sub>i</sub> [μM]	Entry	R	K <sub>i</sub> [μM]
17		4	20		14
18a		3	21		8.5
18b		1.5	22		11.8
19a		5			
19b		1.4			

**Table 3:** FKBP51 binding affinities of amide analogs with branched side chains containing aromatic and non-aromatic 6-membered rings; K<sub>i</sub> values were determined by competitive fluorescence polarization assay.<sup>33</sup>

FKBP51 has two hydrogen bond acceptors, the carbonyls of Gly84 and of Gln85, that are close to the pipecolate ester substituents of FKBP51-bound ligands. The high-affinity ligands FK506 and rapamycin gain part of their binding energy by donating direct or water-mediated hydrogen bonds to these residues.<sup>17, 19</sup> We thus analyzed the effect of substituents containing polar groups in the side chain. As shown in Tab. 4, this did not result in any affinity enhancement over the aliphatic counterparts. As for the branched aliphatic derivatives, we observed a preference for substituents with the (*R*)-configuration (**24b** > **24a**, **25b** > **25a**). The exception was the histamine derivatives, where this trend was reversed (**26a** > **26b**).

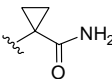
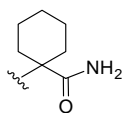
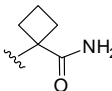
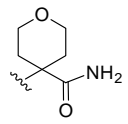
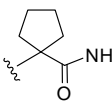
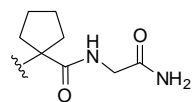
## B. Research Articles – Publication/Manuscript VIII

Entry	R	K <sub>i</sub> [μM]	Entry	R	K <sub>i</sub> [μM]
23a		9.8	25a		59
23b		9.6	25b		3.3
24a		11	26a		3.5
24b		4.2	26b		13

**Table 4:** FKBP51 binding affinities of amide analogs with side chains containing heteroatoms; K<sub>i</sub> values were determined by competitive fluorescence polarization assay.<sup>33</sup>

Intrigued by the promising ligand efficiency of the geminally disubstituted analog **12**, we extended our studies to amide substituents containing geminally substituted carbocycles of different ring sizes (Table 5). While constraining the two geminal substituents by a cyclopropyl ring in **27** reduced affinity, the cyclobutyl (**28**) and 6-membered ring analogs (**30**, **31**) had affinities comparable to **12**. A surprising discovery was the high affinity of the cyclopentyl compound **29**, which showed exceptionally strong inhibition (K<sub>i</sub> = 0.1 μM). The beneficial effect of the cyclopentyl ring was confirmed by the close analog **32** that also showed a significant higher binding affinity, compared to the other carbocycles.

## B. Research Articles – Publication/Manuscript VIII

Entry	R	$K_i$ [ $\mu\text{M}$ ]	Entry	R	$K_i$ [ $\mu\text{M}$ ]
27		17	30		1.6
28		4.7	31		2.3
29		0.1	32		0.7

**Table 5:** FKBP51 binding affinities of amide analogs containing geminally substituted carbocycles or tetrahydropyran;  $K_i$  values were determined by competitive fluorescence polarization assay.<sup>33</sup>

### *Cocrystal Structure of 29*

To better understand the basis for the surprisingly high affinity of **29** we solved the cocrystal structure of **29** in complex with FKBP51 (Fig.4).

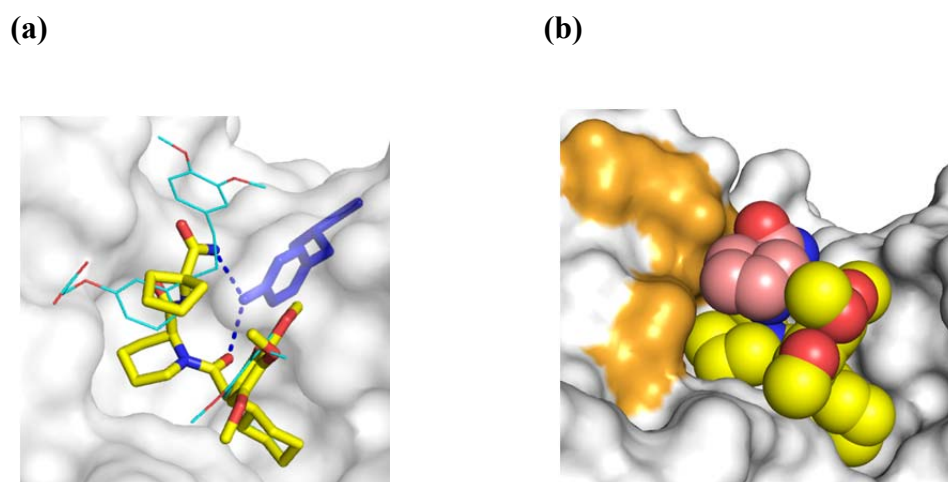


**Fig. 4:** X-ray structure of **29** (yellow) in complex with the FK506-binding domain of FKBP51 (pdb: 5DIV); Lys121 is not shown for clarity; (a) The hydrogen bonds to Tyr113 (blue) are indicated by dotted lines; Compound **3** in complex with FKBP51 is superimposed and shown as cyan lines. (b) **29** in complex with FKBP51 is shown as spheres. The cyclopentane ring and residues Phe77, Gln85, and Val86 have been highlighted in salmon and orange, respectively.

## B. Research Articles – Publication/Manuscript VIII

The cocrystal structure revealed that the pipercolic acid core and the 2-trimethoxyphenyl-2-cyclohexyl acetic acid moiety (derived from **5**) adopt the same conformation and engage in the same interactions as observed for **3** (Fig. 2b). The pipercolic acid core sits tightly in the binding pocket in a chair conformation, positioning both carbonyl groups optimally for forming hydrogen bonds with Ile87 (blue) and Tyr113 (red), respectively. Similar to ligand **3**, the cyclohexyl ring of **29** is deeply buried in a hydrophobic pocket formed by Gly59, Lys60, Leu61, Lys66, Asp68, and Ile122. The trimethoxyphenyl ring points towards the open space. In contrast to **3**, the terminal amide of the pipercolate substituent of **29** donates a hydrogen bond to the hydroxyl group of Tyr113, which in turn donates a hydrogen bond to the carbonyl group of the 2-trimethoxyphenyl-2-cyclohexyl acetic acid moiety. The cyclopentane of **29** neatly fills the space between the piperidine of **29**, the trimethoxyphenyl of **29** and Phe77, Gln85 and Val86 of FKBP51 (Fig. 4b). This tight, sandwich-like, intramolecular packing explains, why even small deviations in the carbocycle size dramatically affect the interactions with FKBP51.

### Conclusion

SAFit1 and SAFit2 were just recently reported as the best selective FKBP51 ligands so far, but they are too large for further drug optimization studies. In this study we have shown, that replacing the pipercolic ester moiety by a low molecular weight amide containing a geminally substituted cyclopentyl ring leads to ligands with high binding affinities ( $K_i = 0.1 \mu\text{M}$ ) and low molecular weight, while retaining selectivity for FKBP51 over FKBP52. Especially with **29** we were able to reduce the molecular weight by 34 % (MW = 529.7 g/mol compared to 802 g/mol for SAFit2) and to improve key physicochemical parameters (clogD = 3.1, tPSA =  $120 \text{ \AA}^2$ , 9 HA, LE = 0.25). Due to these enhanced properties as well as the well-understood molecular binding mode, **29** represents a substantially improved starting point for the further development of FKBP51-directed drug candidates.

### Experimental Section

#### *Chemistry*

Chromatographic separations were performed either by manual flash chromatography or automated flash chromatography using an Interchim Puriflash 430 with an UV detector.  $^1\text{H}$  NMR spectra,  $^{13}\text{C}$  NMR spectra, 2D HSQC, HMBC, and COSY of all intermediates were obtained from the Department of Chemistry and Pharmacy, LMU, on a Bruker Avance III HD 400/800 or a Varian NMR-System 300/400/600 at room temperature. Chemical shifts for  $^1\text{H}$

## B. Research Articles – Publication/Manuscript VIII

or  $^{13}\text{C}$  are given in ppm ( $\delta$ ) downfield from tetramethylsilane using residual protio solvent as an internal standard.

Mass spectra ( $m/z$ ) were recorded on a Thermo Finnigan LCQ DECA XP Plus mass spectrometer at the Max Planck Institute of Psychiatry, while the high resolution mass spectrometry was carried out at MPI for Biochemistry (Microchemistry Core Facility) on Bruker Daltonics MicrOTOF.

The purity of the compounds was verified by reversed phase HPLC (see supporting information for detailed conditions). All of the final compounds synthesized and tested had a purity of > 95 %.

### General Synthetic procedure for solid phase coupling reaction

All steps were performed at RT. Sieber amide resin (108 mg, 80  $\mu\text{mol}$ ) was treated with 20 % 4-methylpiperidine in DMF (2.0 mL) for 20 min for removing the Fmoc-group. The resin was filtered and washed with DMF (2.0 mL x 4). To the resin was added a solution of the Fmoc-protected amino acid (400  $\mu\text{mol}$ , 5 eq.), HBTU (145 mg, 386  $\mu\text{mol}$ , 4.8 eq.), HOBt (52 mg, 386  $\mu\text{mol}$ , 4.8 eq.) and DIPEA (140  $\mu\text{L}$ , 800  $\mu\text{mol}$ , 10 eq.) in DMF (2.0 mL). The mixture was then mixed on a shaker for 2 h. In the following step the resin was filtered and washed with DMF (2 mL x 4). Fmoc deprotection and washing was performed as before. In the following step (S)-N-Fmoc-piperidine-2-carboxylic acid (112 mg, 320  $\mu\text{mol}$ , 4 eq.), HBTU (115mg, 304  $\mu\text{mol}$ , 3.8 eq.), HOBt (41 mg, 304  $\mu\text{mol}$ , 4.8 eq.) and DIPEA (120  $\mu\text{L}$ , 640  $\mu\text{mol}$ , 8 eq.) in DMF (2.0 mL) was added to the resin and mixed for 2 h. Washing and deprotecting was repeated as before, followed by the addition of **5** (48 mg, 136  $\mu\text{mol}$ , 1.7 eq.), HATU (61 mg, 144  $\mu\text{mol}$ , 1.8 eq.) and DIPEA (60  $\mu\text{L}$ , 320  $\mu\text{mol}$ , 4 eq.). The suspension was mixed for 16 h. Then the resin was washed with DMF, MeOH, DCM and Et<sub>2</sub>O (2 mL x 4 each) and dried in vacuo. The compounds were cleaved from the resin using DCM + 1 % TFA + 1 % TIS (2.0 mL) for 2 min. This was repeated 5 times and after every step the solution, containing the cleaved product, was neutralized using saturated NaHCO<sub>3</sub> solution. The aqueous solution was then extracted three times with DCM. The combined organics were dried over MgSO<sub>4</sub>, filtered and the solvent was removed to obtain the compounds after removing the solvent under reduced pressure. If necessary the compounds were purified by flash chromatography. (Note: The synthesis of **14a+b**, **19a+b** and **20** were conducted starting with 160  $\mu\text{mol}$  resin. The coupling step with **5** was performed with **5** (3 eq.), HATU (2.8 eq.) and DIPEA (6 eq.).)

## B. Research Articles – Publication/Manuscript VIII

The purity of the compounds was verified by reversed phase HPLC. All of the final compounds synthesized and tested have a purity of more than 95%.

### **2-(3-((*R*)-1-((*S*)-1-((*S*)-2-cyclohexyl-2-(3,4,5-trimethoxyphenyl)acetyl)piperidine-2-carboxamido)-3-(3,4-dimethoxyphenyl)propyl)phenoxy)acetic acid (3)**

**5** (30 mg, 0.20 mmol), HATU (110 mg, 0.29 mmol) and DIPEA (0.13 mL, 0.78 mmol) were dissolved in DCM (2.0 mL) at RT and stirred for 30 min. Then **3-2** (50 mg, 0.20 mmol), dissolved in DCM (300  $\mu$ L) was added and the reaction mixture was stirred for 16 h at RT. The crude product was concentrated and purified by flash chromatography (0-20 % EtOAc in cyclohexane). Then the carboxylic acid was liberated using 10% TFA in DCM (2.0 mL) at RT for 5 h. The reaction mixture was concentrated and flash purified by preparative HPLC (Gradient: 65-75% B in 20min) to obtain the title compound (15 mg, 20  $\mu$ mol, 24 %) as a colourless oil.

**HPLC** [0-100% Solvent B, 20 min]:  $R_t$  = 11.7 min. **HRMS**: calculated 747.3857 [ $C_{42}H_{55}N_2O_{10} + H$ ] $^+$ , found 747.3854 [ $M+H$ ] $^+$ .  **$^1H$  NMR** (400 MHz, DMSO- $d_6$ )  $\delta$  7.13 – 7.08 (m, 1H), 6.95 – 6.90 (m, 1H), 6.84 (t,  $J$  = 8.4 Hz, 1H), 6.75 (dq,  $J$  = 11.8, 2.0 Hz, 2H), 6.72 – 6.67 (m, 1H), 6.66 – 6.60 (m, 1H), 6.59 – 6.54 (m, 2H), 5.15 – 5.07 (m, 1H), 4.82 – 4.69 (m, 1H), 4.69 – 4.56 (m, 3H), 3.76 – 3.72 (m, 1H), 3.72 – 3.69 (m, 6H), 3.65 – 3.64 (m, 1H), 3.58 – 3.54 (m, 9H), 2.96 – 2.84 (m, 2H), 2.82 – 2.70 (m, 2H), 2.43 – 2.30 (m, 2H), 2.19 – 2.05 (m, 2H), 1.99 – 1.87 (m, 2H), 1.88 – 1.76 (m, 3H), 1.59 (d,  $J$  = 8.2 Hz, 2H), 1.34 (d,  $J$  = 9.6 Hz, 1H), 1.16 – 1.10 (m, 2H), 0.95 – 0.86 (m, 2H).  **$^{13}C$  NMR** (101 MHz, DMSO- $d_6$ )  $\delta$  171.99, 170.28, 170.12, 157.65, 152.52, 148.61, 147.00, 145.30, 135.97, 133.59, 130.71, 127.70, 120.01, 112.62, 112.31, 112.26, 111.74, 105.56, 64.33, 63.08, 59.70, 55.96, 55.52, 55.48, 55.34, 52.42, 51.79, 51.45, 42.79, 39.52, 38.52, 38.17, 31.59, 27.34, 27.03, 26.09, 24.87, 20.68, 19.97.

### **(*S*)-1-((*S*)-2-cyclohexyl-2-(3,4,5-trimethoxyphenyl)acetyl)-*N*-ethylpiperidine-2-carboxamide (4)**

(*S*)-*N*-ethylpiperidine-2-carboxamide (40.0 mg, 0.26 mmol) and **5** (60 mg, 0.39 mmol) were dissolved in DCM (1.0 mL). HATU (0.38 g, 0.26 mmol) and DIPEA (0.17 mL, 1.02 mmol) were added and the reaction was stirred at RT for 16 h. Then the organic solvent was removed and the title compound (68.0 mg, 0.15 mmol, 59.5 %) was obtained after purification by flash chromatography (EtOAc/cyclohexane 1:2).

## B. Research Articles – Publication/Manuscript VIII

**HPLC** [0-100% Solvent B, 20 min]:  $R_t = 18.8$  min. **HRMS**: calculated 447.2859  $[\text{C}_{25}\text{H}_{38}\text{N}_2\text{O}_5 + \text{H}]^+$ , found 447.2863  $[\text{M} + \text{H}]^+$ .  **$^1\text{H}$  NMR** (300 MHz,  $\text{CDCl}_3$ )  $\delta$  6.52 (s, 2H), 5.50 (t, 1H), 5.23 (d,  $J = 5.3$  Hz, 1H), 4.00 (d,  $J = 14.1$  Hz, 1H), 3.84 – 3.83 (m, 6H), 3.82 – 3.80 (m, 3H), 3.42 – 3.29 (m, 2H), 3.08 – 2.97 (m, 2H), 2.78 – 2.71 (m, 1H), 2.38 – 2.31 (m, 1H), 2.22 – 2.08 (m, 2H), 1.91 (d,  $J = 12.6$  Hz, 2H), 1.66 – 1.60 (m, 4H), 1.52 – 1.44 (m, 2H), 1.34 – 1.26 (m, 2H), 1.20 – 1.15 (m, 2H), 0.92 – 0.86 (m, 1H), 0.81 (t,  $J = 7.2, 0.7$  Hz, 3H).  **$^{13}\text{C}$  NMR** (75 MHz,  $\text{CDCl}_3$ )  $\delta$  172.77, 170.10, 153.41, 137.08, 133.71, 105.14, 60.75, 56.24, 55.23, 52.16, 43.71, 40.83, 34.03, 32.77, 30.49, 26.50, 26.10, 26.01, 25.84, 25.00, 20.61, 14.48.

### **(S)-N-(2-amino-2-oxoethyl)-1-((S)-2-cyclohexyl-2-(3,4,5-trimethoxyphenyl)acetyl)piperidine-2-carboxamide (6)**

The general procedure was used with Fmoc-Gly-OH and **6** was obtained after purification by flash chromatography (0% - 100% [EtOAc + 2% MeOH + 0.1% TEA] in cyclohexane) as colourless oil (22 mg, 46  $\mu\text{mol}$ , 57.5 %).

**HPLC** [0-100% Solvent B, 20 min]:  $R_t = 19.2$  min. **HRMS**: calculated 476.2761  $[\text{C}_{25}\text{H}_{38}\text{N}_3\text{O}_6 + \text{H}]^+$ , found 476.2772  $[\text{M} + \text{H}]^+$ .  **$^1\text{H}$  NMR** (400 MHz,  $\text{DMSO}-d_6$ )  $\delta$  6.57 (d,  $J = 1.1$  Hz, 1H), 6.52 (d,  $J = 1.1$  Hz, 2H), 4.94 – 4.90 (m, 1H), 4.75 (d,  $J = 5.1$  Hz, 1H), 4.31 (d,  $J = 13.0$  Hz, 1H), 3.67 – 3.62 (m, 9H), 3.10 (d,  $J = 3.8$  Hz, 1H), 2.68 (td,  $J = 12.9, 2.7$  Hz, 1H), 2.45 – 2.40 (m, 4H), 1.88 – 1.76 (m, 2H), 1.68 – 1.44 (m, 8H), 1.34 – 1.27 (m, 2H), 1.05 – 0.89 (m, 4H).  **$^{13}\text{C}$  NMR** (101 MHz,  $\text{DMSO}-d_6$ )  $\delta$  172.90, 172.28, 170.97, 170.55, 153.08, 152.88, 136.32, 134.97, 134.22, 106.02, 105.82, 60.26, 56.32, 56.12, 53.56, 52.63, 48.98, 32.37, 32.19, 30.23, 27.17, 26.51, 26.05, 25.50, 21.14, 20.37.

### **(S)-N-(3-amino-3-oxopropyl)-1-((S)-2-cyclohexyl-2-(3,4,5-trimethoxyphenyl)acetyl)piperidine-2-carboxamide (7)**

The general procedure was used with Fmoc- $\beta$ -Ala-OH and **7** was obtained after purification by flash chromatography (0% - 100% [EtOAc + 2% MeOH + 0.1% TEA] in cyclohexane) as colourless oil (19 mg, 39  $\mu\text{mol}$ , 48.6 %).

**HPLC** [0-100% Solvent B, 20 min]:  $R_t = 15.9$  min. **HRMS**: calculated 490.2917  $[\text{C}_{26}\text{H}_{39}\text{N}_3\text{O}_6 + \text{H}]^+$ , found 490.2945  $[\text{M} + \text{H}]^+$ .  **$^1\text{H}$  NMR** (599 MHz,  $\text{CDCl}_3$ )  $\delta$  6.52 (s, 2H), 5.94 – 5.81 (m, 2H), 5.35 (s, 1H), 5.22 – 5.17 (m, 1H), 4.65 – 4.60 (m, 1H), 4.01 – 3.96 (m, 1H), 3.88 – 3.80 (m, 9H), 3.44 – 3.37 (m, 2H), 3.17 – 3.11 (m, 1H), 2.83 – 2.76 (m, 1H), 2.30

## B. Research Articles – Publication/Manuscript VIII

(d,  $J = 13.6, 3.3, 1.8$  Hz, 1H), 2.19 – 2.13 (m, 1H), 2.12 – 2.04 (m, 2H), 1.90 – 1.85 (m, 1H), 1.73 – 1.61 (m, 4H), 1.60 – 1.55 (m, 1H), 1.50 – 1.42 (m, 2H), 1.37 – 1.29 (m, 2H), 1.19 – 1.10 (m, 2H), 0.93 – 0.85 (m, 1H), 0.76 (qd,  $J = 12.1, 3.6$  Hz, 1H).  $^{13}\text{C}$  NMR (151 MHz,  $\text{CDCl}_3$ )  $\delta$  173.00, 172.65, 170.80, 153.32, 136.90, 133.83, 105.41, 105.13, 60.87, 56.33, 56.26, 55.15, 52.30, 43.75, 40.97, 40.88, 35.29, 35.03, 32.70, 30.52, 26.48, 26.10, 26.01, 25.76, 25.25, 20.54, 14.18.

### **(S)-N-(4-amino-4-oxobutyl)-1-((S)-2-cyclohexyl-2-(3,4,5-trimethoxyphenyl)acetyl)piperidine-2-carboxamide (8)**

The general procedure was used with Fmoc-GABA-OH and **7** was obtained after purification by flash chromatography (0% - 100% [EtOAc + 2% MeOH + 0.1% TEA] in cyclohexane) as colourless oil (15 mg, 29  $\mu\text{mol}$ , 36.3 %).

**HPLC** [0-100% Solvent B, 10 min]:  $R_t = 16.2$  min. **HRMS**: calculated 504.3074 [ $\text{C}_{27}\text{H}_{41}\text{N}_3\text{O}_6 + \text{H}$ ] $^+$ , found 504.3093 [ $\text{M} + \text{H}$ ] $^+$ .  $^1\text{H}$  NMR (599 MHz,  $\text{CDCl}_3$ )  $\delta$  6.52 (s, 2H), 6.30 ( $s_{\text{br}}$ , 1H), 5.69 (t,  $J = 6.1$  Hz, 1H), 5.32 ( $s_{\text{br}}$ , 1H), 5.23 (d,  $J = 5.3, 2.2$  Hz, 1H), 4.00 (d, 1H), 3.84 – 3.79 (m, 9H), 3.40 (d,  $J = 10.2$  Hz, 1H), 3.23 (dq,  $J = 13.1, 6.5$  Hz, 1H), 2.89 (h, 1H), 2.76 – 2.68 (m, 1H), 2.36 – 2.30 (m, 1H), 2.19 – 2.11 (m, 1H), 1.96 – 1.83 (m, 4H), 1.74 – 1.64 (m, 5H), 1.61 – 1.55 (m, 1H), 1.52 – 1.46 (m, 3H), 1.37 – 1.33 (m, 1H), 1.32 – 1.27 (m, 1H), 1.20 – 1.11 (m, 2H), 0.94 – 0.85 (m, 1H), 0.77 (qd,  $J = 12.2, 3.7$  Hz, 1H).  $^{13}\text{C}$  NMR (151 MHz,  $\text{CDCl}_3$ )  $\delta$  174.56, 172.93, 170.93, 153.42, 136.88, 133.89, 105.21, 60.86, 56.31, 55.20, 52.32, 43.85, 41.00, 40.87, 38.41, 32.73, 32.47, 30.49, 26.46, 26.09, 26.00, 25.74, 25.11, 20.58.

### **(S)-N-(5-amino-5-oxopentyl)-1-((S)-2-cyclohexyl-2-(3,4,5-trimethoxyphenyl)acetyl)piperidine-2-carboxamide (9)**

The general procedure was used with Fmoc-Ava-OH and **9** was obtained after purification by flash chromatography (0% - 100% [EtOAc + 2% MeOH + 0.1% TEA] in cyclohexane) as colourless oil (22 mg, 41.5  $\mu\text{mol}$ , 51.9 %).

**HPLC** [0-100% Solvent B, 10 min]:  $R_t = 16.9$  min. **HRMS**: calculated 518.3230 [ $\text{C}_{28}\text{H}_{43}\text{N}_3\text{O}_6 + \text{H}$ ] $^+$ , found 518.3264 [ $\text{M} + \text{H}$ ] $^+$ .  $^1\text{H}$  NMR (400 MHz,  $\text{CDCl}_3$ )  $\delta$  6.44 (s, 2H), 6.01 (s, 1H), 5.47 – 5.37 (m, 1H), 5.32 ( $s_{\text{br}}$ , 1H), 5.15 (d,  $J = 4.6$  Hz, 1H), 3.93 (d,  $J = 14.2$  Hz, 1H), 3.78 – 3.70 (m, 9H), 3.32 (d,  $J = 10.2$  Hz, 1H), 3.14 – 3.04 (m, 1H), 2.80 – 2.70 (m, 1H), 2.65 (td,  $J = 13.4, 2.7$  Hz, 1H), 2.27 (d,  $J = 14.3$  Hz, 1H), 2.12 – 2.03 (m, 1H), 2.02 –

## B. Research Articles – Publication/Manuscript VIII

1.91 (m, 4H), 1.82 (d,  $J = 12.5$  Hz, 1H), 1.66 – 1.56 (m, 4H), 1.53 – 1.46 (m, 1H), 1.37 (m, 2H), 1.30 – 1.17 (m, 4H), 1.13 – 0.94 (m, 3H), 0.87 – 0.75 (m, 1H), 0.74 – 0.62 (m, 1H).  $^{13}\text{C}$  NMR (101 MHz,  $\text{CDCl}_3$ )  $\delta$  175.37, 172.80, 170.43, 153.38, 136.61, 134.04, 105.07, 60.87, 56.22, 55.18, 52.26, 43.84, 40.97, 40.88, 38.61, 34.84, 32.72, 30.48, 28.73, 26.48, 26.09, 25.99, 25.81, 25.04, 22.47, 20.63.

### **(S)-N-((S)-1-amino-1-oxopropan-2-yl)-1-((S)-2-cyclohexyl-2-(3,4,5-trimethoxyphenyl)acetyl)piperidine-2-carboxamide (10a)**

The general procedure was used with Fmoc-Ala-OH and **10a** was obtained as colourless oil (15 mg, 31  $\mu\text{mo}$ , 19.4 %).

**HPLC** [0-100% Solvent B, 20 min]:  $R_t = 16.4$  min. **HRMS**: calculated 490.2917  $[\text{C}_{26}\text{H}_{39}\text{N}_3\text{O}_6 + \text{H}]^+$ , found 490.2945  $[\text{M} + \text{H}]^+$ .  $^1\text{H}$  NMR (400 MHz,  $\text{DMSO}-d_6$ )  $\delta$  6.63 (s, 1H), 6.59 (s, 2H), 5.04 – 4.98 (m, 1H), 4.82 (d,  $J = 5.2$  Hz, 1H), 4.33 – 4.25 (m, 1H), 4.10 – 4.00 (m, 2H), 3.70 (d,  $J = 3.7$  Hz, 9H), 3.60 (s, 2H), 2.04 (d,  $J = 10.0$  Hz, 1H), 1.96 – 1.90 (m, 2H), 1.70 (d,  $J = 12.5$  Hz, 2H), 1.60 – 1.46 (m, 5H), 1.42 – 1.35 (m, 2H), 1.24 – 1.17 (m, 2H), 1.11 – 1.03 (m, 2H), 0.91 (d,  $J = 7.0$  Hz, 3H), 0.82 – 0.70 (m, 1H).  $^{13}\text{C}$  NMR (75 MHz,  $\text{DMSO}-d_6$ )  $\delta$  174.22, 172.67, 170.28, 153.14, 153.03, 136.48, 134.34, 106.02, 60.44, 60.28, 56.45, 56.17, 53.46, 51.74, 48.27, 47.95, 43.26, 41.23, 32.31, 32.17, 30.20, 26.59, 26.09, 25.82, 19.29, 18.84.

### **(S)-N-((R)-1-amino-1-oxopropan-2-yl)-1-((S)-2-cyclohexyl-2-(3,4,5-trimethoxyphenyl)acetyl)piperidine-2-carboxamide (10b)**

The general procedure was used with Fmoc-D-Ala-OH and **10b** was obtained as colourless oil (8 mg, 17  $\mu\text{mol}$ , 21.3 %).

**HPLC** [0-100% Solvent B, 20 min]:  $R_t = 17.1$  min. **HRMS**: calculated 490.2917  $[\text{C}_{26}\text{H}_{39}\text{N}_3\text{O}_6 + \text{H}]^+$ , found 490.2923  $[\text{M} + \text{H}]^+$ .  $^1\text{H}$  NMR (400 MHz,  $\text{DMSO}-d_6$ )  $\delta$  6.65 (s, 1H), 6.54 (s, 2H), 4.93 – 4.87 (m, 1H), 4.85 (d,  $J = 5.3$  Hz, 1H), 4.31 – 4.24 (m, 1H), 4.10 – 3.99 (m, 2H), 3.70 – 3.68 (m, 6H), 3.60 – 3.58 (m, 3H), 3.08 – 2.96 (m, 1H), 2.78 – 2.68 (m, 1H), 1.98 (t,  $J = 12.2$  Hz, 2H), 1.71 (d,  $J = 11.9$  Hz, 2H), 1.64 – 1.46 (m, 6H), 1.06 (s, 2H), 1.04 (s, 2H), 1.02 – 1.02 (m, 3H), 0.95 (d,  $J = 0.7$  Hz, 3H).  $^{13}\text{C}$  NMR (101 MHz,  $\text{DMSO}-d_6$ )  $\delta$  174.38, 173.07, 170.90, 153.10, 152.98, 136.38, 135.02, 134.13, 105.98, 60.44, 60.27, 56.39, 56.18, 52.75, 48.05, 41.13, 30.24, 26.96, 26.10, 25.43, 20.29, 19.67, 19.28, 18.53.

## B. Research Articles – Publication/Manuscript VIII

### **(S)-N-((S)-1-amino-1-oxobutan-2-yl)-1-((S)-2-cyclohexyl-2-(3,4,5-trimethoxyphenyl)acetyl)piperidine-2-carboxamide (11a)**

The general procedure was used with Fmoc-Abu-OH and **11a** was obtained after purification by flash chromatography (0% - 100% [EtOAc + 2% MeOH + 0.1% TEA] in cyclohexane) as pale yellow oil (29 mg, 58  $\mu$ mol, 72.5 %).

**HPLC** [0-100% Solvent B, 20 min]:  $R_t$  = 17.8 min. **HRMS**: calculated 504.3074  $[\text{C}_{27}\text{H}_{41}\text{N}_3\text{O}_6+\text{H}]^+$ , found 504.3086  $[\text{M}+\text{H}]^+$ .  **$^1\text{H}$  NMR** (400 MHz,  $\text{DMSO}-d_6$ )  $\delta$  6.63 (s, 1H), 6.52 (s, 2H), 4.97 – 4.89 (m, 1H), 4.31 (d,  $J$  = 13.3 Hz, 1H), 3.73 – 3.60 (m, 9H), 3.45 – 3.38 (m, 1H), 3.02 (t,  $J$  = 12.5 Hz, 1H), 2.06 – 1.80 (m, 4H), 1.73 – 1.63 (m, 3H), 1.55 – 1.46 (m, 6H), 1.31 – 1.20 (m, 3H), 1.06 – 0.98 (m, 3H), 0.94 – 0.82 (m, 3H), 0.69 – 0.60 (m, 3H).  **$^{13}\text{C}$  NMR** (101 MHz,  $\text{DMSO}-d_6$ )  $\delta$  173.54, 172.98, 171.00, 152.91, 136.34, 134.97, 134.13, 105.93, 60.37, 60.19, 56.35, 56.10, 53.44, 52.60, 43.18, 41.09, 32.29, 30.18, 27.22, 26.50, 26.04, 25.93, 25.40, 20.32, 10.30.

### **(S)-N-((R)-1-amino-1-oxobutan-2-yl)-1-((S)-2-cyclohexyl-2-(3,4,5-trimethoxyphenyl)acetyl)piperidine-2-carboxamide (11b)**

The general procedure was used with Fmoc-D-Abu-OH and **11b** was obtained after purification by flash chromatography (0% - 90% [EtOAc + 2% MeOH + 0.1% TEA] in cyclohexane) as colourless oil (10 mg, 20  $\mu$ mol, 24.8 %).

**HPLC** [0-100% Solvent B, 20 min]:  $R_t$  = 17.3 min. **HRMS**: calculated 504.3074  $[\text{C}_{27}\text{H}_{41}\text{N}_3\text{O}_6+\text{H}]^+$ , found 504.3100  $[\text{M}+\text{H}]^+$ .  **$^1\text{H}$  NMR** (599 MHz,  $\text{CDCl}_3$ )  $\delta$  6.51 (s, 2H), 6.03 (d,  $J$  = 7.9 Hz, 1H), 5.85 ( $s_{\text{br}}$ , 1H), 5.34 ( $s_{\text{br}}$ , 1H), 5.22 – 5.18 (m, 1H), 4.16 – 4.13 (m, 1H), 4.05 (dt,  $J$  = 13.7, 3.4 Hz, 1H), 3.84 – 3.78 (m, 11H), 3.41 (d,  $J$  = 10.2 Hz, 1H), 3.04 – 2.96 (m, 1H), 2.32 – 2.27 (m, 1H), 2.17 – 2.11 (m, 1H), 1.86 (d,  $J$  = 12.5 Hz, 1H), 1.71 – 1.64 (m, 8H), 1.39 – 1.31 (m, 3H), 1.18 – 1.09 (m, 3H), 0.94 – 0.86 (m, 2H), 0.77 – 0.69 (m, 1H).  **$^{13}\text{C}$  NMR** (151 MHz,  $\text{CDCl}_3$ )  $\delta$  173.63, 173.50, 171.12, 153.36, 137.11, 133.46, 105.24, 60.77, 60.37, 56.22, 55.03, 53.94, 52.60, 43.89, 41.06, 32.63, 30.47, 26.47, 26.07, 26.02, 25.61, 25.30, 24.73, 20.42, 14.18, 9.79.

## B. Research Articles – Publication/Manuscript VIII

### **(S)-N-(1-amino-2-methyl-1-oxopropan-2-yl)-1-((S)-2-cyclohexyl-2-(3,4,5-trimethoxyphenyl)acetyl)piperidine-2-carboxamide (12)**

The general procedure was used with Fmoc-Aib-OH and **12** was obtained after purification by flash chromatography (0% - 100% [EtOAc + 2% MeOH + 0.1% TEA] in cyclohexane) as pale white oil (29 mg, 58  $\mu$ mol, 72.5 %).

**HPLC** [0-100% Solvent B, 20 min]:  $R_t$  = 17.1 min. **HRMS**: calculated 504.3074 [ $C_{27}H_{41}N_3O_6+H$ ]<sup>+</sup>, found 504.3108 [ $M+H$ ]<sup>+</sup>. **<sup>1</sup>H NMR** (400 MHz, DMSO-*d*<sub>6</sub>)  $\delta$  6.59 (s, 1H), 6.51 (s, 2H), 4.86 – 4.76 (m, 1H), 3.95 (d,  $J$  = 13.5 Hz, 1H), 3.68 – 3.60 (m, 7H), 3.60 – 3.51 (m, 4H), 2.86 (td,  $J$  = 14.3, 13.8, 2.9 Hz, 1H), 1.96 – 1.83 (m, 2H), 1.71 – 1.61 (m, 2H), 1.57 – 1.46 (m, 4H), 1.35 – 1.25 (m, 2H), 1.13 (d,  $J$  = 3.7 Hz, 6H), 1.09 – 0.96 (m, 4H), 0.85 – 0.70 (m, 3H). **<sup>13</sup>C NMR** (101 MHz, DMSO-*d*<sub>6</sub>)  $\delta$  176.37, 172.96, 170.58, 152.91, 136.31, 134.11, 105.97, 60.21, 56.13, 55.93, 53.68, 52.78, 43.13, 32.36, 30.18, 26.53, 26.03, 25.43, 24.88, 24.51, 20.18.

### **(S)-N-(4-amino-2-methyl-4-oxobutan-2-yl)-1-((S)-2-cyclohexyl-2-(3,4,5-trimethoxyphenyl)acetyl)piperidine-2-carboxamide (13)**

The general procedure was used with Fmoc-3-amino-3-methyl-butyric acid and **13** was obtained as colorless oil (34 mg, 66  $\mu$ mol, 82.5 %).

**HPLC** [0-100% Solvent B, 15 min]:  $R_t$  = 14.6 min. **HRMS**: calculated 518.3230 [ $C_{28}H_{43}N_3O_6+H$ ]<sup>+</sup>, found 518.3264 [ $M+H$ ]<sup>+</sup>. **<sup>1</sup>H NMR** (300 MHz, CDCl<sub>3</sub>)  $\delta$  6.52 (s, 2H), 5.99 (s<sub>br</sub>, 1H), 5.70 (s, 2H), 5.14 (d,  $J$  = 4.1 Hz, 1H), 4.05 (d,  $J$  = 14.0 Hz, 1H), 3.90 – 3.73 (m, 9H), 3.39 (d,  $J$  = 10.2 Hz, 1H), 2.97 – 2.86 (m, 1H), 2.66 – 2.48 (m, 2H), 2.30 – 2.10 (m, 2H), 1.84 (d,  $J$  = 13.2 Hz, 1H), 1.70 – 1.57 (m, 4H), 1.51 – 1.41 (m, 3H), 1.31 – 1.22 (m, 2H), 1.17 – 1.12 (m, 3H), 1.06 – 1.00 (m, 6H), 0.93 – 0.86 (m, 1H), 0.79 – 0.67 (m, 1H). **<sup>13</sup>C NMR** (75 MHz, CDCl<sub>3</sub>)  $\delta$  173.45, 173.23, 170.88, 153.35, 137.14, 133.68, 105.32, 60.73, 56.24, 54.92, 52.75, 52.22, 44.74, 43.68, 40.97, 32.61, 30.44, 27.57, 27.52, 26.46, 26.04, 25.97, 25.72, 25.11, 20.51, 17.67, 12.27.

### **(S)-N-((S)-1-amino-3-methyl-1-oxobutan-2-yl)-1-((S)-2-cyclohexyl-2-(3,4,5-trimethoxyphenyl)acetyl)piperidine-2-carboxamide (14a)**

The general procedure was used with Fmoc-Val-OH and **14a** was obtained after purification by flash chromatography (50% - 100% [EtOAc + 0.1% TEA] in cyclohexane) as white crystals (24 mg, 46  $\mu$ mol, 28.8 %).

## B. Research Articles – Publication/Manuscript VIII

**HPLC** [0-100% Solvent B, 20 min]:  $R_t = 15.1$  min. **HRMS**: calculated 518.3230  $[\text{C}_{28}\text{H}_{43}\text{N}_3\text{O}_6+\text{H}]^+$ , found 518.3264  $[\text{M}+\text{H}]^+$ .  **$^1\text{H NMR}$**  (599 MHz,  $\text{CDCl}_3$ )  $\delta$  6.54 (s, 2H), 6.17 (d,  $J = 8.9$  Hz, 1H), 5.23 – 5.18 (m, 1H), 4.10 – 4.07 (m, 2H), 3.83 (s, 6H), 3.78 (s, 3H), 3.37 (s, 1H), 2.87 – 2.79 (m, 1H), 2.34 – 2.27 (m, 1H), 2.14 (qt,  $J = 11.0, 3.4$  Hz, 2H), 1.93 – 1.88 (m, 1H), 1.85 – 1.81 (m, 1H), 1.73 – 1.67 (m, 3H), 1.66 – 1.59 (m, 2H), 1.55 – 1.47 (m, 2H), 1.36 – 1.25 (m, 2H), 1.19 – 1.09 (m, 3H), 0.97 (dd,  $J = 29.5, 6.8$  Hz, 1H), 0.91 – 0.84 (m, 1H), 0.77 – 0.69 (m, 1H), 0.62 (d,  $J = 6.8$  Hz, 3H), 0.35 (d,  $J = 6.8$  Hz, 3H).  **$^{13}\text{C NMR}$**  (151 MHz,  $\text{CDCl}_3$ )  $\delta$  173.81, 172.93, 171.06, 153.46, 137.12, 133.32, 105.18, 60.67, 57.82, 56.18, 55.18, 52.73, 43.84, 41.51, 32.54, 30.43, 29.26, 26.44, 26.01, 25.95, 25.63, 24.91, 20.46, 19.16, 16.71.

### **(S)-N-((R)-1-amino-3-methyl-1-oxobutan-2-yl)-1-((S)-2-cyclohexyl-2-(3,4,5-trimethoxyphenyl)acetyl)piperidine-2-carboxamide (14b)**

The general procedure was used with Fmoc-D-Val-OH and **14b** was obtained after purification by flash chromatography (50% - 100% [EtOAc + 0.1% TEA] in cyclohexane) as colourless solid (31 mg, 63  $\mu\text{mol}$ , 39.4 %).

**HPLC** [0-100% Solvent B, 20 min]:  $R_t = 15.6$  min. **HRMS**: calculated 518.3230  $[\text{C}_{28}\text{H}_{43}\text{N}_3\text{O}_6+\text{H}]^+$ , found 518.3254  $[\text{M}+\text{H}]^+$ .  **$^1\text{H NMR}$**  (400 MHz,  $\text{DMSO}-d_6$ )  $\delta$  6.58 (s, 2H), 5.07 – 5.02 (m, 1H), 4.95 (d,  $J = 5.1$  Hz, 1H), 4.10 (d,  $J = 13.9$  Hz, 1H), 4.02 – 3.98 (m, 1H), 3.69 (s, 6H), 3.58 (s, 3H), 2.87 – 2.80 (m, 1H), 2.08 – 2.02 (m, 1H), 1.88 – 1.79 (m, 2H), 1.73 – 1.61 (m, 3H), 1.58 – 1.48 (m, 6H), 1.07 – 1.00 (m, 3H), 0.90 – 0.86 (m, 3H), 0.83 (dd,  $J = 6.7, 3.6$  Hz, 3H), 0.72 (d,  $J = 6.8$  Hz, 3H), 0.59 (d,  $J = 6.8$  Hz, 3H).  **$^{13}\text{C NMR}$**  (101 MHz,  $\text{DMSO}-d_6$ )  $\delta$  173.07, 172.83, 171.00, 152.98, 136.65, 136.44, 135.02, 134.27, 106.00, 60.41, 60.23, 57.12, 56.42, 56.13, 53.39, 52.50, 46.55, 43.29, 41.23, 35.51, 32.29, 32.22, 31.33, 30.43, 30.24, 27.46, 26.56, 26.50, 26.09, 26.03, 25.65, 20.50, 19.84, 19.69, 18.17, 17.51, 14.51.

### **(S)-N-((S)-1-amino-4-methyl-1-oxopentan-2-yl)-1-((S)-2-cyclohexyl-2-(3,4,5-trimethoxyphenyl)acetyl)piperidine-2-carboxamide (15)**

The general procedure was used with Fmoc-Leu-OH and **15** was obtained after purification by flash chromatography (0% - 80% [EtOAc + 2 % MeOH + 0.1% TEA] in cyclohexane) as colourless oil (8 mg, 15  $\mu\text{mol}$ , 18.8 %).

## B. Research Articles – Publication/Manuscript VIII

**HPLC** [0-100% Solvent B, 20 min]:  $R_t = 18.8$  min. **HRMS**: calculated 532.3387  $[C_{29}H_{45}N_3O_6+H]^+$ , found 532.3215  $[M+H]^+$ .  **$^1H$  NMR** (599 MHz,  $CDCl_3$ )  $\delta$  6.53 (s, 2H), 6.26 (s, 1H), 5.84 (d,  $J = 8.4$  Hz, 1H), 5.34 (s, 1H), 5.22 – 5.17 (m, 1H), 4.26 (ddd,  $J = 10.1, 8.4, 4.9$  Hz, 1H), 4.10 – 4.04 (m, 1H), 3.87 – 3.77 (m, 9H), 3.37 (d,  $J = 10.2$  Hz, 1H), 2.83 – 2.71 (m, 1H), 2.40 – 2.32 (m, 1H), 2.13 (qt,  $J = 10.9, 3.8$  Hz, 1H), 1.76 – 1.61 (m, 6H), 1.60 – 1.48 (m, 4H), 1.37 – 1.29 (m, 1H), 1.18 – 1.06 (m, 3H), 0.99 – 0.85 (m, 3H), 0.78 – 0.71 (m, 1H), 0.70 (d,  $J = 6.6$  Hz, 3H), 0.66 (d,  $J = 6.6$  Hz, 3H).  **$^{13}C$  NMR** (151 MHz,  $CDCl_3$ )  $\delta$  173.89, 173.74, 170.91, 153.51, 137.21, 133.22, 104.98, 60.81, 56.20, 55.30, 52.85, 51.07, 43.83, 41.43, 39.60, 32.66, 30.41, 26.45, 26.04, 25.97, 25.49, 24.93, 24.85, 22.73, 21.21, 20.49.

### **(S)-N-((2S,3S)-1-amino-3-methyl-1-oxopentan-2-yl)-1-((S)-2-cyclohexyl-2-(3,4,5-trimethoxyphenyl)acetyl)piperidine-2-carboxamide (16a)**

The general procedure was used with Fmoc-Ile-OH and **16a** was obtained after purification by flash chromatography (0% - 80% [EtOAc + 2 % MeOH + 0.1% TEA] in cyclohexane) obtained as colourless oil (13 mg, 25  $\mu$ mol, 31.3 %).

**HPLC** [0-100% Solvent B, 20 min]:  $R_t = 18.3$  min. **HRMS**: calculated 532.3387  $[C_{29}H_{45}N_3O_6+H]^+$ , found 532.3417  $[M+H]^+$ .  **$^1H$  NMR** (599 MHz,  $CDCl_3$ )  $\delta$  6.55 (s, 2H), 6.17 (d,  $J = 8.9$  Hz, 1H), 6.08 (s, 1H), 5.51 (s, 1H), 5.21 (d,  $J = 5.1$  Hz, 1H), 4.16 (dd,  $J = 8.9, 6.0$  Hz, 1H), 4.10 – 4.04 (m, 1H), 3.85 (s, 9H), 3.36 (d,  $J = 10.2$  Hz, 1H), 2.90 – 2.77 (m, 1H), 2.35 – 2.29 (m, 1H), 2.13 (qt,  $J = 11.0, 3.5$  Hz, 1H), 1.86 – 1.79 (m, 1H), 1.76 – 1.59 (m, 6H), 1.56 – 1.47 (m, 2H), 1.38 – 1.30 (m, 1H), 1.29 – 1.22 (m, 1H), 1.19 – 1.07 (m, 2H), 1.02 – 0.95 (m, 1H), 0.95 – 0.85 (m, 2H), 0.78 – 0.70 (m, 1H), 0.68 – 0.56 (m, 6H), 0.48 – 0.41 (m, 1H).  **$^{13}C$  NMR** (151 MHz,  $CDCl_3$ )  $\delta$  173.86, 172.97, 170.94, 153.40, 153.31, 137.13, 133.32, 105.12, 60.72, 57.07, 56.17, 55.14, 52.81, 43.86, 41.69, 35.64, 32.56, 30.47, 26.45, 26.02, 25.97, 25.63, 24.99, 24.00, 20.51, 15.45, 10.86.

### **(S)-N-((2R,3R)-1-amino-3-methyl-1-oxopentan-2-yl)-1-((S)-2-cyclohexyl-2-(3,4,5-trimethoxyphenyl)acetyl)piperidine-2-carboxamide (16b)**

The general procedure was used with Fmoc-D-Ile-OH and **16b** was obtained after purification by flash chromatography (0% - 80% [EtOAc + 2 % MeOH + 0.1% TEA] in cyclohexane) as colourless oil (26 mg, 49  $\mu$ mol, 61.3 %).

**HPLC** [0-100% Solvent B, 20 min]:  $R_t = 18.0$  min. **HRMS**: calculated 532.3387  $[C_{29}H_{45}N_3O_6+H]^+$ , found 532.3411  $[M+H]^+$ .  **$^1H$  NMR** (400 MHz,  $CDCl_3$ )  $\delta$  6.45 (s, 2H), 6.13

## B. Research Articles – Publication/Manuscript VIII

(d,  $J = 8.8$  Hz, 1H), 5.70 (s, 1H), 5.39 (s, 1H), 5.14 – 5.08 (m, 1H), 4.24 (dd,  $J = 8.7, 4.4$  Hz, 1H), 3.99 (d,  $J = 13.2$  Hz, 1H), 3.73 (d,  $J = 12.1$  Hz, 9H), 3.34 (d,  $J = 10.2$  Hz, 1H), 2.97 (ddd,  $J = 13.8, 12.3, 2.7$  Hz, 1H), 2.24 – 2.15 (m, 1H), 2.07 (qt,  $J = 11.0, 3.4$  Hz, 1H), 1.80 – 1.70 (m, 2H), 1.65 – 1.54 (m, 5H), 1.48 – 1.36 (m, 2H), 1.30 – 1.21 (m, 2H), 1.19 – 1.12 (m, 2H), 1.10 – 0.97 (m, 3H), 0.90 – 0.82 (m, 1H), 0.78 (t,  $J = 7.4$  Hz, 3H), 0.72 – 0.62 (m, 1H), 0.54 (d,  $J = 6.9$  Hz, 3H).  $^{13}\text{C}$  NMR (101 MHz,  $\text{CDCl}_3$ )  $\delta$  173.97, 173.65, 171.20, 153.32, 137.10, 133.48, 105.36, 60.78, 56.19, 55.84, 54.97, 52.81, 43.95, 41.32, 36.45, 32.58, 30.50, 26.46, 26.40, 26.06, 26.03, 25.62, 25.35, 20.40, 14.00, 11.60.

### **(S)-N-((S)-2-amino-1-cyclohexyl-2-oxoethyl)-1-((S)-2-cyclohexyl-2-(3,4,5-trimethoxyphenyl)acetyl)piperidine-2-carboxamide (17)**

The general procedure was used with Fmoc-Chg-OH and **17** was obtained after purification by flash chromatography (0% - 100% [EtOAc + 2% MeOH + 0.1% TEA] in cyclohexane) as colourless oil (22 mg, 39  $\mu\text{mol}$ , 48.8 %).

**HPLC** [0-100% Solvent B, 20 min]:  $R_t = 18.7$  min. **HRMS**: calculated 558.3543  $[\text{C}_{31}\text{H}_{47}\text{N}_3\text{O}_6+\text{H}]^+$ , found 558.3574  $[\text{M}+\text{H}]^+$ .  $^1\text{H}$  NMR (400 MHz,  $\text{DMSO}-d_6$ )  $\delta$  6.62 (s, 2H), 6.57 (s, 1H), 5.04 (d,  $J = 4.1$  Hz, 1H), 4.19 – 4.10 (m, 1H), 4.02 (dd,  $J = 8.8, 5.6$  Hz, 1H), 3.69 – 3.64 (m, 6H), 3.55 – 3.52 (m, 3H), 2.72 – 2.60 (m, 1H), 2.45 – 2.40 (m, 3H), 2.00 (d,  $J = 12.6$  Hz, 1H), 1.94 – 1.82 (m, 2H), 1.66 – 1.57 (m, 4H), 1.53 – 1.41 (m, 5H), 1.39 – 1.25 (m, 5H), 1.13 – 0.90 (m, 8H), 0.79 – 0.60 (m, 3H).  $^{13}\text{C}$  NMR (101 MHz,  $\text{DMSO}-d_6$ )  $\delta$  172.79, 172.53, 170.15, 153.02, 136.33, 134.11, 105.56, 60.36, 60.04, 56.31, 56.08, 55.94, 53.33, 51.74, 46.04, 43.45, 41.58, 32.23, 30.10, 29.78, 27.29, 26.50, 26.08, 25.93, 25.87, 25.60, 20.74.

### **(S)-N-((S)-2-amino-2-oxo-1-phenylethyl)-1-((S)-2-cyclohexyl-2-(3,4,5-trimethoxyphenyl)acetyl)piperidine-2-carboxamide (18a)**

The general procedure was used with Fmoc-Phg-OH and **18a** was obtained as pale yellow oil (38 mg, 69  $\mu\text{mol}$ , 86.3 %).

**HPLC** [0-100% Solvent B, 20 min]:  $R_t = 18.6$  min. **HRMS**: calculated 552.3074  $[\text{C}_{31}\text{H}_{41}\text{N}_3\text{O}_6+\text{H}]^+$ , found 552.3057  $[\text{M}+\text{H}]^+$ .  $^1\text{H}$  NMR (400 MHz,  $\text{DMSO}-d_6$ )  $\delta$  7.35 – 7.24 (m, 5H), 6.60 (s, 2H), 5.83 (s, 1H), 5.62 (s, 2H), 5.24 (t,  $J = 3.3$  Hz, 1H), 3.74 – 3.70 (m, 10H), 3.45 – 3.41 (m, 1H), 2.97 (dt,  $J = 12.3, 5.3$  Hz, 1H), 2.41 – 2.32 (m, 1H), 2.12 – 2.02 (m, 1H), 1.92 – 1.65 (m, 5H), 1.62 – 1.39 (m, 7H), 1.32 – 1.22 (m, 2H).  $^{13}\text{C}$  NMR (101 MHz,

## B. Research Articles – Publication/Manuscript VIII

DMSO-*d*<sub>6</sub>)  $\delta$  176.49, 172.83, 172.02, 155.39, 138.52, 137.39, 130.48, 128.88, 128.38, 127.05, 108.27, 60.70, 57.77, 57.51, 57.41, 56.83, 43.29, 41.29, 32.44, 26.81, 26.27, 26.02, 25.47, 22.24.

### **(S)-N-((R)-2-amino-2-oxo-1-phenylethyl)-1-((S)-2-cyclohexyl-2-(3,4,5-trimethoxyphenyl)acetyl)piperidine-2-carboxamide (18b)**

The general procedure was used with Fmoc-D-Phg-OH and **18b** was obtained after purification by flash chromatography (0% - 100% [EtOAc + 2% MeOH + 0.1% TEA] in cyclohexane) as pale yellow oil (24 mg, 43  $\mu$ mol, 53.2%).

**HPLC** [0-100% Solvent B, 20 min]:  $R_t$  = 17.8 min. **HRMS**: calculated 552.3074 [C<sub>31</sub>H<sub>41</sub>N<sub>3</sub>O<sub>6</sub>+H]<sup>+</sup>, found 552.3065 [M+H]<sup>+</sup>. **<sup>1</sup>H NMR** (400 MHz, CDCl<sub>3</sub>)  $\delta$  7.44 – 7.33 (m, 2H), 7.34 – 7.29 (m, 2H), 7.16 – 7.06 (m, 2H), 6.83 – 6.76 (m, 1H), 6.62 (s, 1H), 6.54 (s, 1H), 5.88 (s<sub>br</sub>, 1H), 5.78 – 5.75 (m, 2H), 5.34 – 5.30 (m, 1H), 5.29 – 5.24 (m, 1H), 3.84 – 3.77 (m, 9H), 3.39 (dd,  $J$  = 32.2, 10.1 Hz, 1H), 2.57 – 2.44 (m, 1H), 2.31 – 2.10 (m, 3H), 1.95 – 1.83 (m, 1H), 1.75 – 1.56 (m, 7H), 1.22 – 1.10 (m, 3H), 0.98 – 0.86 (m, 1H), 0.83 – 0.69 (m, 1H). **<sup>13</sup>C NMR** (101 MHz, CDCl<sub>3</sub>)  $\delta$  173.32, 171.74, 170.38, 153.35, 153.23, 138.16, 137.12, 133.73, 29.11, 128.89, 127.01, 126.61, 105.19, 60.81, 60.40, 56.91, 56.74, 55.36, 52.68, 43.57, 41.56, 32.74, 26.53, 25.67, 25.38, 21.06, 20.35.

### **(S)-N-((S)-1-amino-1-oxo-3-phenylpropan-2-yl)-1-((S)-2-cyclohexyl-2-(3,4,5-trimethoxyphenyl)acetyl)piperidine-2-carboxamide (19a)**

The general procedure was used with Fmoc-Phe-OH and **19a** was obtained after purification by flash chromatography (EtOAc + 0.1% TEA) as colourless solid (15 mg, 23  $\mu$ mol, 28.8 %).

**HPLC** [0-100% Solvent B, 20 min]:  $R_t$  = 19.1 min. **HRMS**: calculated 566.3230 [C<sub>32</sub>H<sub>43</sub>N<sub>3</sub>O<sub>6</sub> +H]<sup>+</sup>, found 566.3253 [M+H]<sup>+</sup>. **<sup>1</sup>H NMR** (400 MHz, DMSO-*d*<sub>6</sub>)  $\delta$  8.29 (s, 1H), 7.21 – 7.16 (m, 1H), 7.15 – 7.12 (m, 4H), 6.60 (s, 2H), 6.45 (s, 2H), 5.08 (t,  $J$  = 7.3 Hz, 1H), 5.01 (t,  $J$  = 3.2 Hz, 1H), 3.78 – 3.67 (m, 10H), 3.56 (dd,  $J$  = 12.4, 7.2 Hz, 1H), 3.39 (d,  $J$  = 1.8 Hz, 1H), 3.02 (dd,  $J$  = 12.4, 7.3 Hz, 1H), 2.88 (dt,  $J$  = 12.5, 5.3 Hz, 1H), 2.61 – 2.50 (m, 1H), 2.29 – 2.18 (m, 1H), 1.90 – 1.78 (m, 1H), 1.73 – 1.59 (m, 4H), 1.55 – 1.40 (m, 8H), 1.35 – 1.20 (m, 2H). **<sup>13</sup>C NMR** (101 MHz, DMSO-*d*<sub>6</sub>)  $\delta$  173.39, 172.96, 170.95, 153.11, 152.90, 138.43, 138.20, 136.67, 136.40, 134.95, 134.23, 129.67, 129.44, 128.38, 128.33, 126.54, 106.14, 105.97, 60.44, 60.27, 56.43, 56.16, 53.75, 52.56, 41.23, 37.92, 30.27, 26.54, 26.11, 20.03.

## B. Research Articles – Publication/Manuscript VIII

### **(S)-N-((R)-1-amino-1-oxo-3-phenylpropan-2-yl)-1-((S)-2-cyclohexyl-2-(3,4,5-trimethoxyphenyl)acetyl)piperidine-2-carboxamide (19b)**

The general procedure was used with Fmoc-D-Phe-OH and **19b** was obtained after purification by flash chromatography (50% [EtOAc + 0.1% TEA] - 100% [EtOAc + 1% TEA] in hexane) as white solid (19 mg, 34  $\mu$ mol, 21.3 %).

**HPLC** [0-100% Solvent B, 20 min]:  $R_t$  = 19.4 min. **HRMS**: calculated 566.3230  $[\text{C}_{32}\text{H}_{43}\text{N}_3\text{O}_6 + \text{H}]^+$ , found 566.3248  $[\text{M} + \text{H}]^+$ .  **$^1\text{H}$  NMR** (400 MHz, DMSO- $d_6$ )  $\delta$  7.29 (s, 1H), 7.21 – 7.12 (m, 3H), 7.10 – 7.04 (m, 1H), 6.55 (s, 1H), 6.51 (s, 2H), 4.91 – 4.81 (m, 1H), 4.67 (d,  $J$  = 4.8 Hz, 1H), 4.35 – 4.26 (m, 1H), 3.92 (d,  $J$  = 13.4 Hz, 1H), 3.72 – 3.62 (m, 7H), 3.61 – 3.51 (m, 3H), 3.30 – 3.24 (m, 3H), 2.98 – 2.84 (m, 2H), 1.92 – 1.83 (m, 1H), 1.77 – 1.67 (m, 2H), 1.62 – 1.52 (m, 3H), 1.45 (d,  $J$  = 12.9 Hz, 1H), 1.32 – 1.21 (m, 2H), 1.12 – 0.98 (m, 4H), 0.92 – 0.83 (m, 2H), 0.78 – 0.60 (m, 1H).  **$^{13}\text{C}$  NMR** (101 MHz, DMSO- $d_6$ )  $\delta$  173.39, 172.96, 170.95, 153.11, 152.90, 138.43, 138.20, 136.67, 136.40, 134.95, 134.23, 129.67, 129.44, 128.38, 128.33, 126.54, 106.14, 105.97, 60.44, 60.27, 56.43, 56.16, 53.75, 52.56, 41.23, 37.92, 30.27, 26.54, 26.11, 20.03.

### **(S)-N-((S)-1-amino-3-cyclohexyl-1-oxopropan-2-yl)-1-((S)-2-cyclohexyl-2-(3,4,5-trimethoxyphenyl)acetyl)piperidine-2-carboxamide (20)**

The general procedure was used with Fmoc-Cha-OH and **20** was obtained after purification by flash chromatography (50% - 100% [EtOAc + 0.1% TEA] in cyclohexane) as white solid (19 mg, 34  $\mu$ mol, 21.3 %).

**HPLC** [30-100% Solvent B, 10 min]:  $R_t$  = 18.5 min. **HRMS**: calculated 572.3700  $[\text{C}_{32}\text{H}_{49}\text{N}_3\text{O}_6 + \text{H}]^+$ , found 572.3736  $[\text{M} + \text{H}]^+$ .  **$^1\text{H}$  NMR** (400 MHz, DMSO- $d_6$ )  $\delta$  7.00 (s, 1H), 6.64 (s, 2H), 6.57 (s, 2H), 5.09 – 5.06 (m, 2H), 4.74 (d,  $J$  = 4.6 Hz, 1H), 4.39 – 4.29 (m, 2H), 4.23 – 4.12 (m, 2H), 3.72 (s, 3H), 3.70 (s, 6H), 2.71 (t,  $J$  = 12.3 Hz, 2H), 2.08 (d,  $J$  = 10.3 Hz, 1H), 1.99 – 1.90 (m, 2H), 1.65 – 1.51 (m, 9H), 1.44 – 1.34 (m, 4H), 1.22 – 1.15 (m, 4H), 0.85 – 0.76 (m, 3H), 0.67 – 0.58 (m, 3H).  **$^{13}\text{C}$  NMR** (101 MHz, DMSO- $d_6$ )  $\delta$  174.17, 172.78, 170.20, 153.10, 136.32, 134.23, 105.51, 60.14, 55.97, 55.48, 54.11, 53.48, 51.77, 50.48, 49.67, 43.39, 41.46, 34.06, 33.52, 32.28, 32.22, 31.78, 30.15, 26.39, 26.29, 26.12, 26.05, 20.79, 19.67, 18.28, 12.51, 10.09.

## B. Research Articles – Publication/Manuscript VIII

### **(S)-N-((S)-1-amino-1-oxo-4-phenylbutan-2-yl)-1-((S)-2-cyclohexyl-2-(3,4,5-trimethoxyphenyl)acetyl)piperidine-2-carboxamide (21)**

The general procedure was used with Fmoc-Homophe-OH and **21** was obtained after purification by flash chromatography (40% - 100% [EtOAc + 2 % MeOH + 0.1% TEA] in cyclohexane) as white solid (34 mg, 58  $\mu$ mol, 72.5 %).

**HPLC** [0-100% Solvent B, 10 min]:  $R_t$  = 19.2 min. **HRMS**: calculated 580.3387  $[C_{33}H_{45}N_3O_6+H]^+$ , found 580.3434  $[M+H]^+$ .  **$^1H$  NMR** (400 MHz, DMSO- $d_6$ )  $\delta$  7.23 – 7.12 (m, 2H), 6.98 – 6.80 (m, 3H), 6.63 (s, 2H), 5.06 (s, 1H), 4.37 (s, 1H), 4.24 – 4.01 (m, 2H), 3.64 – 3.48 (m, 3H), 3.06 – 2.93 (m, 9H), 2.93 – 2.82 (m, 1H), 2.42 – 2.16 (m, 2H), 2.05 – 1.90 (m, 3H), 1.74 (d,  $J$  = 12.6 Hz, 2H), 1.58 – 1.44 (m, 5H), 1.23 – 1.04 (m, 5H), 0.90 – 0.71 (m, 2H).  **$^{13}C$  NMR** (101 MHz, DMSO- $d_6$ )  $\delta$  173.39, 172.96, 170.95, 153.11, 152.90, 138.43, 138.20, 136.67, 136.40, 134.95, 134.23, 129.67, 129.44, 128.38, 128.33, 126.54, 106.14, 105.97, 60.44, 60.27, 56.43, 56.16, 53.75, 52.56, 41.23, 37.92, 30.27, 26.54, 26.11, 20.03.

### **(S)-N-((S)-1-amino-4-cyclohexyl-1-oxobutan-2-yl)-1-((S)-2-cyclohexyl-2-(3,4,5-trimethoxyphenyl)acetyl)piperidine-2-carboxamide (22)**

The general procedure was used with Fmoc-L-HomoCha-OH and **22** was obtained after purification by flash chromatography (0% - 80% [EtOAc + 2% MeOH + 0.1% TEA] in cyclohexane) as pale white oil (37 mg, 63  $\mu$ mol, 78.8 %).

**HPLC** [0-100% Solvent B, 10 min]:  $R_t$  = 19.2 min. **HRMS**: calculated 586.3856  $[C_{33}H_{51}N_3O_6+H]^+$ , found 586.3893  $[M+H]^+$ .  **$^1H$  NMR** (400 MHz,  $CDCl_3$ )  $\delta$  6.44 (s, 2H), 6.14 ( $s_{br}$ , 1H), 5.90 (d,  $J$  = 8.3 Hz, 1H), 5.49 ( $s_{br}$ , 1H), 5.19 – 5.09 (m, 1H), 4.15 – 4.07 (m, 1H), 3.94 (d,  $J$  = 6.5 Hz, 1H), 3.79 – 3.67 (m, 12H), 3.28 (d,  $J$  = 10.1 Hz, 1H), 2.77 – 2.65 (m, 1H), 2.32 – 2.23 (m, 1H), 2.09 – 2.01 (m, 1H), 1.82 – 1.74 (m, 1H), 1.69 – 1.44 (m, 12H), 1.11 – 0.98 (m, 6H), 0.94 – 0.81 (m, 3H), 0.74 – 0.66 (m, 3H), 0.63 – 0.52 (m, 2H).  **$^{13}C$  NMR** (101 MHz,  $CDCl_3$ )  $\delta$  173.68, 173.61, 170.92, 153.49, 137.18, 133.19, 104.93, 60.74, 60.38, 56.14, 55.36, 52.78, 52.53, 43.79, 41.49, 36.36, 33.26, 32.94, 32.90, 32.74, 30.45, 28.40, 26.91, 26.48, 26.47, 26.21, 26.15, 26.07, 26.01, 25.58, 24.96, 21.04, 20.53, 14.19.

### **(S)-N-((S)-1-amino-3-hydroxy-1-oxopropan-2-yl)-1-((S)-2-cyclohexyl-2-(3,4,5-trimethoxyphenyl)acetyl)piperidine-2-carboxamide (23a)**

The general procedure was used with Fmoc-L-Ser(OTrt)-OH and **23a** was obtained as pale yellow oil (32 mg, 63  $\mu$ mol, 78.8 %).

## B. Research Articles – Publication/Manuscript VIII

**HPLC** [0-100% Solvent B, 20 min]:  $R_t = 15.8$  min. **HRMS**: calculated 506.2866  $[C_{26}H_{39}N_3O_7+H]^+$ , found 506.2865  $[M+H]^+$ .  **$^1H$  NMR** (300 MHz,  $CDCl_3$ )  $\delta$  6.49 (s, 2H), 6.03 (s, 1H), 5.18 – 5.10 (m, 2H), 4.35 – 4.25 (m, 2H), 3.99 (d,  $J = 13.6$  Hz, 2H), 3.82 (s, 6H), 3.79 (s, 3H), 3.70 (dd,  $J = 11.3, 3.9$  Hz, 2H), 3.37 – 3.24 (m, 6H), 2.96 – 2.87 (m, 2H), 2.27 – 2.20 (m, 1H), 2.14 – 2.08 (m, 1H), 1.61 – 1.50 (m, 3H), 1.17 – 1.09 (m, 3H), 0.95 – 0.86 (m, 2H), 0.74 – 0.68 (m, 1H).  **$^{13}C$  NMR** (75 MHz,  $CDCl_3$ )  $\delta$  173.75, 173.27, 171.70, 153.28, 143.86, 137.02, 133.32, 129.40, 128.25, 126.24, 105.49, 61.78, 60.79, 56.27, 55.32, 53.00, 45.65, 43.75, 41.14, 32.64, 30.45, 26.45, 26.04, 25.35, 20.27, 17.67.

### **(S)-N-((R)-1-amino-3-hydroxy-1-oxopropan-2-yl)-1-((S)-2-cyclohexyl-2-(3,4,5-trimethoxyphenyl)acetyl)piperidine-2-carboxamide (23b)**

The general procedure was used with Fmoc-D-Ser(OTrt)-OH and **23b** was obtained after purification by flash chromatography (0% - 100% [EtOAc + 5% MeOH] in cyclohexane) as colourless oil (7 mg, 14  $\mu$ mol, 17.3 %).

**HPLC** [0-100% Solvent B, 20 min]:  $R_t = 16.9$  min. **HRMS**: calculated 506.2866  $[C_{26}H_{39}N_3O_7+H]^+$ , found 506.2881  $[M+H]^+$ .  **$^1H$  NMR** (599 MHz,  $CDCl_3$ )  $\delta$  6.71 (d,  $J = 8.0$  Hz, 1H), 6.47 (s, 2H), 6.44 (s<sub>br</sub>, 1H), 5.43 (s<sub>br</sub>, 1H), 5.08 (t,  $J = 4.3$  Hz, 1H), 4.38 – 4.30 (m, 1H), 4.01 – 3.94 (m, 2H), 3.82 (d,  $J = 12.4$  Hz, 9H), 3.53 (dd,  $J = 11.3, 4.8$  Hz, 1H), 3.37 (d,  $J = 10.0$  Hz, 1H), 3.02 (td,  $J = 13.7, 13.0, 2.9$  Hz, 1H), 2.23 – 2.15 (m, 2H), 2.11 (ddt,  $J = 10.8, 6.8, 3.3$  Hz, 1H), 1.84 (d,  $J = 12.6$  Hz, 1H), 1.72 – 1.61 (m, 5H), 1.33 – 1.27 (m, 3H), 1.18 – 1.10 (m, 2H), 0.93 – 0.84 (m, 2H), 0.79 – 0.70 (m, 2H).  **$^{13}C$  NMR** (151 MHz,  $CDCl_3$ )  $\delta$  173.92, 172.88, 171.73, 153.28, 137.11, 133.17, 105.52, 62.13, 60.82, 56.31, 55.37, 53.68, 53.23, 43.88, 41.16, 32.76, 30.51, 29.67, 26.47, 26.09, 25.48, 25.33, 20.22.

### **(S)-N-((S)-1-amino-4-hydroxy-1-oxobutan-2-yl)-1-((S)-2-cyclohexyl-2-(3,4,5-trimethoxyphenyl)acetyl)piperidine-2-carboxamide (24a)**

The general procedure was used with Fmoc-L-Homoser(Trt)-OH and **24a** was obtained after purification by flash chromatography (40% - 100% [EtOAc + 2 % MeOH + 0.1% TEA] in cyclohexane) as colourless oil (25 mg, 39  $\mu$ mol, 48.8 %).

**HPLC** [0-100% Solvent B, 20 min]:  $R_t = 14.8$  min. **HRMS**: calculated 503.2995  $[C_{27}H_{40}N_3O_6+H]^+$ , found 503.2771  $[M-O]^+$ .  **$^1H$  NMR** (400 MHz,  $DMSO-d_6$ )  $\delta$  6.64 (s, 1H), 6.60 (s, 2H), 5.09 – 5.04 (m, 1H), 4.80 (d,  $J = 5.1$  Hz, 1H), 4.31 – 4.27 (m, 1H), 4.23 – 4.13 (m, 2H), 4.08 – 3.97 (m, 2H), 3.72 – 3.71 (m, 6H), 3.63 – 3.62 (m, 3H), 3.10 – 2.99 (m, 1H),

## B. Research Articles – Publication/Manuscript VIII

2.76 – 2.68 (m, 1H), 2.36 – 2.26 (m, 2H), 2.09 – 2.00 (m, 2H), 1.95 – 1.88 (m, 1H), 1.84 – 1.67 (m, 2H), 1.62 – 1.54 (m, 4H), 1.51 – 1.43 (m, 2H), 1.42 – 1.32 (m, 3H), 1.14 – 1.01 (m, 3H).  $^{13}\text{C}$  NMR (101 MHz, DMSO- $d_6$ )  $\delta$  175.63, 175.61, 172.62, 171.11, 152.89, 148.19, 136.37, 134.45, 128.78, 128.19, 127.95, 106.18, 65.62, 60.33, 56.38, 56.17, 52.02, 48.17, 43.30, 41.57, 32.38, 30.32, 28.51, 28.30, 27.93, 27.00, 26.56, 26.11, 25.72, 24.53, 20.54, 18.29.

### **(S)-N-((R)-1-amino-4-hydroxy-1-oxobutan-2-yl)-1-((S)-2-cyclohexyl-2-(3,4,5-trimethoxyphenyl)acetyl)piperidine-2-carboxamide (24b)**

The general procedure was used with Fmoc-L-Homoser(Trt)-OH and **24b** was obtained as colourless oil (4 mg, 8  $\mu\text{mol}$ , 10.0 %).

**HPLC** [0-100% Solvent B, 20 min]:  $R_t$  = 14.9 min. **HRMS**: calculated 503.2995  $[\text{C}_{27}\text{H}_{40}\text{N}_3\text{O}_6+\text{H}]^+$ , found 503.2774  $[\text{M}-\text{O}]^+$ .  $^1\text{H}$  NMR (400 MHz, DMSO- $d_6$ )  $\delta$  6.64 (s, 1H), 6.60 (s, 2H), 5.09 – 5.04 (m, 1H), 4.80 (d,  $J$  = 5.1 Hz, 1H), 4.31 – 4.27 (m, 1H), 4.23 – 4.13 (m, 2H), 4.08 – 3.97 (m, 2H), 3.72 – 3.71 (m, 6H), 3.63 – 3.62 (m, 3H), 3.10 – 2.99 (m, 1H), 2.76 – 2.68 (m, 1H), 2.36 – 2.26 (m, 2H), 2.09 – 2.00 (m, 2H), 1.95 – 1.88 (m, 1H), 1.84 – 1.67 (m, 2H), 1.62 – 1.54 (m, 4H), 1.51 – 1.43 (m, 2H), 1.42 – 1.32 (m, 3H), 1.14 – 1.01 (m, 3H).  $^{13}\text{C}$  NMR (101 MHz, DMSO- $d_6$ )  $\delta$  175.63, 175.61, 172.62, 171.11, 152.89, 148.19, 136.37, 134.45, 128.78, 128.19, 127.95, 106.18, 65.62, 60.33, 56.38, 56.17, 52.02, 48.17, 43.30, 41.57, 32.38, 30.32, 28.51, 28.30, 27.93, 27.00, 26.56, 26.11, 25.72, 24.53, 20.54, 18.29.

### **(S)-2-((S)-1-((S)-2-cyclohexyl-2-(3,4,5-trimethoxyphenyl)acetyl)piperidine-2-carboxamido)pentanediamide (25a)**

The general procedure was used with Fmoc-Gln-OH and **25a** was obtained as colorless oil (25 mg, 46  $\mu\text{mol}$ , 57.5 %).

**HPLC** [0-100% Solvent B, 20 min]:  $R_t$  = 15.1 min. **HRMS**: calculated 547.3132  $[\text{C}_{28}\text{H}_{42}\text{N}_4\text{O}_7+\text{H}]^+$ , found 547.3187  $[\text{M}+\text{H}]^+$ .  $^1\text{H}$  NMR (300 MHz,  $\text{CDCl}_3$ )  $\delta$  6.77 (s<sub>br</sub>, 1H), 6.70 (d,  $J$  = 7.7 Hz, 1H), 6.54 (s<sub>br</sub>, 2H), 6.14 (s<sub>br</sub>, 1H), 5.76 (s<sub>br</sub>, 1H), 5.52 (s<sub>br</sub>, 1H), 5.17 – 5.07 (m, 1H), 4.42 – 4.30 (m, 1H), 4.00 (d,  $J$  = 14.2 Hz, 1H), 3.81 (dd,  $J$  = 14.3, 0.8 Hz, 9H), 3.38 (d,  $J$  = 10.1 Hz, 1H), 2.94 (t,  $J$  = 12.9 Hz, 1H), 2.24 – 1.99 (m, 3H), 1.96 – 1.77 (m, 3H), 1.73 – 1.52 (m, 6H), 1.38 – 1.22 (m, 3H), 1.18 – 1.08 (m, 2H), 1.00 – 0.85 (m, 2H), 0.78 – 0.56 (m, 2H).

## B. Research Articles – Publication/Manuscript VIII

$^{13}\text{C}$  NMR (75 MHz,  $\text{CDCl}_3$ )  $\delta$  174.79, 173.56, 173.10, 171.24, 153.23, 136.70, 133.79, 105.45, 60.81, 56.24, 55.21, 52.92, 51.63, 43.72, 41.35, 32.59, 30.76, 30.51, 27.96, 26.46, 26.07, 26.00, 25.38, 20.27.

### **(R)-2-((S)-1-((S)-2-cyclohexyl-2-(3,4,5-trimethoxyphenyl)acetyl)piperidine-2-carboxamido)pentanediamide (25b)**

The general procedure was used with Fmoc-D-Gln-OH and **25b** was obtained as colorless oil (28 mg, 51  $\mu\text{mol}$ , 64.4 %).

**HPLC** [0-100% Solvent B, 20 min]:  $R_t$  = 14.8 min. **HRMS**: calculated 547.3132  $[\text{C}_{28}\text{H}_{42}\text{N}_4\text{O}_7+\text{H}]^+$ , found 547.3196  $[\text{M}+\text{H}]^+$ .  $^1\text{H}$  NMR (300 MHz,  $\text{CDCl}_3$ )  $\delta$  6.79 (s<sub>br</sub>, 1H), 6.51 (s, 2H), 6.35 (s<sub>br</sub>, 1H), 5.85 (s<sub>br</sub>, 1H), 5.72 (s<sub>br</sub>, 1H), 5.16 – 5.08 (m, 1H), 4.38 – 4.28 (m, 1H), 4.02 (d,  $J$  = 13.7 Hz, 1H), 3.86 – 3.74 (m, 9H), 3.44 (d,  $J$  = 10.0 Hz, 1H), 3.20 – 3.06 (m, 2H), 2.56 – 2.41 (m, 2H), 2.28 – 2.19 (m, 1H), 2.16 – 2.06 (m, 3H), 1.83 (d,  $J$  = 11.8 Hz, 1H), 1.73 – 1.54 (m, 4H), 1.39 – 1.27 (m, 3H), 1.18 – 1.09 (m, 2H), 0.97 – 0.84 (m, 3H), 0.82 – 0.69 (m, 2H).  $^{13}\text{C}$  NMR (75 MHz,  $\text{CDCl}_3$ )  $\delta$  175.02, 173.79, 173.24, 171.24, 153.22, 136.92, 133.60, 105.53, 60.78, 56.24, 54.98, 53.24, 40.97, 32.62, 30.54, 27.97, 26.89, 26.46, 26.07, 25.44, 20.34, 17.68, 12.28.

### **(S)-N-((S)-1-amino-3-(1H-imidazol-4-yl)-1-oxopropan-2-yl)-1-((S)-2-cyclohexyl-2-(3,4,5-trimethoxyphenyl)acetyl)piperidine-2-carboxamide (26a)**

The general procedure was used with Fmoc-His(Trt)-OH. The trityl protection group was cleaved with 1% TFA and 1%TIS in DCM at RT for 5 h. The crude product was loaded on silica and purified by flash chromatography (50% [EtOAc + 2% MeOH + 0.1% TEA] -100% [EtOAc + 10% MeOH + 0.1% TEA] in cyclohexane) to obtain **26b** as colourless oil (20 mg, 36  $\mu\text{mol}$ , 45.0 %).

**HPLC** [0-100% Solvent B, 20 min]:  $R_t$  = 13.2 min. **HRMS**: calculated 556.3135  $[\text{C}_{29}\text{H}_{41}\text{N}_5\text{O}_6 +\text{H}]^+$ , found 556.3229  $[\text{M}+\text{H}]^+$ .  $^1\text{H}$  NMR (599 MHz,  $\text{CDCl}_3$ )  $\delta$  7.30 (s<sub>br</sub>, 1H), 7.06 (d,  $J$  = 8.4 Hz, 1H), 6.57 (s, 2H), 6.33 (s, 1H), 6.18 (s<sub>br</sub>, 1H), 5.10 – 5.04 (m, 1H), 4.71 – 4.64 (m, 1H), 4.02 – 3.93 (m, 1H), 3.79 (d,  $J$  = 57.4 Hz, 9H), 3.41 (d,  $J$  = 10.0 Hz, 1H), 2.98 (dd,  $J$  = 15.1, 4.9 Hz, 1H), 2.75 – 2.66 (m, 1H), 2.54 – 2.46 (m, 1H), 2.17 – 2.08 (m, 1H), 2.03 (d,  $J$  = 12.8 Hz, 1H), 1.82 (d,  $J$  = 12.1 Hz, 1H), 1.74 – 1.59 (m, 4H), 1.59 – 1.52 (m, 2H), 1.48 – 1.41 (m, 2H), 1.34 – 1.25 (m, 3H), 1.15 (q,  $J$  = 12.7 Hz, 2H), 0.95 – 0.86 (m, 1H), 0.82 – 0.73 (m, 1H).  $^{13}\text{C}$  NMR (151 MHz,  $\text{CDCl}_3$ )  $\delta$  173.85, 172.04, 171.54, 153.30, 136.71,

## B. Research Articles – Publication/Manuscript VIII

133.81, 133.30, 129.38, 116.83, 105.45, 60.78, 56.21, 55.11, 52.62, 51.50, 43.74, 41.19, 40.92, 32.50, 30.46, 28.08, 26.41, 26.03, 25.98, 25.12, 25.05, 19.94.

### **(S)-N-((R)-1-amino-3-(1H-imidazol-4-yl)-1-oxopropan-2-yl)-1-((S)-2-cyclohexyl-2-(3,4,5-trimethoxyphenyl)acetyl)piperidine-2-carboxamide (26b)**

The general procedure was used with Fmoc-D-His(Trt)-OH. The trityl protection group was cleaved with 1% TFA and 1%TIS in DCM at RT for 5 h. The crude product was loaded on silica and purified by flash chromatography (50% [EtOAc + 2% MeOH + 0.1% TEA] -100% [EtOAc + 10% MeOH + 0.1% TEA] in cyclohexane) to obtain **26a** as colourless oil (13 mg, 23  $\mu$ mol, 28.8 %).

**HPLC** [0-100% Solvent B, 20 min]:  $R_t$  = 13.7 min. **HRMS**: calculated 556.3135 [ $C_{29}H_{41}N_5O_6 + H$ ]<sup>+</sup>, found 556.3217 [ $M+H$ ]<sup>+</sup>. **<sup>1</sup>H NMR** (599 MHz,  $CDCl_3$ )  $\delta$  7.61 (s, 1H), 7.10 – 7.01 (m, 2H), 6.77 – 6.70 (m, 1H), 6.47 (s, 2H), 5.61 (s, 1H), 5.02 – 4.95 (m, 1H), 4.59 – 4.52 (m, 1H), 3.99 – 3.92 (m, 0H), 3.84 – 3.72 (m, 9H), 3.66 – 3.60 (m, 1H), 3.43 (d,  $J$  = 10.0 Hz, 1H), 3.23 – 3.12 (m, 1H), 2.94 – 2.81 (m, 2H), 2.18 – 2.03 (m, 2H), 1.80 (d,  $J$  = 12.4 Hz, 1H), 1.70 – 1.58 (m, 5H), 1.48 (tdd,  $J$  = 13.0, 8.2, 4.6 Hz, 2H), 1.34 – 1.28 (m, 3H), 1.17 – 1.07 (m, 2H), 0.98 – 0.86 (m, 1H), 0.79 – 0.70 (m, 1H). **<sup>13</sup>C NMR** (151 MHz,  $CDCl_3$ )  $\delta$  174.15, 173.14, 171.19, 153.17, 136.88, 134.53, 133.44, 105.60, 60.80, 56.28, 56.20, 55.14, 53.82, 52.48, 44.01, 41.07, 40.96, 32.67, 30.57, 28.73, 26.44, 26.10, 25.84, 25.19, 20.11.

### **(S)-N-(1-carbamoylcyclopropyl)-1-((S)-2-cyclohexyl-2-(3,4,5-trimethoxyphenyl)acetyl)piperidine-2-carboxamide (27)**

The general procedure was used with Fmoc-1-amino-cyclopropane carboxylic acid and **27** was obtained after purification by flash chromatography (0% - 100% [EtOAc + 2 % MeOH + 0.1% TEA] in cyclohexane) as colourless oil (18 mg, 36  $\mu$ mol, 45.0 %). **HPLC** [0-100% Solvent B, 20 min]:  $R_t$  = 16.8 min. **HRMS**: calculated 502.2917 [ $C_{27}H_{39}N_3O_6 + H$ ]<sup>+</sup>, found 502.2950 [ $M+H$ ]<sup>+</sup>. **<sup>1</sup>H NMR** (400 MHz,  $CDCl_3$ )  $\delta$  6.39 (s, 2H), 6.21 (s, 1H), 5.33 (s, 1H), 4.94 – 4.83 (m, 1H), 3.89 (d,  $J$  = 13.8 Hz, 1H), 3.75 (d,  $J$  = 5.1 Hz, 9H), 3.30 (d,  $J$  = 10.1 Hz, 1H), 2.70 (ddd,  $J$  = 14.5, 11.6, 3.2 Hz, 1H), 2.21 – 2.10 (m, 1H), 2.04 (qt,  $J$  = 11.0, 3.3 Hz, 1H), 1.67 – 1.40 (m, 9H), 1.36 – 1.16 (m, 5H), 1.14 – 0.99 (m, 2H), 0.83 (qd,  $J$  = 12.3, 3.3 Hz, 1H), 0.76 – 0.62 (m, 2H), 0.42 (ddd,  $J$  = 10.3, 7.6, 4.5 Hz, 1H). **<sup>13</sup>C NMR** (101 MHz,  $CDCl_3$ )  $\delta$  174.08, 173.91, 172.17, 153.63, 137.31, 132.96, 105.12, 60.85, 56.26, 55.62, 53.44, 43.83, 40.95, 34.33, 32.77, 30.42, 26.46, 26.08, 26.03, 25.05, 24.79, 19.98, 17.37, 16.87.

## B. Research Articles – Publication/Manuscript VIII

### **(S)-N-(1-carbamoylcyclobutyl)-1-((S)-2-cyclohexyl-2-(3,4,5-trimethoxyphenyl)acetyl)piperidine-2-carboxamide (28)**

The general procedure was used with Fmoc-1-amino-cyclobutane carboxylic acid and **28** was obtained after purification by flash chromatography (0% - 100% [EtOAc + 2 % MeOH + 0.1% TEA] in cyclohexane) as colourless oil (17 mg, 33  $\mu$ mol, 41.3 %).

**HPLC** [0-100% Solvent B, 20 min]:  $R_t$  = 18.9 min. **HRMS**: calculated 516.3074  $[\text{C}_{28}\text{H}_{41}\text{N}_3\text{O}_6+\text{H}]^+$ , found 516.3069  $[\text{M}+\text{H}]^+$ .  **$^1\text{H NMR}$**  (400 MHz,  $\text{CDCl}_3$ )  $\delta$  6.47 (s, 1H), 6.44 (s, 2H), 6.11 (s, 1H), 5.13 – 5.03 (m, 2H), 4.02 – 3.96 (m, 1H), 3.76 – 3.67 (m, 9H), 3.33 (d,  $J$  = 10.2 Hz, 1H), 2.80 (ddd,  $J$  = 13.9, 12.3, 2.8 Hz, 1H), 2.54 – 2.42 (m, 2H), 2.21 (dd,  $J$  = 13.5, 3.5 Hz, 1H), 2.13 – 2.03 (m, 1H), 1.83 – 1.70 (m, 2H), 1.69 – 1.52 (m, 8H), 1.52 – 1.39 (m, 3H), 1.31 – 1.21 (m, 2H), 1.13 – 1.00 (m, 2H), 0.88 – 0.75 (m, 1H), 0.68 (qd,  $J$  = 12.0, 3.4 Hz, 1H).  **$^{13}\text{C NMR}$**  (101 MHz,  $\text{CDCl}_3$ )  $\delta$  175.20, 173.73, 171.13, 153.55, 137.28, 133.33, 105.14, 60.76, 59.06, 56.28, 55.27, 52.59, 43.87, 41.10, 32.66, 31.42, 31.02, 30.42, 26.91, 26.47, 26.06, 26.00, 25.47, 24.84, 20.29, 15.53.

### **(S)-N-(1-carbamoylcyclopentyl)-1-((S)-2-cyclohexyl-2-(3,4,5-trimethoxyphenyl)acetyl)piperidine-2-carboxamide (29)**

The general procedure was used with Fmoc-1-amino-cyclopentane carboxylic acid and **29** was obtained as colourless oil (32 mg, 60  $\mu$ mol, 75.0 %).

**HPLC** [0-100% Solvent B, 20 min]:  $R_t$  = 18.1 min. **HRMS**: calculated 530.3230  $[\text{C}_{29}\text{H}_{43}\text{N}_3\text{O}_6+\text{H}]^+$ , found 530.3266  $[\text{M}+\text{H}]^+$ .  **$^1\text{H NMR}$**  (300 MHz,  $\text{CDCl}_3$ )  $\delta$  6.52 (s, 2H), 5.94 (s, 1H), 5.19 ( $s_{\text{br}}$ , 1H), 5.10 – 5.03 (m, 1H), 4.06 (dd,  $J$  = 13.2, 4.2 Hz, 1H), 3.88 – 3.73 (m, 9H), 3.39 (d,  $J$  = 10.2 Hz, 1H), 2.95 – 2.82 (m, 1H), 2.26 (d,  $J$  = 13.4 Hz, 1H), 2.17 – 1.98 (m, 3H), 1.88 – 1.75 (m, 2H), 1.74 – 1.44 (m, 10H), 1.41 – 1.24 (m, 4H), 1.23 – 1.06 (m, 3H), 0.96 – 0.84 (m, 1H), 0.83 – 0.68 (m, 1H).  **$^{13}\text{C NMR}$**  (75 MHz,  $\text{CDCl}_3$ )  $\delta$  175.86, 173.91, 171.21, 153.49, 137.33, 133.37, 105.24, 66.96, 60.73, 56.28, 55.10, 52.98, 43.82, 41.28, 37.23, 36.25, 32.54, 30.40, 26.42, 26.01, 25.96, 25.44, 24.88, 23.87, 23.67, 20.23.

### **(S)-N-(1-carbamoylcyclohexyl)-1-((S)-2-cyclohexyl-2-(3,4,5-trimethoxyphenyl)acetyl)piperidine-2-carboxamide (30)**

The general procedure was used with Fmoc-1-amino-cyclohexane carboxylic acid and **30** was obtained after purification by flash chromatography (0% - 100% [EtOAc + 2% MeOH + 0.1% TEA] in cyclohexane) as colourless oil (21 mg, 38  $\mu$ mol, 47.8 %).

## B. Research Articles – Publication/Manuscript VIII

**HPLC** [0-100 % Solvent B, 20 min]:  $R_t = 18.9$  min. **HRMS**: calculated 544.3387  $[\text{C}_{30}\text{H}_{45}\text{N}_3\text{O}_6+\text{H}]^+$ , found 544.3438  $[\text{M}+\text{H}]^+$ .  **$^1\text{H}$  NMR** (400 MHz,  $\text{CDCl}_3$ )  $\delta$  6.55 (s, 3H), 5.95 (s, 1H), 5.28 ( $s_{\text{br}}$ , 1H), 5.20 – 5.12 (m, 1H), 4.19 – 4.14 (m, 1H), 3.88 – 3.77 (m, 9H), 3.63 (ddt,  $J = 24.9, 12.1, 4.0$  Hz, 2H), 3.45 (d,  $J = 10.3$  Hz, 1H), 3.24 (td,  $J = 11.6, 2.6$  Hz, 1H), 3.14 – 2.95 (m, 2H), 2.37 – 2.25 (m, 1H), 2.22 – 2.12 (m, 1H), 2.10 – 2.06 (m, 1H), 2.05 – 1.96 (m, 2H), 1.86 – 1.73 (m, 4H), 1.73 – 1.63 (m, 4H), 1.62 – 1.55 (m, 2H), 1.55 – 1.41 (m, 2H), 1.39 – 1.29 (m, 2H), 1.17 (qd,  $J = 12.3, 2.9$  Hz, 2H), 0.93 (qd,  $J = 12.3, 3.4$  Hz, 1H), 0.77 (qd,  $J = 12.0, 3.5$  Hz, 1H).  **$^{13}\text{C}$  NMR** (101 MHz,  $\text{CDCl}_3$ )  $\delta$  175.06, 174.24, 171.35, 153.51, 137.37, 133.30, 105.29, 62.96, 62.70, 60.74, 57.22, 56.33, 54.99, 53.23, 44.04, 41.30, 32.79, 32.51, 31.83, 30.43, 26.43, 26.01, 25.98, 25.45, 24.89, 20.27.

### **(S)-N-(1-carbamoylcyclohexyl)-1-((S)-2-cyclohexyl-2-(3,4,5-trimethoxyphenyl)acetyl)piperidine-2-carboxamide (31)**

The general procedure was used with Fmoc-4-amino-tetrahydropyran-4-carboxylic acid and **31** was obtained after purification by flash chromatography (0% - 100% [EtOAc + 2% MeOH + 0.1% TEA] in cyclohexane) as colourless oil (19 mg, 35  $\mu\text{mol}$ , 43.5 %).

**HPLC** [0-100% Solvent B, 20 min]:  $R_t = 18.9$  min. **HRMS**: calculated 546.3179  $[\text{C}_{29}\text{H}_{44}\text{N}_3\text{O}_7 + \text{H}]^+$ , found 546.3201  $[\text{M}+\text{H}]^+$ .  **$^1\text{H}$  NMR** (400 MHz,  $\text{CDCl}_3$ )  $\delta$  6.55 (s, 3H), 5.95 (s, 1H), 5.28 (s, 1H), 5.20 – 5.12 (m, 1H), 4.19 – 4.14 (m, 1H), 3.88 – 3.77 (m, 9H), 3.63 (ddt,  $J = 24.9, 12.1, 4.0$  Hz, 2H), 3.45 (d,  $J = 10.3$  Hz, 1H), 3.24 (td,  $J = 11.6, 2.6$  Hz, 1H), 3.14 – 2.95 (m, 2H), 2.37 – 2.25 (m, 1H), 2.22 – 2.12 (m, 1H), 2.10 – 2.06 (m, 1H), 2.05 – 1.96 (m, 2H), 1.86 – 1.73 (m, 4H), 1.73 – 1.63 (m, 4H), 1.62 – 1.55 (m, 2H), 1.55 – 1.41 (m, 2H), 1.39 – 1.29 (m, 2H), 1.17 (qd,  $J = 12.3, 2.9$  Hz, 2H), 0.93 (qd,  $J = 12.3, 3.4$  Hz, 1H), 0.77 (qd,  $J = 12.0, 3.5$  Hz, 1H).  **$^{13}\text{C}$  NMR** (101 MHz,  $\text{CDCl}_3$ )  $\delta$  175.06, 174.24, 171.35, 153.51, 137.37, 133.30, 105.29, 62.96, 62.70, 60.74, 60.40, 57.22, 56.33, 54.99, 53.23, 44.04, 41.30, 32.79, 32.51, 31.83, 30.43, 26.43, 26.01, 25.98, 25.45, 24.89, 20.27, 14.20.

### **(S)-N-(1-((2-amino-2-oxoethyl)carbamoyl)cyclopentyl)-1-((S)-2-cyclohexyl-2-(3,4,5-trimethoxyphenyl)acetyl)piperidine-2-carboxamide (32)**

The general procedure was used with Fmoc-Gly-OH and Fmoc-1-amino-cyclopentane carboxylic acid (first coupling step repeated). **32** was obtained after purification by flash chromatography (0% - 100% [EtOAc + 2% MeOH + 0.1% TEA] in cyclohexane) as colourless oil (14 mg, 24  $\mu\text{mol}$ , 30.2 %).

## B. Research Articles – Publication/Manuscript VIII

**HPLC** [0-100% Solvent B, 20 min]:  $R_t = 19.1$  min. **HRMS**: calculated 587.3445  $[\text{C}_{31}\text{H}_{46}\text{N}_4\text{O}_7 + \text{H}]^+$ , found 587.3530  $[\text{M} + \text{H}]^+$ .  **$^1\text{H}$  NMR** (400 MHz,  $\text{CDCl}_3$ )  $\delta$  6.87 (s, 1H), 6.81 (t, 1H), 6.47 (s, 2H), 6.11 (s, 1H), 5.34 (s, 1H), 4.97 (t, 1H), 4.00 (d, 1H), 3.86 (dd, 1H), 3.76 (s, 6H), 3.72 (s, 3H), 3.62 (dd, 1H), 3.34 (d, 1H), 2.86 (m, 1H), 2.19 – 2.02 (m, 3H), 1.90 – 1.84 (m, 3H), 1.74 (d, 2H), 1.65 – 1.52 (m, 8H), 1.32 – 1.16 (m, 5H), 1.11 – 1.01 (m, 2H), 0.82 (qd, 1H), 0.75 – 0.57 (m, 1H).  **$^{13}\text{C}$  NMR** (101 MHz,  $\text{CDCl}_3$ )  $\delta$  174.27, 173.39, 172.17, 172.03, 153.56, 137.39, 133.37, 105.23, 66.78, 60.77, 56.32, 55.10, 53.26, 44.12, 43.10, 41.30, 37.56, 36.40, 32.52, 30.39, 26.41, 26.00, 25.96, 25.38, 24.82, 23.88, 20.31.

### ASSOCIATED CONTENT

Full characterization and synthetic procedures of all intermediates as well as crystallography information can be found in the supporting information. This material is available free of charge via the Internet at <http://pubs.acs.org>.

### AUTHOR INFORMATION

#### Corresponding Author

\* Dr. Felix Hausch, Max Planck Institute of Psychiatry, Dept. Translational Research in Psychiatry, Kraepelinstrasse 2, 80804 Munich, Germany; e-mail: [hausch@psych.mpg.de](mailto:hausch@psych.mpg.de)

#### Author Contributions

\*These authors contributed equally. All authors have given approval to the final version of the manuscript.

#### Notes

The authors declare no competing financial interest

#### ACKNOWLEDGMENT

This work was supported by the M4 award 2011 to F.H. We are indebted to Claudia Dubler (Ludwig-Maximilians-University, München) and Elisabeth Weyher (Max Planck Institute of Biochemistry, Martinsried) for measurement of the NMR spectra and high-resolution mass spectra, respectively. We thank the staff at the European Synchrotron Radiation Facility (ESRF) in Grenoble, France, and at SLS beamline PX-II, Villigen, Switzerland.

#### ABBREVIATIONS

FKBP, FK506-binding protein; HA, hydrogen bond acceptor; FP, fluorescence polarization.

## B. Research Articles – Publication/Manuscript VIII

### REFERENCES

1. Cioffi, D. L.; Hubler, T. R.; Scammell, J. G., Organization and function of the FKBP52 and FKBP51 genes. *Curr Opin Pharmacol* 2011, 11, (4), 308-13.
2. Sanchez, E. R., Chaperoning steroidal physiology: Lessons from mouse genetic models of Hsp90 and its cochaperones. *Biochim Biophys Acta* 2012, 1823, (3), 722-29.
3. Storer, C. L.; Dickey, C. A.; Galigniana, M. D.; Rein, T.; Cox, M. B., FKBP51 and FKBP52 in signaling and disease. *Trends Endocrinol Metab* 2011, 22, (12), 481-90.
4. Albu, S.; Romanowski, C. P.; Letizia Curzi, M.; Jakubcakova, V.; Flachskamm, C.; Gassen, N. C.; Hartmann, J.; Schmidt, M. V.; Schmidt, U.; Rein, T.; Holsboer, F.; Hausch, F.; Paez-Pereda, M.; Kimura, M., Deficiency of FK506-binding protein (FKBP) 51 alters sleep architecture and recovery sleep responses to stress in mice. *J Sleep Res* 2014, 23, (2), 176-85.
5. Hartmann, J.; Wagner, K. V.; Liebl, C.; Scharf, S. H.; Wang, X.-D.; Wolf, M.; Hausch, F.; Rein, T.; Schmidt, U.; Touma, C.; Cheung-Flynn, J.; Cox, M. B.; Smith, D. F.; Holsboer, F.; Müller, M. B.; Schmidt, M. V., The involvement of FK506-binding protein 51 (FKBP5) in the behavioral and neuroendocrine effects of chronic social defeat stress. *Neuropharmacology* 2012, 62, (1), 332-39.
6. Touma, C.; Gassen, N. C.; Herrmann, L.; Cheung-Flynn, J.; Bull, D. R.; Ionescu, I. A.; Heinzmann, J. M.; Knapman, A.; Siebertz, A.; Depping, A. M.; Hartmann, J.; Hausch, F.; Schmidt, M. V.; Holsboer, F.; Ising, M.; Cox, M. B.; Schmidt, U.; Rein, T., FK506 binding protein 5 shapes stress responsiveness: modulation of neuroendocrine reactivity and coping behavior. *Biol Psychiatry* 2011, 70, (10), 928-36.
7. Zannas, A. S.; Binder, E. B., Gene–environment interactions at the FKBP5 locus: sensitive periods, mechanisms and pleiotropism. *Genes Brain Behav* 2014, 13, (1), 25-37.
8. Zannas, A. S.; Wiechmann, T.; Gassen, N. C.; Binder, E. B., Gene-Stress-Epigenetic Regulation of FKBP5: Clinical and Translational Implications. *Neuropsychopharmacology* 2015, doi: 10.1038/npp.2015.235.
9. Schmidt, M. V.; Paez-Pereda, M.; Holsboer, F.; Hausch, F., The Prospect of FKBP51 as a Drug Target. *ChemMedChem* 2012, 7, (8), 1351-9.
10. Hausch, F., FKBP5 and their role in neuronal signaling. *Biochim Biophys Acta* 2015, 1850, 2035-40.
11. Babine, R. E.; Villafranca, J. E.; Gold, B. G., FKBP immunophilin patents for neurological disorders. *Expert Opin Ther Patents* 2005, 15, (5), 555-73.
12. Blackburn, E. A.; Walkinshaw, M. D., Targeting FKBP isoforms with small-molecule ligands. *Curr Opin Pharmacol* 2011, 11, (4), 365-71.
13. Feng, X.; Pomplun, S.; Hausch, F., Recent progress in FKBP ligand development. *Curr Mol Pharmacol* 2015, DOI: 10.2174/1874467208666150519113313.
14. Gaali, S.; Gopalakrishnan, R.; Wang, Y.; Kozany, C.; Hausch, F., The chemical biology of immunophilin ligands. *Curr Med Chem* 2011, 18, (35), 5355-79.
15. Wang, X. J.; Etkorn, F. A., Peptidyl-prolyl isomerase inhibitors. *Biopolymers* 2006, 84, (2), 125-46.
16. Bracher, A.; Kozany, C.; Hähle, A.; Wild, P.; Zacharias, M.; Hausch, F., Crystal Structures of the Free and Ligand-Bound FK1-FK2 Domain Segment of FKBP52 Reveal a Flexible Inter-Domain Hinge. *J Mol Biol* 2013, 425, (22), 4134-44.
17. Bracher, A.; Kozany, C.; Thost, A. K.; Hausch, F., Structural characterization of the PPIase domain of FKBP51, a cochaperone of human Hsp90. *Acta Crystallogr D Biol Crystallogr* 2011, 67, (6), 549-59.
18. LeMaster, D. M.; Mustafi, S. M.; Brecher, M.; Zhang, J.; Heroux, A.; Li, H.; Hernandez, G., Coupling of conformational transitions in the N-terminal domain of the 51 kDa FK506-binding protein (FKBP51) near its site of interaction with the steroid receptor proteins. *J Biol Chem* 2015, 290, 15746-57.
19. Marz, A. M.; Fabian, A.-K.; Kozany, C.; Bracher, A.; Hausch, F., Large FK506-Binding Proteins Shape the Pharmacology of Rapamycin. *Mol Cell Biol* 2013, 33, (7), 1357-1367.
20. Mustafi, S. M.; Lemaster, D. M.; Hernandez, G., Differential conformational dynamics in the closely homologous FK506-binding domains of FKBP51 and FKBP52. *Biochem J* 2014, 461, (1), 115-23.
21. Sinars, C. R.; Cheung-Flynn, J.; Rimerman, R. A.; Scammell, J. G.; Smith, D. F.; Clardy, J., Structure of the large FK506-binding protein FKBP51, an Hsp90-binding protein and a component of steroid receptor complexes. *Proc Natl Acad Sci U S A* 2003, 100, (3), 868-73.
22. Wu, B.; Li, P.; Liu, Y.; Lou, Z.; Ding, Y.; Shu, C.; Ye, S.; Bartlam, M.; Shen, B.; Rao, Z., 3D structure of human FK506-binding protein 52: implications for the assembly of the glucocorticoid receptor/Hsp90/immunophilin heterocomplex. *Proc Natl Acad Sci U S A* 2004, 101, (22), 8348-53.

## B. Research Articles – Publication/Manuscript VIII

23. Bischoff, M.; Sippel, C.; Bracher, A.; Hausch, F., Stereoselective Construction of the 5-Hydroxy Diazabicyclo[4.3.1]decane-2-one Scaffold, a Privileged Motif for FK506-Binding Proteins. *Org Lett* 2014, 16, 5254-7.
24. Gopalakrishnan, R.; Kozany, C.; Gaali, S.; Kress, C.; Hoogeland, B.; Bracher, A.; Hausch, F., Evaluation of Synthetic FK506 Analogues as Ligands for the FK506-Binding Proteins 51 and 52. *J Med Chem* 2012, 55, (9), 4114-22.
25. Gopalakrishnan, R.; Kozany, C.; Wang, Y.; Schneider, S.; Hoogeland, B.; Bracher, A.; Hausch, F., Exploration of Pipecolate Sulfonamides as Binders of the FK506-Binding Proteins 51 and 52. *J Med Chem* 2012, 55, (9), 4123-31.
26. Pomplun, S.; Wang, Y.; Kirschner, A.; Kozany, C.; Bracher, A.; Hausch, F., Rational Design and Asymmetric Synthesis of Potent and Neurotrophic Ligands for FK506-Binding Proteins (FKBPs). *Angew Chem Int Ed Engl* 2015, 54, 345-8.
27. Wang, Y.; Kirschner, A.; Fabian, A. K.; Gopalakrishnan, R.; Kress, C.; Hoogeland, B.; Koch, U.; Kozany, C.; Bracher, A.; Hausch, F., Increasing the Efficiency of Ligands for FK506-Binding Protein 51 by Conformational Control. *J Med Chem* 2013, 56, (10), 3922-35.
28. Gaali, S.; Kirschner, A.; Cuboni, S.; Hartmann, J.; Kozany, C.; Balsevich, G.; Namendorf, C.; Fernandez-Vizarra, P.; Sippel, C.; Zannas, A. S.; Draenert, R.; Binder, E. B.; Almeida, O. F. X.; Rühter, G.; Uhr, M.; Schmidt, M. V.; Touma, C.; Bracher, A.; Hausch, F., Selective inhibitors of the FK506-binding protein 51 by induced fit. *Nat Chem Biol* 2015, 11, (1), 33-37.
29. Hartmann, J.; Wagner, K. V.; Gaali, S.; Kirschner, A.; Kozany, C.; Rühter, G.; Hoeijmakers, L.; Westerholz, S.; Uhr, M.; Chen, A.; Holsboer, F.; Hausch, F.; Schmidt, M. V., Pharmacological inhibition of the psychiatric risk factor FKBP51 has anxiolytic properties. *J Neurosci* 2015, 35, 9007-16.
30. Romano, S.; Xiao, Y.; Nakaya, M.; D'Angelillo, A.; Chang, M.; Jin, J.; Hausch, F.; Masullo, M.; Feng, X.; Romano, M. F.; Sun, S. C., FKBP51 employs both scaffold and isomerase functions to promote NF-kappaB activation in melanoma. *Nucleic Acids Res* 2015, 43, (14), 6983-93.
31. Wager, T. T.; Chandrasekaran, R. Y.; Hou, X.; Troutman, M. D.; Verhoest, P. R.; Villalobos, A.; Will, Y., Defining desirable central nervous system drug space through the alignment of molecular properties, *in vitro* ADME, and safety attributes. *ACS Chem Neurosci* 2010, 1, (6), 420-34.
32. Devigny, C.; Perez-Balderas, F.; Hoogeland, B.; Cuboni, S.; Wachtel, R.; Mauch, C. P.; Webb, K. J.; Deussing, J. M.; Hausch, F., Biomimetic screening of class-B G protein-coupled receptors. *J Am Chem Soc* 2011, 133, (23), 8927-33.
33. Kozany, C.; März, A.; Kress, C.; Hausch, F., Fluorescent Probes to Characterise FK506-Binding Proteins. *ChemBioChem* 2009, 10, (8), 1402-10.

## B. Research Articles – Publication/Manuscript VIII

### SUPPORTING INFORMATION

#### **Rapid, structure-based exploration of pipecolic acid amides as novel selective antagonists of the FK506-binding protein 51**

Steffen Gaali\*, Xixi Feng\*, Claudia Sippel\*, Andreas Bracher<sup>#</sup>, Felix Hausch\*

\* Max Planck Institute of Psychiatry, Dept. Translational Research in Psychiatry, Kraepelinstrasse 2, 80804 Munich, Germany

<sup>#</sup> Max Planck Institute of Biochemistry, Am Klopferspitz 18, 82152 Martinsried, Germany

#### **Table of contents**

- I. Crystallography
- II. Chemistry
- III. References

## I. Crystallography

Dataset	FKBP51·3	FKBP51·14
<b>Data collection</b>		
Space group	$P2_12_12_1$	$P6_3$
Cell dimensions a, b, c (Å)	45.029, 48.414, 56.852	82.16, 82.16, 50.19
$\alpha, \beta, \gamma$ (°)	90, 90, 90	90, 90, 120
Wavelength (Å)	1.03679	0.97895
Resolution (Å)	48.41 - 1.3 (1.37 – 1.3)*	41.08 - 1.65 (1.68 - 1.65)
$R_{\text{merge}}$	0.053 (1.043)	0.077 (0.922)
$I/\sigma I$	15.7 (1.7)	12.1 (1.3)
Completeness (%)	99.5 (97.0)	99.1 (89.6)
Redundancy	8.3 (7.4)	4.8 (3.0)
<b>Refinement</b>		
Resolution (Å)	30 – 1.3	30 - 1.65
No reflections	29490	21944
$R_{\text{work}} / R_{\text{free}}$	0.144 / 0.186	0.261 / 0.297
Number of atoms		
Protein	1042	966
Ligand/ion	54	38
Water	141	63
<i>B</i> -factors		
Protein	21.37	26.69
Ligand/ion	15.74	18.59
Water	34.43	33.91
R.m.s. deviations		
Bond length (Å)	0.025	0.011
Bond angles (°)	2.350	1.513

\* Values in parenthesis for outer shell.

*Crystallization*

**3:** The complex was prepared by mixing FKBP51 (16-140)-A19T protein at 1.75 mM with 20 mM **3** dissolved in DMSO in 9:1 ratio. Crystallization was performed at 20 °C using the hanging drop vapor-diffusion method, equilibrating mixtures of 1  $\mu$ l protein complex and 1  $\mu$ l reservoir against 500  $\mu$ l reservoir solution. Rod-shaped crystals were obtained with reservoir solution containing 10 % PEG-3350, 0.2 M  $\text{NH}_4$ -acetate and 0.1 M HEPES-NaOH pH 7.5.

**29:** The complex was prepared by mixing FKBP51 (16-140)-A19T protein at 1.75 mM with 30 mM **29** dissolved in DMSO in 9:1 ratio. Crystallization was performed at 20 °C using the hanging drop vapor-diffusion method, equilibrating mixtures of 1  $\mu$ l protein complex and 1  $\mu$ l

## B. Research Articles – Publication/Manuscript VIII

reservoir against 500  $\mu$ l reservoir solution. Needle-shaped crystals were obtained with reservoir solution containing 16 % PEG-3350, 0.2 M  $\text{NH}_4$ -acetate and 0.1 M HEPES-NaOH pH 7.5.

### *Structure Solution and Refinement*

The diffraction data were collected at beamlines X10SA (3) of the Swiss Synchrotron Light Source (SLS) in Villigen, Switzerland, and ID29 (29) of the European Synchrotron Radiation Facility (ESRF) in Grenoble, France. Diffraction data were integrated with XDS<sup>1</sup>, and further processed with Aimless and Ctruncate<sup>2</sup>, as implemented in the CCP4i interface<sup>3</sup>. The crystal structures were solved by molecular replacement employing the program Molrep<sup>4</sup>. Iterative model improvement and refinement were performed with Coot<sup>5</sup> and Refmac5<sup>6</sup>. The dictionaries for the compounds were generated with the PRODRG server<sup>7</sup>. Residues facing solvent channels without detectable side chain density were modeled as alanines.

Large solvent channels running through the crystal lattice of the FKBP51·29 complex contained considerable density for disordered molecules. The disorder could not be resolved, even when the data were processed in spacegroup *P*1, and was not included into the crystallographic model. The difference density for the ligand in the ordered molecules was however clear and readily interpretable.

Molecular graphics figures were generated with the program Pymol<sup>8</sup>. (DeLano, 2002).

## II. Chemistry

Chromatographic separations were performed either by manual flash chromatography or automated flash chromatography using an Interchim Puriflash 430 with an UV detector.

Merck F-254 (thickness 0.25 mm) commercial plates were used for analytical TLC. <sup>1</sup>H NMR spectra, <sup>13</sup>C NMR spectra, 2D HSQC, HMBC, and COSY of all intermediates were obtained from the Department of Chemistry and Pharmacy, LMU, on a Bruker AC 300, a Bruker XL 400, or a Bruker AMX 600 at room temperature. Chemical shifts for <sup>1</sup>H or <sup>13</sup>C are given in ppm ( $\delta$ ) downfield from tetramethylsilane using residual protio solvent as an internal standard.

Mass spectra (*m/z*) were recorded on a Thermo Finnigan LCQ DECA XP Plus mass spectrometer at the Max Planck Institute of Psychiatry, while the high resolution mass spectrometry was carried out at MPI for Biochemistry (Microchemistry Core Facility) on Bruker Daltonics MicrOTOF.

The purity of the compounds was verified by reversed phase HPLC. All gradients were started after 1 min of equilibration with starting percentage of solvent mixture. All of the final compounds synthesized and tested have a purity of more than 95%.

### Analytical HPLC:

<b>Pump:</b>	Beckman System Gold 125S Solvent Module
<b>Detector:</b>	Beckman System Gold Diode Array Detector Module 168
<b>Column:</b>	Phenomenex Jupiter 4 $\mu$ Proteo 90Å, 250 x 4.6 mm 4 micron
<b>Solvent A:</b>	95% H <sub>2</sub> O, 5% MeCN, 0.1% TFA
<b>Solvent B:</b>	95% MeCN, 5% H <sub>2</sub> O, 0.1% TFA
<b>Methods:</b>	Described for the specific compound

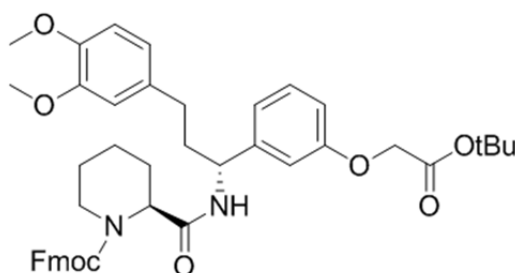
## B. Research Articles – Publication/Manuscript VIII

### Preparative HPLC:

<b>Pump:</b>	Beckman System Gold Programmable Solvent Module 126 NMP
<b>Detector:</b>	Beckman Programmable Detector Module 166
<b>Column:</b>	Phenomenex Jupiter 10 $\mu$ Proteo 90 Å, 250 x 21.2 mm 10 micron
<b>Solvent A:</b>	95% H <sub>2</sub> O, 5% MeOH, 0.1% TFA
<b>Solvent B:</b>	95% MeOH, 5% H <sub>2</sub> O, 0.1% TFA

**Methods:** Described for the specific compound

### **(S)-1-((9H-Fluoren-9-yl)methyl)ester-2-((R)-1-(3-(2-(tert-butoxy)-2-oxoethoxy) phenyl)-3-(3,4-dimethoxyphenyl)propyl) piperidine-2-carboxylate (3-1)**



**3-1**

(S)-Fmoc-Pip-OH (0.25 g, 0.71 mmol), DIPEA (0.50 mL, 2.85 mmol) and HATU (410 mg, 1.07 mmol) were dissolved in DMF (1.5 mL) and stirred for 30 min at RT. Then (R)-tert-butyl-2-(3-(1-amino-3-(3,4-dimethoxyphenyl)propyl)phenoxy)acetate (0.29 g, 0.71 mmol)\* dissolved in DCM (2.0 mL) was added to the reaction mixture and stirred at RT for 16 h. The solvent was removed *in vacuo* and the crude product was purified by flash chromatography (EtOAc/cyclohexane 3:7) to afford the title compound (0.48 g, 0.65 mmol, 92.1 %) as a light yellow solid.

\* provided by Lead Discovery Center GmbH, Dortmund (LDC046341)

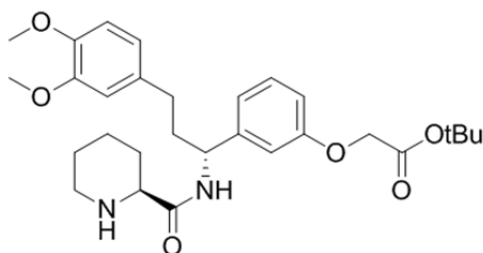
**HPLC** [0-100% Solvent B, 20 min]:  $R_t = 20.5$  min.

**Mass:** (ESI<sup>+</sup>), calculated 531.25 [C<sub>44</sub>H<sub>50</sub>N<sub>2</sub>O<sub>8</sub>+H]<sup>+</sup>, found 531.21 [M+H]<sup>+</sup>.

**<sup>1</sup>H NMR** (400 MHz, DMSO)  $\delta$  7.83-7.80 (m, 2H), 7.63-7.58 (m, 2H), 7.46 – 7.39 (m, 4H), 7.32 – 7.20 (m, 2H), 7.04-7.02 (m, 2H), 6.88-6.84 (m, 3H), 6.80 – 6.74 (m, 2H), 5.20-5.17 (m, 1H), 5.00 – 4.93 (m, 4H), 4.83 (t, J = 6.2 Hz, 1H), 4.17-4.11 (m, 1H), 3.83 (s, 3H), 3.75 (s, 3H), 3.53-3.47 (m, 1H), 2.82 (t, J = 4.3 Hz, 1H), 2.69 (t, J = 7.9 Hz, 2H), 2.34-2.20 (m, 2H), 2.08-1.91 (m, 2H), 1.79-1.66 (m, 3H), 1.34 (s, 9H).

**<sup>13</sup>C NMR** (101 MHz, DMSO)  $\delta$  170.45, 168.32, 162.49, 158.23, 155.70, 148.71, 147.54, 145.61, 144.45, 141.16, 134.01, 129.35, 128.18, 127.22, 125.45, 120.40, 119.48, 113.43, 112.65, 112.08, 81.47, 64.94, 59.93, 55.91, 54.51, 51.97, 46.97, 41.90, 38.41, 36.27, 32.22, 31.25, 28.31, 26.80, 24.78, 21.20.

**tert-Butyl-2-(3-((R)-3-(3,4-dimethoxyphenyl)-1-((S)-piperidine-2-carboxamido)propyl)phenoxy) acetate (3-2)**



**3-2**

**3-1** (0.43 g, 0.59 mmol) was dissolved in DCM (4.5 mL) and 4-methylpiperidine (0.5 mL). After stirring at RT for 16 h, the reaction mixture was concentrated and the crude product purified by flash chromatography (0-100 % (EtOAc + 1 % MeOH + 1 % TEA) in cyclohexane). The title compound (160 mg, 0.31 mmol, 53.1 %) was obtained as a colourless solid.

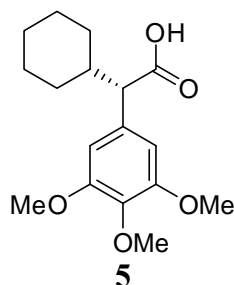
**Mass:** (ESI<sup>+</sup>), calculated 530.30 [C<sub>29</sub>H<sub>40</sub>N<sub>2</sub>O<sub>6</sub>+H]<sup>+</sup>, found 530.28 [M+H]<sup>+</sup>.

**HPLC** [0-100% Solvent B, 20 min]: R<sub>t</sub> = 14.8 min.

**<sup>1</sup>H NMR** (300 MHz, CDCl<sub>3</sub>) δ 7.26 – 7.20 (m, 1H), 7.18 (d, *J* = 9.4 Hz, 1H), 6.94 – 6.88 (m, 1H), 6.86 (dd, *J* = 2.6, 1.5 Hz, 1H), 6.78 – 6.72 (m, 2H), 6.69 – 6.64 (m, 2H), 4.96 (q, *J* = 7.7 Hz, 1H), 4.49 (s, 2H), 3.85 (s, 3H), 3.83 (s, 3H), 3.23 – 3.15 (m, 1H), 3.02 – 2.91 (m, 1H), 2.68 – 2.58 (m, 1H), 2.59 – 2.50 (m, 2H), 2.21 – 2.00 (m, 4H), 1.98 – 1.87 (m, 1H), 1.80 – 1.70 (m, 1H), 1.59 – 1.49 (m, 1H), 1.47 (s, 9H).

**<sup>13</sup>C NMR** (75 MHz, CDCl<sub>3</sub>) δ 172.71, 167.65, 158.24, 148.73, 146.82, 144.02, 133.90, 129.60, 120.08, 119.82, 113.37, 112.87, 111.74, 111.20, 82.20, 65.69, 60.12, 55.90, 52.51, 45.68, 37.93, 32.24, 29.75, 28.02, 25.69, 23.88.

**(S)-2-cyclohexyl-2-(3,4,5-trimethoxyphenyl)acetic acid (5)**



Synthesized as previously described.<sup>10</sup>

## B. Research Articles – Publication/Manuscript VIII

### III. References

1. Kabsch, W. (2010). XDS. *Acta Crystallogr. D Biol. Crystallogr.* *66*, 125-132.
2. Potterton, E., Briggs, P., Turkenburg, M., and Dodson, E. (2003). A graphical user interface to the CCP4 program suite. *Acta crystallographica* *59*, 1131-1137.
3. French, G.S., and Wilson, K.S. (1978). On the treatment of negative intensity observations. *Acta Crystallogr. A* *34*, 517-525.
4. Collaborative Computational Project, N. (1994). The CCP4 suite: programs for protein crystallography. *Acta Crystallogr. D Biol. Crystallogr.* *50*, 760-763.
5. Vagin, A.A., and Isupov, M.N. (2001). Spherically averaged phased translation function and its application to the search for molecules and fragments in electron-density maps. *Acta Crystallogr. D Biol. Crystallogr.* *57*, 1451-1456.
6. Emsley, P., and Cowtan, K. (2004). Coot: model-building tools for molecular graphics. *Acta Crystallogr. D Biol. Crystallogr.* *60*, 2126-2132.
7. Evans, P.R. (1997). Scala. *Joint CCP4 and ESF-EACBM Newsletter* *33*, 22-24.
8. Schüttelkopf, A.W., and van Aalten, D.M. (2004). PRODRG: a tool for high-throughput crystallography of protein-ligand complexes. *Acta Crystallogr. D Biol. Crystallogr.* *60*, 1355-1363.
9. DeLano, W.L. (2002). The PyMOL Molecular Graphics System.
10. Gaali S, Kirschner A, Cuboni S, Hartmann J, Kozany C, Balsevich G, Namendorf C, Fernandez-Vizarra P, Sippel C, Zannas AS, et al.: Selective inhibitors for the psychiatric risk factor FKBP51, *Nat. Chem. Biol* 2015, 11: 33-39.

## C. Summary and Outlook

### C. Summary and Outlook

In the presented thesis the first structure-affinity-relationship analysis on FKBP51-selective ligands, after the discovery of SAFit1 and 2, is shown. Using rational drug design methods, three different ligand series were designed, synthesized and evaluated. The overall aim was to find promising lead structures as starting point for further drug development since the SAFit compounds are not suitable for this. Based on the building blocks used for the synthesis we developed two “Bottom Group” (BG) and one “Top Group” (TG) series.

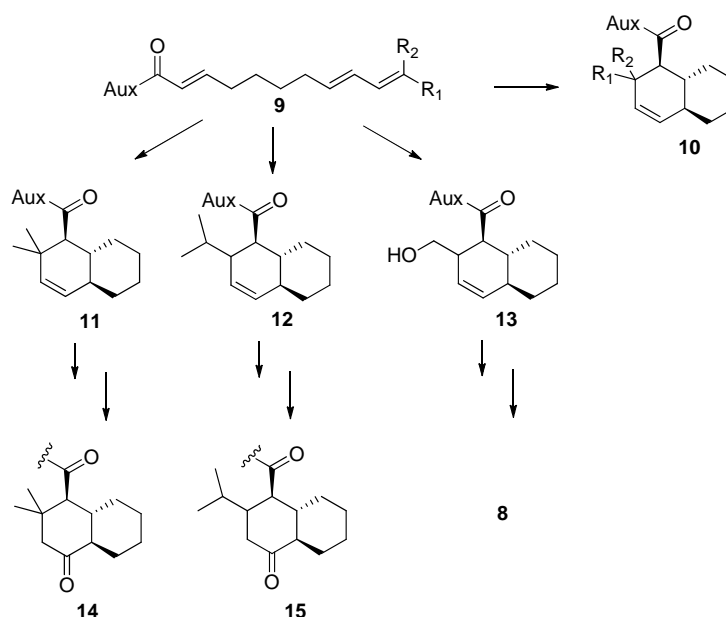
In all series we were able to reproduce the FKBP51 selective binding mode by induced fit that was discovered by Gaali et. al.[...]. This was confirmed by solving cocrystal structures of representative ligands with FKBP51. Additionally, we could show that neither modifications in the TG nor substitutions in the BG affect the selective binding mode. The correct conformation of the cyclohexyl ring seems to be the most important factor. Although we were not able to retain the high binding affinities of SAFit1 and 2, the developed ligands and building blocks exhibit much lower molecular weights. Together with their moderate binding affinity and the possibility for further chemical modification, they could serve as promising lead structures.

During our studies we found out that an  $\alpha$ -methyl-cyclohexyl group is the minimum requirement for selective binding. Inducing a hydroxyl group to the BG building group by an aldol reaction does not lead to an additional interaction with the protein but, nevertheless, leads to FKBP51 selective compounds with moderate binding affinities. We also recognized that rigidification of the cyclohexyl ring can be realized via a trans decalin scaffold as BG and that substituents can be positioned in a novel way with this scaffold. In the TG series we discovered a piperonic acid amide containing a geminally substituted cyclopentyl ring as promising new scaffold that leads to ligands with much lower molecular weight. Additionally, the solid phase-assisted method that was developed for the synthesis of this series is a useful novel method for further the rapid generation of FKBP51-focused libraries.

The chemical synthesis of SAFit1 and SAFit2 was scaled up and adapted in a way that we were able to synthesize both compounds in gram scales to provide them for further *in vivo* and *in vitro* studies. Thereby FKBP51 was confirmed as possible target for the treatment of obesity and melanoma and discovered as new target for treating musculoskeletal chronic pain.

## C. Summary and Outlook

These findings reinforce further FKBP51 drug development. Within the explored scaffolds particularly the decalin series (BG) exhibits a lot of potential for further exploration. Using the developed synthesis the 2-position of the bicycle could (9->10) be further substituted, e.g. by a dimethyl (11), an isopropyl (12) or a hydroxymethyl (13) group. Affinities could then be increased by inducing a carbonyl group (14+15) in the 4-position (that currently represents the best ligand of the series). It's also further worth trying to introduce an oxygen in the 2-position (8). A possible way would be the conversion of a hydroxymethyl group, which was described by Inoue et al.<sup>60</sup>.



**Scheme 7:** Possible further modifications of the bicyclic scaffold.

Most exciting will be the combination of the best building blocks that were discovered during this work, e.g. the geminally substituted piperolic ester amide with the best BG from the aldol-series (16) and the decalin-series (17).

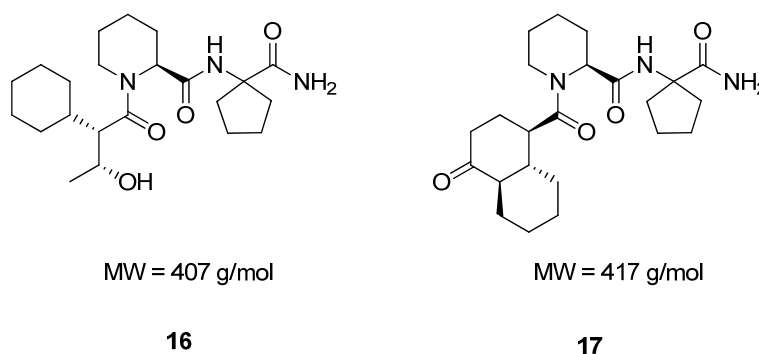


**Fig. 12:** Chemical structures of combined, promising building blocks

## C. Summary and Outlook

Although we initially expect a reduction of binding affinity, we postulate that when these low molecular weight (< 500 g/mol) compounds still exhibit moderate binding affinity they can serve as new lead structure for further optimization.

## D. References

### D. REFERENCES

1. Zannas AS, Binder EB: Gene–environment interactions at the FKBP5 locus: sensitive periods, mechanisms and pleiotropism. *Genes, Brain and Behavior* 2014, 13:25-37.
2. Klengel, T.; Mehta, D.; Anacker, C.; Rex-Haffner, M.; Pruessner, J. C.; Pariante, C. M.; Pace, T. W. W.; Mercer, K. B.; Mayberg, H. S.; Bradley, B.; Nemeroff, C. B.; Holsboer, F.; Heim, C. M.; Ressler, K. J.; Rein, T.; Binder, E. B., Allele-specific FKBP5 DNA demethylation mediates gene-childhood trauma interactions. *Nat Neurosci* 2013, 16, (1), 33-41.
3. Albu, S.; Romanowski, C. P.; Letizia Curzi, M.; Jakubcakova, V.; Flachskamm, C.; Gassen, N. C.; Hartmann, J.; Schmidt, M. V.; Schmidt, U.; Rein, T.; Holsboer, F.; Hausch, F.; Paez-Pereda, M.; Kimura, M., Deficiency of FK506-binding protein (FKBP) 51 alters sleep architecture and recovery sleep responses to stress in mice. *J Sleep Res* 2014, 23, (2), 176-85.
4. Hartmann, J.; Wagner, K. V.; Liebl, C.; Scharf, S. H.; Wang, X.-D.; Wolf, M.; Hausch, F.; Rein, T.; Schmidt, U.; Touma, C.; Cheung-Flynn, J.; Cox, M. B.; Smith, D. F.; Holsboer, F.; Müller, M. B.; Schmidt, M. V., The involvement of FK506-binding protein 51 (FKBP5) in the behavioral and neuroendocrine effects of chronic social defeat stress. *Neuropharmacology* 2012, 62, (1), 332-339.
5. Hoeijmakers, L.; Harbich, D.; Schmid, B.; Lucassen, P. J.; Wagner, K. V.; Schmidt, M. V.; Hartmann, J., Depletion of FKBP51 in female mice shapes HPA axis activity. *PLoS One* 2014, 9, (4), e95796.
6. O'Leary, J. C., 3rd; Dharia, S.; Blair, L. J.; Brady, S.; Johnson, A. G.; Peters, M.; Cheung-Flynn, J.; Cox, M. B.; de Erausquin, G.; Weeber, E. J.; Jinwal, U. K.; Dickey, C. A., A new anti-depressive strategy for the elderly: ablation of FKBP5/FKBP51. *PLoS One* 2011, 6, (9), e24840.
7. Yeh, W.; Li, T.; Bierer, B. E.; McKnight, S. L., Identification and Characterization of an Immunophilin Expressed During the Clonal Expansion Phase to Adipocyte Differentiation. *PNAS* 1995, 92, (24), 11081-11085.
8. Warriar, M., Role of Fkbp51 and Fkbp52 in Glucocorticoid Receptor Regulated Metabolism. Thesis, University of Toledo 2008.
9. Romano, S.; D'Angelillo, A.; Pacelli, R.; Staibano, S.; De Luna, E.; Bisogni, R.; Eskelinen, E. L.; Mascolo, M.; Cali, G.; Arra, C.; Romano, M. F., Role of FK506-binding protein 51 in the control of apoptosis of irradiated melanoma cells. *Cell Death Differ* 2010, 17, 145–157.

## D. References

10. Romano, S.; Staibano, S.; Greco, A.; Brunetti, A.; Nappo, G.; Ilardi, G.; Martinelli, R.; Sorrentino, A.; Di Pace, A.; Mascolo, M.; Bisogni, R.; Scalvenzi, M.; Alfano, B.; Romano, M. F., FK506 binding protein 51 positively regulates melanoma stemness and metastatic potential. *Cell Death Dis* 2013, 4, e578.
11. Srivastava, S. K.; Bhardwaj, A.; Arora, S.; Tyagi, N.; Singh, A. P.; Carter, J. E.; Scammell, J. G.; Fodstad, O.; Singh, S., Interleukin-8 is a key mediator of FKBP51-induced melanoma growth, angiogenesis and metastasis. *Br J Cancer* 2015.
12. Romano, S.; Mallardo, M.; Romano, M. F., FKBP51 and the NF-kappaB regulatory pathway in cancer. *Curr Opin Pharmacol* 2011, 11, 288-93.
13. Romano, S.; Sorrentino, A.; Di Pace, A. L.; Nappo, G.; Mercogliano, C.; Romano, M. F., The emerging role of large immunophilin FK506 binding protein 51 in cancer. *Curr Med Chem* 2011, 18, (35), 5424-9.
14. Bortsov, A. V., Smith, J. E., Diatchenko, L., Soward, A. C., Ulirsch, J. C., Rossi, C., ... & McLean, S. A.: Polymorphisms in the glucocorticoid receptor co-chaperone FKBP5 predict persistent musculoskeletal pain after traumatic stress exposure. *Pain* 2013, 154 (8), 1419-1426.
15. Gaali, S.; Gopalakrishnan, R.; Wang, Y.; Kozany, C.; Hausch, F., The chemical biology of immunophilin ligands. *Curr Med Chem* 2011, 18, (35), 5355-79.
16. Schmidt, M. V.; Paez-Pereda, M.; Holsboer, F.; Hausch, F., The Prospect of FKBP51 as a Drug Target. *ChemMedChem* 2012, 7, (8), 1351-9.
17. Hausch, F., FKBP5 and their role in neuronal signaling. *Biochim Biophys Acta* 2015, doi: 10.1016/j.bbagen.2015.01.012.
18. Price, R. D., Yamaji, T., Yamamoto, H., Higashi, Y., Hanaoka, K., Yamazaki, S., ... & Gold, B. G.: FK1706, a novel non-immunosuppressive immunophilin: neurotrophic activity and mechanism of action. *Eur. J. Pharmacol.* 2005, 509 (1), 11-19.
19. Kozany C, März A, Kress C, Hausch F: Fluorescent Probes to Characterise FK506-Binding Proteins. *ChemBioChem* 2009, 10:1402-1410.
20. Gopalakrishnan R, Kozany C, Gaali S, Kress C, Hoogeland B, Bracher A, Hausch F: Evaluation of Synthetic FK506 Analogues as Ligands for the FK506-Binding Proteins 51 and 52. *J Med Chem* 2012, 55:4114-4122.
21. Gopalakrishnan R, Kozany C, Wang Y, Schneider S, Hoogeland B, Bracher A, Hausch F: Exploration of Pipecolate Sulfonamides as Binders of the FK506-Binding Proteins 51 and 52. *J Med Chem* 2012, 55:4123-4131.

## D. References

22. Wang Y, Kirschner A, Fabian AK, Gopalakrishnan R, Kress C, Hoogeland B, Koch U, Kozany C, Bracher A, Hausch F: Increasing the Efficiency of Ligands for FK506-Binding Protein 51 by Conformational Control. *J Med Chem* 2013, 56:3922-3935.
23. Pomplun S, Wang Y, Kirschner A, Kozany C, Bracher A, Hausch F: Rational design and asymmetric synthesis of potent and neurotrophic FKBP ligands. *Angew Chem Int Ed* 2014:DOI: 10.1002/ange.201408776R201408771.
24. Gaali, S.; Kirschner, A.; Cuboni, S.; Hartmann, J.; Kozany, C.; Balsevich, G.; Namendorf, C.; Fernandez-Vizarra, P.; Sippel, C.; Zannas, A. S.; Draenert, R.; Binder, E. B.; Almeida, O. F. X.; Rühler, G.; Uhr, M.; Schmidt, M. V.; Touma, C.; Bracher, A.; Hausch, F. Selective inhibitors of the FK506-binding protein 51 by induced fit. *Nat. Chem. Biol.* 2015, 11 (1), 33–37.
25. Hartmann, J.; Wagner, K. V.; Gaali, S.; Kirschner, A.; Kozany, C.; Rühler, G.; Hoeijmakers, L.; Westerholz, S.; Uhr, M.; Chen, A.; Holsboer, F.; Hausch, F.; Schmidt, M. V., Pharmacological inhibition of the psychiatric risk factor FKBP51 has anxiolytic properties. *J Neurosci* 2015, in press.
26. Galat, A: Functional drift of sequence attributes in the FK506-binding proteins (FKBPs). *J Chem Inf Model* 2008, 48, (5), 1118-30.
27. Sinars, C. R.; Cheung-Flynn, J.; Rimerman, R. A.; Scammell, J. G.; Smith, D. F.; Clardy, J., Structure of the large FK506-binding protein FKBP51, an Hsp90-binding protein and a component of steroid receptor complexes. *Proc Natl Acad Sci U S A* 2003, 100, (3), 868-73.
28. Weiwad, M.; Edlich, F.; Kilka, S.; Erdmann, F.; Jarczowski, F.; Dorn, M.; Moutty, M. C.; Fischer, G., Comparative analysis of calcineurin inhibition by complexes of immunosuppressive drugs with human FK506 binding proteins. *Biochemistry* 2006, 45, (51), 15776-84.
29. de Kloet, E. R.; Joels, M.; Holsboer, F., Stress and the brain: from adaptation to disease. *Nat Rev Neurosci* 2005, 6, (6), 463-75.
30. Patrick, G. L. (2013). *An introduction to medicinal chemistry*. Oxford university press.
31. Cox, M. B.; Smith, D. F., *Functions of the Hsp90-Binding FKBP Immunophilins*. Austin, 2007.
32. Cheung-Flynn, J.; Prapapanich, V.; Cox, M. B.; Riggs, D. L.; Suarez-Quian, C.; Smith, D. F., Physiological role for the cochaperone FKBP52 in androgen receptor signaling. *Mol Endocrinol* 2005, 19, (6), 1654-66.

## D. References

33. Riggs, D. L.; Roberts, P. J.; Chirillo, S. C.; Cheung-Flynn, J.; Prapapanich, V.; Ratajczak, T.; Gaber, R.; Picard, D.; Smith, D. F., The Hsp90-binding peptidylprolyl isomerase FKBP52 potentiates glucocorticoid signaling *in vivo*. *Embo J* 2003, 22, (5), 1158-67.
34. Tranguch, S.; Cheung-Flynn, J.; Daikoku, T.; Prapapanich, V.; Cox, M. B.; Xie, H.; Wang, H.; Das, S. K.; Smith, D. F.; Dey, S. K., Cochaperone immunophilin FKBP52 is critical to uterine receptivity for embryo implantation. *Proc Natl Acad Sci U S A* 2005, 102, (40), 14326-31.
35. Storer, C. L.; Dickey, C. A.; Galigniana, M. D.; Rein, T.; Cox, M. B., FKBP51 and FKBP52 in signaling and disease. *Trends Endocrinol Metab* 2011.
36. Yong, W.; Yang, Z.; Periyasamy, S.; Chen, H.; Yucel, S.; Li, W.; Lin, L. Y.; Wolf, I. M.; Cohn, M. J.; Baskin, L. S.; Sanchez, E. R.; Shou, W., Essential Role for Co-chaperone Fkbp52 but Not Fkbp51 in Androgen Receptor-mediated Signaling and Physiology. *Journal of Biological Chemistry* 2007, 282, (7), 5026-5036.
37. Yang, Z.; Wolf, I. M.; Chen, H.; Periyasamy, S.; Chen, Z.; Yong, W.; Shi, S.; Zhao, W.; Xu, J.; Srivastava, A.; Sanchez, E. R.; Shou, W., FK506-binding protein 52 is essential to uterine reproductive physiology controlled by the progesterone receptor A isoform. *Mol Endocrinol* 2006, 20, (11), 2682-94.
38. Kirschner, A., Charakterisierung neuronaler Effekte von FKBP51. Dissertation. Ludwig-Maximilians-Universität München 2013.
39. Wager, T. T.; Chandrasekaran, R. Y.; Hou, X.; Troutman, M. D.; Verhoest, P. R.; Villalobos, A.; Will, Y., Defining desirable central nervous system drug space through the alignment of molecular properties, *in vitro* ADME, and safety attributes. *ACS Chem Neurosci* 2010, 1, (6), 420-34.
40. Leeson, P. D., & Springthorpe, B. (2007). The influence of drug-like concepts on decision-making in medicinal chemistry. *Nature Reviews Drug Discovery*, 6(11), 881-890.
41. Gaali, S., Design and Synthesis of Selective Ligands for the FK506-binding Protein 51. Dissertation. Ludwig Maximilians University Munich, 2012.
42. Crimmins, M. T., & Chaudhary, K. (2000). Titanium enolates of thiazolidinethione chiral auxiliaries: Versatile tools for asymmetric aldol additions. *Organic letters*, 2(6), 775-777.
43. Evans, D. A., Downey, C. W., Shaw, J. T., & Tedrow, J. S. (2002). Magnesium halide-catalyzed anti-aldol reactions of chiral N-acylthiazolidinethiones. *Organic letters*, 4(7), 1127-1130.
44. Nagao, Y., Ikeda, T., Yagi, M., Fujita, E., & Shiro, M. (1982). A new design for chiral induction: a highly regioselective differentiation between two identical groups in an acyclic

## D. References

- compound having a prochiral center. *Journal of the American Chemical Society*, 104(7), 2079-2081.
45. Wu, Y., Sun, Y. P., Yang, Y. Q., Hu, Q., & Zhang, Q. (2004). Removal of thiazolidinethione auxiliaries with benzyl alcohol mediated by DMAP. *The Journal of organic chemistry*, 69(18), 6141-6144
46. Evans, D. A., Britton, T. C., & Ellman, J. A. (1987). Contrasteric carboximide hydrolysis with lithium hydroperoxide. *Tetrahedron Letters*, 28(49), 6141-6144.
47. Evans, D. A., Tedrow, J. S., Shaw, J. T., & Downey, C. W. (2002). Diastereoselective magnesium halide-catalyzed anti-aldol reactions of chiral N-acyloxazolidinones. *Journal of the American Chemical Society*, 124(3), 392-393.
48. Walker, M. A., & Heathcock, C. H. (1991). Acyclic stereoselection. 54. Extending the scope of the Evans asymmetric aldol reaction: preparation of anti and "non-Evans" syn aldols. *The Journal of Organic Chemistry*, 56(20), 5747-5750.
49. Gómez-Vidal, J. A., Forrester, M. T., & Silverman, R. B. (2001). Mild and selective sodium azide mediated cleavage of p-nitrobenzoic esters. *Organic letters*, 3(16), 2477-2479.
50. Gemal, A. L., & Luche, J. L. (1981). Lanthanoids in organic synthesis. 6. Reduction of  $\alpha$ -enones by sodium borohydride in the presence of lanthanoid chlorides: synthetic and mechanistic aspects. *Journal of the American Chemical Society*, 103(18), 5454-5459.
51. Paintner, F. F., Bauschke, G., & Polborn, K. (2003). Toward the synthesis of tetrodecamycin: asymmetric synthesis of a direct precursor of the C6 · C18 trans-decalin portion. *Tetrahedron letters*, 44(12), 2549-2552.
52. Evans, D. A., & Adams, D. J. (2007). Total synthesis of (+)-galbulimima alkaloid 13 and (+)-hingaline. *Journal of the American Chemical Society*, 129(5), 1048-1049.
53. Evans, D. A., Chapman, K. T., & Bisaha, J. (1988). Asymmetric Diels-Alder cycloaddition reactions with chiral  $\alpha$ ,  $\beta$ -unsaturated N-acyloxazolidinones. *Journal of the American Chemical Society*, 110(4), 1238-1256.
54. Roush, W. R., Gillis, H. R., & Ko, A. I. (1982). Stereochemical aspects of the intramolecular Diels-Alder reactions of deca-2, 7, 9-trienoate esters. 3. Thermal, Lewis acid catalyzed, and asymmetric cyclizations. *Journal of the American Chemical Society*, 104(8), 2269-2283.
55. Iqbal, J., & Khan, M. A. (1989). An Efficient Synthesis of Silyl Dienol Ethers from  $\alpha$ ,  $\beta$ -Unsaturated Aldehydes and Ketones. *Synthetic Communications*, 19(3-4), 515-521.
56. Tsypysheva, I. P., Kunakova, A. M., Shitikova, O. V., Spirikhin, L. V., Valeev, F. A., & Tolstikov, G. A. (2002). Synthesis of the Eleutheside Core from (+)- $\Delta$ -Cadinol:

## D. References

- Construction of Side Chains on the Menthane Ring. *Chemistry of natural compounds*, 38(2), 154-160.
57. Silvestre, S. M., & Salvador, J. A. (2007). Allylic and benzylic oxidation reactions with sodium chlorite. *Tetrahedron*, 63(11), 2439-2445.
58. Zhao, Y., & Yeung, Y. Y. (2010). An unprecedented method for the generation of tert-butylperoxy radical using DIB/TBHP protocol: Solvent effect and application on allylic oxidation. *Organic letters*, 12(9), 2128-2131.
59. Catino, A. J., Forslund, R. E., & Doyle, M. P. (2004). Dirhodium (II) caprolactamate: An exceptional catalyst for allylic oxidation. *Journal of the American Chemical Society*, 126(42), 13622-13623.
60. Inoue, A., Kanematsu, M., Yoshida, M., & Shishido, K. (2010). Total synthesis of (+)-aspermytin A. *Tetrahedron Letters*, 51(30), 3966-3968.



## E. Curriculum Vitae

### E. CURRICULUM VITAE

**Xixi Feng**

#### Education

12/2015 **PhD** candidate at Max Planck Institute of Psychiatry, Munich, PG Hausch (Chemical Genomics)

Research Project: “Rational Drug Design and Synthesis of Selective FKBP51 ligands”

03/2012 **Master of Science**, Pharmaceutical Sciences, LMU Munich

Thesis: “Synthesis of Enzyme Inhibitors as Potential Cancer Therapeutics“ (in cooperation with Merck KGaA in Darmstadt, Medicinal Chemistry Division, supervisor: Dr. Buchstaller)

08/2010 **Bachelor of Science**, Pharmaceutical Sciences, LMU Munich

Thesis: “Synthesis of Potential GABA-Uptake-Inhibitors with Chelat-controlled Heck-Reaction“ (Dept. Pharmacy, Center of Drug Research, supervisor: Prof. Wanner)

07/2007 **Abitur** at Friedrich-Ludwig-Jahn-Gymnasium, Greifswald

#### Publications

- Feng X., Sippel C., Bracher A., Hausch F.: Structure-activity relationship analysis of selective FKBP51 ligands. *J. Med. Chem.* 2015, 58, 7796-7806. (doi: 10.1021/acs.jmedchem.5b00785)
- Feng X., Pomplun S., Hausch F.: Recent progress in FKBP ligand development. *Current Molecular Pharmacology*, 2015.
- Romano S., Xiao Y., Nakaya M., D’Angelillo A., Chang M., Jin J., Hausch F., Masullo M., Feng X., Romano M., Sun S.: FKBP51 employs both scaffold and isomerase functions to promote NF- $\kappa$ B activation in melanoma. *Nucleic Acids Research* 2015, 43 (14), 6983-6993. (doi: 10.1093/nar/gkv615).

#### Patent

- Selective FKBP51 ligands for treatment of psychiatric disorders  
International Application No.: PCT/EP2014/002542